
Università degli Studi di Napoli Federico II
Facoltà di Ingegneria



Gilda Florio

VULNERABILITY OF HISTORICAL MASONRY
BUILDINGS UNDER EXCEPTIONAL ACTIONS

*Tesi di Dottorato
XXIII ciclo*

*Il Coordinatore
Prof. Ing. Federico M. MAZZOLANI*

Dottorato di Ricerca in Ingegneria delle Costruzioni

ACKNOWLEDGMENTS

I have been waiting from three years to write this page.

Three special years of my lifetime, in which I went through many experiences.

Three years throughout which I have acquired a *forma mentis* and an internal richness I couldn't gained elsewhere. For this I have to thank Prof. Federico Massimo Mazzolani and Prof. Raffaele Landolfo.

I would like to truly thank Prof. Mazzolani, the Coordinator of this Doctoral Course. In this three years, He has represented a reference model for me, with His wisdom and vast knowledge. Even if He was not directly a teacher of mine when I was just a student, I have quickly learnt to greatly admire Him and the intense feeling that He still has for every new study He is going to tackle.

I wish to express my deep and sincere gratitude to my supervisor, Prof. Landolfo, who guided me during the whole Doctoral period, giving me the possibility to enrich my erudition.

I still remember his nice lessons which have strongly influenced my life choices. He taught me the civil engineering basis, transmitting to me the interest for structural field.

The regard and the esteem I have for him are very high (although he sometimes tease playfully the architects...).

I am infinitely grateful to Eng Antonio Formisano for his immense helpfulness to aid me and for the encouragement constantly provided during the period of my Doctoral studies. He gave me the essential enthusiasm to research in the field, involving me in some interesting study activities. Thank to him, I have really improved my way-work.

His professional, but at the same time, friendly presence has represented a steady reference point in each phase of this work.

On top of everything, I could thank him only for his patience: throughout this period, I sent to him about 1000 email!

I want to thank my affectionate PhD-room fellows for their friendly and selfless support in these three years: Renata Marmo, because she is always in

good spirit; Susanna Tortorelli and Marina Annecchiarico for their constructive suggestions and Maria Rosaria Gargiulo, for her outspokenness.

We shared meaningful pieces of our life.

I would like to acknowledge Lucrezia Cascini, Mario D'Aniello, Gianmaria Di Lorenzo, Ornella Iuorio, Oreste Mammana and Francesco Portioli, for their ready answers to all of my questions. They have accompanied me in my way, giving a friendly contribute to this work.

I also want to thank Carmine Castaldo, Daniela De Gregorio and Pierpaolo Di Feo, who shared with me study and survey activities, and the *new entries* of the research group, Giusy Terracciano and Maria Teresa Terracciano, for the time spent together.

Also I extend my acknowledgements to professors L. Krstevska and Lj. Tashkov of the *Institute of Earthquake Engineering and Engineering Seismology*, for the aid provided in the experimental activity in Abruzzo developed in the current thesis.

A special thank goes to my friends Caterina Dattilo, because together we started this adventure before to become architects and together we're finishing, and, *dulcis in fundo* (in each sense!) Marina Parrilli, for her extraordinary capacity of listening and always finding the right words.

Last but not least, my deepest gratitude goes to my parents and to my brother Vincenzo for their love and for their guide in every single day of my life.

My father taught me to never surrender and to get some of my zip back every time I needed. My mother has supported me...always.

What you have made for me is inestimable.

I will never forget.

November, 2010

Gilda

RINGRAZIAMENTI

Sto aspettando da tre anni per scrivere questa pagina.

Tre anni speciali della mia vita, in cui ho fatto molte esperienze.

Ho acquisito una *forma mentis* ed una ricchezza interiore che mai avrei potuto acquisire altrove. Per questo devo ringraziare il Prof. Federico Massimo Mazzolani ed il Prof. Raffaele Landolfo.

Ringrazio sinceramente il Prof. Mazzolani, Coordinatore di questo Corso di Dottorato. In questi tre anni, Egli ha rappresentato un modello di riferimento per me, con la sua saggezza e vasta cultura. Anche se Egli non è stato direttamente un mio professore quando ancora ero studentessa, ho imparato presto ad avere grande ammirazione di Lui e della passione che Egli ancora mette in ogni nuovo studio che si accinge ad intraprendere.

Esprimo la mia profonda e sincera gratitudine al mio tutor, Prof. Landolfo, che mi ha guidata durante l'intero periodo di Dottorato, dandomi la possibilità di arricchire la mia conoscenza.

Ricordo ancora le sue belle lezioni che hanno fortemente influenzato le mie scelte di vita. Egli mi ha insegnato le basi dell'ingegneria civile, trasmettendomi l'interesse per le discipline strutturali.

Il rispetto e la stima che ho per lui sono elevatissimi (anche se talvolta scherza sugli architetti...)

Sono infinitamente grata all'Ing. Antonio Formisano, per la sua immensa disponibilità ad aiutarmi e per avermi costantemente incoraggiata durante il Dottorato.

Egli mi ha fornito l'entusiasmo necessario per portare avanti la ricerca in questa disciplina, coinvolgendomi in interessanti attività di studio. Grazie a lui, ho davvero migliorato il mio modo di lavorare.

La sua presenza, professionale ma al contempo amichevole ha rappresentato un costante punto di riferimento in ciascuna fase di questo lavoro.

Al di là di tutto, potrei ringraziarlo solo per la sua pazienza: in questo periodo gli ho mandato circa 1000 e-mail!

Voglio ringraziare le mie affettuose compagne di stanza per il loro supporto, amichevole ed altruista, in questi tre anni: Renata Marmo, perché è sempre di buon umore, Susanna Tortorelli e Marina Annecchiarico, per i loro

suggerimenti costruttivi e Maria Rosaria Gargiulo, per la sua schiettezza. Abbiamo condiviso momenti significativi della nostra vita.

Voglio, inoltre, ringraziare Lucrezia Cascini, Mario D'Aniello, Gianmaria Di Lorenzo, Ornella Iuorio, Oreste Mammana e Francesco Portioli, per le pronte risposte alle mie domande. Mi hanno accompagnata nel mio percorso, dando un amichevole contributo a questo lavoro.

Voglio inoltre ringraziare Carmine Castaldo, Daniela De Gregorio e Pierpaolo Di Feo, che hanno condiviso con me attività di studio e di rilievo sul campo, e le *new entry* del gruppo di ricerca, Giusy Terracciano e Maria Teresa Terracciano per il tempo trascorso insieme.

Ancora vorrei estendere i ringraziamenti ai professori L. Krstevska and Lj. Tashkov dell' *Institute of Earthquake Engineering and Engineering Seismology*, per l' aiuto fornito nel corso dell'attività sperimentale oggetto di questa tesi.

Un ringraziamento speciale va alle mie amiche Caterina Dattilo, perché insieme abbiamo cominciato questa avventura prima di diventare architetti ed insieme la stiamo finendo, e *dulcis in fundo* (in tutti i sensi!) Marina Parrilli per la sua straordinaria capacità di ascoltare e di trovare sempre le parole giuste.

Ultimi, ma non meno importanti, ringrazio profondamente i miei genitori e mio fratello Vincenzo, per il loro affetto e per il loro essermi di guida in ogni giorno della mia vita.

Mio padre mi ha insegnato a non arrendermi mai e a ritrovare la giusta grinta ogni volta che ne avevo bisogno. Mia madre mi ha appoggiato...sempre.

Quello che avete fatto per me non ha prezzo.

Non lo dimenticherò mai.

Novembre, 2010

Gilda

ABOUT THE AUTHOR

Gilda Florio was born in Castellammare di Stabia (NA), Italy, on March 12th, 1983. She graduated cum laude in Architecture at the University “Federico II” of Naples on July 19th 2007, with a thesis developed in the field of Structural Engineering about the possibility of the cold formed steel system use in the emergency management. In the same year, she won the public competitive examination for the XXIII cycle of the PhD in Engineering of Constructions at the University of Naples, Faculty of Engineering, starting the PhD student activity. She’s actively involved in several studies and research activities in the Department of Constructions and Mathematical Methods in Architecture, mainly focusing on the seismic vulnerability assessment of historical masonry blocks and monumental buildings.

She also has been involved in the European project COST Action C26 “Urban habitat constructions under catastrophic events”. She is co-authoress of some scientific publications, on topic of seismic vulnerability of masonry structures.

Gilda Florio è nata a Castellammare di Stabia (NA), Italia, il 12 marzo 1983. Si è laureata con lode in Architettura presso l’Università di Napoli “Federico II” il 19 luglio 2007, con in Ingegneria Strutturale sulla possibilità di impiego dei sistemi in acciaio formato a freddo nella gestione delle emergenze. Nello stesso anno, ha vinto il concorso pubblico per il XXIII ciclo di Dottorato in Ingegneria delle Costruzioni, Facoltà di Ingegneria, cominciando l’attività di dottorato. È attualmente impegnata in numerosi studi ed attività di ricerca presso il Dipartimento di Costruzioni e Metodi Matematici in Architettura, riguardanti principalmente il tema della valutazione della vulnerabilità sismica di edifici storici in aggregato e monumentali.

Ella è stata inoltre coinvolta nel progetto di ricerca Europeo COST Action C26: “Urban habitat constructions under catastrophic events”. È coautrice di alcune pubblicazioni scientifiche concernenti la vulnerabilità sismica delle strutture murarie.

A Papà e a Mamma

LIST OF CONTENTS

LIST OF FIGURES	VII
LIST OF TABLES	XIII
INTRODUCTION	1
MOTIVATION AND SCOPE OF THE STUDY	1
FRAMING OF THE ACTIVITY	3
CHAPTER 1	7
THE SEISMIC RISK	
1.1. THE SEISMIC PHENOMENON	7
1.2. SEISMIC MEASURE SCALES	10
1.3. THE SEISMIC RISK ANALYSIS	16
1.3.1. General remarks	16
1.3.2. Hazard	17
1.3.3. Exposure	20
1.3.4. Vulnerability	22
1.4. RISK MANAGEMENT AND TOOLS	25
1.5. THE SEISMIC RISK IN ITALY: MICROZONATION, GUIDELINES AND MITIGATION PROJECTS	27
CHAPTER 2	31
MASONRY STRUCTURES	
2.1. INTRODUCTION	31
2.2. HISTORICAL REMARKS	32

2.3.	THE CONSTRUCTIVE SYSTEM	38
2.3.1.	General remarks	38
2.3.2.	Main typologies of masonry	38
2.4.	THE MATERIAL	43
2.4.1.	The base components	43
2.4.2.	Mechanical properties of units and mortars	46
2.4.3.	Mechanical properties of masonry	49
2.4.4.	The stress-strain relationships	53
2.4.5.	Material modelling approaches	56
2.5.	STRUCTURAL BEHAVIOUR	58
2.5.1	Modelling techniques	58
2.5.2	Under vertical loads	61
2.5.2.1.	<i>Calculation methods</i>	61
2.5.2.2.	<i>Check methods</i>	62
2.5.3	Under seismic loads	64
2.5.3.1.	<i>Masonry, earthquake and vulnerability factors</i>	64
2.5.3.2.	<i>Calculation methods</i>	68
2.5.3.3.	<i>Analysis type</i>	69
2.5.3.4.	<i>Strength criteria</i>	72
2.6.	TECHNICAL CODES APPROACHES	75
2.6.1.	Regulations for masonry buildings	75
2.6.2.	New masonry structures	76
2.6.3.	Existing masonry structures	77
CHAPTER 3		81
SEISMIC VULNERABILITY ASSESSMENT METHODOLOGIES		
3.1.	THE HISTORICAL HERITAGE IN ITALY	81

3.2.	METHODOLOGICAL APPROACHES	84
3.3.	ISOLATED MASONRY BUILDINGS	86
3.3.1.	Local scale methodologies	86
3.3.1.1.	<i>SAVE</i>	86
3.3.1.2.	<i>FaMIVE</i>	87
3.3.1.3.	<i>VULNUS</i>	90
3.3.1.4.	<i>Mechanical approaches</i>	93
3.3.2.	Large scale methodologies	96
3.3.2.1.	<i>Damage Probability Matrix Method</i>	96
3.3.2.2.	<i>The I level GNDT methodology</i>	97
3.3.2.3.	<i>The II level GNDT methodology</i>	99
3.3.2.4.	<i>Fully displacement – based methods</i>	102
3.3.2.5.	<i>The macroseismic method</i>	103
3.3.2.6.	<i>The electronic database MEDEA</i>	108
3.4.	MASONRY BLOCKS	112
3.4.1.	Introductory remarks	112
3.4.2.	Calculation Methods	112
3.4.2.1.	<i>General remarks</i>	112
3.4.2.2.	<i>In - plane analysis</i>	114
3.4.2.3.	<i>Out - of- plane analysis</i>	117
3.4.3.	Proposal of a vulnerability assessment approach	125
3.4.3.1.	<i>Revision of the Benedetti and Petrini’s form</i>	125
3.4.3.2.	<i>Numerical calibration of additional scores and weights</i>	125
3.4.3.3.	<i>Validation of the results: study cases in the historical centres of Sessa Aurunca (Ce)</i>	130
3.3.4.1.	<i>Further validation of the results: study cases in the historical centres of Torre del Greco (Na)</i>	134

3.3.4.2.	<i>Methodology application to the historical centre of Torre del Greco: seismic vulnerability and damage assessment by GIS</i>	139
3.3.4.3.	<i>Conclusions and further developments</i>	147

CHAPTER 4 **149**

THE VESUVIUS STUDY CASE: VULNERABILITY EVALUATION OF A MONUMENTAL BUILDING

4.1.	INTRODUCTION	149
4.2.	THE STUDY CASE: THE PALAZZO DI CITTÀ IN TORRE DEL GRECO (NA)	151
4.2.1	Historical and descriptive and information	151
4.2.2	Structural features	156
4.3.	QUICK METHODOLOGY APPROACHES	157
4.3.1	The Benedetti and Petrini's form	157
4.3.2	The Italian Guidelines	160
4.3.3	The SAVE Method	164
4.3.4	Mechanical model for masonry buildings	166
4.4.	NUMERICAL ANALYSIS	172
4.4.1	Theoretical basis	172
4.4.2.1.	<i>The Capacity Spectrum Method</i>	172
4.4.2.2.	<i>Horizontal elastic response spectra</i>	173
4.4.2.3.	<i>Conversion of the curve</i>	177
4.4.2.4.	<i>The index calculation: N2 and ATC 40 Methods</i>	179
4.4.2	The AeDES software	183
4.4.2.1.	<i>The FEM Model</i>	183
4.4.2.2.	<i>The static non linear analysis</i>	186
4.4.2.3.	<i>Vulnerability indexes assessment</i>	188
4.4.3	The SAP 2000 program	192

4.4.3.1.	<i>Theoretical basis</i>	192
4.4.3.2.	<i>The FEM model</i>	193
4.4.3.3.	<i>The static non linear analysis</i>	194
4.4.3.4.	<i>Vulnerability indexes assessment</i>	198
4.4.4	Comparison among results	201
4.5.	COMPARISON AMONG VULNERABILITY ASSESSMENT PROCEDURES	202
4.6.	VOLCANIC VULNERABILITY ASSESSMENT	205
4.6.1	Introductory observations	205
4.6.2	Volcanic eruption effects	205
4.6.2.1.	<i>General remarks</i>	205
4.6.2.2.	<i>Tephra deposits</i>	207
4.6.2.3.	<i>Pyroclastic flows</i>	208
4.6.2.4.	<i>Flying fragments and ballistic missiles</i>	208
4.6.2.5.	<i>Lahars</i>	209
4.6.2.6.	<i>Earthquakes</i>	210
4.6.3	Volcanic analysis	211
4.6.3.1.	<i>Tephra</i>	211
4.6.3.2.	<i>Ground motion</i>	214
4.7.	CONCLUSIVE REMARKS	215
 CHAPTER 5		217
SEISMIC BEHAVIOUR OF A MONUMENTAL PALACE UNDER EXCEPTIONAL ACTIONS: THE L'AQUILA EARTHQUAKE STUDY CASE		
5.1.	L'AQUILA EARTHQUAKE	217
5.1.1.	Characteristics of the seism	217
5.1.2.	Why an exceptional action	219

5.1.3.	Post-event consequences	221
5.2.	MEASUREMENTS IN ABRUZZO	223
5.2.1	Introduction	223
5.2.2	Poggio Picenze and Castelnuovo historical centres	224
5.2.3	The investigated buildings in Poggio Picenze	228
5.2.4	Environmental dynamic tests	230
5.2.4.1.	<i>Theoretical basis</i>	230
5.2.4.2.	<i>Experimental results</i>	231
5.3.	THE STUDY CASE: PALAZZO SIDONI IN CASTELNUOVO	235
5.3.1	Historical news and structural features	235
5.3.2	Experimental tests on masonry	238
5.3.3	Dynamic identification tests	240
5.3.4	Numerical activity	242
5.3.4.1.	<i>Calibration of the experimental results</i>	242
5.3.4.2.	<i>Modal behaviour of the undamaged building</i>	245
5.3.5	Interpretation and comparison of results	246
5.3.6	Retrofitting interventions	248
5.3.1	Vulnerability curves	250
5.4.	CONCLUSIVE REMARKS	252
	CONCLUSIVE REMARKS	253
	REFERENCES	257

LIST OF FIGURES

Figure 1.1 Tectonic faults: (a) fracture of the lithosphere; (b) main types of faults.....	8
Figure 1.2 Phenomena induced by earthquake: (a) landslide; (b) tsunami.....	10
Figure 1.3 Damage classification according to EMS 98.....	14
Figure 1.4 Damage classification according to EMS 98.....	14
Figure 1.5 The Seismic Risk Analysis	17
Figure 1.6 Microzonation according to OPCM 3274.....	28
Figure 2.1 Egyptian pyramids at Giza (2800-2000 BC).....	33
Figure 2.2 Brick making in Egypt, as depicted in a wall painting in the tomb of.....	33
Figure 2.3 The Parthenon at Athens	34
Figure 2.4 Roman masonry walls: (a) bonded brick wall; (b) brick faced wall with header courses; (c) brick faced wall (Drysdale et al., 1999)	35
Figure 2.5 Dry stone constructions: (a) Colosseum; (b) Segovia's aqueduct	35
Figure 2.6 Famous Gothic Cathedrals: (a) Amiens; (b) Beauvais	36
Figure 2.7 Church of St. Maria del Fiore, Florence.....	37
Figure 2.8 Different types of structural masonry walls:.....	39
Figure 2.9 Different types of stone masonry:.....	40
Figure 2.10 Different kinds of reinforced masonry: (a) cavity wall; (b) pocket wall;.....	41
Figure 2.11 Masonry confined within: (a) reinforced concrete frame;.....	42
Figure 2.12 Different kinds of concrete masonry units:	44
Figure 2.13 EC6, geometrical requirements for grouping of masonry units.....	45
Figure 2.14 Definition of failure planes: (a) failure parallel to the bed joints f_{vk1}	52
Figure 2.15 Stress – strain relationships for masonry material and its base components	53
Figure 2.16 Stress-strain relationship for masonry in compression.....	54
Figure 2.17 Reference system for plane stress states.....	55
Figure 2.18 Different modes of failure of solid clay brickwork panels under biaxial loading	56
Figure 2.19 Modelling strategies for masonry structures: (a) detailed micro-modelling; (b) simplified micro-modelling; (c) macro-modelling	57
Figure 2.20 (a) Structural component of masonry walls;	58
Figure 2.21 Different modelling techniques for masonry structures:	61
Figure 2.22 (a) I Mode Collapse Mechanisms (D'Ayala e Speranza, 2003); (b) II Mode Collapse Mechanism (Magenes, 2006)	66
Figure 2.23 Examples of: (a) I Mode Mechanism; (b) II Mode Mechanism.....	66
Figure 2.24 In-plane behaviour (a) action in the mean plane (b) rocking collapse; (c) diagonal shear; (d) sliding shear.....	73
Figure 3.1 Monumental buildings in Naples: (a) Royal Palace; (b) New Castle.....	82
Figure 3.2 Italian Monumental buildings:(a) Pisa Tower and (b) Main Cathedral in Milan	83
Figure 3.3 Italian Monumental buildings:	83
Figure 3.4 Samples of Italian historical centres:.....	83
Figure 3.5 FaMIVE spreadsheet	89
Figure 3.6 Out-of-plane collapse mechanism identified by FaMIVE program.....	90
Figure 3.7 Building capacity curve vs. demand spectrum (FEMA, 1999)	93

Figure 3.8 Fragility curves corresponding to the different damage limit states	95
Figure 3.9 EMS-98 building typologies and correlated vulnerability classes.....	97
Figure 3.10 Vulnerability functions to relate damage ratio and peak ground acceleration (PGA) for different values of index I_v	101
Figure 3.11 The MEDEA glossary and archive	109
Figure 3.12 Abacus of the global collapse mechanisms.....	110
Figure 3.13 Abacus of the local collapse mechanisms	110
Figure 3.14 MEDEA training section	111
Figure 3.15 In-plane collapse mechanisms	116
Figure 3.16 In-plane collapse mechanisms for buildings included in aggregate	116
Figure 3.17 Overturning mechanism.....	119
Figure 3.18 Vertical bending mechanism.....	120
Figure 3.19 Horizontal bending mechanism	121
Figure 3.20 Sample of horizontal bending failure: gable collapse	121
Figure 3.21 Possible composed overturning failure mode in case of good connections	122
Figure 3.22 Composed overturning mechanism	122
Figure 3.23 The 3MURI numerical model of a typical structural unit of Sessa Aurunca	126
Figure 3.24 Presence of adjacent building with different height	128
Figure 3.25 Possible positions of the building in the aggregate.....	128
Figure 3.26 Number of staggered floors among aggregated buildings	129
Figure 3.27 The investigated aggregate: a) plan view; b) building n.1; c) building n.2; d) building n.3; e) building n.4; f) building n.5.....	131
Figure 3.28 The implemented 3MURI model.....	132
Figure 3.29 Distribution of the two calculated vulnerability indexes I_M and I_V	133
Figure 3.30 Plan and bird-eye views of the study masonry aggregate in Torre del Greco.....	134
Figure 3.31 Plan view of the masonry block ground floor.....	136
Figure 3.32 FEM model of the aggregate in Sessa Aurunca	137
Figure 3.33 Pushover curves of the entire aggregate in the longitudinal (X) direction (a) and the transverse (Y) one (b).....	138
Figure 3.34 The building n. 1 and n. 2 within the masonry building block examined in Torre del Greco.....	139
Figure 3.35 The pilot area selected within the historical centre of Torre del Greco.	140
Figure 3.36 The investigated pilot area: a) main structural typologies; b) age classes.....	142
Figure 3.37 The investigated area: a) number of floors; b) conservation state	142
Figure 3.38 The investigated area: main vertical structures.....	143
Figure 3.39 The investigated area: main horizontal structures.....	143
Figure 3.40 Seismic vulnerability maps developed by applying: (a) Benedetti and Petrini's procedure and (b) the proposed one.....	144
Figure 3.41 Damage map for an earthquake with: (a) $T_R = 101$ years; (b) $T_R = 475$ years.....	146
Figure 3.42 Damage map for an earthquake with: (a) $T_R = 975$ years; (b) $T_R = 2475$ years	146
Figure 4.1 Pilot study building identification	150
Figure 4.2 Oil paintings by: (a) N. De Corsi, "Le cento Fontane" (1939);	152
Figure 4.3 Historical photographs of the façades:.....	152
Figure 4.4 Views of the building before the refurbishment intervention started in 1989.....	152
Figure 4.5 Views of the palace main façade after restoration works finished in 2003.....	153
Figure 4.6 Present-day pictures: (a) from via Fontana; (b) from via Barbacane.....	153

Figure 4.7 Present-day pictures: (a) from via Barbacane; (b) from the sea.....	153
Figure 4.8 Plan layout of the first floor of the building	154
Figure 4.9 South geometrical view of the building (from Piazza Plebiscito).....	154
Figure 4.10 North geometrical view of the building (from via Barbacane).....	155
Figure 4.11 East and West geometrical views of the building.....	155
Figure 4.12 Structural plan view of the building and structural details.....	156
Figure 4.13 Relation between damage levels according to EMS 98 and vulnerability indexes.....	160
Figure 4.14 Graphic representation of the shear strength of the examined construction.....	164
Figure 4.15 Shear-displacement relation according to (a) X direction and (b) Y direction.....	166
Figure 4.16 Simplified capacity curve of the Palazzo di Città:	171
Figure 4.17 Fragility curves of the structure according to the simplified method.....	172
Figure 4.18 Canonical shape of the elastic response spectrum (EC8)	176
Figure 4.19 Traditional and ADRS formats for the response spectra representation	177
Figure 4.20 Phases of conversion of MDOF curve into SDOF equivalent bilinear one.....	178
Figure 4.21 Performance point identification by means of the N2 method	181
Figure 4.22 Derivation of damping for spectral reduction	182
Figure 4.23 Derivation of energy dissipated by damping E_D	182
Figure 4.24 PC.M model 3D view	184
Figure 4.25 FEM model plan within the PC.M software.....	185
Figure 4.26 3D View of the equivalent frame model in PC.E environment.....	185
Figure 4.27 Push-over curves in (a) longitudinal and (b) in transverse direction according to the load distribution (A).....	186
Figure 4.28 Push-over curves in (a) longitudinal and (b) in transverse direction according to the load distribution (B).....	187
Figure 4.29 Aedes results: SDOF curves for (a) longitudinal (X) and (b) transverse (Y) directions according to the force distributions considered (A and B)	187
Figure 4.30 Aedes results: SDOF mean curves between distribution A and B for longitudinal (X) and transverse (Y) directions	188
Figure 4.31 Capacity spectrum for (a) longitudinal (X) and (b) transverse (Y) directions	189
Figure 4.32 Performance Point detection at LLS according to the N2 method:.....	190
Figure 4.33 Performance Point detection at CLS according to the N2 method:	190
Figure 4.34 Performance Point detection at LLS according to the ATC method:	191
Figure 4.35 Performance Point detection at LLS according to the ATC method:	191
Figure 4.36 Relationships assumed in SAP 2000 v.10 (Pasticier et al., 2007):.....	193
Figure 4.37 Plane Equivalent Frame Model of the examined building.....	194
Figure 4.38 3D Equivalent Frame Model of the Palazzo di Città	194
Figure 4.39 Deformed shape of the structure in the longitudinal direction	195
Figure 4.40 Deformed shape of the structure in the transverse direction	195
Figure 4.41 MDOF static push over curves for load distribution proportional to masses: (a) longitudinal and (b) transverse direction.....	195
Figure 4.42 MDOF static push over curves for load distribution proportional to vibration mode displacements: (a) longitudinal and (b) transverse direction	196
Figure 4.43 SAP results: SDOF curves for (a) longitudinal (X) and (b) transverse (Y) directions according to the force distributions considered (A and B)	196
Figure 4.44 SAP results: SDOF mean curves between distribution A and B for longitudinal (X) and transverse (Y) directions	197
Figure 4.45 Capacity spectrum for (a) longitudinal (X) and (b) transverse (Y) directions	198

Figure 4.46 Performance Point detection at LLS according to the N2 method:	199
Figure 4.47 Performance Point detection at CLS according to the N2 method:	199
Figure 4.48 Performance Point detection at LLS according to the ATC method:	200
Figure 4.49 Comparison between SDOF curves both for (a) longitudinal (X) and (b) transverse (Y) directions developed by means of the AeDes and SAP 2000 programs	201
Figure 4.50 Vulnerability index distribution : (a) SLS; (b) CLS.....	203
Figure 4.51 Capacity curves of the examined structure for longitudinal direction (X) according to different analysis methodologies.....	204
Figure 4.52 Eruption typologies: (a) effusive; (b) explosive.....	206
Figure 4.53 Comparison between the response spectra of the tectonic (1980) and the volcanic (1999) earthquakes in the Vesuvius area.....	210
Figure 4.54 Map of the isopachs of the ash deposits during the eruption occurred in 1631	212
Figure 4.55 Reduction factor detection for strength parallel to grain softwood	213
Figure 4.56 Effect of temperature on modulus of elasticity parallel to grain of softwood.....	213
Figure 5.1 Traces of L'Aquila earthquake: (a) the hour of the event; (b) the surface fracture; (b) the fault geometry	218
Figure 5.2 Mainshock maps (Italian National Institute of Geophysics and Vulcanology - INGV): (a) MCS map; (b) (PGA) map	218
Figure 5.3 (a) Sequence of seismic events occurred in the L'Aquila district (INGV);.....	219
Figure 5.4 Near-field and far-field site distances	220
Figure 5.5 Geologic section corresponding to the centre of L'Aquila (Bertini et al. 1992)	221
Figure 5.6 The Church of St. Massimo: (a) before and (b) after the earthquake; (c) detail of the damaged dome	222
Figure 5.7 Monumental buildings of L'Aquila after the earthquake:	222
Figure 5.8 (a) Building of the New Town; (b) wooden cabin in Onna.....	223
Figure 5.9 The work team.....	224
Figure 5.10 Location of Poggio Picenze and Catelnuovo as respect L'Aquila	225
Figure 5.11 Poggio Picenze: (a) plan view; (b) the Medieval House	226
Figure 5.12 Part of the destroyed centre of Poggio Picenze	227
Figure 5.13 The historical centre of Castelnuovo: (a) collapse of old masonry building on the hilltop; (b) limited damage to masonry building at the toe of the hill	228
Figure 5.14 Detection of the monumental building investigated in Poggio Picenze	228
Figure 5.15 Churches in Poggio Picenze: (a); Visitazione (b) St. Giuliano	229
Figure 5.16 (a) Seismometer Ranger type; (b) adjustment of the seismometer	231
Figure 5.17 Applied equipment for ambient vibration measurements: (a) Kinematics product; (b) Four Channel Signal Conditioner; (c) high-speed data acquisition system	231
Figure 5.18 Visitazione Church: (a) Test set-up (the RP is highlighted in blue);.....	232
Figure 5.19 Mode shapes of vibration: (a) transverse, $f = 3.51$ Hz; (b) rotational, $f = 5.08$; (c) longitudinal, $f=7.32$ Hz.....	232
Figure 5.20 St. Giuliano Church: (a) Test set-up (the RP is highlighted in blue);.....	233
Figure 5.21 Mode shapes of vibration: (a) longitudinal $f=5.37$ Hz; (b) longitudinal $f=6.64$ Hz; (c) rotational, $f=7.03$ Hz.....	233
Figure 5.22 Ferrari Palace: (a) Test set-up (the RP is highlighted in blue);	234
Figure 5.23 Mode shapes of vibration: (a) longitudinal; (b) transverse; (c) rotational	234
Figure 5.24 Palazzo Sidoni: (a)before earthquake(b) after earthquake.....	235
Figure 5.25 Palazzo Sidoni: plan view	236

Figure 5.26 Palazzo Sidoni: front view.....	236
Figure 5.27 Section AA	237
Figure 5.28 Main damages: (a) and (b) vaults; (c) debris and (d) remaining part of the collapsed vault over the stairs	237
Figure 5.29 3D views of Palazzo Sidoni.....	238
Figure 5.30 (a) Flat jack test; (b) present state.....	239
Figure 5.31 Stress-strain law: (a) mean vertical deformations; (b) horizontal deformations.....	240
Figure 5.32 Sidoni Palace: (a) seismometer; (b) detection of the RP;	241
Figure 5.33 Sidoni Palace: (a) test set-up (the RP is highlighted in blue);.....	241
Figure 5.34 Mode shapes of vibration: (a) transverse, $f = 5.08\text{Hz}$;.....	241
Figure 5.35 Transversal vibration mode of the damaged model: $f = 5.06\text{ Hz}$;.....	244
Figure 5.36 Longitudinal vibration mode of the damaged model: $f = 5.17\text{ Hz}$;.....	244
Figure 5.37 Torsional vibration mode of the damaged model corresponding to $f = 6.59\text{ Hz}$	245
Figure 5.38 Transversal vibration mode of the undamaged model: $f = 4.00\text{ Hz}$;	245
Figure 5.39 Longitudinal vibration mode of the undamaged model: $f = 5.32\text{ Hz}$;.....	246
Figure 5.40 Torsional vibration mode of the undamaged model: $f = 7.09\text{ Hz}$;.....	246
Figure 5.41 Damage evolution curve of Sidoni Palace.....	248
Figure 5.42 Modes shape of vibrations of the retrofitted building.....	249
Figure 5.43 Vulnerability curve of Sidoni Palace according to (X) direction.....	250
Figure 5.44 Vulnerability curve of Sidoni Palace according to (Y) direction	251

LIST OF TABLES

Table 1.1 The Modified Mercalli Intensity Scale (MMI).....	11
Table 1.2 European Macroseismic Scale (EMS 98).....	13
Table 1.3 Comparison between the Richter magnitude scale and the corresponding Mercalli Degree one.....	15
Table 1.4 Correlation between magnitudes and the earthquake effects	15
Table 1.5 Classification proposed by RISK-UE project.....	21
Table 1.6 EMS 98 vs HAZUS building typology classification	24
Table 1.7 The Giovinazzi's proposal for European building typology classification	25
Table 2.1 Classification of clay elements.....	44
Table 2.2 Classification of concrete elements	44
Table 2.3 Value of the shape factor δ relatively to the unit dimensions.....	48
Table 2.4 Typical guaranteed performance classes of mortars.....	48
Table 2.5 Typical prescribed composition classes of mortars.....	49
Table 2.6 Values of the initial shear strength of masonry f_{vk0} according to EC6.....	51
Table 2.7 Values of f_{vk1} for failure parallel to bed joints according to EC6.....	52
Table 2.8 Values of f_{vk2} for failure perpendicular to bed joints according to EC6	52
Table 2.9 Comparison among the modelling issue of EFM and FEM.....	60
Table 2.10 Factors influencing the seismic vulnerability of masonry buildings.....	67
Table 3.1 Resumptive draft of vulnerability analyses	85
Table 3.2 Score values corresponding to the vulnerability classes.....	92
Table 3.3 Weights related to the vulnerability factors of the constructions	92
Table 3.4 Linguistic relationship between I_3 and (a).....	92
Table 3.5 The Benedetti and Petrini original survey data form.	99
Table 3.6 Scores and relative weight of the significant factors to compute I_V according to the GNDT II level form.....	100
Table 3.7 Damage Model provided by EMS 98 for each of the six vulnerability class	105
Table 3.8 Most probable value of the vulnerability index for each vulnerability class	105
Table 3.9 Most probable value of the vulnerability index for each vulnerability class	106
Table 3.10 Scores for behavior modifier factors for Masonry and RC buildings.....	107
Table 3.11 Vulnerability increments ΔV evaluated for EC8 Ground types and for different building categories.....	108
Table 3.12 Resumptive draft of main failure out-of-plane modes.....	123
Table 3.13 Proposal of a survey data form for masonry block.....	130
Table 3.14 Mechanical indexes obtained by means of the numerical model, considering the building both as isolated and as part of the aggregate.....	132
Table 3.15 Comparison between the results of the two vulnerability assessment forms.	133
Table 3.16 Masonry mechanical properties of the aggregate structural units.	136
Table 3.17 Vulnerability index I_V according to the proposed procedure	136
Table 3.18 Mechanical vulnerability indexes obtained by means of the numerical analyses.....	138
Table 3.19 Comparison between vulnerability indexes achieved by applying the two assessment methods.....	139

Table 3.20 Earthquakes considered in the damage analysis.....	145
Table 4.1 Structural data of the examined construction.....	156
Table 4.2 The Benedetti and Petrini's procedure applied to the Palazzo di Città.....	157
Table 4.3 Parameters related to the calculation of factor n_4	158
Table 4.4 Mean damage grades related to macro-seismic levels of EMS 98.....	159
Table 4.5 Parameters for the evaluation of the masonry shear strengths at each levels.....	163
Table 4.6 Evaluation of the collapse acceleration.....	163
Table 4.7 Peak Ground Acceleration (Operational Limit State).....	164
Table 4.8 Peak Ground Acceleration (Near Collapse Limit State).....	165
Table 4.9 Shear resistance at each level.....	165
Table 4.10 Building typology classification.....	170
Table 4.11 Values for the parameters involved in the capacity curves evaluation.....	170
Table 4.12 Specific values of the parameter assumed for the investigated building.....	171
Table 4.13 Simplified mechanical model results.....	171
Table 4.14 Probability of each LS to be surpassed in the Reference Period.....	174
Table 4.15 Formulations for S_s and C_c	175
Table 4.16 Maximum values of the coefficient of topographical amplification S_T	175
Table 4.17 Aedes results: SDOF bilinear curves parameters.....	187
Table 4.18 Aedes results: SDOF mean curves between A and B load distribution.....	188
Table 4.19 Capacity spectrum parameter according to X and Y directions.....	189
Table 4.20 Target displacement of the structure capacity curve.....	191
Table 4.21 Seismic vulnerability indexes according to the numerical model.....	192
Table 4.22 SAP results: SDOF bilinear parameters.....	197
Table 4.23 SAP results: SDOF bilinear parameters of the mean curve.....	197
Table 4.24 Capacity spectrum parameter according to X and Y directions.....	198
Table 4.25 Target displacement of the structure capacity curve.....	199
Table 4.26 Seismic vulnerability indexes according to the numerical analysis performed.....	200
Table 4.27 Summary draft of the vulnerability indexes assessed by means of the two applied methodologies.....	202
Table 4.28 Summary draft of the vulnerability indexes assessed by means of the two applied methodologies.....	202
Table 4.29 Summary draft of all the vulnerability indexes assessed.....	203
Table 4.30 Values of the shape coefficient μ_i	211
Table 4.31 Tephra load evaluation.....	212
Table 4.32 Performance ratios for different value of the tephra density.....	214
Table 4.33 Vulnerability indexes of the building towards a volcanic earthquake.....	215
Table 5. 1 Earthquake effects at different epicentre distances.....	219
Table 5.2 Dominant frequencies and damping coefficients.....	232
Table 5. 3 Dominant frequencies and damping coefficients.....	233
Table 5.4 Dominant frequencies and damping coefficients.....	234
Table 5.5 Double flat jack test: parameters.....	240
Table 5.6 Dominant frequencies and damping coefficients.....	242
Table 5.7 Dominant frequencies corresponding to different value of E.....	243
Table 5.8 Parameter used in the adopted numerical model.....	243
Table 5.9 Dominant frequencies corresponding to different value of t.....	244

Table 5.10 Comparison among frequencies	246
Table 5.11 Comparison among experimental and numerical frequencies	247
Table 5.12 Dominant frequencies	247
Table 5.13 Dominant frequencies and damping coefficients	250

Introduction

MOTIVATION AND SCOPE OF THE STUDY

This work focuses on the vulnerability of historical masonry buildings under exceptional actions. So, the three key-concepts of this thesis are:

1. *Vulnerability*
2. *Historical masonry construction*
3. *Exceptional action*

The vulnerability of a constructions represents its propensity to suffer a certain damage level under a catastrophic event, seismic or not. It is commonly expressed by functions or matrices which may be obtained either by statistical studies of damaged buildings in earthquake-struck areas or by simulations using numerical models of the structure.

Seismic vulnerability topic is included in the field of seismic risk, which also involves hazard and exposure. The importance of seismic risk is related to the public safety that requires suitable management measures in order to protect people, properties, infrastructures and the built up cultural heritage. Therefore, a seismic risk analysis is aimed at the assessment and the hypothetical, quantitative description of the consequences of earthquakes upon a geographical area in a certain period of time.

The most vulnerable construction, but also the most valuable ones, are the historical ones, mostly made of oldest building material, that is masonry.

In fact, on one hand ancient masonry structures are particularly vulnerable to dynamic actions, especially seismic actions, since they were designed to resist ordinary vertical loads only, in compliance with the technical rules of their time of construction, so that they present an insufficient safety level against the exceptional actions. On the other hand, old constructions constitute the cultural

heritage of a nation, because they are imbued with historicity. This historicity does not only coincides with the concept of monuments or with the formal architectural language, but also to the specific structural features, applied materials and building techniques and, due to their age, to the fact that they are a part of human life. Thus, the historical heritage include monumental buildings, which may have great artistic values and are characterized by their own unique history, and historical centres, which represent the sign of the human past.

The issue of the protection of historic building is very important in Italy. In fact, this Nation is characterized by a large number of ancient monuments and dwellings, apart from innumerable minor centres. This need of preservation of the built up heritage is strongly related to the past lessons. Italy, indeed, has experienced destructive earthquakes throughout its history, which have provoked considerable social and economic losses. For this reasons, the public awareness is very sensitized of this issue and the conservation of the historic heritage becomes a pressing need.

The third concept concerns the risk induced by exceptional loading conditions.

In fact, buildings in the urban habitat are designed according to rules aimed at ensuring an adequate structural safety level under normal loading conditions. Nonetheless, all structures can be exposed to certain extreme conditions due to natural or human-made hazards in their design lifetime. So the behaviour of constructions when exposed to extreme events (e.g. volcanic actions and earthquakes in non-seismic areas) may not be neglected; on the contrary it should be ordinarily investigated in order to predict the structural response and ensure an adequate safety level.

In particular, an earthquake is exceptional when it is characterised by an extra-long return period, which corresponds to very strong seismic event. Also ground motions due to volcanic eruptions can be considered as exceptional events. For example, the Vesuvius risk is very high, due to both the presence of a wide cultural heritage and the high density of population. Furthermore, exceptional is the quake different from the one which the constructions has been designed to withstand, as for instance near-field seismic events often ignored by the seismic design codes. The damage scenario during L'Aquila earthquake in Abruzzo in 2009 was a clear example of such an unexpected effect. Finally, an earthquake may also be defined as exceptional when it hits historical zones. In fact, in this cases, as aforesaid, historic structures are not specifically designed or reinforced against earthquake, so the possible seismic event represents a totally unexpected event which can produce catastrophic effects.

For all this reasons, this thesis has been developed in the framework of the Research Project COST (*European Cooperation in the field of Scientific and Technical*

Research) Action C26 “Urban Habitat Constructions under Catastrophic Events”, which is related to the research activity in the field of risks due to exceptional loads.

On the basis of the above considerations, the analysis of the structural behaviour of historical masonry constructions subjected to exceptional actions has been done in order to evaluate their true levels of safety, as well as the potential risk induced by extreme conditions, which represent the main targets of the present study.

FRAMING OF THE ACTIVITY

The topic of this thesis is the vulnerability assessment of historical masonry building under exceptional actions. In order to develop the study, the structural performance of masonry aggregates and isolated monumental buildings under extreme loading condition have been investigated.

A scheme of the activity framing is shown in Figure 1.

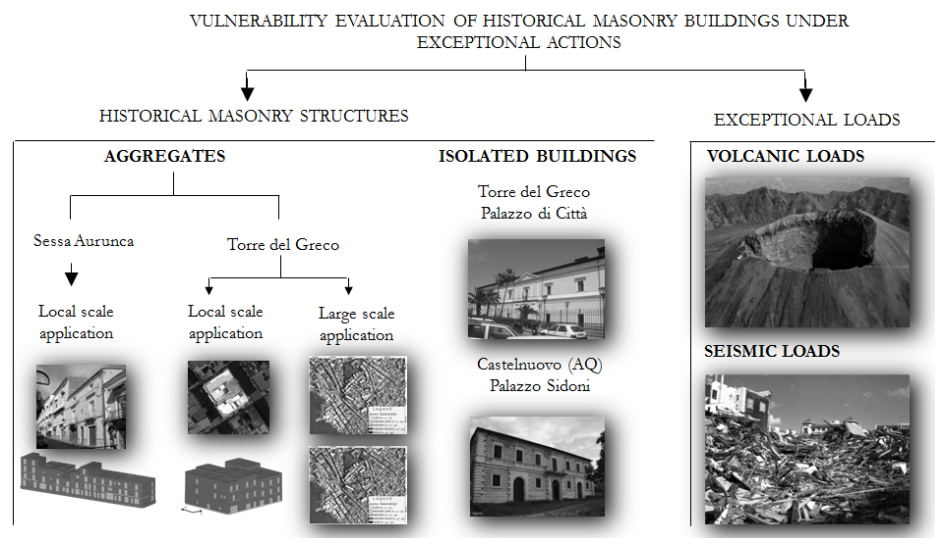


Figure 1 Framing of the activity

In detail, the thesis is organized in five chapters.

In **Chapter 1**, as a preliminary study phase, the seismic risk, with particular reference to seismic physic phenomenon, is described. The seismic risk issue involves hazard, exposure and vulnerability; each of this topic is fully described. In addition, a look to the Italian situation is taken, with particular reference to the

seismic zonation. Moreover, the importance of GIS tool in the risk management is emphasized.

In **Chapter 2**, a review of masonry structure properties has been done. Masonry is the most diffuse constructive material on the Italian territory and, also, the most ancient one. So, some historic news about masonry construction show the oldness of this material and its large application field. Then, the material is examined from the structural viewpoint, by describing the mechanical properties of both the basis components and the composite material. The constitutive laws present in literature are mentioned and the main material modelling techniques are described. Subsequently, the structural behaviour under vertical and horizontal loadings is investigated, in order to detect the most vulnerable factors which may influence the structural performance and the weak points of this structural typology.

In **Chapter 3** a complete state-of-the-art on seismic vulnerability assessment methodologies, both on the local scale and the large one, is performed. This represents a very crucial issue, since the vulnerability of most historical masonry building is very high, since they were designed to resist to vertical loads only. Thus, a large number of approaches available in literature are described and examined. In addition, a study on the seismic behaviour of masonry blocks is presented, by investigating both their in-plane collapse mechanisms and the out-of-plane ones. This study has led to the proposal of a form for the quick vulnerability evaluation of the structurally independent units belonging to aggregates. The procedure is applied and validated on study cases in Sessa Aurunca (Ce) and Torre del Greco (Na), respectively. This proposed methodology has been also applied to the aggregates of a historical centre area of Torre del Greco by means of the GIS instrument, in order to evaluate their susceptibility to damage under different return period seismic events.

The **Chapter 4** is based on the application of several seismic vulnerability assessment methodologies to a study case, represented by a monumental building, *Palazzo di Città* in Torre del Greco (Na). This palace is within the historical centre of the city and represents a strategic building, since it hosts the town municipality offices. Furthermore, it has been selected as an interesting edifice to be studied in the framework of the research project COST Action C26. Many vulnerability evaluation procedures have been applied to this construction in order to test the effective validity of the several approaches available in literature. Thus both simplified and mechanical procedures have been used for

both the calculation of the seismic vulnerability indicator, expressed by an appropriate index, and the estimation of the damage grade. In particular, since the mechanical model is applicable only when a capacity curve is available, the implementation of numerical models by means of two different non-linear numerical program has represented the preliminary phase of the study. Finally, according to the objectives of this thesis, a volcanic vulnerability analysis has been performed by considering two kinds of actions related to the volcanic activity, that is tephra and quake, in order to examine the structural behaviour of the study building in case of a possible eruption of Vesuvius.

In **Chapter 5** a very interesting and recently investigated topic, namely L'Aquila earthquake occurred on 2009, April 6th, has been treated. This represent a clear example of exceptional quake for intensity and physical aspects. This event caused many victims, fatalities and injuries, homeless, apart from the inestimable damages to the built up heritage. An experimental campaign, developed in cooperation with the University of L'Aquila and the University of Skopje, has been undertaken within the COST Action C26 project by performing environmental vibration tests on monuments of two Abruzzo municipalities, namely Poggio Picenze and Castelnuovo, gravely hit by the earthquake. The study is focused on a monumental palace in Castelnuovo, named Palazzo Sidoni, whose experimental dynamic frequencies have been numerically calibrated with the aim to set-up appropriate retrofitting interventions.

Finally, interesting **Conclusions** on the main results provided by this work have been drawn.

Chapter 1

The seismic risk

1.1. THE SEISMIC PHENOMENON

Earthquakes are very complex natural phenomena which represent the natural catastrophe producing major damages to constructions and people. According to the various causes that generated earthquakes, they can be classified in:

- tectonic earthquakes, generated by the sudden sliding of plates along a fault plane;
- volcanic earthquakes, related to volcanic eruptions and caused by the fracture of rocks due to heat stress of the intrusion of magma in the volcanic areola;
- subsident earthquakes, consisting in localized seismic events caused by the collapse of underground caverns.

Other possible earthquakes may be also caused by human activities, i.e. large excavations in mines, explosions and large water reservoirs.

In particular, tectonic earthquake can be defined as a ground tremor caused by the natural fracture and slippage of rock layers in the Earth crust, according to the generally accepted plates tectonic theory. The fracture in the lithosphere, where in the past sections of rock have slipped each other, is called tectonic fault (Figure 1.1a). Along these faults, the crust rupture produces a sudden release of energy under form of low-frequency sound waves called seismic waves due to the accumulated strains. The relative displacement of the two sides of a fault and the fault length both increase approximately exponentially with earthquake intensity. Generally, the relative displacement during high intensity earthquakes may be as much as 20 to 30 m, while the fault length in a single event may be hundreds of kilometres long. In most cases, the faults are formed deep within the lithosphere and they are not visible on the surface of the Earth.

The main types of faults that may cause a ground motion are: normal, reverse, thrust and strike-slip (Figure 1.1b). Normal and reverse faulting are dip-slip motions, in which the displacement along the fault involves a vertical component. In particular, the normal faults occur when ground on one side moves down the dip of the fault relative to the adjacent ground and mainly in areas where the Earth crust is being extended. Instead, reverse and thrust faults occurs when ground on one side moves up the dip of the fault relative to the adjacent ground and interests the areas where the crust is being shortened.

Last, the strike-slip, occur where the two sides of the fault slip horizontally each other. In particular, the two blocks of the fault can move to the right (right lateral fault) or to the left (left lateral fault). Generally, most earthquakes are caused by the movement of faults having components of both dip-slip and strike-slip, known as oblique slip.

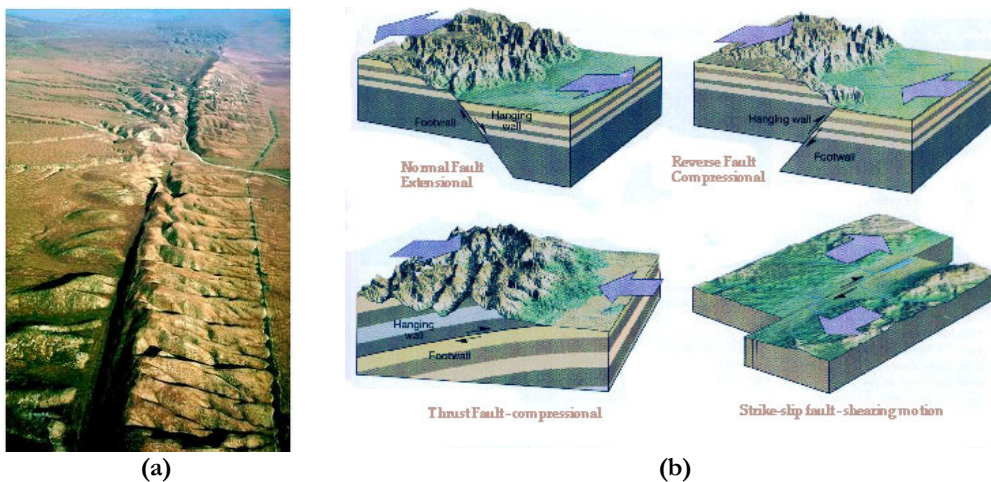


Figure 1.1 Tectonic faults: (a) fracture of the lithosphere; (b) main types of faults

The surface of slippage generating seismic elastic waves is called focus or hypocentre and its projection onto the Earth surface is defined epicentre. Although the hypocentre and the epicentre are commonly idealised as two points, they respectively represent the area of slippage between two tectonic blocks and the zone of the Earth where the seismic impact is most severe. In general, the size of the epicentral area depends on the intensity of the quake, on the size of the ground fracture and on the depth of the hypocentre (Tomazevic, 1999).

The size of the ground rupture and the degree of the slippage also determine the quake magnitude. The released energy deforms the rocks near the fault and

propagates in the form of seismic elastic waves transmitted through the Earth. Although the time of a seismic shock ranges from a few seconds to a minute, the waves continue to propagate after the movement across the globe for about 20 minutes. The vibrations cause significant damages near the epicentre, although they may be felt at large distances from the epicentre too.

Two types of seismic waves, generated at the slippage zone, are carried by seismographs, instruments that record the ground motion and determine the epicentre and the fault extension and orientation. The first type of waves are called body waves since they travel through the Earth inner layers, while the second type are called surface waves and are the result of the reflection and the refraction of the body waves during the propagation in stratified formation of the Earth crust.

Body waves includes both primary or compressive waves (P) and secondary or shear waves (S). The P waves are longitudinal waves, characterized by alternative compressions and dilations along the direction of propagation and perpendicular to the wavefront. These waves can move through solid rocks and fluids and are the fastest waves, having a velocity of about 5 – 7 km/s in typical Earth crust, less than 8 km/s in Earth mantle and core, about 1.5 km/s in water and 0.3 km/s in air.

The S waves are transverse waves slower than P ones. These waves do not propagate through fluids and present a velocity of about 3 – 4 km/s in typical Earth crust, less than 4.5 km/s in Earth mantle and less than 2.5-3.0 km/s in solid inner core. Surface waves includes Love (L) and Rayleigh (R) ones.

The L waves vibrate in a plane parallel to the Earth surface by a transverse horizontal motion perpendicular to the direction of propagation. Love waves are largest at the surface and decrease in amplitude with depth; their velocity, in general, depends on frequency and ranges from 2.0 to 4.5 km/s.

The R waves presents, instead, a typical elliptical motion, vibrating in a plane perpendicular to the Earth surface. These waves amplitudes, generally, decrease with depth in the Earth and their velocity depends on frequency, ranging from 2.0 to 4.5 km/s.

In general, the frequency of oscillation and the amplitude of a wave is dependent on the way of propagation. Therefore, the wave that reaches the surface inducing vibrations to a building reflects not only the characteristics of the seism but also the effect of the bedrock and the soil under the site of construction.

The earthquakes also cause other indirect phenomena as for instance landslides (Figure 1.2a), fires and dam failures. In general, the seismic event occurred under or near the ocean may also generate waves tide, more properly called tsunamis or seismic sea waves (Figure 1.2b). High as 15 m, these waves can cross an ocean in

a few hours, causing considerable damage also on the coasts are very distant from the epicentre of the earthquake.



Figure 1.2 Phenomena induced by earthquake: (a) landslide; (b) tsunami

1.2. SEISMIC MEASURE SCALES

In order to measure and classify the earthquake intensity, the seismologists have elaborated different measurement scales. One of the first scale was developed by Michele de Rossi and Francois Forel in 1883 and ranged from I to X intensity level (De Rossi, 1883).

Nowadays, various scale are used in the different continents. In particular, the Japan Meteorological Agency (JMA) official seismic intensity scale is the Omori one, a eight-point scale developed by Fusakichi Omori and calibrated on damages suffered by various types of Nippon structures (Omori, 1900).

In America and in Europe, the standard official scales are based on the one devised in 1902 by an Italian man called Giuseppe Mercalli (1850-1914) and hereafter modified. In particular, the official American scale is the Modified Mercalli (MMI) one, based on the Mercalli scale modified by a H. O. Wood and Frank Neumann in 1931. The MMI scale is characterised by ten grades which measure seismic severity by means of the classification of earthquake effects at different sites of the Earth surface. Intensity ratings are expressed as Roman numerals between I (lower grade) and XII (higher grade) (Table 1.1).

In Europe, instead, the twelve grade Mercalli-Cancani-Sieberg (MCS) has been used from the beginning of the 20th century.

Table 1.1 The Modified Mercalli Intensity Scale (MMI)

Tremor level	Degree and Description	Average PGA
Instrumental	I. People do not feel any Earth movement	
Lightest	II. A few people might notice movement if they are at rest and/or on the upper floors of tall buildings.	
Light	III. Many people indoors feel movement. Hanging objects swing back and forth. People outdoors might not realize that an earthquake is occurring.	
Mediocre	IV. Most people indoors feel movement. Hanging objects swing. Dishes, windows, and doors rattle. The earthquake feels like a heavy truck hitting the walls. A few people outdoors may feel movement. Parked cars rock.	0.015 g – 0.02 g
Strongly	V. Almost everyone feels movement. Sleeping people are awakened. Doors swing open or close. Dishes are broken. Pictures on the wall move. Small objects move or are turned over. Trees might shake. Liquids might spill out of open containers.	0.03 g – 0.04 g
Much fort	VI. Everyone feels movement. People have trouble walking. Objects fall from shelves. Pictures fall off walls. Furniture moves. Plaster in walls might crack. Trees and bushes shake. Damage is slight in poorly built buildings. No structural damage.	0.06 g – 0.07 g
Strong	VII. People have difficulty standing. Drivers feel their cars shaking. Some furniture breaks. Loose bricks fall from buildings. Damage is slight to moderate in well-built buildings; considerable in poorly built buildings.	0.10 g – 0.15 g
Violent	VIII. Drivers have trouble steering. Houses that are not bolted down might shift on their foundations. Tall structures such as towers and chimneys might twist and fall. Well-built buildings suffer slight damage. Poorly built structures suffer severe damage. Tree branches break. Hillsides might crack if the ground is wet. Water levels in wells might change.	0.25 g – 0.30 g
Disastrous	IX. Well-built buildings suffer considerable damage. Houses that are not bolted down move off their foundations. Some underground pipes are broken. The ground cracks. Reservoirs suffer serious damage.	0.50 g – 0.55 g
Most Disastrous	X. Most buildings and their foundations are destroyed. Some bridges are destroyed. Dams are seriously damaged. Large landslides occur. Water is thrown on the banks of canals, rivers, lakes. The ground cracks in large areas. Railroad tracks are bent slightly.	More than 0.60 g
Catastrophic	XI. Most buildings collapse. Some bridges are destroyed. Large cracks appear in the ground. Underground pipelines are destroyed. Railroad tracks are badly bent.	
Great catastrophe	XII. Almost everything is destroyed. Objects are thrown into the air. The ground moves in waves or ripples. Large amounts of rock may move.	

Other seismic scales are also based on the released energy in the focus, as for instance the Richter magnitude one developed in 1935 by the seismologist Charles F. Richter from the California Institute of Technology. According to the Richter scale, the seismic severity depends on the magnitude M estimation, expressed by the logarithm of the maximum displacement amplitude A (in μm)

recorded by a standardised seismograph located at exactly 100 km from the epicentre, as reported in the following equation:

$$M = \log A \quad (1.1)$$

Adjustments are included for the variation in the distance between the various seismographs and the epicentre of an earthquakes. The local magnitude M_L for a shallow local earthquake is defined as follows:

$$M_L = \log A - \log A^0 \quad (1.2)$$

where $\log A^0$ is the calibration factor.

The Richter Scale does not measure the damage suffered by a building under earthquake, since the concept of magnitude is directly related to the amount of released energy. It is worth to precise that great part of this energy is dissipated in the crushing process and only the minor part contributes to the seismic waves formation. Thus, the Richter Scale is a logarithmic scale, in which each whole number increase in magnitude represents a tenfold increase in the correspondent measured amplitude. Therefore, in terms of energy, each step in the magnitude scale corresponds to the release of about thirty-one times more energy than the amount associated with the preceding whole number value. For example, if a magnitude 5.3 might be computed for a moderate earthquake, a magnitude 6.3 might be evaluated for a strong earthquake.

In order to assess the relation between the magnitude M and the epicentre intensity I , the seismologist have proposed the following empirical equation:

$$M = a \cdot I + b \cdot \log h + c \quad (1.3)$$

where a , b and c are constant depending on the site and h is the depth of the hypocentre.

This correlation between magnitude and intensity is very complex and, in so many cases, not very clear. Indeed, the so-called macro-seismic scale has been defined on the basis of the earthquake effects on the different building typologies. This type of classification varies from country to country, in relation to the built environment, to the quality of constructions and to the human feelings. In order to consider all of these aspects, in 1995 the European Committee defined the European Macroseismic Scale (EMS), the actual reference scale for European Countries which took its basis from the Medvedev-Sponhever-Karnik (MSK) scale, firstly proposed in 1964 (MSK-64) and subsequently modified in 1976 and 1978 (MSK-76 and MSK-78) with the purpose to quantify the damage suffered by constructions under earthquake.

Analogously to the MMI scale, the EMS 98 has twelve grades, but the latter is more detailed than the former. In particular, higher intensity levels are assigned to earthquakes on the basis of damages provoked to buildings, they being associated to both a specific value of ground acceleration and a picture related to the damage level suffered by the building (Grunthal, 1998). The European Macroseismic Scale is synthetically described in Table 1.2.

Table 1.2 European Macroseismic Scale (EMS 98)

Intensity	Description
I	Not felt
II	Scarcely felt
III	Weak
IV	Largely observed
V	Strong
VI	Slightly damaging
VII	Damaging
VIII	Heavily damaging
IX	Destructive
X	Very destructive
XI	Devastating
XII	Completely devastating

It is worth noticing that EMS 98 scale appears equivalent to MSK in terms of the intensity degree definition. Thus, in the range of intensities meaningful for the building damage description ($I > V$), since the MSK scale and the MMI one are equivalent, EMS 98 is equivalent to the MMI scale. This is an important observation because, thanks to this assumption, comparisons between data and intensity based vulnerability models from different countries are allowed.

The conversion of the MCS levels towards the EMS ones is, instead, a little bit more problematic and it is often solved setting the EMS intensity a degree level lower than the MCS one, even if a precise and complex relationship between the two scales exists.

This EMS 98 scale also classifies damaged masonry (Figure 1.3) and reinforced concrete (Figure 1.4) buildings on the basis of the structural and geometrical features of the constructions. In particular, for masonry constructions, the EMS-98 considers seven different typologies which distinguish each other for materials, installation techniques and constructive details. This aspect has been treated into detail within the Chapter 3 on the building vulnerability analysis.

<p>Grade 0: No damages</p> 	<p>Grade 3: Substantial to heavy damages Moderate structural damages and heavy non structural damages Large and extensive cracks in most walls; pantiles or slates slip off; chimneys are broken at the roof line; failure of individual non structural elements</p> 
<p>Grade 1: Negligible structural damages or non structural damages Hair-line cracks in many few walls, fall of small pieces of plaster; fall of loose stones from upper parts of building</p> 	<p>Grade 4: Very heavy damages Heavy structural damages and very heavy non structural damages; serious failure of walls; partial structural failure</p> 
<p>Grade 2: Moderate damages Slight structural damages and moderate non structural damages Cracks in many walls Fall of fairly large pieces of plaster, parts of chimneys fall down</p> 	<p>Grade 5: Destruction Very heavy structural damages Total or near total collapse</p> 

Figure 1.3 Damage classification according to EMS 98

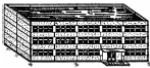
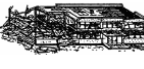
<p>Grade 0: No damages</p> 	<p>Grade 3: Substantial to heavy damages Moderate structural damages and heavy non structural damages Cracks in columns and beam column joints of frames at the base and at joints of coupled walls Spalling of concrete cover, buckling of reinforced rods Large cracks in partition and infill walls, failure of individual infill pannels</p> 
<p>Grade 1: Negligible structural damages or non structural damages Fine cracks in plaster over frame members or in walls at base Fine cracks in partitions and infills</p> 	<p>Grade 4: Very heavy damages Heavy structural damages and very heavy non structural damages; Large cracks in structural elements with compression failure of concrete fracture of rebar; bond failures of beam reinforced bars; tilting of columns. Collapse of few columns or of a single upper floor</p> 
<p>Grade 2: Moderate damages Slight structural damages and moderate non structural damages Cracks in columns and beams of frames and in structural walls Cracks in partition and infill walls; fall of brittle cladding and Plaster Falling mortar from the joints of wall pannels</p> 	<p>Grade 5: Destruction Very heavy structural damages Total or near total collapse</p> 

Figure 1.4 Damage classification according to EMS 98

A comparison between the Richter magnitudes and the Mercalli degrees has been made in Table 1.3, where also the corresponding quantity of free energy released is reported. Finally, in Table 1.4 the effects on the built-up related to earthquakes of given Richter magnitude are described.

Table 1.3 Comparison between the Richter magnitude scale and the corresponding Mercalli Degree one

Richter Magnitude	Energy [joule]	Mercalli Degree
< 3.5	< 1.6 E+7	I
3.5	1.6 E+7	II
4.2	7.5 E+8	III
4.5	4 E+9	IV
4.8	2.1 E+10	V
5.4	5.7 E+11	VI
6.1	2.8 E+13	VII
6.5	2.5 E+14	VIII
6.9	2.3 E+15	IX
7.3	2.1 E+16	X
8.1	> 1.7 E+18	XI
> 8.1		XII

Table 1.4 Correlation between magnitudes and the earthquake effects

Richter magnitude	Earthquake effects
less than 3.5	Generally not felt, but recorded.
3.5-5.4	Often felt, but rarely causes damage.
under 6.0	At most slight damage to well-designed buildings. Can cause major damage to poorly constructed buildings over small regions.
6.1-6.9	Can be destructive in areas up to about 100 kilometres across where people live.
7.0-7.9	Major earthquake. Can cause serious damage over larger areas.
8 or greater	Great earthquake. Can cause serious damage in areas several hundred kilometres across.

1.3. THE SEISMIC RISK ANALYSIS

1.3.1. General remarks

Earthquakes are one of the most costly and complex natural hazards, posing a significant risk in many parts of the World. The general risks related to the seismic event include fatalities, injuries, collapses of houses, homeless population, bridges impassable, road length damaged, water supply pipes, telephone and electric lines damaged and economic losses. So, Seismic Engineering has the purpose to study the behaviour of constructions in order to reduce life and economic losses under earthquakes.

Seismic risk is the probability of negative consequences and losses directly or indirectly provoked by earthquakes that may occur in a specific zone and in a period of time. In particular, losses might be suffered either by the population or by the built up environment as well as by the economic and social systems. Historically, the term has been used to describe an assortment of earthquake effects that ranges from ground shaking to economic loss and casualties, but the terminology has become more precise as more quantitative methods for estimating the effects of earthquakes have been developed.

According to the definition given by United National Disaster Relief Office, (U.N.D.R.O., 1979), the seismic risk R_l is the damage probability of level l for a fixed period of time within a population of risk elements (grouped into categories) due to the seismic probability at site. A general expression for the defined risk is given by the equation below:

$$R_l = \sum_m q_m \left(\sum_i H_i \cdot V_{lim} \right) \quad (1.4)$$

in which:

- i is the severity of the event;
- m is the category of the exposed elements;
- q_m is the percentage of the exposed elements;
- l is the damage level;
- H_i is the seismic hazard, defined as the probability of the occurrence of a seismic event of severity i within a fixed site and in a fixed exposure time, considered, in so many cases, as the design lifetime of a construction;
- V_{lim} is the seismic vulnerability expressed by the probability of attaining a damage level l caused by a seismic event with intensity i from a number m of categories of risk elements, such as people, cultural heritage and human activities.

In particular, primary, secondary and tertiary hazards H_i can be distinguished (Hi. Dong et al., 1988). Fault break and ground motion are identified as primary hazards, while all the potentially dangerous phenomena caused by primary hazards are defined as secondary hazards, i.e. tsunami, foundation settlement, foundation failure, liquefaction and landslides caused by ground shaking. Finally, fire following earthquake and flooding produced by dam break can be considered as tertiary hazards.

The seismic risk analysis is based on three essential components to be separately quantified and analysed: Hazard, Exposure and Vulnerability. Each category includes several parameters to be evaluated by means of specific studies and methodologies investigation. The summary scheme for seismic risk analysis is depicted in Figure 1.5.

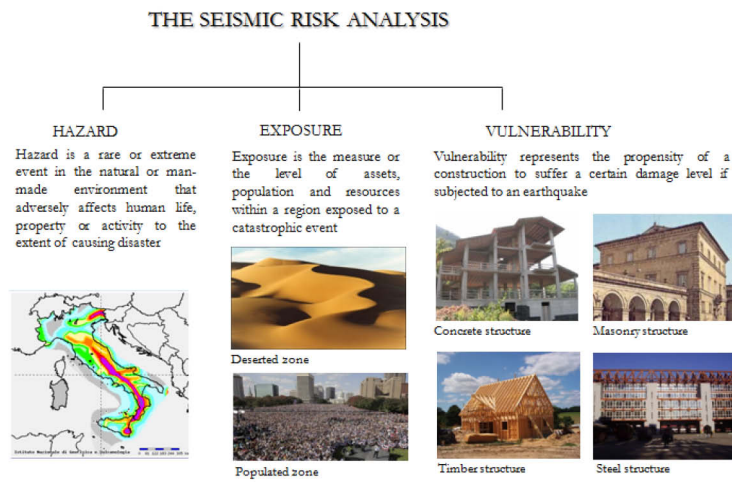


Figure 1.5 The Seismic Risk Analysis

1.3.2. Hazard

Hazard is a rare or extreme event in the natural or man-made environment that adversely affects human life, property or activity to the extent of causing disaster. In engineering, the term is used in a mathematical sense to mean the probability of the occurrence, within a specified period of time and a given area, of a potentially damaging phenomenon of a given intensity (Coburn et al., 1994). Therefore, a seismic hazard analysis consists on the estimation of the ground-shaking motion for a given magnitude earthquake by an appropriate parameter which is represented under form of maps. Thus, hazard assessment involves

studies of historical data, skilled interpretations of existing topographical and geological maps.

In order to perform a macro-seismic hazard assessment, two universally methods have been defined: the *Deterministic Seismic Hazard Assessment* (DSHA) and the *Probabilistic Seismic Hazard Assessment* (PSHA). From these two methods, other two approaches are derived: the *mixed* approach and the so-called *of site* one.

The DSHA represent the earliest approach taken for seismic hazard analysis, which takes its origin from nuclear power industry applications. This approach attempts to determine a maximum credible intensity of ground-motion at a given site through estimation of a maximum credible earthquake likely to take place in the proximity of that site (Suckale et al., 2005). In fact, the method is based on the assumption of an earthquake scenario of a particular location, by considering several seismograms and a source synthetic ground motion generation model.

In particular, the methodology is articulated into four steps.

The first step is the identification and characterization of all sources by providing an exhaustive documentation of the seismic history of the selected site, related to the geological faults, the magnitude of the maximum historical earthquakes and their distance from the site. The information can be acquired referring to specific data source, such as earthquake catalogues or seismo-tectonic studies. In general, the territory is divided with cells in order to define a grid. The centre of each cell is constituted by a seismogenetic source, where the maximum magnitude observed in the epicentre area and the distance from the studied region are fixed. The second step is the selection of the source-site distance parameter, generally assumed in order to represent the most unfavourable situation, the so-called worst scenario. The third step is the selection of a “controlling earthquake”, calculating by using an attenuation relationship enabling to estimate the ground shaking within the area of interest. Finally, the hazard can be defined as the maximum expected value on the assumption that the catalogues maximum magnitude is a representation of the maximum possible earthquake.

The PSHA aims to quantify the probability of exceeding various ground-motion levels at a site by the identification of all the possible earthquakes that could affect the site. According to this approach, indeed, the seismic hazard $H(A)$ is defined as the annual rate of earthquakes that produce a ground-motion amplitude (a) exceeding the expectation (A) at a specific site. The random variable (a) may generally represent an arbitrary hazard-relevant quantity describing the ground shaking, as for example the Peak Ground Acceleration (PGA).

The probabilistic methodology is based on the Cornell (1968) and McGuire (1976) original formulation, and represents the most widely used approach to the

problem of determining the characteristic of strong ground motion for engineering design. On the basis of this approach, the overall hazard is composed of the respective contribution $H_i(A)$ from each source zone (i) out of the set of zones (I). Thus, the seismic hazard is evaluated for each zone separately and then summed over, according to the below total-probability theorem:

$$H(A) = \sum_{i \in I} H_i(A) = \sum_{i \in I} v_i \int_{m_{\min}}^{m_{\max}} \int_{r_{\min}}^{r_{\max}} P(a > A | m, r) f_{(R_i|M_i)}(r|m) f_{M_i} dr dm \quad (1.5)$$

where

- v_i is the annual rate of earthquakes with a magnitude higher than a yet to be specified threshold value M_{\min} in the zone i ;
- f_{M_i} and $f_{(R_i|M_i)}(r|m)$ are the probability density functions on magnitude and distance
- $P(a > A | m, r)$ is the probability that the expectation A of the ground acceleration is exceeded under the condition that an earthquake of magnitude m occurred at distance r .

Throughout this analysis, the seismicity is evaluated according to a Poisson process, as follows:

$$P(K = k, \Delta t) = \frac{\lambda^k}{k!} \cdot \exp(-\lambda) \quad (1.6)$$

where $P(K = k)$ is the probability that k events occur during a time interval Δt and λ the expectation of the number of earthquakes in Δt .

The seismicity of the examined area can be characterised in terms of a magnitude M and the number of earthquake correlation. In fact, in case of a sufficient number of historical data about earthquake in the zone, the magnitude is related to seismic frequency through the equation below:

$$\log n = a - b \cdot M \quad (1.7)$$

where a and b are the parameters depending on both the zone and the time interval and n is the annual frequency for the magnitude M (Tomazevic, 1999). Considering that probability of the occurrence of the event P_T in a given time period Δt is expressed as follows:

$$P_T = 1 - P(0) \quad (1.8)$$

and assuming the Poisson distribution, the defined probabilistic hazard is obtained by assessing the probability of an earthquake with a magnitude M to be overcome during a period of time Δt , given by:

$$P_T = 1 - \exp^{-\lambda} \quad (1.9)$$

Both probabilistic and deterministic methods have a role in seismic hazard and risk analyses performed for decision-making purposes. These two methods can complement each other to provide additional insights to the seismic hazard or risk problem. One method will have priority over the other, depending on the seismic environment and on the scope of the assessment.

In general, probabilistic methods can be viewed as inclusive of all deterministic events with a finite probability of occurrence. In this context, proper deterministic methods that focus on a single earthquake ensure that event is realistic, i.e. that has a finite probability of occurrence.

This two specific analyses may be complementary deterministic events and can be checked with a probabilistic analysis to ensure that the event is realistic (and reasonably probable). Moreover, probabilistic analyses can be checked with deterministic events to see that rational and realistic hypotheses of concern have been included in the analyses.

1.3.3. Exposure

Exposure evaluation aims to measure the level of assets, population and resources within a region exposed to a catastrophic event. In fact, an earthquake in a densely populated area, which results in many deaths and considerable damage, may have the same magnitude as a shock in a remote area that does nothing more than frighten the wildlife. Large-magnitude earthquakes that occur beneath the oceans may not even be felt by humans.

Therefore, an exposure analysis is performed by considering the built environment, the demographics and the environmental uses of the examined zone.

An exposure assessment is achieved by means of an inventory of the elements at risk, consisting of a wide range of things, such as people and their economic activities, their jobs, equipment, crops and livestock, the houses, the roads and the community services. These elements are not easily aggregated and have to be treated as a number of separate categories, having a different importance or value. For this reason, firstly it is necessary to establish a classification criterion for buildings and other facilities, in order to define an inventory of the resources within the interest zone.

Referring to the building category, the classification system depends on the scope for which it is established. On one hand the classification criterion groups together the constructions that would be expected to present a similar seismic behaviour.

According to vulnerability assessment, buildings have been usually classified by means of the development of some vulnerability classes, selected on the basis of the used vulnerability model.

On the other hand, it is necessary to take into account the building use and the relative social function. Therefore, an occupational classification system is employed, in order to take into account for the influence of occupancy upon the internal layout of the building. In this sense, a classification has been proposed in Table 1.5 by the RISK- UE project, whose research activity, together with an efficient vulnerability assessment method, will be fully described in Chapter 3.

Table 1.5 Classification proposed by RISK-UE project

General building stock	Essential facilities
Residential	Government functions and civil defence
Commercial	Health and medical care
Cultural	Emergency response
Multiple use	Education facilities
Monuments and historical Heritage	
Religion	
Industrial	
Agricultural	
Temporary buildings	

Once defined the classification criterion and identified the consistence of the social and built environment, the inventory may be developed, by enumerating the buildings and facilities in each of the typology defined with the assumed classification system.

Since the cost and the time necessary to perform the inventory are high, the objective of the analysis have to be defined. The inventories, indeed, can have different detail threshold and they can be achieved at regional level or on the single building scale.

In developing a regional inventory, the knowledge has to be intended in a statistical sense, assuming a determined area as the analysis unit. From this viewpoint, the availability of data to be collected is subordinate to all the available possible sources, as database belonging to state, regional local and private sectors. It is worth to precise that these data often are overlapping and incomplete and, in the most cases, they not include information about structural

characteristics. Thus, the inventory techniques must be supported by expert judgments coupled with limited field reconnaissance.

A single building inventory, instead, is required when particular exigencies are requested, such as in case of historical centres of cities, having a particular cultural and historical value, or in case of overcrowded areas, characterized by high exposure. According to this type of inventory, each construction should be identified individually. Many procedures exist to survey in a quick way all the buildings of given zone (GNDT I and II, 1994, FEMA154, 1988) in order to make a vulnerability assessment analysis. A large part of the present study is dedicated to this in-situ activity, as deeply illustrated in Chapter 3.

1.3.4. Vulnerability

The vulnerability of a built system is its susceptibility to be damaged by a catastrophic event. In particular, the seismic vulnerability for a building represents its propensity to suffer a certain damage level if subjected to an earthquake.

Dealing with the definition of Sandi (1986), the vulnerability of a building is a behavioural character described by a cause - effect law in which the cause is the earthquake and the effect is the damage.

In order to have a correct and reliable vulnerability measure, it is necessary to select the right parameters to express cause and effect. Depending on the methodology employed, earthquake is generally measured in terms of macro-seismic intensity, acceleration or displacement. The possible damage parameters are, instead, economic estimates of the reconstruction costs, with respect to the costs of the construction of a similar new building, values corresponding to arbitrary damage states, mechanical parameters of numerical structure models and so on.

A vulnerability evaluation method aims to provide a measure of the possible damage level of a construction in case of occurrence of a calamitous event, by giving in most cases the so-called vulnerability index. In particular, the current method must correlate the seismic hazard evaluation to the physical damage suffered by the buildings.

Several methods for the vulnerability assessment have been developed and proposed in the recent years, in order to evaluate and reduce the propensity to the damage of the classes of building defined on the basis of a proper classification system.

In fact, the vulnerability of a built system depends especially on the type of construction and on its geometrical and structural features. To this purpose, the

buildings are usually grouped in terms of vulnerability classes, through various classification criterion (see par. 3.3.2.5).

In particular, the classes employed by the MKS scale are:

1. Class A: buildings with dry stone, or clay, adobe or mud walls;
2. Class B: buildings with walls made from brick, mortar blocks, masonry and mortar, stone block, timber frame;
3. Class C: buildings with metal structure or reinforced concrete.

A similar example of approximate classification of building types has been developed in Turkey (Coburn et al., 1994). This criterion identifies three building categories, as follows:

1. Type A: Rubble and adobe walls;
2. Type B: Brick and timber walls;
3. Type C: Reinforced concrete frame.

Different classification systems have been elaborated, due to the necessity of a deep diversification of the structural behaviour of the constructions under horizontal and exceptional loading condition.

In America, the ATC 13 classification is commonly used, it being developed on the basis of the one proposed by Steinbrugge in 1984, in which about 21 building typologies were identified.

The HAZUS (1999) and EMS-98 (Grunthal, 1998) classification systems, instead, introduce some subcategories, in order to be representative of the diversification of in the built environment of a specified territory. With reference to these latter building classification systems, in Table 1.6 it can be noted that unreinforced masonry, reinforced or confined masonry, reinforced concrete, steel and wood buildings are taken into account by both of them, while pre-cast buildings and mobile homes are provided only by the HAZUS system. Furthermore, the HAZUS classification presents a building subdivisions on the basis of three height classes, distinguished each other by the number of floors. In addition, a further classification of each structural system is provided with reference to four code level: high-code, moderate-code, low-code and pre-code.

Table 1.6 EMS 98 vs HAZUS building typology classification

EMS 98	HAZUS
Unreinforced masonry Rubble stone Adobe (earth brick) Simple stone Massive stone U Masonry (old brick) U Masonry – r.c. floors	Masonry typologies Unreinforced Masonry Bearing Walls
Reinforced/ confined masonry Reinforced/ confined masonry	Reinforced/ confined masonry RM Bearing walls with wood or metal deck diaphragms RM Bearing walls with precast concrete diaphragms
Reinforced concrete Frame in reinforced concrete Shear wall	Reinforced concrete Concrete Moment Frame Concrete Shear Walls Concrete Frame with U. Masonry Infill Walls
Steel typologies Steel structures	Steel typologies Steel Moment Frame Low-Rise Steel Braced Frame Steel Light Frame Steel Frame with Cast-in-Place Concrete Shear Walls Steel Frame with Unreinforced Masonry Infill Walls
Timber typologies Timber structures	Timber typologies Wood, Light frame Wood, Commercial and Industrial
	Pre-Cast typologies Precast Concrete Tilt-Up Walls Precast Concrete Frames with Concrete Shear Walls
	Mobile Homes

An innovative classification has been also proposed by Giovinazzi (2005), it being different from the one adopted by EMS-98 and HAZUS. This way to classify the structures has been originated from the consciousness that the HAZUS classification is representative of American built environment, while the EMS-98 classification is particularly referenced to masonry constructions, with a poor consideration of other constructive materials. The Giovinazzi proposal for the European building typology classification is shown in Table 1.7.

Table 1.7 The Giovinazzi's proposal for European building typology classification

Class	Building Typology
	Unreinforced Masonry
M1	Rubble Stone
M2	Adobe (earth brick)
M3	Simple stone
M4	Massive stone
M5	U Masonry (old brick)
M6	U Masonry –RC. floors
	Reinforced/ confined masonry
M7	Reinforced/ confined masonry
	Reinforced concrete
RC1	Concrete Moment Frame
RC2	Concrete Shear Walls
RC3	Dual System
S	Steel
W	Timber

1.4. RISK MANAGEMENT AND TOOLS

A risk management involves specific planning, practices of mitigation before earthquakes and provision of critical and timely information to improve response of the society after the calamitous event. Therefore, a specific program for risk reduction could be developed in order to reduce the losses in terms of human life and built up. An approach aimed at the reduction of the catastrophic impact in densely populated areas may be carried out by means of constant security measurements and monitoring of some environmental factors. In fact, a calamitous event is generally preceded by accumulation of tension and deteriorating rocks, that can give a warning signal. Also a sudden drop in water level ground or the increase of concentrations of rare gases in groundwater can characterize the period immediately prior to the seismic event.

However, even if some events could be predicted, it is necessary to set up appropriate strategies in order to manage and reduce the risk.

To this purpose, different analytical approaches are commonly employed, they including scenario mapping, potential loss studies and annualized risk mapping.

A scenario mapping is developed on the basis of a single hazard occurrence and is often used to estimate the resources likely to be needed to handle the reference emergency.

Instead, the potential loss studies indicate the effects of an expected and probable hazard across a region or country and shows the location of zone which should be priorities for loss-reduction programs.

Finally, the annualized risk mapping represents a calculation of the probable levels of losses occurring from all levels of hazards over a period of time. The probability of each level of hazard occurring within that unit time period is combined with the consequences of that hazard level to generate the expected loss within that time. Summing up the losses over all levels of hazard, the total losses expected with time are given (Coburn et al., 1994).

In the framework of the risk management, the GIS (Geographic Information System) represents, nowadays, a suitable instrument for multi-disciplinary studies and for the scenario or risk analysis performance. In fact, the GIS system permits to cross different kind of data and verify, from many points of view, the effects deriving from specific territorial phenomena. In particular, a GIS allows to computerize capture, store, analyse, manage and show data linked to a specific zone by means the use of the personal computer. Moreover, in the emergency management, the GIS approach is a strategic support for development of analyses, studies and procedures for the evaluation of urban and territorial risks. Indeed, throughout a GIS employment, it is possible to control various and complex aspects of large territories and to develop a complete seismic risk analysis by means of the interaction of hazard estimation, exposure identification and vulnerability assessment.

In particular, GIS is useful for scenario and risk analysis. In fact, in the first case, a deterministic analysis can be achieved by means of the simulation of a specific catastrophic event recorded in the seismic catalogues in order to identify all the possible damaged structures and the most vulnerable buildings for the model adopted. More in detail, it is possible to determine the strategic structures present on the territory and all the possible alternative roots and available networks so that, in this way, the risk management is aided.

On the other hand, for risk analysis, a probabilistic approach can be used by means of the calculation of the probable losses occurring from all levels of hazards during a period of time. In this case, all the possible damages for structures and infrastructures are identified for all the probable events which may occur in the period of time considered.

The analysis may be performed by using various detail levels: from country or state level to addresses, municipalities or postcodes. In general, the level of detail depend on the type of analysis to be performed. For example, data of medium quality are available at the municipalities scales, in order to produce quite realistic analyses for seismic risk. A fine data detail, instead, means that information are provided by individual buildings in order to work on the small scale.

Also, GIS is a suitable tool for the seismic and volcanic vulnerability assessment, for the hazard and exposure level estimation, for the expected damage grade

representation. In this work, the potentialities of GIS have been extensively proved in developing vulnerability and damage analyses of a historical centre, as it will be shown in Chapter 3.

1.5. THE SEISMIC RISK IN ITALY: MICROZONATION, GUIDELINES AND MITIGATION PROJECTS

Seismic risk in Italy is very high, especially in terms of exposure. In fact, according to UNESCO, Italy hosts a large part of the known cultural but up heritage of the World. This important aspect may be highlighted, as an example, by the damages of the frescoed vault of the San Francesco basilica in Assisi during the 1997 Umbria-Marche seismic event or of the S. Bernardino Church during the recent L'Aquila seismic event (2009).

The seismic Italian history is long and tragic, since past earthquake have left a strong imprint on the country landscape and traditions. In fact, in the past years, several strong seismic events have occurred in Italian regions, each one recorded in a specific catalogue, in which the phenomenon effects were not described in a scientific way.

After the Benevento seism of 1688, the seismic catalogue become more detailed, although the first catalogue used as scientific tool was implemented during the 19th century. Referring to these catalogues, it is possible to partially predict a disastrous event, by observing the regularity and the characteristics of some phenomena (Valensise et al., 2003).

After the Friuli and Irpinia catastrophic earthquakes occurred in 1976 and 1980, respectively, the research into historical seismicity has become a national priority. In particular, the seismic design conception was significantly changed and new technical codes were developed in order to sensitize the designers awareness of the issue.

The 1990s brought another revolution in the task of retrieving, analyzing and storing historical earthquake data. Some techniques were carried out in order to forecast an earthquake and plan opportune countermeasures for the risk reduction. The main studies concern especially the characteristics and the nature of the faults, the surface of ruptures, the impact on the environment, the frequency of various phenomena and the monitoring of volcano activities.

Nowadays, Italian modern seismological instrumentation allows to identify the location and depth of the focus, the source size, the faulting mechanism and details of the fracture process. Tens of thousands of earthquakes having magnitudes between 1.5 and 6.0 have been recorded.

This study activities are useful to identify the areas in which a seismic event could occur and the related intensity. This identification is noted as seismic classification or microzonation of the territory and it is adopted by the Nations by means of specific regulations.

The first valid seismic classification was achieved in 1980. According to this classification, the 45% of the Italian territory was considered as a seismic zone.

Recently, the OPCM 3274 (2003) subdivided Italy into four homogeneous zones, each one characterized by the following different values of a_g (horizontal maximum acceleration on a rock ground):

- Zone 1: $a_g = 0.35 g$
- Zone 2: $a_g = 0.25 g$
- Zone 3: $a_g = 0.15 g$
- Zone 4: $a_g = 0.05 g$

where g is the gravity acceleration, equal to $9.81 \text{ m}\cdot\text{s}^{-2}$.

Dealing with this classification, the 67% of the whole national territory was identified as a high seismicity zone (Figure 1.6).

The in force New Technical Italian Code (M.D. 2008) subdivides the Italian territory into cells in order to define a grid. Each square cell has a length of 5 km and is identified by univocal geographic coordinates (longitude and latitude). The seismic parameters corresponding to each cell allows to determine the seismicity level in the corresponding zone. Thus, the seismicity is precisely detected by uniquely referring to the geographic coordinates.

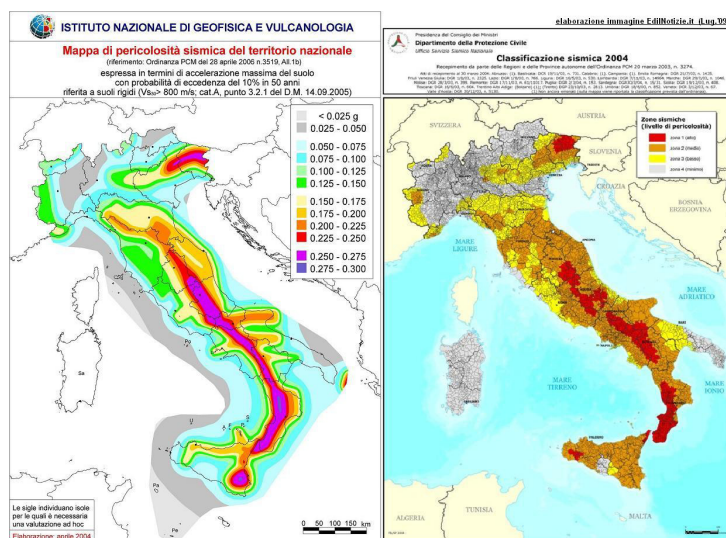


Figure 1.6 Microzonation according to OPCM 3274

Other instruments for the mitigation of the seismic risk are constituted by the various guidelines enacted on either the Regional or National scale. In general, guidelines offer rules aiming to evaluate the seismic vulnerability of buildings by means of simplified methods. In the framework of this Ph.d thesis, a specific reference to “*Guidelines for the evaluation and reduction of the seismic risk of the cultural heritage referring to the Constructions Technical Code*” (in Italian, “*Linee Guida per la valutazione e riduzione del rischio sismico del patrimonio culturale con riferimento alle norme tecniche per le costruzioni*”) will be made in the Chapter 4.

In the framing of the issue of the seismic risk in Italy, it is worth to mention some of the several research projects and programs implemented for seismic risk reduction. For instance, in 1999, the Italian Civil Protection Department planned a seismic protection and retrofitting program for the Italian historical centres and required the scientific community support in order to establish intervention priorities.

The scientific approach was aimed at the determination of the rates of non-destructive earthquakes, limiting the maximum credible magnitude over extended regions and providing probabilistic estimates of the expected ground motion. Although this method was based on the combined contribution of historical and instrumental seismicity, geodesy, geology and tectonic data, it was quite problematic to anticipate the location and the size of future large earthquakes or to evaluate the characteristics of the associated ground shaking

An important research project for the risk management in Italy was also developed by GNDT (*National Group for Defence from Earthquakes*, in Italian: *Gruppo Nazionale per la Difesa dai Terremoti*) funded in 2000 by the Italian Civil Protection (<http://gndt.ingv.it>). The project, entitled “*Probable earthquakes in Italy 2000–2030: guidelines for determining priorities in seismic risk mitigation*”, was aimed at the identification of the priority areas requiring seismic risk mitigation. The studies included faults detection and characterization with different tools, evaluation of seismic and geodetic strains, study of the propagation and attenuation of the seismic waves. In particular, a time-dependent hazard estimation tools incorporating innovative information on fault behaviour and earthquake recurrence was developed. To this purpose, it was significant the role of different tools, as the historical catalogues, the seismic instrumentation and the GIS-supported database.

New sources were added or improved during the GNDT project, particularly in poorly documented and strategic areas of the country.

Chapter 2

Masonry structures

2.1. INTRODUCTION

Masonry represents the oldest techniques that still finds wide use in today's building industries. Although the technique of assembling bricks and blocks are essentially the same as the ones developed some thousand years ago, innumerable variations in masonry materials, in constructive systems and in the several applications occurred during the course of time.

The main aspects that have influenced the evolution of masonry construction are the local cultures and wealth, the knowledge of materials and tools, the availability of the base components and the architectural reasons. The spread of this constructive system is, substantially, related to the simplicity of the technique, consisting in the assembling of pieces of stone or bricks on top of each other, either with or without cohesion via mortar, and to aesthetics reasons, solidity, durability and low maintenance, sound absorption and fire protection.

Nowadays, the role of masonry material has become less important due to the development of other modern technologies and to the progressive adoption of the other structural materials, as concrete and steel.

The underlying reason is the lack of insight and models for the complex behaviour of units, mortar, joints and masonry as a composite material. So, the material modelling represents a very problematic issue related to the knowledge of the material, which may be acquired by means of experimental tests, whereas possible. Only a complete material description allows the full knowledge and understanding of the material behaviour.

The material characterization has also huge importance when the use of accurate numerical models is intended. Numerical tools may only give realistic results if

adequate experimental data are available; this represents a very crucial points, especially for historic buildings.

Therefore, the above considerations confirm the importance and the interest of this research field.

2.2. HISTORICAL REMARKS

In the Early History of Mankind, three stages may be recognized: the *Stone Age*, the *Bronze Age* and the *Iron Age*. During these periods, livelihood came from hunting, fishing and food gathering, while the first form of habitation consisted into caverns.

The dawning of civilization began about 10,000 years ago, when the first human communities started. The first habitations were crystallized into houses of stone, clay or timber: dry-stone circular and semisubterranean huts represent the earliest examples of the first permanent stone masonry houses found in near Lake Hullen, (Israel) date back to 9000-8000 BC.

As tools became available and skills developed, stone units were shaped in regular forms. The first bricks were made of mud or clay, shaped to form bricks and dried by the sun. The bricks were then laid with mud mortar into walls. This simple process has been widely used for millennia to construct dwellings, particularly in the valleys of the Mesopotamia and Nile.

During the *Mesopotamian Age* (6000 BC) masonry buildings were constructed from any available material at hand. The Mesopotamians used bricks, made from alluvial deposits of the nearby River Euphrates and Tigris to build their cities beside these two rivers.

During the *Egyptian Age*, the pyramids were built, they representing the first typical example of stone monuments. Apart from the architectural value, their structural behaviour did not present any particular problem, as the inner space was limited and the stresses were low and perfectly compatible with the material strength. The most famous pyramids are undoubtedly the *Egyptian Pyramids at Giza* (Fig. 2.1). In particular, the *Cheope Great Pyramid* is the only survivors of the Seven Wonders of the World and remained the tallest structure in the world until the 20th century.

In general, in Egypt from pre-dynastic times (5000 BC) until the Roman occupation (AD 50) the main material for building houses was sun dried brick, commonly made of Nile mud. In particular, the pure mud was shrunk over 30% in the drying process, but the addition of chopped straw and sand to the mud prevented the formation of cracks.



Figure 2.1 Egyptian pyramids at Giza (2800-2000 BC)

Probably, in the 3rd millenium BC started the practice of burning bricks. This technique, almost certainly, was generated by the observation that the brick near a cooking fire or the brick remaining after a thatch roof burnt seemed to be stronger and more durable than the adobe one.

The earliest recorded reference to burnt brick is a papyrus of the 19th Dynasty in Egypt (1300 BC), but the most famous reference is found in the Bible, Genesis XI, 3-4, when the inhabitants of Babylonia “said to one another ‘Come, let us make bricks and bake them’. They used brick for stone and bitumen for mortar. Then they said ‘Let us build ourselves a city and tower with its top in the heavens’”. They probably built the first ever skyscraper as it is estimated that the 17th level of the Tower of Babel.

In Thebes, the capital of the Upper Egypt, was discovered a wall painting in the tomb of Rekhmara (1500 BC) showing the various stages involved in the manufacture of mud-bricks (Fig. 2.2) (Fields et al., 2004).



Figure 2.2 Brick making in Egypt, as depicted in a wall painting in the tomb of Rekhmara at Thebes (1500 BC).

With time, the structural typology evolved. The *Lion Gate* at Mycenae, Greece (13th century B.C.), which spanned about 3 m and weighed between 25 and 30 tons, shows the beginning of the arched behaviour that would dominate the following millennium.

During the classical period, columns and the corresponding capitals rose were the most distinctive elements of the temples. In this type of construction, the reduced distance between the columns was mostly a structural need. In fact, spanning large distances could not be achieved because it was difficult to transport large stone blocks and at the same time stone has a rather low tensile strength.

Greek temples were aesthetically perfect and based on strict rules of proportion and symmetry between the different elements, which represented an important milestone in the history of buildings. Limestone was usually the stone used to build structural elements as walls, columns and beams. The most famous temple was the *Parthenon* built in the 5th century B.C. (Fig. 2.3).



Figure 2.3 The Parthenon at Athens

Other significant architectures were the *Roman* and *Romanesque* ones (AD 0-1200), with their temples, columns, churches, bridges, roads and aqueducts. *Romans* introduced many innovations directly related to materials, structural concepts and constructive processes.

In fact, the large and centralized Empire fulfilled the conditions to the wide spread of brick. There were many kinds of clayey materials suitable for making bricks and tiles readily available in all the areas of the *Roman Empire* and the desire to obtain domination and homogenization of architecture and building techniques made the rest. The size of bricks became more standardized: different shapes were manufactured for special purposes, and seals, trademarks or decorative motifs began to be impressed in the brick.

During the *Roman period*, also innovative techniques were introduced in the construction of walls, using bricks or stones as facing, finely finished, and filling the inner space with concrete (Fig. 2.4).

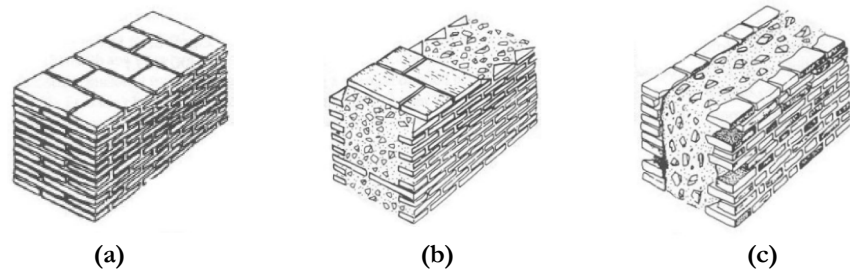


Figure 2.4 Roman masonry walls: (a) bonded brick wall; (b) brick faced wall with header courses; (c) brick faced wall (Drysdale et al., 1999)

The technique of dry stone block was also greatly improved and remarkable structures were built, such as the *Colosseum* (1st century A.D., Fig. 2.5.a) and *Segovia's aqueduct* (1st century A.D., 2.5b), represented.



Figure 2.5 Dry stone constructions: (a) Colosseum; (b) Segovia's aqueduct

Another noteworthy structural advance was the change from linear to arched or curved structures, i.e. arches and vaults. In curved elements, it is common to find only compressive stresses in a given section, therefore no tensile resistant materials are needed, so that masonry represents a very suitable material. Exploiting the structural form of the arch, the Romans constructed magnificent bridges and aqueducts all over their Empire.

The fall of the Roman Empire caused an anonymous period in western architecture and it is only from the 11th century on that structural advances were made with the use of semicircular arches and barrel vaults. Churches and castles were marked by the presence of masonry towers.

During the *Gothic period* (AD 1200-1600) the art of cutting stone reached the maximum splendour. In fact, Gothic architecture represents the step forward

where both architectural and structural functions were extraordinarily integrated together. The main aspects of the Gothic architecture are: the incorporation of the arch ribs into roof structures, so that the thickness of the masonry spanning between the ribs was reduced; the substitution of the semicircular arch by a pointed arch allowed a further reduction in weight; the substitution of the heavy supporting walls running across the thrust lines by flying buttresses and towers more aligned with the thrusts. These further developments of this constructive techniques have led to the masonry-framed structures based on linear elements working in compression. Cathedrals were the most meaningful Gothic structures (Fig. 2.6).



(a)



(b)

Figure 2.6 Famous Gothic Cathedrals: (a) Amiens; (b) Beauvais

During the *Renaissance period*, born in Florence (Italy), new concepts of form and proportions were conceived, they consisting in regular forms and geometrical symmetry in plan and elevation. Churches, and in particular domes, are of great structural interest, e.g. the church of *St. Maria del Fiore* in Florence (15th century, Fig. 2.7). The dome of this church, designed by the Italian Architect Filippo Brunelleschi, was characterized by the use of main ribs and by the construction of two shells connected between them by these ribs.



Figure 2.7 Church of St. Maria del Fiore, Florence

Following the Renaissance, the *Baroque* period did not bring relevant or innovative solutions concerning the structural conception.

The *Industrial Revolution* represents a milestone in the history of the masonry constructions (18th and 19th centuries). In fact, the traditional handwork and manufacturing procedures were replaced by the use of the machineries. The turning point of the brick industry came, finally, in 1858 with the introduction of the Hoffman kiln which enabled all the stages of firing to be carried out concurrently and continuously. Since then, further research and developments led to the creation of efficient brick making industries.

Nowadays, in the building industry, it is possible to find units of different materials and shapes, different types of mortar and different techniques.

Presently, however, masonry constructions seems have lost its fundamental role in the building trade because the material is heavy and expensive. In the last few centuries other more light and economical materials have taken hold in the building industry. In particular, reinforced concrete and steel can be used for several structural applications because they are more competitive, while stone material is commonly used as facings.

2.3. THE CONSTRUCTIVE SYSTEM

2.3.1. General remarks

The low tensile strength is the main reason for which masonry material is normally used for components subjected to compressive loads as load-bearing walls, arches, columns, vaults and domes. History has demonstrated as this mechanical characteristics has determined the shape of the ancient constructions. Nowadays, buildings are the most diffused and important masonry constructions. In particular, three main typologies may be identified (Augenti, 2004):

1. *First class buildings*: constructions made only of masonry (oldest buildings).
2. *Second class buildings*: constructions made with vertical masonry box supporting horizontal slabs made with beams of different material and not connected with masonry in the edge points.
3. *Third class buildings*: constructions made with vertical and horizontal components well connected each other.

In the first case the horizontal floors are realized with arches and vaults that push horizontally the vertical walls, which support gravity loads and the horizontal forces generated by arches.

In the second case, instead, each wall is disconnected from the adjacent one, because rigid horizontal slabs do not exist. The external walls are usually not stable because the section reduction is done only on the internal side for aesthetic reasons. This generates eccentricity on the gravity loads and a tendency on the external walls to overturn toward the exterior side.

Finally, the third type of buildings presents an horizontal RC ring beam at each floor slab, it avoiding the relative displacement between the vertical walls and the floor slab.

2.3.2. Main typologies of masonry

A masonry structural wall is an assemblage of units laid in a specified pattern and joined together with or without mortar. Horizontal and vertical joints are called bed and head or perpend joint, respectively. Units can be stone or concrete bricks, blocks, ashlar, adobes, irregular stones and others types available in a large number of size, while mortar can be made of clay, bitumen, chalk, lime-cement, glue or other. In particular, the European Code EC6 (CEN, 2005a) defines the following structural walls typologies:

- 1 *single-leaf wall* (Figure 2.8a), which is a solid wall without a cavity or continuous vertical joint in its plain;

- 2 *double-leaf wall* (Figure 2.8b), which is a solid wall consisting of a two parallel leaves with the longitudinal joint between filled solidly with mortar and securely tied together with wall ties so as to achieve common action under vertical and horizontal loading condition;
- 3 *cavity wall* (Figure 2.8c), consisting of two parallel single-leaf walls, effectively tied together with wall ties or bed joint reinforcement increasing the global stiffness. The space between the leaves is left as a continuous cavity or filled or partially filled with non-load-bearing thermal or acoustic insulating material;
- 4 *grouted cavity wall*, consisting of two parallel leaves with the cavity filled with concrete or grout and securely tied together with wall ties or bed joint reinforcement so as to result in common action under load.

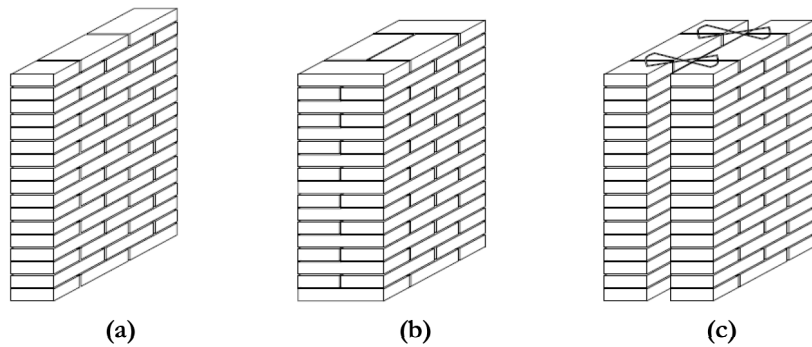


Figure 2.8 Different types of structural masonry walls:
(a) single-leaf wall; (b) double-leaf wall; (c) cavity wall

Although there are no restriction about the use of any wall typologies in EC6, the employment of single-leaf walls should be preferred to double-leaf ones in seismic areas, since they ensure a monolithic behaviour under horizontal loads.

Both traditional and engineered types of masonry construction systems are used in several countries. In general, the following main typologies of techniques can be distinguished:

- *unreinforced masonry*, consisting of units joined with mortar;
- *reinforced masonry*, consisting of units, mortars, reinforcing steel and concrete infill;
- *confined masonry*, consisting of units, mortars and r.c. frame;
- *pre-stressed masonry*, in which internal compressive stresses are introduced in order to eliminate the tensile stresses.

Unreinforced masonry represents the traditional and the most diffused masonry construction system bonded together by intermediate layers of mortar or simply for friction (dry masonry).

In general, an unreinforced masonry wall can be made of natural stones or artificial elements.

In case of walling made of stone, two main typologies exist: rubble and ashlar walls (McKenzie, 2001). Rubble walls (Fig. 2.9a), generally, consist of irregular quarried stones, in which the variation of the stone size results in laps of differing random lengths. Transverse bonding through the wall thickness is normally achieved by using larger stones called bonders, while the space between the stones is filled with small pieces of stone.

Ashlar walls (Fig. 2.9b, 2.9c), are, instead, built with squared stone blocks cut to sizes which correspond to a set number of brickwork courses.

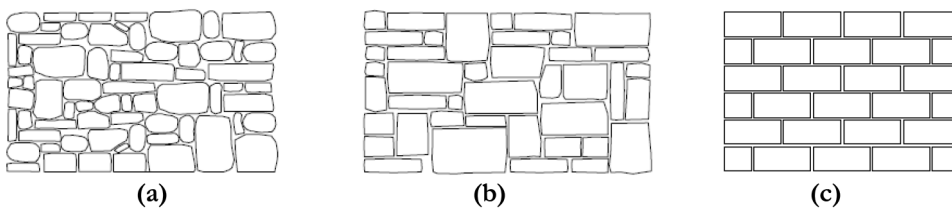


Figure 2.9 Different types of stone masonry:
(a) rubble masonry; (b) ashlar masonry; (c) coursed ashlar masonry

In case of walls made of bricks or blocks, the geometry, nature and arrangement of units produces a huge number of possible combination of masonry typologies, as solid, cavity and fin walls (Fig. 2.10).

Solid walls can be built of any thickness according to the technical codes. Due to architectural reasons, a solid wall can be a faced wall or a veneered one. A faced wall comprises two different kinds of structural unit bonded together to form a solid wall, in which the global strength is based on the full width and on the weaker of the units used. A veneering wall is, instead, covered by a not load-bearing veneer facing, tied to the effective structural wall.

An unreinforced cavity wall is commonly built as exterior wall of a construction in order to resist both vertical and lateral actions, while a fin wall is essentially a wall stiffened through masonry piers in order to increase the bending and shear resistance.

Reinforced masonry represents a construction system in which the tensile resistance is increased by means the insertion of additional element, as wooden or steel reinforcement. In general, a reinforced masonry typology consists of

hollow blocks in which steel bars are vertically and horizontally introduced. Despite being introduced during the XIX century, the use of steel to enhance the strength of brickwork has not been researched and developed extensively as with concrete.

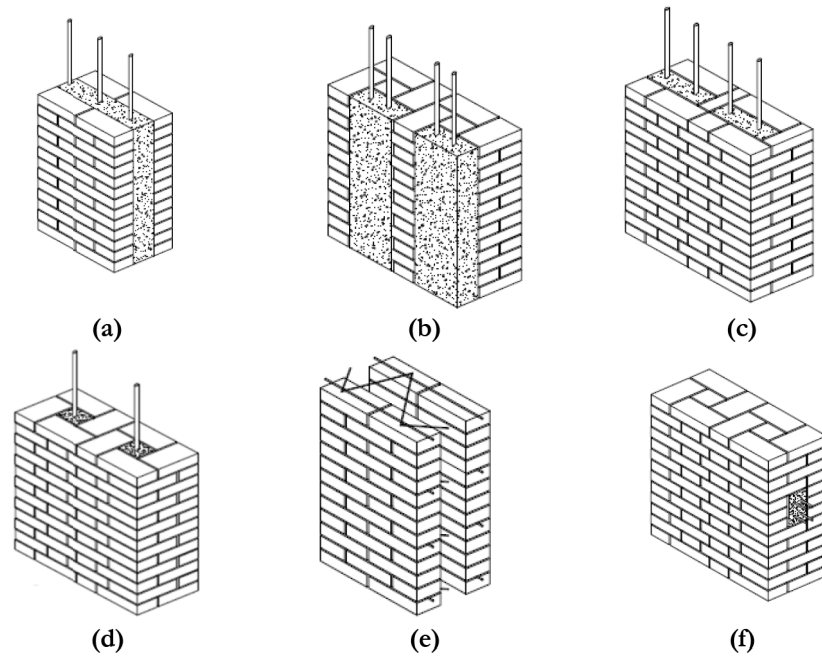
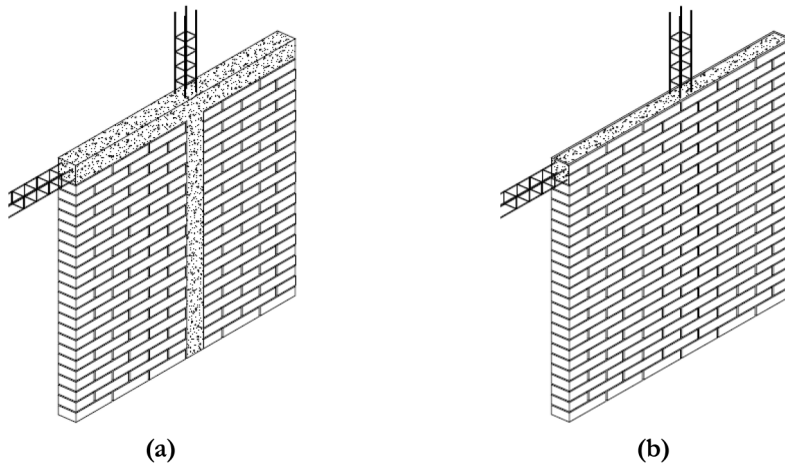


Figure 2.10 Different kinds of reinforced masonry: (a) cavity wall; (b) pocket wall; (c) rat-trap bond; (d) quetta bond; (e) bed reinforcement; (f) reinforced beam

Confined masonry (Figure 2.11) is a construction system in which the all four sides of the masonry structural walls are confined with a RC frame or reinforced masonry vertical and horizontal confining elements, not designed to perform as a moment-resisting frame, but to increase the global stiffness of the structure. Finally, pre-stressed masonry is based on the well known principles established and widely used for concrete industry.



**Figure 2.11 Masonry confined within: (a) reinforced concrete frame;
(b) reinforced masonry**

For the various aspects involved in the construction, masonry represents a structural system or a composite material, in which the mechanical properties depend on the base component characteristics. In fact, whether steel, aluminium and plastic materials are analysed as homogeneous materials, due to their specific and recognizable mechanical properties, masonry is a very heterogeneous material.

Different variable factors may condition masonry design. On one hand, the different and various qualities of mortar and units have to be considered; on the other hand, the random variables of realization process play a significant role, as like the geometry of the units, the structural organization of the components, the different thickness of mortar joints. In other words, the structural behaviour of a masonry construction is heavily influenced by the following parameters (Augenti, 2004):

- 1 *Construction formality*: geometry and placing of the stone elements; filling of the joints at the head; ratio of the joint thickness and dimensions of the stone elements; placing hand crafty; dis-uniformity of the layers;
- 2 *Properties of the units*: compression and tension strength with uniaxial and pluriaxial stresses; elastic and shear moduli, Poisson coefficient, ductility and creep; water proof and superficial (roughness) characteristics; chemical agent resistance; volume variation for humidity, temperature and chemical reaction; weight, shape and holes dimensions.
- 3 *Properties of the mortar* such as: compression strength and behaviour under pluriaxial stresses; elasticity module, Poisson coefficient, ductility and

creep; adhesive force; workmanship, plasticity and capacity of detaining water.

In the last few years, the efficiency of masonry has significantly improved by several studies about higher allowable stresses involving refined possibilities of design. For this reason, the design of masonry and the research about the material properties and modelling is, nowadays, a task of civil engineering.

2.4. THE MATERIAL

2.4.1. The base components

The base components of a masonry structural system are units and mortar.

A unit is a preformed component intended for use in masonry construction (CEN, 2005a) and it can be made from natural stone or artificial concrete elements or bricks. The choice of a particular type of unit depends on technical needs, e.g. strength, durability, adhesion, fire resistance, thermal, acoustic and aesthetical properties.

Natural stones can be cut from different types of stone material as limestone, sandstone, marble, slate or granite and they are still used for the construction of masonry walls. According to the regulation in force, only the use of dimensioned stone units, i.e. squared stone elements with parallel horizontal faces, is allowed for the construction of masonry buildings in seismic areas. Traditional sack masonry made of uncoursed stones is not considered seismic resistant.

Artificial elements can be lightweight or normal weight clay or concrete units. Clay masonry units consist of clay, shale or similar naturally occurring earthy substances, water and additives; most clays are composed mainly of silica and alumina of extremely small particle size formed by decomposition of rocks. The colour and the strength of clay elements generally depend on the chemical composition, surface treatment and burning intensity, and methods of burning control.

Three classes of concrete masonry units exist: normal, medium and lightweight, depending on the base materials. These types of elements are produced by mixing portland cement or blended cement, aggregate and water. In some cases, hydrated lime or pozzolans as air entraining agents can be added. Concrete elements are available in several sizes and shapes, as shown in Figure 2.12.

In general, elements can be distinguished as bricks or blocks on the basis of the volume. Furthermore, dealing with the Italian classification (M. D. 1987, M. D. 2008), artificial units can be distinguished as solid, perforated and hollow or

cellular referring to the volume of the holes expressed in percentage, as shown in Tables 2.1 and 2.2.

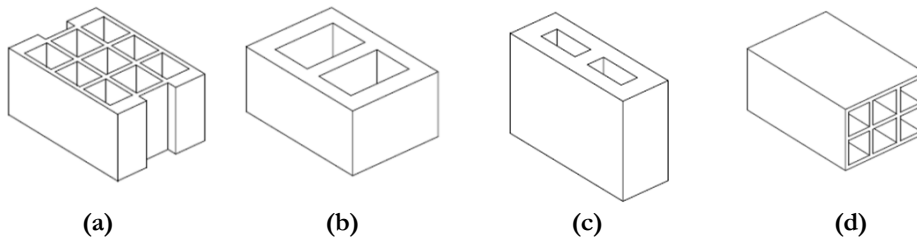


Figure 2.12 Different kinds of concrete masonry units:
(a) perforated unit; b) hollow unit; c) cellular unit; d) horizontally perforated unit

Table 2.1 Classification of clay elements

Element	Volume of all holes (% of the gross volume)	Gross area (f) of the section
Solid	$\Phi \leq 15\%$	$f \leq 9 \text{ cm}^2$
Perforated	$15\% \leq \Phi \leq 45\%$	$f \leq 12 \text{ cm}^2$
Hollow	$45\% \leq \Phi \leq 55\%$	$f \leq 15 \text{ cm}^2$

Table 2.2 Classification of concrete elements

Element	Volume of all holes (% of the gross volume)	Gross area (f) of the section	
		$A \leq 900 \text{ cm}^2$	$A > 900 \text{ cm}^2$
Solid	$\Phi \leq 15\%$	$f \leq 0.10 A$	$f \leq 0.15 A$
Perforated	$15\% \leq \Phi \leq 45\%$	$f \leq 0.10 A$	$f \leq 0.15 A$
Hollow	$45\% \leq \Phi \leq 55\%$	$f \leq 0.10 A$	$f \leq 0.15 A$

Referring to EC6 (CEN, 2005a), instead, six types of structural units are identified: clay units, calcium silicate units, aggregate concrete units (dense and lightweight aggregate), autoclaved aerate concrete units, manufactured stones units, dimensioned natural stone units. Moreover, masonry units are grouped in four groups: Group 1, Group 2, Group 3 and Group 4. The geometrical requirements for each groups are shown in Figure 2.13.

	Materials and limits for Masonry Units							
	Group 1 (all materials)	Units	Group 2		Group 3		Group 4	
			Vertical holes				Horizontal holes	
Volume of all holes (% of the gross volume)	≤ 25	clay	> 25; ≤ 55		≥ 25; ≤ 70		> 25; ≤ 70	
		calcium silicate	> 25; ≤ 55		not used		not used	
		concrete ^b	> 25; ≤ 60		> 25; ≤ 70		> 25; ≤ 50	
Volume of any hole (% of the gross volume)	≤ 12,5	clay	each of multiple holes ≤ 2 gripholes up to a total of 12,5		each of multiple holes ≤ 2 gripholes up to a total of 12,5		each of multiple holes ≤ 30	
		calcium silicate	each of multiple holes ≤ 15 gripholes up to a total of 30		not used		not used	
		concrete ^b	each of multiple holes ≤ 30 gripholes up to a total of 30		each of multiple holes ≤ 30 gripholes up to a total of 30		each of multiple holes ≤ 25	
Declared values of thickness of webs and shells (mm)	No requirement		web	shell	web	shell	web	shell
		clay	≥ 5	≥ 8	≥ 3	≥ 6	≥ 5	≥ 6
		calcium silicate	≥ 5	≥ 10	not used		not used	
		concrete ^b	≥ 15	≥ 18	≥ 15	≥ 15	≥ 20	≥ 20
Declared value of combined thickness ^a of webs and shells (% of the overall width)	No requirement	clay	≥ 16		≥ 12		≥ 12	
		calcium silicate	≥ 20		not used		not used	
		concrete ^b	≥ 18		≥ 15		≥ 45	
^a The combined thickness is the thickness of the webs and shells, measured horizontally in the relevant direction. The check is to be seen as a qualification test and need only be repeated in the case of principal changes to the design dimensions of units.								
^b In the case of conical holes, or cellular holes, use the mean value of the thickness of the webs and the shells.								

Figure 2.13 EC6, geometrical requirements for grouping of masonry units

Mortar is a mix of inorganic binders, aggregates and water, representing the medium which bonds together the individual structural units in order to create a continuous structural system. In a masonry structure, mortar has a fundamental

role, since it distributes the pressure evenly throughout the individual units and infill the joints increasing the resistance of the structure.

Mortars may be defined hydrated or hydraulic true lime mortars when the inorganic binders are hydrated or hydraulic lime respectively; they having different set and strength characteristics. Mortars are defined as cementitious mortar, instead, when the primary binder material is portland cement. In some cases, a mortar may be composed by two different binders (cement-lime mortar). It can be noted that lime increases the plasticity and improve the workability of the mortars, but cement increases the strength. Since a good mortar must have a fair combination of workability and strength, the proportions of its component and the percentage of water depend on the masonry typology, on the environmental conditions and on the durability of construction.

In addition, specific agents may be added to the mortar mixing in order to improve some properties, as strength, workability, flow, plasticity, water retentivity, etc.

In accordance with the EC6, factory-made mortar, pre-batched mortar and site mixed mortar may be distinguished. Moreover, the mortars may be classified in general purpose mortar, thin layer mortar and lightweight mortar. General purpose mortar is the traditional one used in joints with a thickness larger than 3 mm; thin layer mortar is used for joints of 1 ÷ 3 mm, while the last type is produced from perlite, pumice, expanded clay, expanded shale, etc.

Mechanical properties of units and mortar shall be described in the following paragraphs.

2.4.2. Mechanical properties of units and mortars

Masonry is a heterogeneous and anisotropic composite material, existing in many forms, shape, size and physical characteristics depending on the examined base components. For this reason, the mechanical properties of the composite material are significantly influenced by the properties of units and mortars.

In accordance with the regulation in force, masonry units may be classified of Category I or Category II, in terms of manufacturing control. In general, according to EN 771 (CEN, 2004a) and EN 772-1 (CEN, 2004b) the units may be assumed as belonging to the first category when the manufacturer agrees to supply consignments of masonry units to a specified compressive strength and it has a quality control scheme, the results of which demonstrate that the mean compressive strength of a consignment, when sampled in accordance with the relevant part of EN 771 and tested in accordance with EN 772-1, has a probability of failing to reach the specified compressive strength not exceeding 5%. Category II, instead, should be assumed when the mean value of the

compressive strength of the masonry units complies with the declaration in accordance with the relevant part of EN 771, but the additional requirements for Category I are not met.

In general, natural stone should be considered to belong to Category I.

The characteristic compressive strength f_{bk} is determined from the results of tests on masonry. In accordance with the Eurocode, the compressive strength evaluation is performed on three different specimens each consisting of three elements. The control is positive when:

$$\frac{f_1 + f_2 + f_3}{3} \geq 1.20 \cdot f_{bk} \quad (2.1)$$

$$f_1 \geq 0.90 \cdot f_{bk} \quad (2.2)$$

where f_1 , f_2 , and f_3 are the compressive strength of the three units of each specimen.

The standard EN 771-1-6 (Specification for masonry units - Natural stone masonry unit) also specifies the minimum mean values of compressive strength (f_b) for each type of the masonry units defined:

- 1 clay units: $\min f_b = 2.5$ MPa
- 2 calcium silicate clay units: $\min f_b = 5.0$ MPa (normalised value)
- 3 concrete aggregate units: $\min f_b = 1.8$ MPa
- 4 autoclaved aerated concrete units: $\min f_b = 1.8$ MPa
- 5 manufactured stone units: $\min f_b = 1.8$ MPa

According to EC6, the normalised compressive strength of masonry units should be used in the design as defined in EN 772-1, in order to minimise the effect due to the restraint effect of the platens during standard tests execution. This value is the mean reference strength determined by specific testing on a cubic specimen (1 m^3), that cannot be considered representative of the true strength of the unit. Therefore, the effective unit strength is obtained by multiplying the normalised compressive strength f_b by an appropriate shape factor δ that takes into account the actual dimension of the units. The values of the δ coefficient are specified in Table 2.3.

Table 2.3 Value of the shape factor δ relatively to the unit dimensions.

Height [mm]	Least horizontal dimension [mm]				
	50	100	150	200	> 200
50	0.85	0.75	0.70	-	-
65	0.95	0.85	0.75	0.70	0.65
100	1.15	1.00	0.90	0.80	0.75
150	1.30	1.20	1.10	1.00	0.95
200	1.45	1.35	1.25	1.15	1.10
> 250	1.55	1.45	1.35	1.25	1.15

The compressive strength of a masonry unit may have a large range of values referring to the different types of elements. For example, relatively to natural stones, the compressive strength depends on the quality of the stone and it, usually, ranges from 0,3 MPa to 10-15 MPa for tuff or from 4 to 200 MPa for hard stones as marble or granite. In general, the ratio between compressive and tensile strengths normally ranges from 15 to 40.

Relatively to artificial clay elements, instead, the compressive strength of solid elements may reach very high values (130 MPa), but in the most cases these values decrease for the presence of holes. Therefore, in case of hollow and perforated units the compressive strength generally ranges from 2 ÷ 3 MPa for lightweight clay units with a hole volume of 50 ÷ 55 % to 30 ÷ 35 MPa for perforated bricks. Similarly, for concrete elements the strength range starts from 2÷3 MPa for lightweight concrete up to 20÷30 MPa for normal concrete units (Macchi and Magenes, 2002).

The New Technical Italian (M.D. 2008) code according to the UNI EN 998-2 (2003) defines six guaranteed performance classes of mortar on the basis of the mean compressive strength f_m expressed by the letter M followed by the compressive strength in MPa (Table 2.4).

The mortars may also be classified their prescribed composition as indicated in Table 2.5.

Table 2.4 Typical guaranteed performance classes of mortars

Class	M 2.5	M 5	M 10	M 15	M 20	M d
Compressive strength (MPa)	2.5	5	10	15	20	d

d is a compressive strength greater than 25 MPa declared by the producer

Table 2.5 Typical prescribed composition classes of mortars

Class	Mortar type	Composition				
		Cement	Hydrated lime	Hydraulic lime	Sand	Pozzolans
M 2.5	Hydraulic	-	-	1	3	-
M 2.5	Pozzolanic	-	1	-	-	3
M 2.5	Cement-lime	1	-	2	9	-
M 5	Cement-lime	1	-	1	5	-
M 8	Cement-lime	2	-	1	8	-
M 12	Cement-lime	1	-	-	3	-

2.4.3. Mechanical properties of masonry

Masonry is a rather complex composite material, based on the interaction between units and mortar joints. In fact, despite reliable calculation procedures have been achieved, masonry properties assessment represents a very complex problem, due to the several uncertainties of material. In particular, the mechanical parameters which are most significant for structural analysis are related to strength and elastic properties, e.g. compressive, flexural and shear strengths, modulus of elasticity, friction coefficient, creep, moisture movement and thermal expansion. All these properties are dependent on numerous factors such as the mortar and units strengths, the orientation of the units in relation to the direction of the applied load, the bed-joint thickness, the construction formality. Therefore, the different types of masonry may present different mechanical behaviour, although a common feature exists: a very low tensile stress, which is generally ignored in calculation procedures. For this reason, it is necessary to investigate masonry behaviour by appropriate experimental tests.

The main experimental testing performed on masonry specimens are the following types (Augenti, 2004):

- 1 *Uniaxial compressive test*, performed on a masonry specimen by means flat jacks. In general, initial vertical cracks appear in the units along the middle line of the specimen; upon increasing deformation, additional cracks appear, normally vertical cracks at the smaller side of the specimen that lead to failure by splitting of the prism.
- 2 *Uniaxial tensile test*.
- 3 *Diagonal test*, performed on masonry specimens subjected to diagonal 45° compressive actions respect to the mortar bed joints. The failure mechanism is generally due to diagonal cracks appeared orthogonally to the compressive forces.
- 4 *Compressive and shear test*, performed on a specimen subjected to a constant compressive vertical load and to a horizontal load gradually increased.

This test provides the so called characteristic curve shear-displacement of the masonry wall.

- 5 Adhesion test, performed in order to investigate the interaction between units and mortars.

Thus, the most relevant material property of masonry is clearly the compressive strength. Experimentally, this property can be obtained by testing as provided by the EN 1052-1 (CEN, 2001a) and by the Italian codes too. If data test are not available, the characteristic compressive strength of masonry f_k may be calculated on the basis of the above defined normalised compressive strength of units f_b , as follows:

- 1 for masonry made with general purpose mortar and lightweight mortar:

$$f_k = K \cdot f_b^{0.7} \cdot f_m^{0.3} \quad (2.3)$$

- 2 for masonry made with thin layer mortar, in bed joints of thickness 0.5 mm to 3 mm, and clay units of Group 1 and 4, calcium silicate, aggregate units and autoclaved aerated concrete units:

$$f_k = K \cdot f_b^{0.85} \quad (2.4)$$

- 3 for masonry units made with thin layer mortar, in bed joints of thickness 0.5 mm to 3 mm, and clay units of Group 2 and 3:

$$f_k = K \cdot f_b^{0.7} \quad (2.5)$$

where K is a constant depending on the classification of masonry unit.

Anyway, because experimental tests are relatively costly and, in general, not practical for design purposes, semiempirical and analytical relations to predict masonry behaviour under compression have been proposed by researchers.

Despite tensile strength is normally ignored, the ratio between compressive and tensile strength may be a significant datum in structural analysis. In general, this value varies for the different types of masonry, but the frequent values ranges from 0.03 to 0.09.

Another important property for masonry structure the capacity to resist to lateral forces. Shear strength, indeed, is defined as the combination of initial shear strength under zero compressive strength and increment in strength due to the compressive stress perpendicular to shear in the member at the level examined (Tomazevic, 1999). Masonry shear strength is established by means specific experimental tests according to EN 1052-3 (CEN 2001b), so that only shear stresses develop in the mortar to masonry unit contact planers. The characteristic shear strength f_{vk0} should not be greater than a limit value specified in the codes and it may be taken from the following equation (CEN, 2005a):

$$f_{vk} = f_{vk0} + 0.4 \cdot \sigma_d \quad (2.6)$$

where σ_d is the design is the design compressive stress perpendicular to the shear in the member at the level under consideration, using the appropriate load combination based on the average vertical stress over the compressed part of the wall that is providing shear resistance.

Typical values of the initial shear strength of masonry f_{vk0} provided by EC6 are indicated in Table 2.6.

Referring to out-of-plane mechanical behaviour, another considerable parameter is flexural strength. The non-isotropic nature of masonry results in two principal flexural collapse mechanism: failure parallel to the bed joints and failure perpendicular to the bed joints (Figure 2.14). The characteristic flexural strength parallel to the bed joints f_{xk1} and perpendicular to the bed joints f_{xk2} , shall be determined from the results of tests on masonry. Typical values for f_{xk1} and f_{xk2} strengths are provided by EC6 and reported in tables 2.7 and 2.8.

Table 2.6 Values of the initial shear strength of masonry f_{vk0} according to EC6

Masonry units	f_{vk0} (MPa)		
	General purpose mortar of the given strength class	Thin layer mortar	Lightweight mortar
Clay	M10 - M20	0.30	
	M2.5 - M9	0.20	0.30
	M1 - M2	0.10	0.15
Calcium silicate	M10 - M20	0.20	
	M2.5 - M9	0.15	0.40
	M1 - M2	0.10	0.15
Aggregate concrete Autoclaved aerated concrete	M10 - M20	0.20	
	M2.5 - M9	0.15	0.30
Manufactured stone and dimensioned natural stone	M1 - M2	0.10	0.15

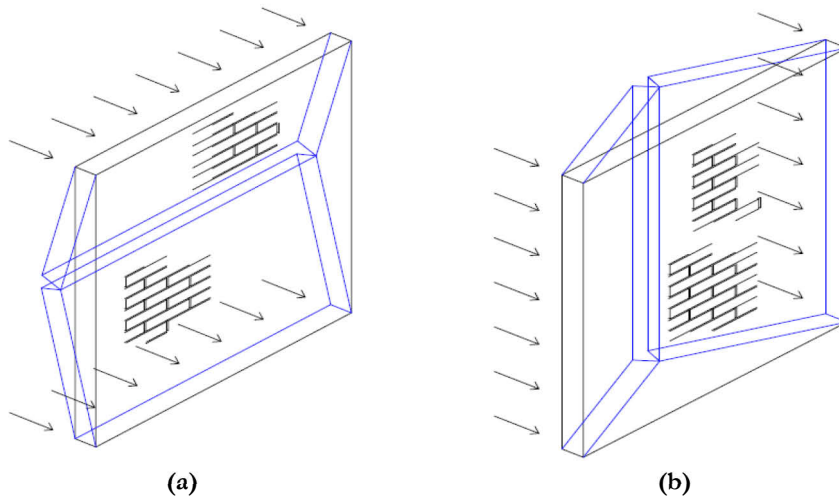


Figure 2.14 Definition of failure planes: (a) failure parallel to the bed joints f_{sk1} ;
(b) failure perpendicular to the bed joints f_{sk2}

Table 2.7 Values of f_{sk1} for failure parallel to bed joints according to EC6

Masonry units	f_{sk1} (MPa)			
	General purpose mortar		Thin layer mortar	Lightweight mortar
	$f_m < 5$ MPa	$f_m \geq 5$ MPa		
Clay	0.10	0.10	0.15	0.10
Calcium silicate	0.05	0.10	0.20	not used
Aggregate concrete	0.05	0.10	0.20	not used
Autoclaved aerated concrete	0.05	0.10	0.15	0.10
Manufactured stone	0.05	0.10	not used	not used
Dimensioned natural stone	0.05	0.10	0.15	not used

Table 2.8 Values of f_{sk2} for failure perpendicular to bed joints according to EC6

Masonry units	f_{sk2} (MPa)			
	General purpose mortar		Thin layer mortar	Lightweight mortar
	$f_m < 5$ MPa	$f_m \geq 5$ MPa		
Clay	0.20	0.40	0.15	0.10
Calcium silicate	0.20	0.40	0.30	not used
Aggregate concrete	0.20	0.40	0.30	not used
Autoclaved aerated concrete	$\rho < 400 \text{ kg/m}^3$	0.20	0.40	0.20
	$\rho \geq 400 \text{ kg/m}^3$	0.20	0.40	0.30
Manufactured stone	0.20	0.40	not used	not used
Dimensioned natural stone	0.20	0.40	0.15	not used

On the basis of compression tests results, the modulus of elasticity E can be estimated too. Nevertheless, the value of Young modulus is variable and depends

on various factors such as materials, stress direction and type of loading condition. In other words, the elastic modulus E is heavily related to the stress-strain relationship of the material, that represents a very complex issue, it treating in the next paragraph.

2.4.4. The stress-strain relationships

The property of heterogeneity and anisotropy influences the mechanical behaviour of masonry materials. Naturally, bed and head joints are responsible for its discontinuous nature, inducing an anisotropic behaviour in both elastic and plastic domains. Therefore, in order to simplify the problematic related to these aspects, an equivalent and homogeneous ideal material is assumed in global modelling.

The stress – strain laws relatively to uniaxial and biaxial loading condition is object of present-day research activities. The most interesting stress-strain relationships refers to uniaxial compressive loading conditions. This law is heavily influenced by the deformation capacity of the mortar. In fact, although both the materials exhibit high compressive strength, the unit behaviour is almost brittle if compared with mortar one. The Figure 2.15 shows a typical stress-strain diagram for units and mortar under uniaxial compression. It may be noted that units shows a quasi-elastic behaviour, while mortar presents a long well definite plastic branch representative of a ductile behaviour. This allows to assume for masonry as composite material the mean behaviour between the ones of the base components.

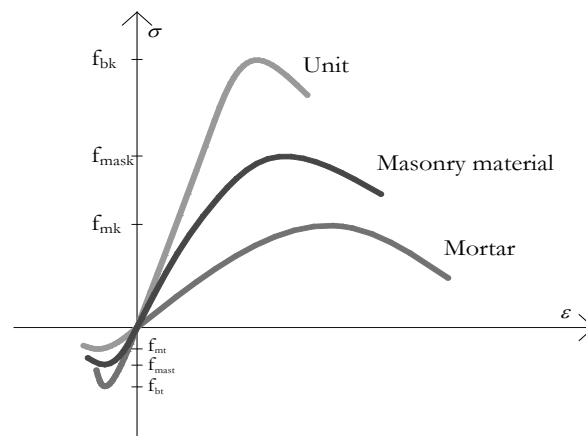


Figure 2.15 Stress – strain relationships for masonry material and its base components

In Augenti (2004), several stress-strain laws for masonry panels under compression are reported on the basis of specific studies.

The most important model are listed in the following:

1. Turnšek and Cacovich (1974):

$$\frac{\sigma}{f_k} = 6.4 \cdot \left(\frac{\varepsilon}{\varepsilon_k} \right) - 5.4 \cdot \left(\frac{\varepsilon}{\varepsilon_k} \right)^{1.17} \quad (2.7)$$

2. Arya – Hegemier (1978):

$$\frac{\sigma}{f_k} = \frac{\varepsilon}{\varepsilon_k} \quad \text{if} \quad 0 \leq \varepsilon \leq \varepsilon \quad (2.8)$$

$$\frac{\sigma}{f_k} = 1 - \left(\frac{\varepsilon - \varepsilon_k}{\varepsilon_{u-} - \varepsilon_k} \right)^2 \quad \text{if} \quad \varepsilon_k \leq \varepsilon \leq \varepsilon_u \quad (2.9)$$

3. Sawko (1982):

$$\frac{\sigma}{f_k} = 2 \cdot \left(\frac{\varepsilon}{\varepsilon_k} \right) - \left(\frac{\varepsilon}{\varepsilon_k} \right)^2 \quad (2.10)$$

4. ANDIL

$$\frac{\sigma}{f_k} = 3.4142 \cdot \left[1 - \left(1 + \frac{\varepsilon}{\varepsilon_k} \right)^{-0.5} \right] \quad (2.11)$$

The EC6 (2005a) also proposes a stress-strain relationship. This law represents a non-linear relation and it may be considered as linear, parabolic, parabolic-rectangular or as simply rectangular, depending on the purposes of designers (Figure 2.16).

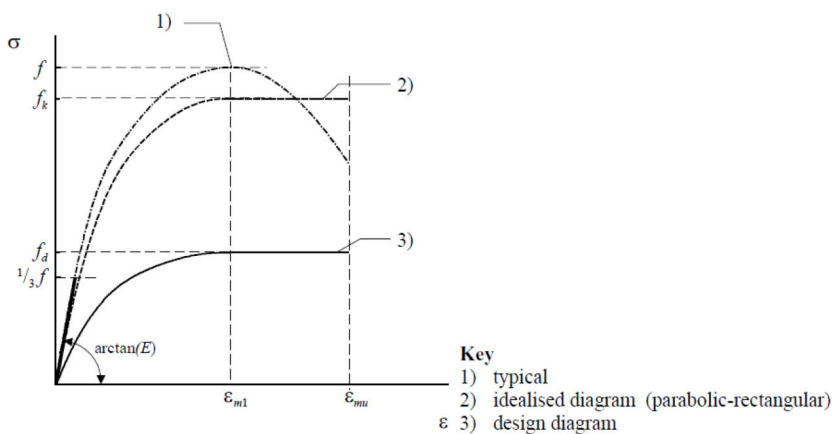


Figure 2.16 Stress-strain relationship for masonry in compression

The constitutive behaviour of masonry under biaxial stress states is almost complex to define, because of the discontinuity nature of the material.

The biaxial strength of masonry is described by means of a three-dimensional surface, employing two different approaches. In the first case, the two principal stresses (σ_1 and σ_2) and the rotation angle between the principal stresses and the material axes (θ) are considered. In the second case, the full stress vector in a fixed set of material axes is defined, indicating the stress components as σ_n (perpendicular to bed joints), σ_p (parallel to bed joints) and τ (Figure 2.17) (Macchi e Magenes, 2002).

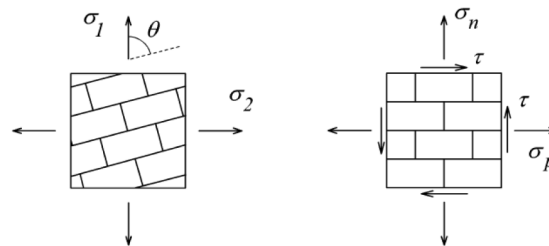


Figure 2.17 Reference system for plane stress states

The most complete experimental research concerning the characterization of biaxial behaviour of masonry was done in Australia, University of Newcastle by Page (1981), and in UK, University of Edinburgh (Page et al., 1980) for brickwork masonry and in USA, California University, in 1980 for concrete units masonry. In particular, the tests performed in Australia shows that both the orientation of the principal stresses relative to the material axes and the principal stress ratio had a great influence in the strength and failure modes. The different failure modes are shown in Figure 2.18. It can be noted that that the biaxial strength envelope obtained for brickwork masonry is not valid for other types of masonry, because of materials differences, shapes and geometry. For this reason it is necessary to develop advanced numerical models in order to generally characterize the constitutive law of masonry under biaxial stress states.

The physic-mathematic abstraction, i.e. transforming the reality into a scheme governed by mathematically treatable laws, can appear arbitrary for masonry. In reality, each material is provided with a micro-structure and the assimilation to a continuum implies an operation of stress average on a suitable reference volume. The masonry material, realized through the assemblage of two components, shows a constitutive bond characterized by a non linear law and intermediate compression strength to both the single components. The limit of the linear behaviour coincides with the beginning of the partialization of the section; it has

to be pointed out that this phenomenon, in a material provided of reduced tension strength, occurs for smaller load levels compared to the bearable ones.

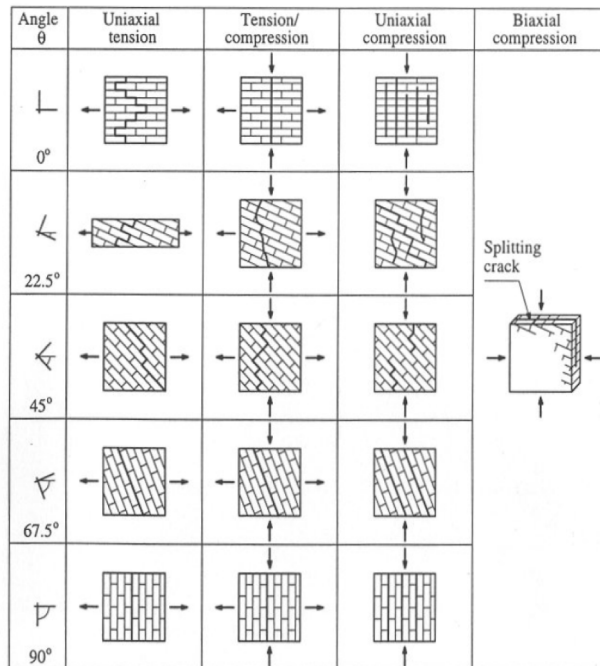


Figure 2.18 Different modes of failure of solid clay brickwork panels under biaxial loading

2.4.5. Material modelling approaches

The above sections have evidenced the heterogeneity of masonry material, it exhibiting distinct directional properties due to the mortar joints which act as planes of weakness. Therefore, the modelling represents a very complex and problematic issue.

In general, three main distinct approaches for modelling masonry have been defined for its numerical representation. These techniques depend on the level of accuracy of the models and they have been implemented as follows (Lourenco, 1998):

- *Detailed micro-modelling*, (Figure 2.19a) in which units and mortar in the joints are represented by continuum elements whereas the unit-mortar interface is represented by discontinuous elements; the Young model, the Poisson coefficient and the inelastic properties of the units and the mortar are taken into account. The interface represents a potential crack/slip

plane with initial dummy stiffness to avoid interpenetration of the continuum.

- *Simplified micro-modelling*, (Figure 2.19b) in which expanded units and mortar joints are represented by continuum elements while the interfaces are represented as discontinuous elements; in other words, masonry is considered as a whole of elastic blocks surrounded by fracture lines in the joints. Poisson coefficient and the inelastic properties of the unit and the mortar are neglected, thus the accuracy is lost.
- *Macro-modelling-units*, (Figure 2.19c) in which mortar, units and their interface are smeared out in the continuum. The difference between the units and the joints does not occur anymore but it is considered as an isotropic or anisotropic homogeneous continuum.

Each of this modelling techniques involves great difficulties, mainly for sack or chaotic masonry, in which the several components are not always distinguishable.

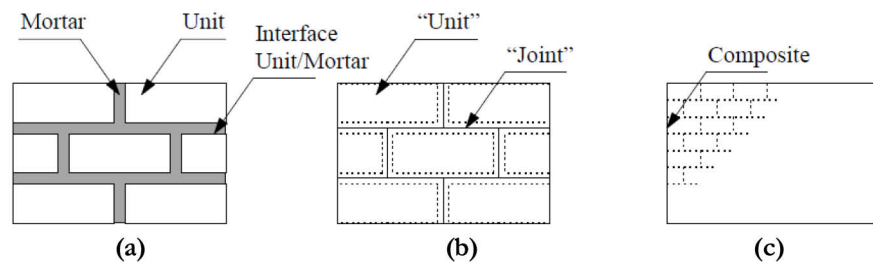


Figure 2.19 Modelling strategies for masonry structures: (a) detailed micro-modelling; (b) simplified micro-modelling; (c) macro-modelling

One modelling strategy cannot be preferred over the other because different application fields exist for micro and macro-models. Micro-modelling studies are necessary to give a better understanding about the local behaviour of masonry structures, while the Macro-models are applicable when the structure is composed of solid walls with sufficiently large dimensions so that the stresses across or along a macro-length will be essentially uniform.

Therefore, macro-modelling is evidently more practice oriented due to the reduced time and memory requirements as well as a user-friendly mesh generation. This type of modelling is most valuable when a compromise between accuracy and efficiency is needed.

In the framework of this thesis, only the macro-modelling technique has been considered in the implementation of the numerical model.

2.5. STRUCTURAL BEHAVIOUR

2.5.1 Modelling techniques

A masonry structure is constituted by walls, structural element of the building of length and a height equal to the total height of the building.

A wall may be regarded as a system of coupled structural components, which are piers and spandrels or “fascias”. The first is a wall element of length and of a height equal to the height of the adjacent opening, while a fascia is that part of the building which lies between two openings in the vertical direction, thus joining the walls in one plane (Figure 2.20a). A wall may be defined regular, if the openings are vertically and horizontally aligned (Figure 2.20b).

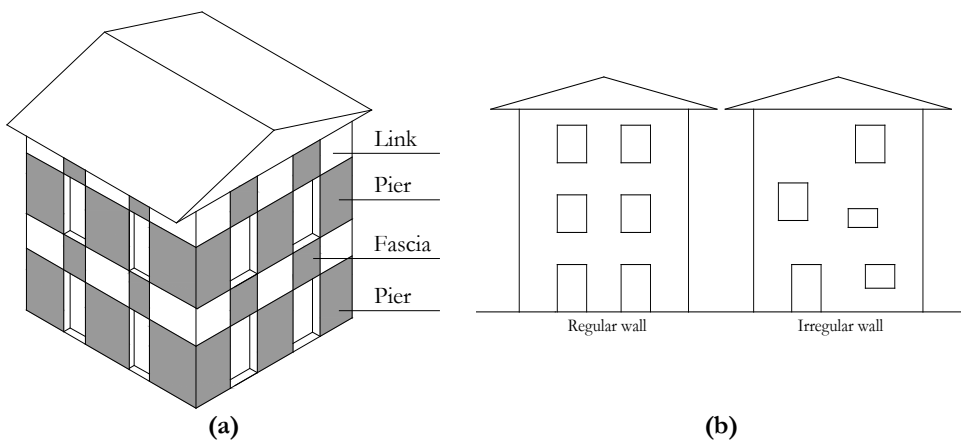


Figure 2.20 (a) Structural component of masonry walls;
(b) Types of wall configuration

A complex issue in the study of masonry structure concerns the choice of a suitable structural model representative of the real response of the system.

With reference to the macro-model approach, two techniques of structural modelling may be distinguished (Romano, 2005):

1. Models with structural components
2. Finite Element Models (FEM)

The models with structural components, may be further subdivided into:

- *Models with lumped masses* or mass-spring-dashpot models, which is an approximation of the geometry of the structure but it can be sufficient in order to determinate the structural dynamic response; consequently, this

kind of model is not able to predict the local or global failure mechanisms or the damage levels of the single structural elements.

- *Models with beams and columns*, well-known as Equivalent Frame Models (EFM), which consist of representing solid walls and spandrels as frame structural elements. The panels are connected by rigid nodes and are distinguished in two types: “piers”, which are the principal vertical resistant elements for both dead and seismic loads; “spandrels” or “fascias”, which are secondary horizontal elements, coupling piers in the case of seismic loads. Usually only in-plane resistant mechanisms are considered. By concentrating damage, slidings and rotations in predefined sections of the structural elements, these models enable one to perform non linear incremental collapse analyses of entire buildings.
- *Macroelements models*, which consider the structure as an assemblage of twodimensional shear walls connected to each other and to flexible floor diaphragms. The structural model may also coincide with identifiable architectural and functional parts of the construction connected each other so that they represent a unitary constructive part even if it is joined and not independent from the whole of the construction. Each shear wall is assumed as consisting of deformable panels, named macroelements, representative of piers and fascias, and by rigid elements that connect the piers and the spandrels themselves. This scheme comes out from the observation that, in most cases, the inelastic and damaging mechanisms in the masonry can be localised in piers and spandrels and are related to both opening of cracks and shear dissipative sliding, while the areas where they are connected seldom experience any kind of damage (Brencich et al., 1998).

The FEM generally work at meso-scale and consider masonry as a continuum equivalent material, whose constitutive model is obtained through homogenization techniques. The model consists of discretizing the masonry continuum in a number of finite elements, adopting a suitable non-linear constitutive law, and, finally, in performing a non-linear incremental analysis.

For masonry modelling, two typologies of finite elements to define exist:

- *bi-dimensional* (shell) elements, that produce faster and more controllable models because of the presence of a smaller number of joints if compared to the brick elements;
- *three-dimensional* (brick) elements, that permit to control the stresses evolution inside the structure.

Although this approach may provide quite an accurate description of the structure and of its material, it requires a high computational effort, which is unsustainable for wide application in engineering practice.

In this study, the analysed buildings have been modeled through EFM and FEM. Models with structural components (EFM) have been used in the analysis of *Palazzo di Città* (Chapter 4), while FEM have been applied in the analysis of *Palazzo Sidoni* (Chapter 5). More in particular, in the first case, the computer codes AeDes (2009) and SAP 2000 (CSI, 2000) have been employed, while in the second case, the code ABAQUS (HKS, 2004) has been used for the analysis.

The main differences between the two approaches are summarized in Table 2.10 and shown in Figure 2.21 (Calderini et al., 2009).

Table 2.9 Comparison among the modelling issue of EFM and FEM

	EFM	FEM
Modeling Scale	Masonry structure is described as an assembly of structural elements.	Masonry structure is described as a non-linear continuum.
	Masonry walls are discretized by a set of masonry panels, in which the non-linear response is concentrated, connected by rigid nodes.	The masonry continuum is discretized into a number of finite elements.
	Structural elements are defined a priori.	Structural elements are identified ex-post.
Constitutive law	Constitutive models are referred to masonry panels and are expressed in term of force-drift relationships.	Constitutive models are referred to the material and are expressed in term of stress-strain relationships.
	Usually elasto-plastic laws are adopted, where stiffness is evaluated by adopting the beam theory computing both the contributions in terms of shear and flexural behaviour, strength is obtained by referring to simplified resistance criteria	They may be defined whether through a phenomenological approach, or homogenization, or direct identification techniques.
Mechanical Properties	The stiffness is computed on the basis of geometric and mechanical properties of panel. Strength parameters may be related to the single constituents or to the masonry as a function of the criterion adopted.	Mechanical parameters of the single constituents of masonry (blocks and mortar joints) have to be defined.

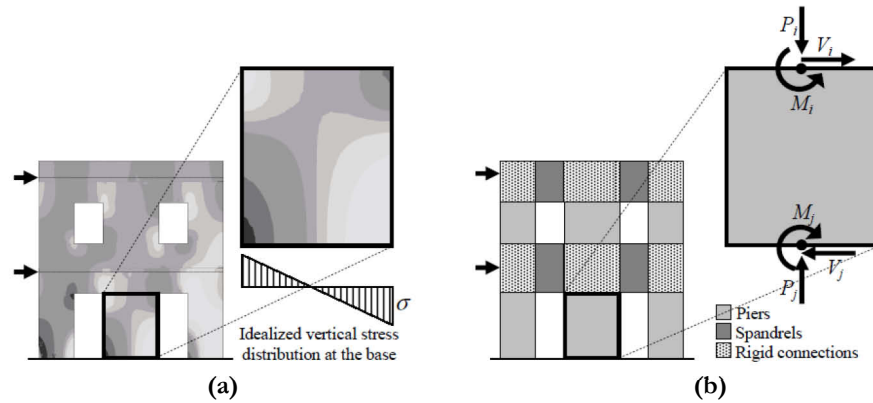


Figure 2.21 Different modelling techniques for masonry structures:
(a) FEM; (b) EFM (Calderini et al., 2009)

2.5.2 Under vertical loads

2.5.2.1. Calculation methods

A calculation method is a mathematical tool which allows to analyze a structural model in order to determine its stress state. Generally, the structural response of a plane wall under vertical loading conditions may be examined by investigating the in-plane behaviour.

The main analysis types under vertical loading condition, are summarizable in three groups (Augenti, 2004):

1. *Linear analysis*: is based on the linear theory of elasticity, assuming a linear relationship between stress and strain with a slope equal to the modulus of elasticity. The structural system may be modelled as an assemblage of panels mutually interconnected, by using the macroelements or the EF approaches. The analysis may be alternatively carried out by considering a framed system pinned or rigidly linked; in the case, the hypothesis of elastic-linear constitutive law permits to solve the global equilibrium by means of the typical force-displacement methods.
2. *Non linear analysis*: this type of calculation takes into account the non-linear behaviour of the material, which coincides with the beginning of the partialization of the section. For a material having a reduced tensile strength, this phenomenon occurs for smaller load levels compared to the design ones, it reducing the effective resistant area of the masonry element. Different types of non linear behaviour exist: mechanical (related to the material non linear behaviour), geometrical (the application

point of the loads changes increasing the actions) and of contact (related to the interaction of two different bodies).

This type of analysis requests the elastic and inelastic properties and the strength of the material. The results that can be gained are the strain behaviour, the stress distribution and the collapse mechanism of the structure.

Calculation models may also be used to study separate parts of the structure (such as walls) independently (i.e. local analysis).

2.5.2.2. Check methods

According to the regulation in force, in order to perform a structural analysis under vertical loading condition, the following combination of the actions may be considered:

$$F_D = \gamma_{G1} \cdot G_{k1} + \gamma_{G2} \cdot G_{k2} + \gamma_P \cdot P + \sum_i \psi_{0i} \cdot Q_{ki} \quad (2.12)$$

in which:

- G_{k1} and G_{k2} express the characteristic value of the permanent loads;
- Q_{ki} expresses the characteristic value of the variable loads;
- γ_G is the partial safety factor for ultimate limit state
- E is the seismic action;
- P are possible pre-stressing actions;
- ψ_{2i} is the combination factor considering the probability of occurrence of the variable actions.

The (2.12) represents a persistent and transient design situations and it is employed for the structural verification for the Ultimate Limit State (ULS).

The safety verification is carried out on each resistant masonry element, by considering the following eccentricity of the vertical total load R :

- structural eccentricity (r) due to vertical loads at the generic i -level:

$$r_i = \frac{R_{i-1} \cdot r_{i-1} + P_i \cdot p_i}{R_{i-1}} \quad (2.13)$$

where P is the action of the horizontal floor system;

- accidental eccentricity (a), depending on the inter-storey height

$$a = \frac{h}{200} \quad (2.14)$$

- transverse eccentricity (t), due to horizontal forces:

$$t = \frac{M_t}{R} \quad (2.15)$$

where M_t is the maximum value of the bending moment due to the wind action;

- longitudinal eccentricity (l), due to horizontal forces:

$$l = \frac{M_t}{R} \leq 0.217 \cdot L \quad (2.16)$$

where L is the length of the wall.

In accordance with EC6, the safety check of unreinforced masonry walls under vertical loading conditions, are defined as follows:

- Verification of walls subjected to mainly vertical loading: it consists into verifying that the design value of the vertical load applied to a masonry wall (N_{Ed}) is less than or equal to the design value of the vertical resistance of the wall (N_{Rd}), according to following relationship:

$$N_{ED} \leq N_{RD} = \Phi \cdot t \cdot f_d \quad (2.17)$$

in which: Φ is the capacity reduction factor, Φ_t , at the top or bottom of the wall, or Φ_m , in the middle of the wall, as appropriate, allowing for the effects of slenderness and eccentricity of loading; t is the thickness of the wall and f_d is the design compressive strength of masonry, equal to the ratio between the characteristic value (f_k) and the safety coefficient.

- Verification of walls subjected to lateral loading: it consists into checking that the design value of the moment applied to a masonry wall (M_{Ed}) is less than or equal to the design value of the resistant moment of the wall (M_{Rd}) according to following formula:

$$M_{ED} \leq M_{RD} = f_{xd} \cdot Z \quad (2.18)$$

where f_{xd} is the design flexural strength appropriate to the plane of bending and Z is the elastic section modulus of unit height or length of the wall.

- Verification of walls subjected to shear loading: it consists into checking that the design value of the shear load applied to a masonry wall (V_{Ed}) is less than or equal to the design value of the shear resistance of the wall (V_{Rd}) according to following expression:

$$V_{ED} \leq V_{RD} = f_{vd} \cdot t \cdot l_c \quad (2.19)$$

where f_{vd} is the design value of the shear strength of masonry, based on the average of the vertical stresses over the compressed part of the wall that is providing the shear resistance; t is the thickness of the wall resisting the shear and l_c is the length of the compressed part of the wall, ignoring any part of the wall that is in tension.

- Verification of walls subjected to concentrate loads: it consists into verifying that the design value of a concentrated vertical load applied to a

masonry wall (N_{Edc}) is less than or equal to the design value of the vertical concentrated load resistance of the wall (N_{Rdc}) as follows:

$$N_{Edc} \leq N_{Rdc} = \beta \cdot A_b \cdot f_d \quad (2.20)$$

where β is an enhancement factor for concentrated loads, A_b is the loaded area, f_d is the design compressive strength of masonry.

2.5.3 Under seismic loads

2.5.3.1. Masonry, earthquake and vulnerability factors

Masonry represent as aforesaid the most ancient constructive material, thus the major part of the seismically active areas of the world are characterized by the presence of ancient structures made of unreinforced masonry.

The effects of earthquake on this structures partially depends on extrinsic aspects (e.g. the magnitude and dynamic characteristics of the seism, the geographical site, the soil conditions, etc), but, above all, on the structural system behaviour.

In Italy, the past experiences have shown the high vulnerability of existing masonry buildings, as for example the Molise earthquake (2002) or the more recent Abruzzo seismic event (cfr. Chapter 5). This experiences have demonstrated the poor performance of historic buildings when subjected to seismic actions. In fact, this type of constructions generally do not meet the seismic requirements stated by the new seismic codes, since they were built to withstand gravity loads only. Thus, they often do not provide the adequate resistance under seismic loads, representing a significant risk during an earthquake. Generally, the seismic vulnerability of masonry buildings derives from several factors, most of which have been recognized for a long time and codified in most modern design provisions.

The most important vulnerability factor is related to the capacity of the building to distribute the loads over all the bearing walls, in order to exhibit a box-type global behaviour. This capacity derives from the quality of the connection between two orthogonal walls and among the floor system and the walls (box effect). Referring to the first case and considering each wall as a system of coupled elements (piers and fascias) mutually interconnected, three types of wall may be distinguished:

1. *Walls only joined by the floors*: the coupling effect is negligible, the whole system can be regarded as interacting cantilever walls. In this case the total overturning moment due to the applied horizontal forces is carried by the walls alone, proportional to their stiffness, resulting in very high bending moments at the base of the wall;

2. *Walls characterized by very deep spandrels*: a considerable coupling effect is produced by the deep spandrels;
3. *Strongly coupled walls*: the total overturning moment due to the applied horizontal forces is mainly carried by high normal forces in the outer walls resulting from the vertical shear forces transmitted by the spandrels.

Generally, in historic masonry structures, the interlocking of a wall with the transverse wall is usually very weak, especially inside the buildings, so that the transfer of shear is not guaranteed.

On the other hand, appropriate connections among the floor system and the walls guarantee a global box-type action. The seismic forces, indeed, originating throughout the building are delivered through structural connections to horizontal diaphragms (floor slabs), which distribute these forces to shear walls. Diaphragms are usually classified as follows (Anderson and Brzev, 2009):

- *Rigid*: shear forces are distributed to vertical elements in proportion to their stiffness. Concrete diaphragms or steel diaphragms with concrete infill, are usually considered rigid.
- *Flexible*: the shear distribution of the forces to vertical elements is independent of their relative rigidity; these diaphragms act like a series of simple beams spanning between vertical elements. This type of diaphragm must have adequate strength to transfer the shear forces to the walls, but cannot distribute torsional forces. Corrugated steel diaphragms without concrete fill and wood diaphragms are generally considered flexible.

To the grade of connection generally corresponds two types of prevent failure mode:

1. *I Mode Collapse Mechanisms* (Figs. 2.22a-2.23a). These type of modes generally involve out-of-plane damage and may be considered as local mechanisms, in the sense that they are usually associated to the local response of structural macroelements. These mechanisms usually occur in case of lack of anchorage of the walls and flexible diaphragms.
2. *II Mode Collapse Mechanisms* (Figs. 2.22b-2.23b) It may be considered as global mechanisms. The resistance of the building to horizontal actions is provided by the combined effect of floor diaphragms and in-plane response of structural walls.

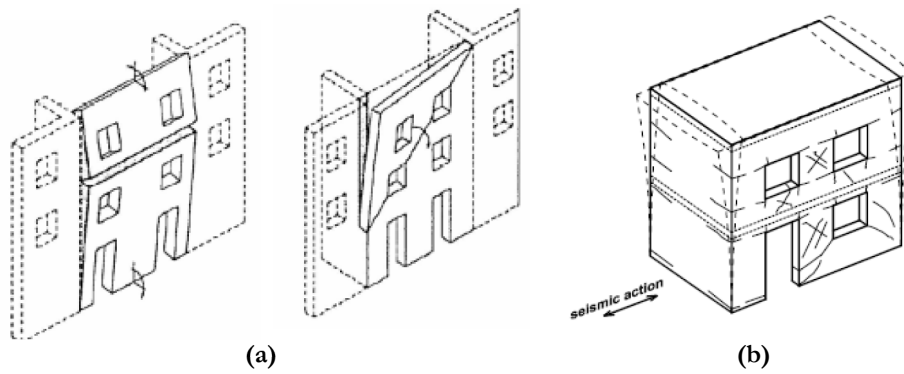


Figure 2.22 (a) I Mode Collapse Mechanisms (D'Ayala and Speranza, 2003); (b) II Mode Collapse Mechanism (Magenes, 2006)



Figure 2.23 Examples of: (a) I Mode Mechanism; (b) II Mode Mechanism

In some cases, the diaphragms continuity is interrupted by split level floors and roofs. Such a discontinuity may cause the diaphragm to function as a cantilever element or three-sided diaphragm.

Other vulnerability factors are related to the configuration of buildings (e.g. dimensions, building form, geometric proportions, location of structural components). Based on past earthquake experiences, it can be stated that symmetrical buildings with simple configurations are more resistant to earthquake shaking than irregular buildings. Typical structural configuration deficiencies include an irregular geometry, a weakness in a given story, a concentration of mass, or a discontinuity in the lateral force resisting system.

Geometric irregularities are usually related to the story-to-story variation in the dimensions of the lateral-force-resisting system, while mass irregularities concerns the story weights. The effective mass consists of the dead load of the structure on each level plus the actual weight of partitions and permanent

equipment on each floor; the validity of this approximation is dependent upon the vertical distribution of mass and stiffness in the building.

The vulnerability is also increased by deteriorated or poor quality of masonry elements. For instance, eroded mortar may easily be scraped away, presenting a low shear strength which results in low wall strength.

Diagonal wall cracks, especially along the masonry joints, may affect the interaction of the masonry units leading to a reduction of strength and stiffness. Crack width is commonly used as a convenient indicator of damage to a wall, but it should be noted that other factors, such as location, orientation, number, distribution and pattern of the cracks could be equally important in measuring the extent of damage present in the shear walls.

All these factors should be considered when evaluating the reduced capacity of a cracked element.

Table 2.10 depicts the main factors which influence the seismic vulnerability of a masonry building (Magenes, 2006).

Table 2.10 Factors influencing the seismic vulnerability of masonry buildings

Higher vulnerability	Lower vulnerability
Insufficient quality of materials (poor mortar, weak/brittle units), poor “internal connection” of masonry	Regular and robust units, good bond and interlocking of units, masonry behaves monolithically through the whole thickness of the wall.
Very slender walls (out-of-plane instability)	Limited slenderness of walls; restraints to out-of-plane failure
Lack of efficient connections among walls and between walls and horizontal structures, lack of structural redundancy	Good interlocking at wall intersections, presence of tie rods and ring beams at each floor (and roof) level to favour “box action”, efficient floor-to-wall connections which reduce stress concentration.
Floors do not provide diaphragm action	Sufficiently stiff and resistant diaphragms to provide restraint to out-of-plane vibration of walls, to increase structural redundancy and favour internal force redistribution.
Presence of horizontal thrusts (e.g. from roof or arched or vaulted structures) equilibrated only by out-of-plane resistance of structural walls	Horizontal thrusts are reacted by in-plane action of strong walls/buttresses or by suitable structural elements (ties, floor diaphragms...) to form a “closed” self equilibrating system.
Excessive unsupported floor spans, widely and irregularly spaced walls High structural and non-structural masses and low material strength	Limited floor spans, regularly spaced shear walls in at least two orthogonal directions Masses and weights produce a low stress/strength ratio
Structural irregularity in plan (torsional effects, stress concentrations) and in elevation (inefficient load path, stress concentrations)	Regular structure, sufficient torsional resistance, regular path of forces from upper structure to foundation

2.5.3.2. Calculation methods

The calculation methods for the study of the seismic behaviour of masonry structures developed in literature refers essentially to models with structural components (macroelements or FE).

In this section, an overview of the main calculation method is provided.

The principal approaches are:

- *VET*: it was the first Italian manual calculation method of walls subjected to seismic actions; it was introduced by the Friuli Venezia Giulia Region (R.L., 1977), after the seismic event of 1976. The method is only based on the shear collapse criterion. The resistance of the whole structure, indeed, coincides with the sum of shear strengths of all the piers according to the seismic direction. In other words, the global crisis condition occurs when all the pier exceed the elastic threshold.
- *POR*: similarly to the *VET*, this method was introduced by the Friuli Venezia Giulia Region (R.L., 1977), after the seismic event of 1976, on the basis of the damage experienced by masonry constructions during the Skopje earthquake (1963). The method is based on the following assumption: the wall thickness is constant at each level; the horizontal floors exhibit a rigid behaviour; the masonry piers have only translational degree of freedom; the constitutive law is elastic-perfectly plastic; the stiffness of each element is constant. Similarly to the *VET* method, the unique reference resistance criterion is the shear one.
- *PORFLEX*: it was proposed by Braga and Dolce (1982) during the 6th *International Brick Masonry Conference*. This procedure is similar to the *POR* one, but it presents the following innovative aspects: the constitutive law is elastic-brittle; the definition of the boundary conditions of each component is improved; the ultimate strength is estimated by performing a level by level analysis; the stiffness of the fascias is unlimited, but their resistance is finite, the horizontal forces are distributed on the basis of the panel stiffness. Contrary, the method does not take into consideration the collapse due to sliding shear and the axial loads applied to fascias.
- *POR 90*: it was developed by Dolce in 1990. The method is based on a storey by storey analysis, neglecting the horizontal loads applied to the upper levels. The height of masonry piers is determined by means of a specific calculation, depending on the spandrels dimensions; therefore, the procedure is particularly useful in case of irregular walls. One of the limit of the method is the fact that it does not provide the load-bearing capacity check in the elastic behavioural phase.

- *VEM*: it was conceived by Fusier and Vignoli (1993) during the 9th *International Brick/Block Masonry Conference*. Scope of this calculus procedure is the identification of the load collapse multiplier of the wall, in order to determine the maximum horizontal force resisted by each level. The fascias element are assumed as rigid structural component, while for the piers three check techniques are provided: diagonal and sliding shear and compressive-bending actions. Similarly to the foregoing analysis, the method does not verify the global equilibrium.
- *SAM*: it was presented by Calvi and Magenes (1994) during the 10th *International Brick/Block Masonry Conference*. The method is aimed at the definition of the global equilibrium of the wall, by avoiding the level by level approach. The analysis is performed by incrementing the horizontal loading up to the wall failure. The maximum horizontal force of the pier is computed by considering the following strength criteria: diagonal and sliding shear and compressive-bending. The maximum horizontal force of the spandrel, instead, is determined by considering only shear criteria.
- *RAN*: devised by Raithel and Augenti (2004), is totally based on the macroelements approach. The method takes into account both the shear and the compressive-bending collapse criteria. The procedure allows not only to determine the maximum load of the wall applied to each slab, but also the failure modes occurred in the masonry panels. Moreover, the constitutive law is elastic-perfectly plastic.

2.5.3.3. *Analysis type*

Several seismic analysis types may be performed on masonry structures.

The Italian Codes (OPCM, 2003, M. D. 2008) provides:

1. *Linear analysis*. This type of analysis is the simplest type in which the material obeying to the Hooke's law is assumed (elastic behaviour). The obtainable results consist into the deformed shapes and the stress distribution in the structure. Due to the assumption of elastic behaviour of the material, this method is not useful into the establishment of the collapse limits. Contrary, it is particular effective into the definition of the global response of the building and into the identification of the structural weak points, subjected to extreme tension-stresses state able to cause fracture in the masonry.

Two kinds of linear analysis may be distinguished: static and dynamic ones.

According to the *linear static technique*, also known as *equivalent static analysis*, the building is modelled as an equivalent single-degree-of-freedom

(SDOF) system with a linear elastic stiffness and an equivalent viscous damping. The seismic input consist in a force system distributed along the height of the building applied to the structural system, hypothesizing a linear distribution of the displacements. In case of multi-storey construction, the horizontal forces are assumed as concentrated and applied at each slab. Such forces are given by the following equations:

$$F_i = F_h \cdot \frac{z_i \cdot W_i}{\sum (z_j \cdot W_j)} \quad (2.21)$$

where:

- F_h is seismic force;
- F_i is the seismic force acting at the generic i-level;
- W_i is a portion of seismic weight (W) that is assigned to i-level, i.e. the floor weight plus a portion of the wall weight above and below that level;
- $\sum W_j$ is the sum of the weigh
- z_i and z_j are the height from the base of the structure up to levels i and j respectively (base of the structure denotes level at which horizontal earthquake motions are considered to be imparted to the structure, usually the top of the foundation);

The (2.21) is based on a linear first mode approximation for the acceleration at each level.

The *linear dynamic* or *modal analysis* allows to determine the mode shapes and the vibration periods of a given structure. Moreover, this kind of analysis, associated with the design response spectrum, permits to obtain the stresses values in the structural components. All the vibration modes with a participating mass bigger than 5% should be considered summing up a number of modes so that the total participating mass is larger than 85%. In order to calculate stresses and displacements in the structure, SRSS (Square Root of the Sum of the Squares) or CQC (Complete Quadratic Combination) rules may be used. In particular the CQC is defined as follows:

$$E_i = \left(\sum E_i^2 \right)^{1/2} = \left(\sum_i \sum_j \rho_{ij} \cdot E_i \cdot E_j \right)^{1/2} \quad (2.22)$$

where:

- E is the total seismic force value;
- E_i is the value of the seismic force according to the i-mode;
- E_j is the value of the seismic force according to the j-mode
- ρ_{ij} is the correlation factor between the i-mode and the j-mode, provided by the code

This type of analysis has been carried out on three-dimensional models of the Sidoni Palace study case (cfr. Chapter 5).

2. *Non Linear analysis*. It is possible to study the complete response of the structure from the elastic field through the cracking, until the complete collapse by means of this approach. Particularly interesting are the damage models very useful into the evaluation of the stiffness loss at global and local level, especially for existing buildings. Similarly to preceding method, static and dynamic analysis may be distinguished.

The *non linear static analysis*, also known as *push over analysis*, consists into the application on the structure of the gravity loads (self weight and dead loads) and a horizontal forces system monotonously increasing until the reaching of the limit conditions. By means of this procedure, it is possible to draw the capacity curve of the structure, i.e. relation between the lateral load resistance of a given structure and its characteristics lateral displacement (Kircher et al., 1997).

This type of analysis, usually adopted in the evaluation of the bearing capacity of existing buildings, has been performed in the present thesis on three-dimensional masonry constructions in order to assess the seismic vulnerability of a monumental building (cfr. Chapter 4).

The *non linear dynamic analysis* or *Time History* is aimed at evaluation of the seismic response of a structural system by integrating the motion equations. The analysis is implemented by means of specific numerical simulations, in which the model is subjected to a time-history (set of accelerograms) record of a certain earthquake ground motion. This is the most sophisticated analysis procedure and time-consuming to perform, and as such, not warranted for low-rise and regular structures. It also requires an advanced level of knowledge of the dynamics of structures. However, the calculated response can be very sensitive to the characteristics of the individual ground motion used as seismic input; therefore several time-history analysis are required using different ground motion records. The main value of nonlinear dynamic procedures is as a research tool with the objective to simulate the behaviour of a building structure in detail, i.e. to describe the exact displacement profiles, the propagation of cracks, the distribution of vertical and shear stresses, the shape of the hysteretic curves, etc.

2.5.3.4. Strength criteria

In accordance with EC8 (CEN, 2005b) the following relation must be satisfied for all structural elements:

$$E_D < R_D \quad (2.23)$$

in which:

- E_D is the design value of the action effect, due to the seismic design situation;
- R_D is the corresponding design resistance of the element.

In particular, the combination of the seismic actions with the others is given by the following relationship:

$$F_D = G_{k1} + G_{k2} + P + E + \sum_i \psi_{2i} \cdot Q_{ki} \quad (2.24)$$

in which:

- G_{k1} and G_{k2} express the characteristic value of the permanent loads;
- Q_{ki} expresses the characteristic value of the variable loads;
- E is the seismic action;
- P are possible pre-stressed actions;
- ψ_{2i} is the combination factor considering the probability of occurrence of the variable actions in case of earthquake.

In order to verify the safety of a masonry construction, simplified formulations exist. The main strength criteria are related to the following state:

1. *in-plane behaviour*, which involves:
 - compressive-bending;
 - diagonal shear;
 - sliding shear;
2. for *out of plane behaviour*, which involves:
 - compressive bending
 - overturning of the wall.

Compressive bending phenomenon is associated to flexural behaviour. This may involve two different modes of failure. If the applied vertical load is low with respect to compressive strength, the horizontal load produces tensile flexural cracking at the corners and the pier begins to behave as a nearly rigid body rotating about the toe (rocking). If no significant flexural cracking occurs, due to a high applied vertical load, the pier is progressively characterized by a widespread damage pattern, with sub-vertical cracks oriented towards the more compressed corners (crushing). In both cases, the ultimate limit state is obtained by failure at the compressed corners (Fig. 2.24b). In order to study the problem, a proper stress distribution for the masonry in compression is introduced and the

tensile strength of bed-joints is neglecting. Referring to Figure 2.24a, the equilibrium leads to the following expression:

$$M_u = \left(\frac{N \cdot l}{2} \right) \cdot \left(1 - \frac{N}{\alpha \cdot f_d \cdot D \cdot t} \right) = \frac{\sigma_0 \cdot D^2 \cdot t}{2} \cdot \left(1 - \frac{\sigma_0}{k \cdot f_d} \right) \quad (2.25)$$

where:

- N is the axial force;
- σ_0 is the mean vertical stress;
- D is the pier width;
- t is the pier thickness;
- k is the coefficient representative of the vertical stress distribution at the compressed toe, assumed equal to 0.85;
- f_d is the design compression strength.

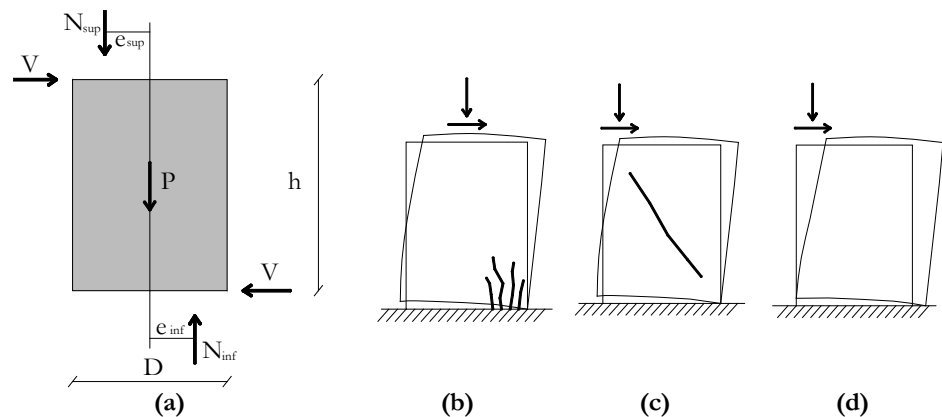


Figure 2.24 In-plane behaviour (a) action in the mean plane (b) rocking collapse; (c) diagonal shear; (d) sliding shear

In diagonal cracking (Fig. 2.24c), failure is attained with the formation of a diagonal crack, which usually develops at the centre of the pier and then propagates towards the corners. The shear strength criterion piers associated with diagonal cracking represents a complex issue, since it is the result of several interacting factors, where the heterogeneity of masonry and the quality of the base components play a dominant role. A general simplified approach for the prediction of shear strength associated to diagonal cracking was formulated by Turnšek and Cačović (1971) and is based on the assumption that the failure occurs when the principal stress at the centre of the pier attains a critical value, defined as a reference tensile strength of the material. Therefore, the diagonal shear strength criterion is expressed by the following equation:

$$V_u^f = \frac{1.5 \cdot f_{v0d} \cdot D \cdot t}{\xi} \cdot \sqrt{1 + \frac{\sigma_0}{1.5 \cdot f_{v0d}}} \quad (2.26)$$

where:

- f_{v0d} is the design conventional strength of masonry;
- ξ is a coefficient related to the pier geometric ratio.

Although the simplification of idealizing masonry as an equivalent isotropic homogeneous continuum is rather drastic, this approach has the main merit of being based on only one parameter, which is the reference tensile strength.

Finally, in sliding shear failure (Figure 2.24d), the development of flexural cracking at the tense corners reduces the resisting section; failure is attained with sliding on a horizontal bed joint plane, usually located at one of the extremities of the pier. The strength criterion is based on the formulation proposed by Mohr in 1776 and reformulated by Coulomb in 1882 and, nowadays, called Mohr-Coulomb criterion. This approach is largely adopted in design and assessment of masonry structures, defined according to the following relationship:

$$\tau_u = c + \mu \cdot \sigma \quad (2.27)$$

where

- c represents the cohesion between mortar and units;
- μ is the friction factor.

It is worth to precise that the parameters τ and σ may assume different interpretation in the practical use, depending on the statement of the criterion. A possible application of the Mohr-Coulomb criterion is the one adopted by EC6 (2005) and absorbed by the Italian Codes. Dealing with this approach, τ_u is the average ultimate shear stress referred to an effective uncracked section length and the ultimate shear capacity may be computed as follows:

$$V_u^s = \frac{\frac{3}{2} \cdot f_{v0d} + \mu \cdot \frac{\sigma_0}{\gamma_m}}{1 + \frac{3 \cdot H_0}{D \cdot \sigma_0} \cdot f_{v0d}} \cdot D \cdot t \quad (2.28)$$

where:

- μ is the friction coefficient equal to 0.4
- H_0 is the effective pier height
- γ_m is the safety factor assumed equal to 2

Another simplified approach for the sliding shear generally concerns the verification of the fascias elements. It is regulated by the following relationship:

$$V_u^u = h \cdot t \cdot f_{v0d} \quad (2.29)$$

where:

- h is the spandrel depth
- t is the spandrel thickness
- f_{vd} is the design shear strength with no axial force

The occurrence of the different aforesaid phenomena is dependent on numerous aspects, such as the geometry of the masonry panel, the boundary conditions, the acting axial load, the mechanical properties of the masonry base components, etc. Rocking generally occurs in slender piers, while bed joint sliding tends to prevail in squat piers. In moderately slender piers, instead, diagonal cracking tends to prevail over rocking and bed joint sliding for increasing levels of vertical compression.

The study of the out-of-plane behaviour is generally achieved by means of the limit analysis fully described in chapter 3 (cfr. section 3.4.2.2).

2.6. TECHNICAL CODES APPROACHES

2.6.1. Regulations for masonry buildings

The main reference codes for design and evaluation of masonry buildings are:

1. M. D. 24/01/1986, Ministerial Decree, *Norme tecniche relative alle costruzioni antisismiche*;
2. M. D. 20/11/1987, Ministerial Decree, *Norme tecniche per la progettazione, esecuzione e collaudo di edifici in muratura e per il loro consolidamento*;
3. D.M 16/01/1996, Ministerial Decree, *Technical regulation for constructions in seismic areas*;
4. OPCM 3274, 20/03/2003, Ordinance of the Prime Minister, *Primi elementi in materia di criteri generali per la classificazione sismica del territorio nazionale e di normative tecniche per le costruzioni in zona sismica* (in English: First elements in the matter of general criteria for seismic classification of the national territory and of technical codes for structures in seismic zones);
5. OPCM 3431, 03/05/2005, Ordinance of the Prime Minister, *Further changes and upgrade to the OPCM 3274/2003*;
6. M.D. 14/09/2005, Ministerial Decree, *NTC 2005 - New Technical Italian Code*;
7. M. D. 14/01/2008, Ministerial Decree: *NTC 2008 - New Technical Italian Code*.
8. ENV 1996-1-1:1995, Eurocode 6. Design of masonry structures., CEN, Brussels, Belgium.

In the following sections the rules of design and analysis of masonry buildings provided by the above regulations are described.

2.6.2. New masonry structures

The objective of the design is to create a new building which shall resist the expected forces (horizontal and vertical) with an appropriate safety margin. Starting from a structural model of the building and the expected applied forces the required sections of the structural elements have to be determined for a chosen material.

The first regulation for masonry structure was the M. D. 1987, in which seismic prescriptive rules for the construction of new buildings are given. The design rules prescribed by the norm concerns essentially the number of storeys, the minimum wall thickness, the seismic global behaviour. In particular, the presence of perimeter RC tie beams or metal ties is prescribed and the box type global response must be guaranteed by means of rigid diaphragms (cfr. 2.5.3.1).

The M.D. 1996 approaches the issue by the seismic viewpoint. The norm introduces specific prescription rules about the material characteristics, the design of particular devise (e.g. RC tie beams, metal ties, etc.) and the global behaviour. Explicit rules provided by the Decree are: the symmetrical shape and the compactness of the plan according two orthogonal directions; the arrangements of RC or metal lintels adequately anchored to the piers and of perimeter RC tie beams; the minimum distance between the foundation level and the first floor intrados; the wall minimum thickness; alignment of the openings inside the facade.

The OPCM 3272 (2003), successively modified by OPCM 3431 (2005) represents a very innovative code for seismic analysis achievement.

Apart the introduction of the new seismic zonation (cfr. 1.5) the Ordinance sanctions the Ultimate Limit State Method as the only reliable and accepted procedure for the seismic calculus. The verifications are based on the strength criteria described in detail in section 2.5.2.6.

The M. D. 2005 and 2008 have substantially absorbed the provisions of the Ordinance. The principal rules prescribed by the code are:

- the masonry building shall exhibit a global box-type behaviour;
- the elements shall be strongly coupled;
- the connections among orthogonal walls and among walls and horizontal floor system shall be guaranteed by means of appropriate RC tie beams or metal ties;
- each masonry panel shall be both bearing element and braced one;
- the floor slab should behave as a rigid diaphragm;

- the conventional slenderness (λ), defined as the ratio between the effective height and the effective thickness of the wall, should not be greater than 20.

Moreover the allowed minimum wall thicknesses for bearing walls are provided. Also the verifications are based on the aforementioned strength criteria (cfr. 2.5.2.6).

The Italian Technical Approaches are conformed to the Eurocode 6 (2005a), with some differences. In particular, the EC6 does not permit to achieve a simplified analysis for well-defined typology of masonry buildings, as provided by the Italian Codes; the slenderness ratio should not be greater than 27; the reduction factors of slenderness and eccentricity (Φ) are averagely bigger, so that the design strength are upper than the ones considered by the Italian regulations. Furthermore, the verification of walls subjected to shear loading conditions is based on the Mohr-Coulomb shear strength.

2.6.3. Existing masonry structures

The objective of the evaluation is to determine how an existing building will respond to a given system of forces. This corresponds to an analysis of a building structure where the structural elements, the materials and the dead loads are given. It is not desired to calculate a worst case scenario by choosing a conservative model and making conservative assumptions on the material properties but to assess the most probable behaviour of the building subjected to the applied action. Thus, the real material properties and the real loading have to be taken without any safety factors as these would falsify the results. Also the model should be as close as possible to reality taking into account all structural elements that help to support the applied forces.

The correct evaluation of historic masonry building is very important in order to protect the built up heritage by means of specific strengthening interventions. Nonetheless, this issue cannot be tackled by adopting the same criteria of the design of masonry building. In fact, in some cases, the adoption, for historical masonry buildings, of the same classes of predictive models developed for new constructions can mislead about the real behaviour of the structures (Binda and Saisi, 2005; Magenes, 2006), and can bring to the choice of useless or even harmful interventions for their seismic protection (Modena et al., 2009).

The most recent seismic events confirmed limits and consequences of some type of interventions, concurrently corroborated also by extensive experimental researches, but also the effectiveness of new methods based on the use of both traditional and innovative materials and techniques.

The Technical Codes approaches for existing buildings are based on the concept of *seismic improvement*.

The M. D. 1986 firstly defined in Italy this concept. According to this Decree, in the case of minor interventions that do not significantly alter the overall structural behaviour, it is not necessary to undertake the seismic upgrading, i.e. the increase of seismic performances to the level required for new constructions. Dealing with the successive M. D. 1996, the concept of *seismic improvement* was referred to the assessment of cultural heritage buildings, since it was considered compatible with their conservation requirements. The norm also prescribes some strengthening techniques to be adopted for improvement and upgrading interventions, which reflected the knowledge and state of art of the years when these were issued.

In this context, a significant step ahead was moved with the enacting of the OPCM 3274 (2003) and OPCM 3431 (2005), which brought significant enhancements to the normative process by introducing the knowledge levels (LC – *Livelli di Conoscenza*, in Italian) and innovative calculation methods in order to assess the seismic vulnerability of ancient masonry constructions. Moreover, the Ordinances set up new strategies for the intervention on existing structures, requiring the designer to estimate the higher safety level reached by means of improvement intervention. In particular, the Chapter 11 of the Ordinance gives an extent treatment of the existing constructions.

Two main intervention typologies are distinguished:

1. *Seismic retrofit*: this type of intervention make the structure able to resist to seismic load according to the design criteria for new buildings.
2. *Seismic improvement*: it consists into specific intervention aimed at upgrading the structural performance.

The norm prescribes the seismic evaluation of an existing building in case of:

- vertical or horizontal addition;
- change of the use destination of the building, when the loading condition increases of 20% as respect to the original one;
- significant structural interventions.

A fundamental issue is the knowledge level of the building, concerning the structural and geometrical features, the details and material properties. Referring to this latter aspect, the norm describes the types of tests to perform on existing masonry in order to exactly compute the mechanical properties, with particular reference to the constitutive law.

Three LC are defined as follows: LC1, LC2 and LC3. To the first knowledge level (LC1) corresponds the lower grade of knowledge, while to the third one

(LC3) corresponds the higher one. To each of these levels, a confidential factor (FC, *Fattore di Confidenza*, in Italian) is assigned, as follows:

1. LC1: FC1 = 1.35
2. LC1: FC1 = 1.20
3. LC1: FC1 = 1.00

The M. D. 2008 has essentially absorbed and arranged the contents of the Ordinance. The EC8 (EN 1998-3, 2005), instead, is not updated with the latest findings and methods introduced in Italy, as for instance the above mentioned concept of *seismic improvement*, which has a significant influence on the design of interventions. Moreover, the Italian regulations provides the general criteria to select the better technique of intervention. For example, the norms prescribe that interventions should be applied as much as possible regularly and uniformly on the building, so to avoid uneven distributions of strength and stiffness. These simple principle derive undoubtedly by the observation of damages experienced by buildings in the past recent years.

The improvement of the seismic performance of a building may be obtained not only by employing traditional techniques but also by using innovative tools and materials (e.g. FRP laminates or steel in order to increase the low tensile strength of masonry structural elements). However, the conservation of original materials and functionality of the structure is the highest priority, therefore interventions should avoid significant alterations to the original structure and provide compatibility to the largest extent.

In conclusion, the EC8 does not deal with the topic of interventions on masonry buildings in a sufficiently consistent and organic way as respect the Italian norms.

Chapter 3

Seismic vulnerability assessment methodologies

3.1. THE HISTORICAL HERITAGE IN ITALY

Constructions may be classified as historical when they become part of our built heritage. Naturally, this does not necessarily mean that the state of an historical building coincides with the monumental one. Historical buildings carry their cultural significance attached not only to their formal architectural language but also to their specific structural features, applied materials and building techniques and, by being old, they have also been a part of Human life. Therefore, scientists have to put their knowledge at the service of culture, in order to respect the historical value of the architectural heritage and to guarantee appropriate safety levels, changing the original design as little as possible.

On the base of the above observations, the historical heritage may be generally subdivided in two categories: monumental buildings and historical centres. Monumental constructions are unique buildings that can have a great architectural and artistic values and are characterized by their own unique history. Therefore, monuments represents the highest pieces of the cultural heritage of a Nation, they including palaces, towers, castles, obelisks, theatres, churches, monasteries, abbeys, triumphal arcs, bridges, etc. In Italy, the monumental heritage is particularly rich (Figs 3.1-3.3).

On the other hand, historical centres represents the so called "minor" architecture. The construction typologies vary from isolated to buildings in aggregate, generally characterized by a rural origin and therefore by a poor level of material choice and construction technique, but worth of being preserved as it is a relevant part of the history of the Country (Fig. 3.4).

In Italy, likewise in all European countries, the intent to preserve the historical heritage is very strong. Large areas of the Mediterranean area are unfortunately characterized by a high level of seismic hazard and, in most cases, the vulnerability of all ancient masonry constructions, monuments or historical centres, is relevant. In fact, it is well known that earthquakes have always represented the main cause of damage and losses to the cultural built heritage.

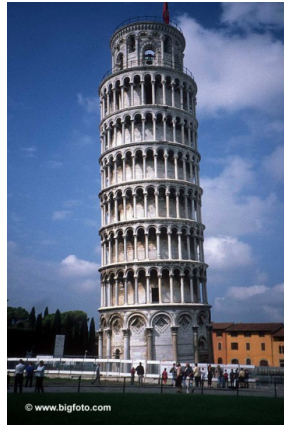
Thus, the necessity to protect such buildings represents an important task for allowing them to survive destroying quakes without collapse and safeguarding the human life. All ancient masonry buildings, indeed, were constructed following the rule of thumb, learning from the experience of previous similar structures. For this reason, they are particularly vulnerable to dynamic actions, especially seismic loads. This awareness and the will to conserve the historic heritage have led to the definition and implementation of several vulnerability assessment model both for the local for the large scale analysis. In the first case, the seismic vulnerability of a single building is assessed on the base of detailed model. In case of territorial analysis, instead, the vulnerability assessment is performed on large areas by means of simplified or quick procedures.



(a)

(b)

Figure 3.1 Monumental buildings in Naples: (a) Royal Palace; (b) New Castle



(a)



(b)

Figure 3.2 Italian Monumental buildings:(a) Pisa Tower and (b) Main Cathedral in Milan



(a)



(b)

Figure 3.3 Italian Monumental buildings:
(a) St. Chiara Monastery in Naples and (b) La Scala theatre in Milan



(a)



(b)

Figure 3.4 Samples of Italian historical centres:
(a) St. Stefano di Sessanio (AQ) and (b) Amalfi (NA)

3.2. METHODOLOGICAL APPROACHES

The seismic vulnerability of a constructions may be defined as its susceptibility to suffer a certain damage level under a seismic event. Therefore, the scope of a seismic vulnerability assessment methodology is to provide a measure of the building propensity to be damaged if hit by an earthquake. In operative terms, a vulnerability estimation approach must correlate the seismic hazard evaluation to the physical damage suffered by the built system depending on the structural, geometric, technological characteristics able to affect the seismic building behaviour.

Several methods for the vulnerability assessment exist and as many are the attempts to provide criteria to classify them.

Depending on the analysis type, three main kinds of vulnerability approaches may be distinguished as follows:

- 1) *Observed vulnerability methods*, based on statistical observations of recorded damage data of past seismic events as a function of the felt intensities. Macroseismic models are representative of this type of methods. For each building examined a vulnerability curve is developed, in which the seismic intensity is correlated to the average expected damage, by means of damage probability matrices, through statistical elaborations. In general, observed damage data are limited and are not able to be representative of each building typology and of each intensity grade, so they are often supported by mechanical analysis.
- 2) *Expert methods*, based on judgment derived from knowledge or experience. The aim is the vulnerability evaluation of a built system, weighting the effects of structural deficiencies, from observed correlations between damage and structural characteristics or from simplified mechanical models. This is the case of method based on score assignments.
- 3) *Analytical methods*, based on numerical models of building structural response. The Capacity Spectrum Method (CSM), which gets more extended treatment in Chapter 4, is representative of this type of methodology. The mechanical models definition, indeed, is based on parameters such as geometrical, technological and dynamical aspects, (fundamental period, ductility, peak acceleration, etc). The analysis is aimed to the capacity curves development by means of appropriate numerical models. The capacity curve is a spectral curve and the structural response is assessed as a demand spectrum. The damage is described by the fragility curves, which represent the probability for the structure to suffer seismic damages.

Another classification of the vulnerability assessment methodologies concerns its field of application. In fact, on the base of the detail of analysis and of the available data, local or large scale methodologies may be distinguished. In the first case, the vulnerability analysis is carried out on the single building or structural unit; in the second case, the analysis is performed by considering buildings within a whole territorial zone. The purposes of the two typologies of analysis are different and dependent on the accuracy and the typology of the available information. In general, the observed and the expert vulnerability models are adopted for large scale analysis, while the analytical models are employed to study the behaviour of isolated buildings, especially monumental constructions. In fact, in this case, parameters as the architectural and historical importance have to be considered, in addition to the structural response.

On the base of the scale of the method, three different levels of knowledge may be defined as follows:

- *Level I*: the vulnerability analysis is traced back to a simple census, in which very few details are surveyed and a typological identification of the constructions is used (church, convent or monastery, palace, tower, etc.); this level of accuracy is related to large scale vulnerability estimation approaches.
- *Level II*: in the census phase the individual buildings are surveyed with quick forms, in which certain information of structural importance are identified (for instance, the structural regularity, the material quality, the state of maintenance, etc.); this second level suits to quick or simplified procedure.
- *Level III*: a vulnerability estimation may be attributed to each building by means of a meticulous and detailed survey; this last level of knowledge provides all the necessary information for the application of a mechanical model.

In so many cases, the employment of one method is not advised, but the combined application of them. In fact, some hybrid techniques have been developed. The resumptive draft of vulnerability analysis is shown in Table 3.1.

Table 3.1 Resumptive draft of vulnerability analyses

Levels of knowledge	Observed	Expert judgement	Analytical
	Macroseismic model	Simplified models	Mechanical model
Level I	Vulnerability index: typology	Simplified analysis: typology	Capacity Curve: typology
Level II	Vulnerability index: single building	Simplified analysis: single building	Capacity Curve: single building
Level III	-	Vulnerability analysis: single building	Capacity Curve: single building

3.3. ISOLATED MASONRY BUILDINGS

3.3.1. Local scale methodologies

3.3.1.1. SAVE

The SAVE methodology (in Italian, *Strumenti Aggiornati per la Vulnerabilità sismica del patrimonio Edilizio e dei sistemi urbani* – Updated Tools for the Seismic Vulnerability Evaluation of the Italian Real Estate and of the Urban Systems) is a simplified procedure developed into the GNDT Research Project coordinated by Mauro Dolce and Giulio Zuccaro (Dolce and Moroni, 2005).

The procedure allows to evaluate the vulnerability of buildings and aims at reducing the seismic risk, on the base of a simplified calculation model. This method permits the evaluation of the seismic acceleration corresponding to two different limit state: the Collapse Limit State (CLS) and the Operational Limit State (OLS).

The structural analysis may be preformed level by level and according to orthogonal seismic directions, by means of a specific spreadsheet implemented by the authors and noted as VC both for masonry and for reinforced concrete structures. For each level and direction examined, the program provides the acceleration value producing the achievement of the two limit state considered. The minimum PGA value calculated for each of the two performance level represents the collapse acceleration of the structure. The PGA is referred to the specific construction site and also to the ground rock (a_g).

In particular, the procedure VC for RC frames has been tested on some large scale experimental models of RC structures, which were subjected to shaking table and pseudo-dynamic tests. A comparison between the experimental and numerical results have shown that the VC procedure represents a valuable tool for the evaluation of the seismic vulnerability of single buildings with RC frame, having low lateral strength and ductility, as often happens in the real cases.

For masonry structures, the in-plane shear and compressive-bending failure mechanisms are assumed. The shear resistance of the single pier is evaluated on the base of the noted Tuck and Caçovic formulation according to (2.25) relationship. As a consequence, the global shear strength of each single storey of the building in each direction is obtained as the sum of the single piers shear resistance in the same direction, as follows:

$$V_j = \sum_i V_{ij} \quad (3.1)$$

The pier stiffness is evaluated as follows:

$$K_{i,j} = r \cdot \frac{G \cdot A}{\chi \cdot h_{\text{def}}} \cdot \frac{1}{1 + \frac{G \cdot h_{\text{def}}^2}{\chi \cdot E \cdot b^2}} \quad (3.2)$$

where:

- r is a reduction factor, it taking into consideration the fractured stiffness and ranging between 0.5 and 1;
- h_{eff} is the pier deformable height equal to the openings dimensions;
- b is the pier width;
- $A_{i,j}$ is the pier horizontal section area;
- χ is the shear factor

The Young (E) and the Shear (G) moduli are computed as follows:

$$E = 6 \cdot G \quad (3.3)$$

$$G = 1100 \cdot \tau_k \quad (3.4)$$

In order to aid the analysis, the spreadsheet is subdivided into the following sections:

- 1) General data: inter-storey height, masonry density, loads;
- 2) Mechanical parameters of walls: elastic and shear moduli, inertia, stiffness
- 3) Resumptive table of the structural data and loading conditions for each direction (X and Y) automatically calculated by the program;
- 4) Results in terms of PGA, a_g and return period (T_R) for each of the considered seismic directions.

Dealing with this method, the vulnerability indicator is provided as the ratio between the collapse acceleration of the structure and the corresponding demand spectra peak accelerations given by the codes. The index is, finally, calculated as follows:

$$I_{\text{SAVE}} = 1 - \frac{a_{\text{Collapse}}}{a_{\text{PGA}}} \quad (3.5)$$

The procedure also provides indications about the structural regularities, the equivalent static forces associated to the masses and the structural ductility.

The reliability of results is closely related to the information quality and to the model accuracy.

3.3.1.2. FaMIVE

The FaMIVE (Failure Mechanisms Identification and Vulnerability Evaluation) analytical method is an integrated procedure aimed at the seismic vulnerability evaluation of single buildings (D'Ayala and Speranza, 2002).

This methodology is based on the preliminary detailed survey of the building to investigate, in order to collect the essential structural and geometrical data. In the survey phase, the identification of the most vulnerable factors and the detection of strengthening devices are very important for the structural appraisal.

Data collected are, afterwards, stored and processed by means a specific spreadsheet elaborated by the authors (Fig. 3.5). The analysis performed on the building is static equivalent type and aims to calculate the lateral loads multiplier which trigger the onset of a specific failure mechanism. This factor, expressed as a percentage of the gravity acceleration (g), allows to predict possible damages and vulnerability levels for the analysed structure, in relation to the expected seismic intensity.

Two important innovative aspects must be highlighted: the procedure takes into account the out-of-plane failure mechanisms as possible collapse causes and, furthermore it permits to reduce the obtainable vulnerability by giving the possibility of introducing specific strengthening devices. In particular, the program considers eight elemental out-of-plane collapse mechanism by means of the limit state analysis, shown schematically in Figure 3.6. Furthermore, it also take into account the occurrence of local collapse, by conducting a storey by storey analysis.

The analysis is performed for each building façade, considering a maximum of five storeys.

INSPECTION FORM FOR THE SURVEY OF ORDINARY BUILDINGS			
Town	RA DEI CQ	Build.	1
Cad. sheet		Type of use	R
Address		Particel n.	
%of use	1	Surveyor	BARBARA
Date	5/5/00		
1 URBANISTIC DATA			
1-1 Block access and escape routes	G	1-4 Position of building within the block	I
1-2 Shape and composition of the block	0	1-5 Connection of the façade to adjacent walls	2C
1-3 Number of buildings in the block	1		
2 GEOMETRIC CHARACTERISTICS OF THE FACADE			
2-1 Façade orientation	S	2-5 Total height of the façade	4.8
2-2 Number of storeys of the building	2	2-6 Presence of gable	<input type="checkbox"/>
2-3 Number of storeys of the façade	2	2-7 Gable height (if present)	
2-4 Length of the façade	8.24	2-8 Additional corner in the façade	<input type="checkbox"/>
3 GEOMETRIC CHARACTERISTICS OF OPENINGS			
3-1 Number of openings per storey	3-3 Openings layout		Disp. n./k.
			left right
storeys			E2 1
2 1 0 0 0			R R
openings	2 2		3-4 Lateral pier
			3-5 Height of upper horizontal spandrel
			0.3
3-2 Estimated opening dimensions	b h		
	0.7 1		
4 PLAN GEOMETRIC CHARACTERISTICS			
4-1 Thickness at basis of façade wall	0.46	4-4 N. int. bearing walls // to the façade	1
4-2 Thickness reduction at the top (%)	0.33	4-5 Total length normal to the façade	4.26
4-3 N. int. bearing walls perp. to façade	1		
5 STRUCTURAL CHARACTERISTICS			
5-1 N. storeys with vaulted structures	0	5-7 Level of maintenance of masonry	B
5-2 Horizontal structure typology	A	5-8 Connection at edges	G G
5-3 Direction of hor. Structure	P	5-9 Out of verticality	<input type="checkbox"/>
5-4 Roof structure typology	A	5-10 Ties/ring beams per storey in the façade	
5-5 Direction of roof	P	storey	2 1 0 0 0
5-6 Masonry type	B1	ties/ring beams	0 M
6 FURTHER VULNERABILITY ELEMENTS			
6-1 Presence of vertical addition	<input type="checkbox"/>	6-3 Specific weight reduction %	
6-2 Dimensions of vertical addition	H I	6-4 Chimney flue within the façade wall	<input type="checkbox"/>

Figure 3.5 FaMIVE spreadsheet

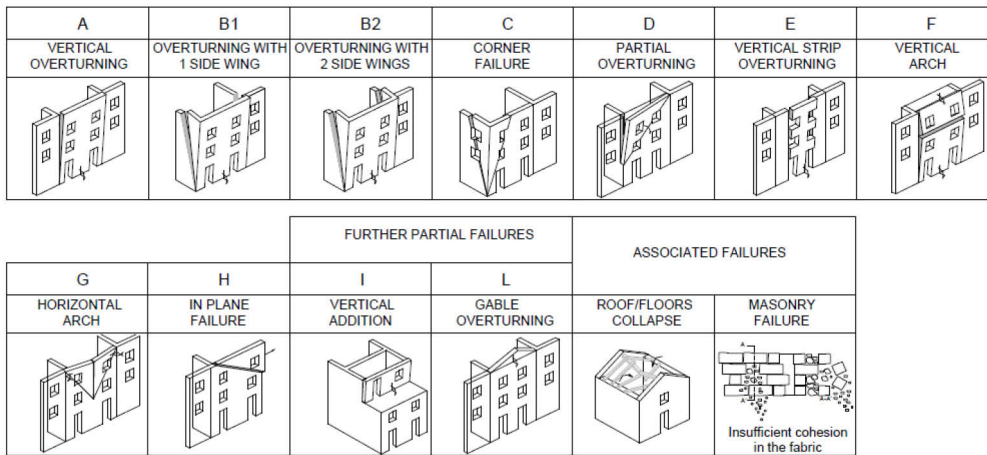


Figure 3.6 Out-of-plane collapse mechanism identified by FaMIVE program

Other innovative characters of this technique lay in the inclusion of proper frictional behaviour for the masonry, in the accurate modelling of the restraint exerted among adjacent walls and in the precise simulation of the effect of strengthening. This allows a more comprehensive and realistic study of possible failure mechanisms, by selecting adequate criteria of intervention.

The FaMIVE approach was applied during a multidisciplinary research activity, funded by the GNDT and the Marche Region (Italy) aimed at the seismic microzonation of four market towns chosen by size and location to be representative of the urban centres in its territory.

The results of this analysis have proven the reliability of the methodology, that is able to provide a realistic seismic behaviour of the structure.

FaMIVE procedure is intermediate between simplified and mechanical models.

3.3.1.3. VULNUS

The VULNUS methodological approach allows to estimate the seismic vulnerability of a single building using the fuzzy-set theory and the definition of collapse multipliers (Bernardini et al., 1990). The method was set up by researchers of University of Padova in the second half of the '80s. The approach is based on building survey, in order to collect geometrical and structural information, handled through qualitative judgement.

A collapse multiplier I_1 for in-plane behaviour considering shear collapse at ground floor is described by means of the following equation:

$$I_1 = \frac{\min(V_x, V_y)}{W} \quad (3.6)$$

where:

- I_1 is the collapse multiplier for in-plane behaviour considering shear collapse at ground floor
- W is the total structural weight
- V_x and V_y are the strengths at mid-storey height of the ground floor in two orthogonal directions considered (X and Y) and computed according to the following relationship:

$$\{V_x, V_y\} = \{F_x, F_y\} \cdot \frac{f_t}{1.5 \cdot \omega} \cdot \left\{ 1 + \frac{W}{f_t \cdot (F_x + F_y)} \right\}^{1/2} \quad (3.7)$$

In the equation (3.7) $\{F_x, F_y\}$ represents the total areas of the wall in the X and Y directions, f_t is the tensile strength of masonry and ω is the regularity plan coefficient. The calculation is based on the hypothesis of wall rigidly jointed to the slabs and subjected to uniform vertical compression.

The collapse multiplier I_2 for out-of-plane behaviour is, instead, found as the ratio between the out-of-plane flexural strength of the most critical external wall and the total weight, evaluated by summing the resistance of the vertical (I_2^I) and horizontal strips (I_2^{II}):

$$I_2 = \min_i (I_2^I + I_2^{II})_i \quad (3.8)$$

Once I_1 and I_2 indexes have been calculated, a third multiplier (I_3) may be evaluated, which is the weighted sum of the scores of seven partial vulnerability factors:

$$I_3 = \sum_i \frac{W_i \cdot S_i}{45 \cdot 3.15} \quad (3.9)$$

where:

- the S_i is the score ranging from 0 (good) to 45 (poor); the values of S_i are shown in Table 3.2
- W_i is the weight of the vulnerability factor (Table 3.3).

The mean absolute acceleration response A of the building (i.e. maximum base shear divided by total weight) is calculated as well as an uncertainty factor (a). This factor depends on the qualitative judgement expressed on the base of Italian databases created by means of several surveys performed in the past years.

Table 3.2 Score values corresponding to the vulnerability classes

Class	Score S_i
1. Good or corresponding to code	0
2. Almost good	15
3. Almost poor	30
4. Poor or unsafe	45

Table 3.3 Weights related to the vulnerability factors of the constructions

Vulnerability factor	Weight W_i
1. Wall system quality	0.15
2. Soil and foundation interaction	0.75
3. Floors interaction	0.50
4. Elevation regularity	0.50
5. Roof interaction	0.50
6. Interaction of non-structural elements	0.25
7. General maintenance conditions	0.50
Total	3.15

Following the calculation of the third index, a linguistic relationship between the uncertainty factor (a) and I_3 is established, in accordance to the Table 3.4.

Table 3.4 Linguistic relationship between I_3 and (a)

$j = 1$	If I_3 is very large than (a) is very large
$j = 2$	If I_3 is large than (a) is large
$j = 3$	If I_3 is medium than (a) is medium
$j = 4$	If I_3 is small than (a) is small
$j = 5$	If I_3 is very small than (a) is very small

Finally, the fuzzy set theory is applied in order to estimate the vulnerability of the construction. In particular, the probability of exceeding a given damage limit state for a building is a function of the aforementioned parameters:

$$V = f(I_1, I_2, A, a) \quad (3.10)$$

3.3.1.4. Mechanical approaches

The vulnerability assessment approaches based on mechanical methodologies allow to evaluate the expected seismic performance of a structural system by means of the development of the capacity curve of the structure.

The most applied procedure is the Capacity Spectrum Method (CSM), which aims at the identification of the performance point (PP) of the structure. In accordance to the American provisions ATC 40, the PP represents the graphical intersection of the global force-displacement capacity curve, obtained by performing a static pushover analysis, with the response spectrum representing the earthquake demand. This method will be fully described in section 4.4.1.1.

Nowadays, the most recent trends in the field of mechanical vulnerability assessment procedures lead to operate with simplified numerical models. In United States, the most worldwide known methodological approach is HAZUS, (acronym for HAZard in U.S.) elaborated by the Federal Emergency Management Agency (FEMA,1999), but often used in other built areas. The aim of the methodology is the estimation of the damages suffered by a construction subjected to a seismic action by means of the PP calculation and its comparison with defined damage limit states. To this purpose, thirty-six different models have been achieved, they providing specific capacity curves for each building class identified in USA. Therefore, the design point is obtained as the intersection point between capacity and demand curves, as depicted in Figure 3.7.

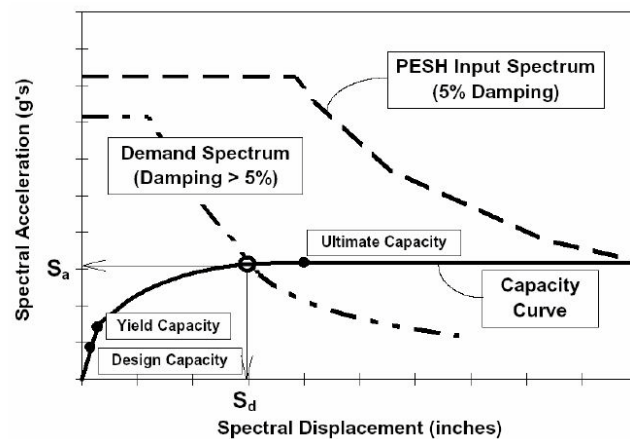


Figure 3.7 Building capacity curve vs. demand spectrum (FEMA, 1999)

On the base of the capacity curve, it is possible to develop the fragility curves related to the analysed structure. A fragility curve is the graphic representation of the probability of reaching or exceeding a specific damage limit state for a given ground motion demand.

According to HAZUS approaches, fragility curves are assumed to be represented by lognormal functions of the expected performance displacement S_d and of the mean displacement limit states $S_{d,ds}$, as in the following equation:

$$P[ds/S_d] = \Phi \cdot \left[\frac{1}{\beta} \cdot \ln \left(\frac{S_d}{S_{d,ds}} \right) \right] \quad (3.11)$$

in which:

- Φ is the standard normal cumulative density function
- β is the lognormal standard deviation of spectral displacement for the damage limit state

The variability of a damage state is given by the following equation:

$$\beta_{ds} = \sqrt{(\text{CONV}[\beta_C, \beta_D])^2 + (\beta_{k,ds})^2} \quad (3.12)$$

where:

- β_D represents the variability of the demand spectrum;
- β_C describes the variability of the capacity spectrum;
- $\beta_{k,ds}$ describes the uncertainty in the estimation of the damage state threshold;
- CONV represents the convolution process applied to the variability of the ground motion demand and the capacity response necessary to achieve, since the demand spectrum depends on building capacity.

Dealing with the normal practice, the capacity and the demand are assumed independent variables, so the total variability may be computed by means of a simplified form considering the square root sum of the square value (SRSS) of all the three uncertainty contributors:

$$\beta_{ds} = \sqrt{\beta_C^2 + \beta_D^2 + \beta_{k,ds}^2} \quad (3.13)$$

Nevertheless, because of the difficulty in determining the variability parameter $\beta_{k,ds}$, the value of the standard deviation $\beta_{k,ds}$ is alternatively calculated as a function of the structural ductility μ , as follows:

$$\beta = 0.45 \cdot \ln(\mu) \quad (3.14)$$

Finally, fragility curves may be developed considering four different damage limit states of the building. In fact, according to the Performance Based Design (PBD) methodology the displacement $S_{d,ds}$ may be consider as a function of both the yielding (d_y) and the ultimate (d_w) displacements of the structure (Cattari et al., 2004). Thus, the following four damage limit states are defined:

- $S_{d1} = 0.7 d_y =$ no damage
- $S_{d2} = 1.5 d_y =$ light damages
- $S_{d3} = 0.5 (d_y + d_u) =$ significant damages
- $S_{d4} = d_u =$ near collapse

Fragility curves corresponding to the different damage limit states are shown in Figure 3.8.

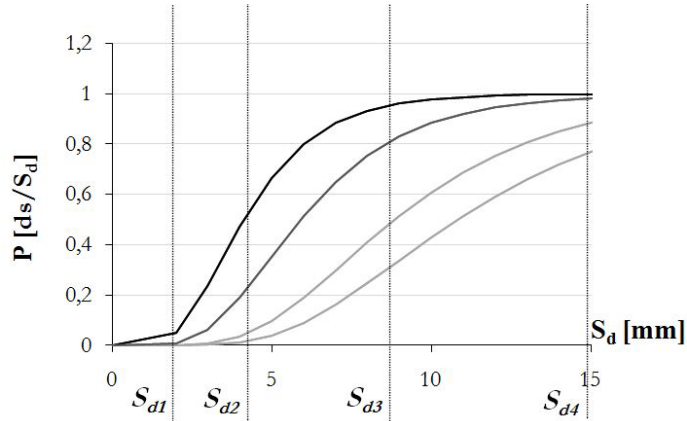


Figure 3.8 Fragility curves corresponding to the different damage limit states

In Europe, an important methodology similar to the American HAZUS and based of mechanical approaches was developed in the framework of RISK UE project (*An advanced approach to earthquake risk scenarios with applications to different European towns*), aimed to the reduction and mitigation of seismic risk. This approach, applied to seven different European towns, is essentially based on the identification of the urban system deficiencies. To this purpose, seven detailed Working Paper (WP) have been developed, related to the seismic risk issue. In particular, “Vulnerability of buildings” and “Vulnerability assessment of historical and monumental buildings” were the topics of WP4 and WP7 respectively.

The RISK UE methodology distinguishes among three different levels of analysis for the vulnerability estimation of the European built up system. The level method depends on the knowledge grade and on the scope of the scenario study. The I and the II level approaches may be classified as macro-seismic methods, used for a large scale vulnerability analysis. Similarly to HAZUS criterion, these procedures have been defined specifically for the European building typologies. These two approaches will be treated in the section 3.3.2.5.

The III level methodology, instead, is applied on the local scale, since it is necessary to define both the geometrical and the structural features and the dynamic parameters of the examined constructions. Therefore, the analysis may

be performed both on the whole structural system or on the single macroelement. In this case, a capacity curve may be defined for the most vulnerable macroelements by means an appropriate numerical model (e.g. FEM or Macroelement modelling techniques, see par. 2.5.3.3). The vulnerability assessment is, finally, achieved by applying the CSM, similar to that adopted by HAZUS.

3.3.2. Large scale methodologies

3.3.2.1. *Damage Probability Matrix Method*

The Damage Probability Matrix (DPM) method is an observed method based on the idea that a set of buildings having the same structural typology would show the same structural response under seismic loading conditions and, consequently, the same level of damage. Therefore, a DPM expresses the statistical distribution of damage grades for different macroseismic intensities. Each element of the matrix is defined by the following expression:

$$\text{DPM}(\text{DV}, \text{I}, \text{T}) = \text{P}(\text{DV} \mid \text{I}, \text{T}) \quad (3.15)$$

in which:

- DV is a given damage grade
- T is a specific structural typology
- I is the earthquake intensity, normally described by some macroseismic scale, for instance EMS 98

The DPM vulnerability model establishes a direct correspondence between vulnerability classes and building typologies, depending on the employed macroseismic scale. According to EMS 98, six different vulnerability levels (A ÷ F) are associated to building typologies, grouped for structural material (masonry, reinforced concrete, steel and wood typologies). Thus, the seismic behaviour of the investigated buildings, in terms of apparent damage, may be examined making directly reference to the seismic behaviour of the six defined vulnerability classes.

The Figure 3.9 shows the six vulnerability classes (A ÷ F) associated to the structural typology according to the EMS 98.

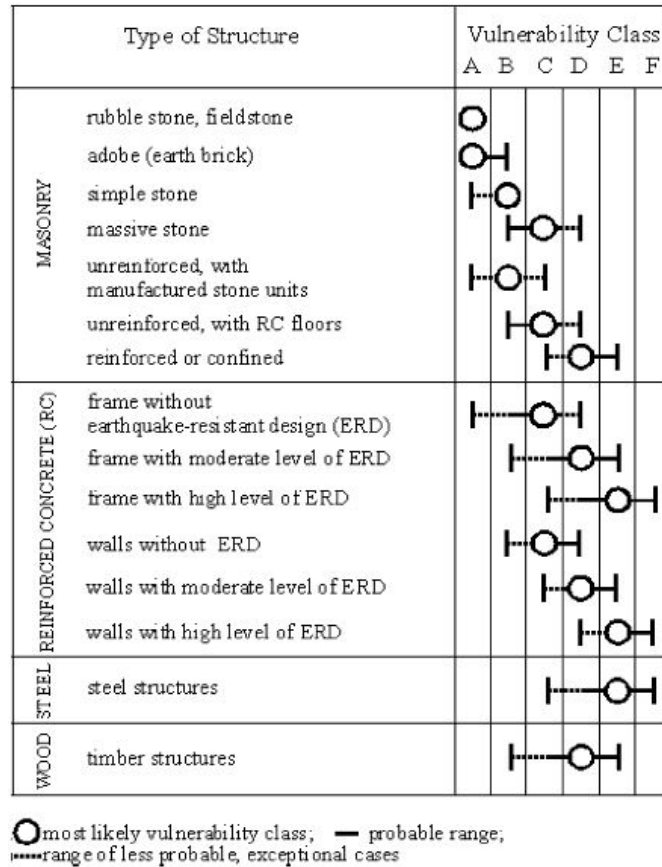


Figure 3.9 EMS-98 building typologies and correlated vulnerability classes.

According to equation (3.15) the DPM would be a matrix having the probability of reaching a specific level of damage, for a given earthquake intensity. The DPM format has become one of the most widely used forms to define the probable distribution of damage, adapted by several other methodologies. However, one of the main disadvantages of this approach is the reference to qualitative and fuzzy measures of the quake intensity, rather than considering parameters for seismic action definition (for instance, acceleration or displacement).

3.3.2.2. The I level GNDT methodology

The I level GNDT methodology, (Corsanego and Petrini, 1994) is an observed vulnerability method based on damages effectively found following the strong

seismic events that have hit the national territory. This methodological approach refers to the above described DPM format.

Therefore, the GNDT I level subdivides the investigated built-system into homogeneous subgroups, by identifying specific building typologies, and defines for each one a statistical distribution of the expected damage.

According to this procedure, the earthquake is considered in terms of macroseismic intensity and the damage is described through qualitative levels, associated with the evidence of particular damaging states or of partial or total collapse.

In particular, three vulnerability classes (A, B and C) are identified, to each one a specific DPM is ascribed. These GNDT DPM probabilistic distributions have been developed on the base of statistical data related to past earthquake subsequently updated and regionalized referring to several seismic events.

The most significant reference earthquake in terms of available data is the Irpinia event occurred in 1980 (Braga et al., 1982), on the base of which the GNDT DPM have been opportunely drawn.

In order to assess the construction vulnerability, all the necessary data are collected in a I level form, divided in the following eight sections:

1. general data related to the building identification, town, team surveyor, etc;
2. location related to the configuration of the building (aggregate or isolated), toponymic information, etc;
3. geometrical data, referring to surfaces, inter-storey heights, minimum or maximum height, etc;
4. use destination, estate and percentage of use;
5. age and type of interventions, etc;
6. state of conservation of finishing and systems;
7. structural typology: main horizontal and vertical partitions;
8. damage level and extension.

It can be pointed out that eighth section is conceptually different respect the other, because it concerns the possible damages of the examined constructions. In fact, in this section the damages of the constructive system (vertical and horizontal structures, stairs, etc) are grouped in four matrixes and codified by means of letter (from A to F).

Each line of the matrix refers to the storey of the building from the bottom to the top. The damage indicator D_{ij} for each level is calculated by assigning to each vulnerability class A, B, C, D, E and F the corresponding numerical values: 0, 0.2, 0.4, 0.6, 0.8, 1.

$$D_{ij} = E \cdot L + \frac{1-E}{3} \cdot M \quad (3.16)$$

where:

- M represents the highest observed damage level;
- L is the most frequent damage;
- E is the damage extension;

The value of D_{ij} ranges from 0 to 1. The damage index of the entire structure is given by the following formula:

$$d = \sum_{ij} S_i \cdot F_j \cdot D_{ij} \quad (3.17)$$

in which F_j are the mass proportional to the volume or to the area of the generic j -level, while S_i are the mass proportional to the economic influence of the same floor.

3.3.2.3. The II level GNDT methodology

The quick GNDT II level procedure was developed in the area of the activities of GNDT (*National Group for Defence from Earthquakes*) over the last twenty years. The GNDT II level method is based on the original Benedetti and Petrini's (1984) form, commonly used both on the local and on the large scale vulnerability assessment. The original form is shown in Table 3.5.

Table 3.5 The Benedetti and Petrini's original survey data form.

Factors	Classes score (s)				Weight (w)
	A	B	C	D	
Organization of the vertical structures	0	5	20	45	1
Nature of the vertical structures	0	5	25	45	0.25
Location of the building and type of foundation	0	5	25	45	0.75
Planimetry	0	5	25	45	1.5
Planimetry: compactness	0	5	25	45	0.5
Regularity	0	5	25	45	variable
Type of slabs	0	5	15	45	variable
Roofing	0	15	25	45	0.75
Details	0	0	25	45	0.25
Physical conditions	0	5	25	45	1

Therefore, the GNDT II level approach is an expert judgement based technique aiming to estimate the seismic vulnerability of buildings, by means the calculation of an appropriate vulnerability index. This index I_v is assigned to each examined

construction after a visual inspection aiming to identify the primary structural system and the significant seismic deficiencies.

The GNDT II level form has been developed both for masonry and reinforced concrete structures. The eleven parameters recognized as the most important in controlling masonry building damage caused by earthquakes are listed in Table 3.6.

Each factor is differentiated into four classes indicated with A, B, C and D, where A and D represent the lowest and highest vulnerability grade, they being characterized by a score (s) equal to 0 and 45, respectively. A given weight (w) is assigned to each vulnerability factor aiming at highlighting the most significant parameters in determining the structural behaviour toward earthquakes.

So, the vulnerability index I_v is calculated combining, by a weighted average, the different scores and the relative weights attributed to these parameters, according to the following equation:

$$I_v = \sum_i s_i \cdot w_i \quad (3.18)$$

The index I_v as expressed in (3.18) ranges from 0 to 382.02, which is the upper index, obtained by the assignment of the maximum score to each factors. The index may be eventually normalized respect to the maximum value from 0 to 100, being 0 the best vulnerability condition and 100 the worst.

Table 3.6 Scores and relative weight of the significant factors to compute I_v according to the GNDT II level form.

Factors	Classes score (s)				Weight (w)
	A	B	C	D	
Type and layout of resistant system	0	5	20	45	1
Structural system quality	0	5	25	45	0.25
Conventional strength	0	5	25	45	1.50
Retaining walls and foundations	0	5	25	45	0.75
Floor system	0	5	15	45	variable
Configuration in plan	0	5	25	45	0.50
Configuration in elevation	0	5	25	45	variable
Maximum distance between walls	0	5	25	45	0.25
Roof type	0	15	25	45	variable
Non structural elements	0	0	25	45	0.25
State of conservation	0	5	25	45	1.00

The data from past earthquakes was used to calibrate vulnerability functions to relate the vulnerability index I_v to a global damage factor of buildings with the same typology for the same macroseismic intensity or PGA. The damage factor ranges between 0 and 1 and is computed in terms of economical losses. The

Figure 3.10 shows the correlation between the acceleration in terms of PGA and the damage (Giovinazzi and Lagomarsino, 2001).

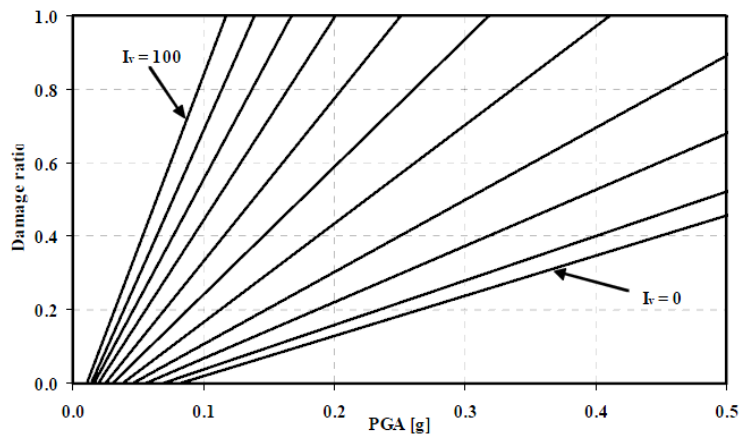


Figure 3.10 Vulnerability functions to relate damage ratio and peak ground acceleration (PGA) for different values of index I_v

The choice of the PGA as a seismic parameter is connected with the desire to use a continuous parameter different from intensity and of clearer mechanical significance. These curves have been derived from the original ones drawn by Guagenti and Petrini (1989), in order to correlate the vulnerability grade with damage level.

Despite seismic vulnerability is the damage which a construction can undergo earthquakes and therefore it depends on both the earthquake grade and the construction parameters, the present procedure does not provide indications about the expected damaged suffered by the assessed structures. For this reason, a deterministic correlation between the seismic input and the expected damage has been elaborated in Frassinè e Giovinazzi (2004). The trigonometric correlation (3.19) represents a vulnerability curve and provides the mean damage grade μ_D as a function of the macroseismic intensity I .

$$\mu_D = 2.5 \left[1 + \tanh \left(\frac{S + 6.25 \cdot V_I - 13.1}{Q} \right) \right] \quad (3.19)$$

in which:

- μ_D represents the mean damage value of the discrete damage distribution (3.20), it ranging from 0 to 5 and defined as the average damage in that represents the barycentre abscissa of the damage histogram expressed by:

$$\mu_D = \sum_{k=0}^5 P_k \cdot k \quad (3.20)$$

- Q is a ductility factor, in general equal to 2.3 for masonry structures;
- S is the macro-seismic level ranging from 5 to 12;
- V_1 is the vulnerability index estimated by applying the macroseismic methodology (Giovinazzi, 2005) and correlated to the GNDT II level vulnerability index I_v by means of the following relationship:

$$I_v = 156.25 \cdot V_1 - 76.25 \quad (3.21)$$

The equation (3.21) is very useful to complete the vulnerability analysis by means the GNDT II level quick procedure, because it allows to forecast the damage level of the structure under a seismic event of a given intensity. An application of this vulnerability assessment methodology is reported in Chapter 4.

3.3.2.4. Fully displacement – based methods

A simplified vulnerability assessment technique was proposed by Calvi (1999) and it is based on the displacement approach rather than on the force one.

This methodology consists in the use of the displacements as the fundamental indicator of damage and a spectral representation of the earthquake demand. This procedure is based on the principles of the Direct Displacement-Based Design method, wherein a Multi-Degree-of-Freedom (MDOF) structure is modelled as a Single-Degree-of-Freedom (SDOF) system.

Thus, different displacement profiles are developed for specific failure mechanisms at a given limit state, by referring to the geometric and material properties of the structures within a defined building class.

The preliminary step is, therefore, the development of the demand spectrum for the considered site. Afterwards, the performance levels or limit states are defined in terms of inter-storey drift.

In particular, four limit states are considered, by accounting structural and non structural damages. The same limit states are also considered in MeBaSe (Mechanical Based Procedure for the Seismic Risk Estimation of Unreinforced Masonry Buildings) (Restrepo Vélez., 2005) for the case of in-plane failure mechanisms and consist in:

- LS1-LS2 - slight structural and non-structural damages: the structural model is defined considering a linear displacement profile;
- LS3 - moderate structural damages, extensive non-structural damages: the structural model is defined considering a soft-storey displacement with failure at the ground floor;

- LS4 - structural collapse: the structural model is defined considering a soft-storey displacement with failure at the ground floor.

The corresponding displacement for each defined limit state is evaluated by means of the following formula:

$$\Delta_{LS} = 0.67 \cdot h_s \cdot n \cdot \delta_y + (\delta_{LS} - \delta_y) \cdot h_s \quad (3.22)$$

where:

- h_s is the typical inter-storey height
- n is the number of storeys
- δ_{LS} is the median drift
- δ_y is the yielding displacement

The equivalent period of vibration is, instead, computed as follows:

$$T_{LS} = 0.04 \cdot (h_s \cdot n)^{3/4} \cdot \sqrt{\mu_{LS}} \quad (3.23)$$

in which μ_{LS} represents the structural ductility.

A joint probability distribution function (JPDF) is, subsequently, defined in the displacement – period format, for which a uniform distribution is assumed. The probability of that the demand should exceed the capacity is calculated by integrating the JPDF function.

This procedure allows to assess the seismic vulnerability of an identified building typology, defined on the base of several features (e.g. the period of construction, the number of stories and the construction material), by considering different levels of data in the refinement in modelling and analysis.

3.3.2.5. The macroseismic method

The macroseismic method for the vulnerability assessment of built-up is derived, by the use of Probability and of Fuzzy Set Theory, considering Macroseismic Scale definitions. Therefore, the basic concept of the method is that if the aim of a Macroseismic Scale is the measure of an earthquake severity, from the observation of the damage suffered by the buildings, it can, in the same way, represent, for forecast purposes, a Vulnerability Model able to supply, for a given intensity, the probable damage distribution.

The methodology makes reference to the damage model developed for each building typology by EMS 98. The six vulnerability classes defined by EMS 98 groups together buildings characterized by a similar seismic behaviour. For each class, the intensity may be estimated from a certain damage pattern, supplied in terms of DPM (Table 3.7).

The EMS vulnerability technique is vague and incomplete, since the definition of the damage amount is provided through the qualitative judgement “Few”,

“Many” and “Most”. The distribution of damage is also incomplete as the EMS only considers the most common and easily observable situations.

On the base of this considerations, the macroseismic methodology is aimed at solving the EMS 98 incompleteness and vagueness matters.

The first matter has been solved by introducing a proper discrete probability distribution of damage grade (μ_D) while the second have been solved by deriving numerical DPM for EMS 98 vulnerability classes (Giovinazzi, 2005).

Thus, an analytical equation is provided by interpolating the curves as a function of an only one parameter. This one represents the vulnerability index (V_I) and correlates the seismic input, in terms of Macroseismic Intensity, with the physical damage, summarized by the mean value of the beta distribution.

In Table 3.8 the most probable value for each of the six vulnerability classes are shown. It can be noticed that the index V_I ranges from -1.02 to 1.02, due to the uncertainties related to the employed probabilistic approach for the calibration.

Finally, the operational implementation of the methodology has led to the analytic expression defined by (3.19) and herein reported:

$$\mu_D = 2.5 \left[1 + \tanh \left(\frac{S + 6.25 \cdot V_I - 13.1}{Q} \right) \right]$$

Table 3.7 Damage Model provided by EMS 98 for each of the six vulnerability class

	Class A					Class B				
I	D ₁	D ₂	D ₃	D ₄	D ₅	D ₁	D ₂	D ₃	D ₄	D ₅
V	Few					Few				
VI	Many	Few				Many	Few			
VII			Many	Few			Many	Few		
VIII				Many	Few			Many	Few	
IX					Many				Many	Few
X					Most					Many
XI										Most
XII										
	Class C					Class D				
I	D ₁	D ₂	D ₃	D ₄	D ₅	D ₁	D ₂	D ₃	D ₄	D ₅
V										
VI	Few									
VII		Few				Few				
VIII		Many	Few				Few			
IX			Many	Few			Many	Few		
X				Many	Few			Many	Few	
XI					Many				Many	Few
XII					Most					Most
	Class E					Class F				
I	D ₁	D ₂	D ₃	D ₄	D ₅	D ₁	D ₂	D ₃	D ₄	D ₅
V										
VI										
VII										
VIII										
IX		Few								
X		Many	Few				Few			
XI			Many	Few			Many	Few		
XII										

Table 3.8 Most probable value of the vulnerability index for each vulnerability class

Class	V_{Imin}^c	V_I^c	V_I^{c*}	V_I^{c+}	V_{Imax}^c
A	1.02	0.94	0.90	0.86	0.78
B	0.86	0.78	0.74	0.70	0.62
C	0.70	0.62	0.58	0.54	0.46
D	0.54	0.46	0.42	0.38	0.30
E	0.38	0.30	0.26	0.22	0.14
F	0.22	0.14	0.10	0.06	-1.02

The macroseismic methodology allows to refer the damage model directly to the building typologies making reference to EMS98 Vulnerability Tables, shown in Figure 3.9, which contains a typological classification representative of the various building types in the European countries. The final index values obtained for all the identified building typologies are shown in Table 3.9.

Table 3.9 Most probable value of the vulnerability index for each vulnerability class

Typologies		Building type	V_{Imin}^c	V_I^{c-}	V_I^{c*}	V_I^{c+}	V_{Imax}^c
Masonry	M1	Rubble stone	0.62	0.81	0.873	0.98	1.02
	M2	Adobe (earth bricks)	0.62	0.687	0.84	0.98	1.02
	M3	Simple stone	0.46	0.65	0.74	0.83	1.02
	M4	Massive stone	0.30	0.49	0.616	0.793	0.86
	M5	Unreinforced (old bricks)	0.46	0.65	0.74	0.83	1.02
	M6	Unreinforced with RC floors	0.30	0.49	0.616	0.79	0.86
	M7	Reinforced or confined masonry	0.14	0.33	0.451	0.633	0.7
RC	RC1	Frame in RC. (without E.R.D)	0.3	0.49	0.644	0.8	1.02
	RC2	Frame in RC. (moderate E.R.D.)	0.14	0.33	0.484	0.64	0.86
	RC3	Frame in RC. (high E.R.D.)	-0.02	0.17	0.324	0.48	0.7
	RC4	Shear walls (without E.R.D)	0.30	0.367	0.544	0.67	0.86
	RC5	Shear walls (moderate E.R.D.)	0.14	0.21	0.384	0.51	0.7
	RC6		-0.02	0.047	0.224	0.35	0.54
Steel	S	Steel structures	0.02	0.17	0.324	0.48	0.7
Timber	W	Timber structures	0.14	0.207	0.447	0.64	0.86

Referring to the identified structural typologies, it can be noted that some structures may behave in a similar way (i.e. massive stone and unreinforced masonry with RC floors). Therefore, even if each type of structure is characterized by a prevailing vulnerability class, it is possible to find buildings with a better or worse seismic behaviour, depending on their constructive or structural characteristics or every other parameter able to affect their seismic resistance.

Thus, according to this consideration, the method also proposes the following definition of the vulnerability index:

$$V_I = V_I^* + \Delta V_R + \Delta V_m \quad (3.24)$$

where:

- V_I^* is a typological vulnerability index, that can be increased or decreased on the basis of the vulnerability factors recognized inside a certain building;
- ΔV_R is the regional vulnerability factor, that takes into account the typifying of some building typologies at a regional level: a major or minor vulnerability could be indeed recognized due to some traditional constructive techniques of a specific built area;
- ΔV_m seismic behaviour modifier factor, computed as follows:

$$\Delta V_m = \sum_k r_k \cdot V_{m,k} \quad (3.25)$$

In the equation (3.25), r_k represents the ratio of building affected by the behaviour modifier k characterized by a $V_{m,k}$ score. For the vulnerability evaluation of isolated buildings, ΔV_m is simply the sum of the scores $V_{m,k}$ for the recognized behaviour modifiers, empirically identified on the basis of the observation of typical damage pattern.

In Table 3.10 the behaviour modifier factors and the corresponding scores are reported for masonry and RC buildings (Giovinazzi and Lagomarsino, 2004).

Table 3.10 Scores for behaviour modifier factors for Masonry and RC buildings

Behaviour modifier	Masonry		RC			
			Low	Medium	High	
		V_{mk}	V_{mk}	V_{mk}	V_{mk}	V_{mk}
State of preservation	Good	-0.04	Good	-	-	-
	Bad	+0.04	Bad	+0.02	+0.02	0
Number of floors	Low (1÷2)	-0.08	Low (1÷3)	-0.02	-0.02	-0.02
	Medium (3÷5)	0	Medium (4÷7)	0	0	0
	High (>6)	+0.08	High (>8)	+0.04	+0.04	+0.04
Structural system	Wall thickness					
	Wall distance	-0.04÷+0.04				
	Wall connection					
Plan irregularity	Geometry		Geometry	+0.04	+0.02	0
	Mass distribution	+0.04	Mass distribution	+0.02	+0.01	0
Vertical irregularity	Geometry		Geometry			
	Mass distribution	+0.04	Mass distribution	+0.04	+0.02	0
Superimposed floors		+0.04				
Roof	Weight, thrust and connections	+0.04				
Retrofitting intervention		-0.08÷+0.08				
Aseismic devices	Barbican, Foil, arches,	-0.04				
Aggregate building position	Middle	-0.04	Insufficient seismic joint	+0.04	0	0
	Corner	+0.04				
	Header	+0.06				
Aggregate building elevation	Staggered floors	+0.04				
	Buildings with different height	-0.04÷+0.04				
Foundation	Different level foundation	+0.04	Beams	-0.04	0	0
			Connected beams	0	0	0
			Isolated footings	+0.04	0	0
			Short-column	+0.02		0
			Bow windows	+0.04		0

Finally, in order to consider “site effects”, further V_1 modifier is defined. This latter is computed as vulnerability increment ΔV evaluated making reference to the Eurocode 8 for the dynamic characterization of both the building categories and the soil types (Table 3.11).

Table 3.11 Vulnerability increments ΔV evaluated for EC8 Ground types and for different building categories

	Ground types according to EC8			
	B/A	C/A	D/A	E/A
Masonry_Low	0.04	0.03	0.08	0.09
Masonry_Medium	0.04	0.03	0.08	0.09
Masonry_High	0.07	0.06	0.10	0.12
RC_Low	0.04	0.03	0.08	0.09
RC_Medium	0.10	0.15	0.24	0.15
RCHigh	0.10	0.15	0.26	0.15

The macroseismic model may be employed both with statistical existent data or properly surveyed data and it may be implemented both for the vulnerability assessment of single buildings and of the entire built-up areas.

It is worth to highlight that this approach is sufficiently representative of the different European building typologies, so it is particularly useful for the vulnerability characterization of traditional masonry constructions.

3.3.2.6. *The electronic database MEDEA*

MEDEA (in Italian: Manuale di Esercitazioni sul Danno Ed Agibilità) is multimedia and didactic handbook for seismic damage evaluation and post-event macroseismic assessment. MEDEA is organized as an electronic database and has been elaborated both for RC and masonry structures. Therefore, the database is structured in different sections representing a guided training path for usability evaluation of damaged buildings (Zuccaro and Papa, 2001).

The first section concerns a glossary of the main terms frequently used in technical and scientific field; some pictures and graphics, a descriptive text and links to other terms in the glossary correspond to each term of the dictionary,

All the terms are organized into five different categories:

- structural elements of constructions;
- structural seismic damages;
- yard equipment in the emergency;
- provisional interventions;
- environment.

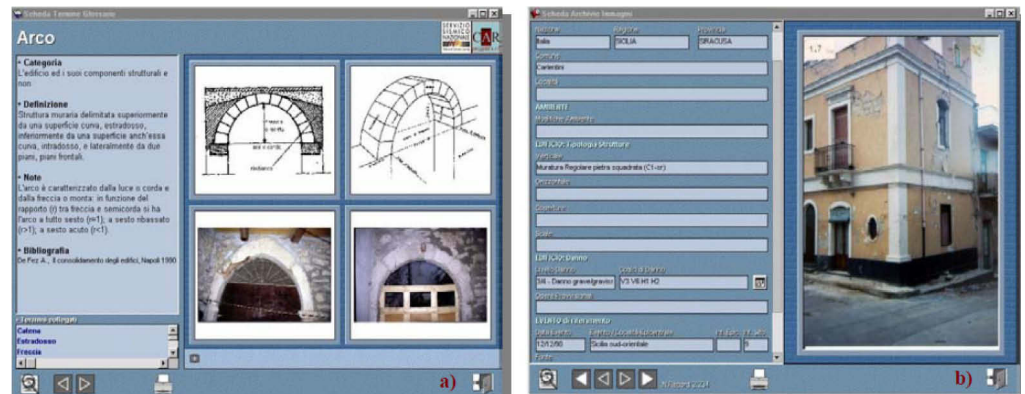


Figure 3.11 The MEDEA glossary and archive

MEDEA second section consists of an archive of pictures showing different structural typologies and different levels and types of damages. The aim of this archive is to provide an essential basic knowledge of the observed damage typologies in order to improve the capability of interpretation and judgment of the technicians during the post-event inspections. In fact, the most important section of MEDEA is the catalogue of the main damages on structural and non structural elements suffered by buildings under seismic events.

This part is a useful tool for the safety check of the damaged constructions in the post event phase. The catalogue is constituted by three sub-sections:

- 1) *Collapse Mechanisms Abacus*, in which the main recognisable collapse mechanisms for a standard structure are classified;
- 2) *Damages Abacus*, in which the main damages that a building may suffer under seismic actions are classified and described by a specific form;
- 3) *Interactive Training*, a table in which to each kind of damage selected by the users is associated a possible collapse mechanism congruent to the chosen damage.

The most interesting part is the one concerning the collapse mechanisms. In fact, both global and local failure mechanism are defined; *global mechanisms* are those ones involving the whole structure such that the evolution of the cracks compromises the structural static and dynamic equilibrium, while *local mechanisms* pertain marginal parts of the structure and generally do not involve the whole structural equilibrium.

In particular, for masonry structures, the structural *global mechanisms* have been subdivided as follows:

- in-plane mechanisms that occur when the classical diagonal cracks due to the poor tensile strength of masonry material are formed in the piers;
- out of plane mechanisms that may occur when out-of-plane kinematics of one or more walls of the masonry box are activated, generally, due to the connection deficiency between the walls of the facade and the orthogonal ones;
- other collapse mechanisms, classified as those mechanisms that couldn't directly be recognized as in-plane or out-of-plane, nevertheless are able to cause the total structural collapse of the structure.

The *local mechanisms* have been, instead, classified as follows:

- for localized dislocation (e.g. for arch or architrave failure);
- for thrusting elements: the mechanism is determined by the action of single elements that produce horizontal thrusts on the supporting structures.

A resumptive scheme of the listed global and local mechanisms is shown in Figures 3.12 and 3.13.

GLOBAL MECHANISMS	
Storey shear mechanism 	Storey shear mechanism Upper storeys 
Whole wall overturning 	Partial wall overturning 
Vertical instability of the wall 	Wall bending rupture 
Horizontal sliding failure 	Foundation subsidence 
Irregularity between adjacent structures 	Floor and roof beam unthreading 

Figure 3.12 Abacus of the global collapse mechanisms

LOCAL MECHANISMS	
Lintel or masonry arch failure 	Material irregularity Local weakness 
Roof gable wall overturning 	Corner overturning in the upper part 
Overturning of the wall supporting the roof 	Vault and arch overturning 

Figure 3.13 Abacus of the local collapse mechanisms

A training section is the final part of MEDEA, in which some examples of damage and usability evaluation are shown (Fig. 3.14). The evaluations is expressed on constructive typology, damage level expressed both for every single element and for the whole building, safety assessment of the building and possible provisional interventions to be adopted. Furthermore, the training form permit to control the judgement capability achieved by the surveyor.

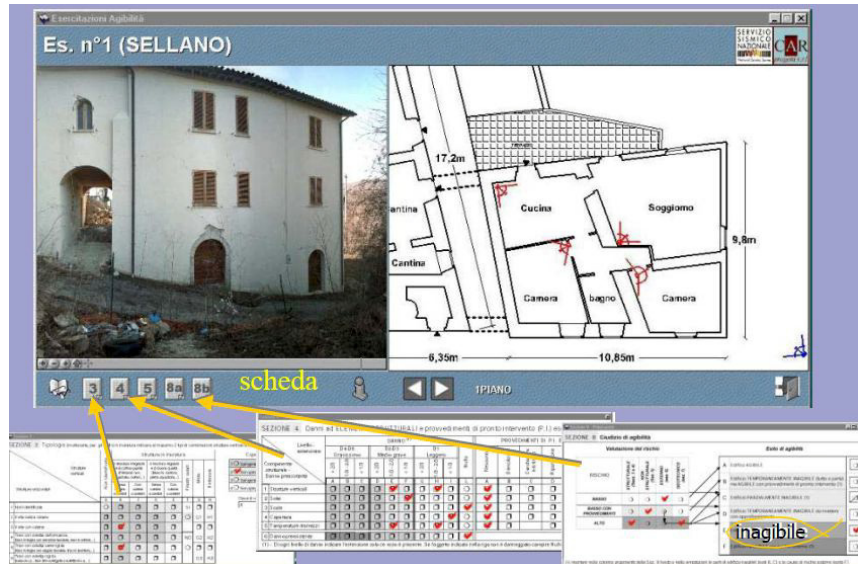


Figure 3.14 MEDEA training section

The electronic database MEDEA is aimed at the identification of the common aspects of the different approaches for seismic vulnerability assessment proposed by the scientific community by means of unambiguous and homogenised survey. MEDEA has been applied in the post-event phase of the recent earthquake of L'Aquila (April 2009), that represent one of the study cases of this thesis.

3.4. MASONRY BLOCKS

3.4.1. Introductory remarks

Italian historical centres are often the result of an uncontrolled urban development, since the major part of buildings located there have been erected in continuity each other, giving rise to structural complexes developed during time without any constructive rule.

As a consequence, historical building aggregates are the result of the progressive growth of towns, in which elevation floors are added to existing buildings and plan enlargements are made by adding structural cells to the previously existing ones, so that adjacent units often share the same boundary wall (Giovinazzi et al., 2004). As a result, it is very difficult, if not impossible, both to distinct the structurally independent units and to identify the global response of the building aggregates. Therefore, seismic vulnerability assessment of masonry blocks in the Italian historical centres represents a specific and very actual problem.

The main difficulties of this task are related to the low knowledge level of the structures, which were in many cases built in absence of anti-seismic design regulations, particularly due to the absence of drawings or reports. In addition, the analysis of these building complexes should require the complete modelling of all structural units. However, reliable methodologies and analytical tools for the analysis of seismic vulnerability of masonry building aggregates are not available and seismic codes provide scarce or insufficient information.

The consciousness of this matter has led to the proposal of a quick procedure for the seismic vulnerability assessment of masonry blocks, described in the following sections.

3.4.2. Calculation Methods

3.4.2.1. *General remarks*

Historic buildings tend to be at greater seismic risk than comparable new constructions, not only because they have been designed to little or no seismic loading requirements, but also because they are not capable of dissipating energy through large inelastic deformations during an earthquake. Furthermore, in many cases the old buildings are aggregate of buildings, structurally dependent on the global behaviour of the entire block. Thus, the analysis of the conditions of the context in which the building is inserted is a fundamental issue for the assessment and reduction of the seismic vulnerability of masonry buildings. In

fact, various factors affecting structural performance exist, depending on the interference between the single structural unit and those adjacent to it.

The types of damage that may occur for buildings included in a masonry block have a particular importance, as well as the criteria and techniques of intervention.

The problem of seismic analysis and modelling of masonry aggregates was considered seriously by the scientific community in Italy after the Friuli earthquake occurred in 1976. In fact, after this tragic event, calculation methods for masonry buildings based on static nonlinear analyses were introduced in the codes, even before this happened for other recurrent structural typologies.

The nonlinear analysis for masonry building in aggregate are generally based on the macroelements approach, although the validity of such model has been substantially demonstrated for sufficiently regular geometrical configurations, that is rarely found in complex of existing buildings. On the other hand, the use of equivalent frame models is in most cases almost impossible due to the relevant dimensions and irregularities of aggregates in historical centres. Thus, any structural analysis that aims at evaluating the global performance should in principle either model the whole block or model the structural unit with suitable boundary conditions that take into account the effect of the adjacent ones

In general, the main problem for the study of the structural response of a masonry aggregate is the local behaviour; this complex structures exhibit often local collapse mechanism. Therefore, the problem of a correct evaluation of the vulnerability to local collapse mechanisms is of fundamental importance in the vulnerability evaluation of building units in complex aggregates in historical centres.

Two main typologies of local mechanisms exist:

- *in-plane mechanisms*, generally due to thick and redundant connection among the building units
- *out-of-plane mechanisms*, generally caused by construction irregularities (for instance, walls not well clamped in the last building units, that obstructed the empty spaces) or the geometric irregularities (for instance, different height between adjacent buildings).

The analysis of local mechanisms can be similar as for isolated building, as concerns the definition of the seismic input and evaluation of the capacity. However, specific mechanisms can take place within aggregates which are induced by the interconnection or contact by adjacent structural subsystems.

In this field, the reading of the damage mechanisms in a historical centre hit by a seismic event may be very useful. In fact, the marks of the past earthquakes are

never totally wipe out and may aid to recognise the set of local and global collapse mechanisms, traceable to in-plane or out-of-plane seismic actions.

3.4.2.2. *In - plane analysis*

The in-plane behaviour of masonry aggregates is generally conditioned by excessive bending or shear actions. Shear in-plane failures are more common and expressed by double-diagonal (X) shear cracking. Fortunately, until the shear cracks become unduly severe, the gravity-load carrying capacity of the walls is not jeopardized.

The failure due to shear is particularly common in masonry facades with numerous window openings, spandrels and short piers between those spandrels. Flexural failure is also possible, particularly for slender piers; the resulting cracking at both ends of a masonry element transforms it into a rigid body of no further lateral-load resisting capacity, unless gravity forces can provide a stabilizing effect.

Mechanisms of lateral force resistance depend primarily on the pier geometry, on their boundary conditions and on the magnitude of vertical loads, and then on the characteristics of the brick, of the mortar and of the brick-mortar interface.

In general, the presence of good connection system ensures a certain level of transmission of the seismic action from the set of walls orthogonal to it to the one parallel, causing the development of in-plane mechanisms rather than out-of-plane ones.

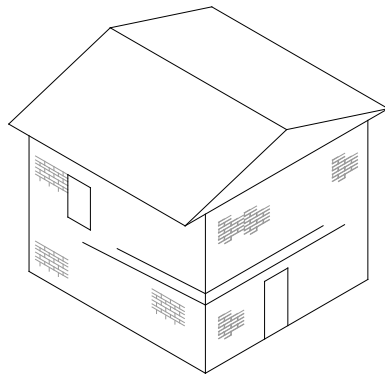
The main in-plane collapse mechanisms of masonry piers under seismic actions are (Magenes and Calvi, 1997):

1. *rocking failure*: as horizontal load or displacement demand increase, bed-joints crack in tension, and shear is carried by the compressed masonry; the failure is obtained by overturning of the wall and simultaneous crushing of the compressed corner;
2. *shear cracking*: peak resistance is governed by the formation and development of inclined diagonal cracks, which may follow the path of bed- and head-joints or may go through the bricks, depending on the relative strength of mortar joints, brick-mortar interface, and bricks; in the case on an included building, the resistant mechanism interest portions of the adjacent buildings that are in the same plan;
3. *sliding*: due to the formation of tensile horizontal crack in the bed-joints, subjected to reversed seismic action, potential sliding planes can form along the cracked bed-joints; this failure mode is possible for low levels of vertical load and/or low friction coefficients.

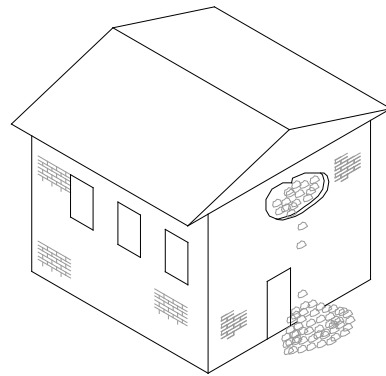
The strength associated to aforesaid failure modes may be calculated by means of the simplified formulations and criteria provided by the codes and literature, as fully described in Chapter 2 (section 2.5.3.4).

In a complex building aggregate, instead, the interaction mechanisms between the adjacent cells must be analysed, generally consisting in: hammering between adjoining buildings, planimetric and altimetric irregularity, hammering due to the offset between the levels of adjacent floors (Fig.3.15).

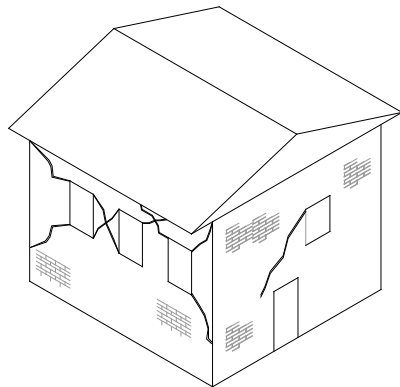
The interaction between adjoining unit structurally independent condition the seismic global response of the whole masonry block. For this reason, the influence of each of this factors on the global performance has been studied in order to implement a specific form for the vulnerability evaluation of buildings included in a historic aggregate.



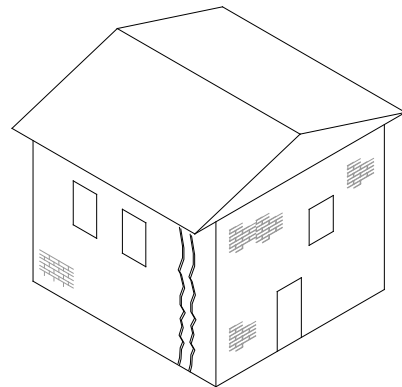
Sliding between tie beams and masonry



Collapse of the outer leaf of the masonry



Widespread shear failure of external walls



Cracks in presence of discontinuity

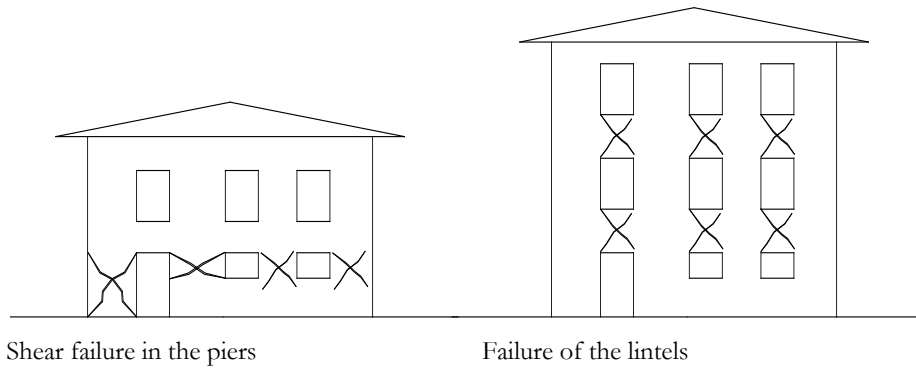


Figure 3.15 In-plane collapse mechanisms

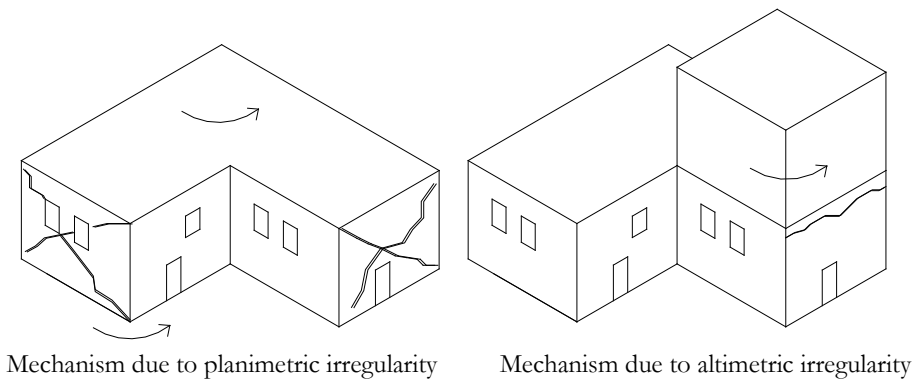
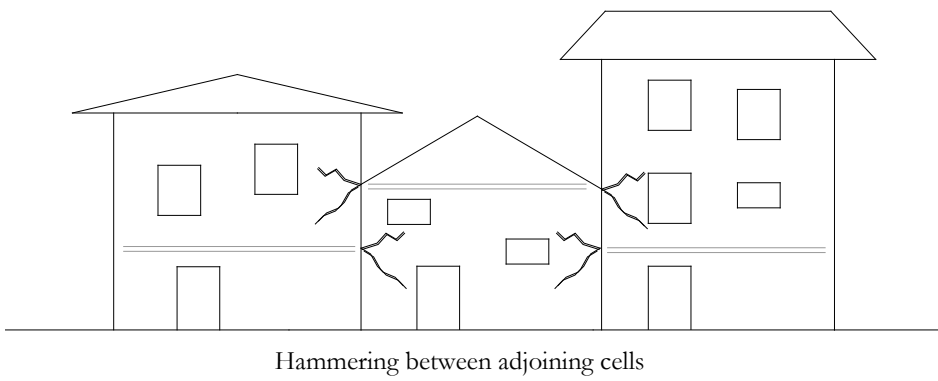


Figure 3.16 In-plane collapse mechanisms for buildings included in aggregate

3.4.2.3. Out - of - plane analysis

Masonry walls aligned orthogonal to the earthquake direction may fail in an out-of-plane mode and this may endanger the gravity load carrying building capacity. The out-of-plane behaviour of masonry walls depends particularly on the floor-wall connection. In fact, for masonry walls which are properly anchored to the floors, the out-of-plane behaviour is usually not critical and the behaviour of the building is determined by its in-plane failure modes.

Generally, out-of-plane mechanisms can be triggered before in-plane ones, when the connection between orthogonal walls and between walls and floors is rather poor. Moreover, the walls are often subjected to both in-plane and out-of-plane actions, considered that the seismic actions do not correspond to one of the principal directions of the building.

Once out-of-plane failure is prevented by proper measures (e.g. reinforced concrete ring beams, steel ties at the floor levels) the in-plane walls provide the stability necessary to avoid collapse. Usually, these walls are pierced by windows or doors, leaving a series of smaller piers to provide both the gravity and lateral load resisting systems.

The study out-of-plane local mechanisms may be achieved by means of the limit analysis, aimed at the evaluation of the collapse load that generates the failure mechanism. The application of this type of analysis is quite complex, because the cause and the extension of the cracks are not immediately recognizable and strains or other damages are in many cases not directly related to the collapse generation.

The limit analysis is based on two different calculus methods of the collapse multiplier (λ) of the load triggered the collapse mechanisms:

1. *static method*: consisting on the basic assumption of a distribution of statically admissible stresses depending on several parameters and search them so that the correspondent load multiplier is maximum;
2. *kinematic method*: consisting into assuming a failure mechanism dependent on some geometrical parameters and in the following minimization of the correspondent multiplier to the considered mechanism.

According to the uniqueness theorem, a multiplier that is statically and kinematically admissible coincides necessarily with the collapse multiplier.

Therefore, in order to apply limit analysis, the following basic assumption regarding masonry material are made:

1. masonry has zero tensile strength;
2. infinite compression strength of the elements;
3. sliding of a stone, or of part of the structure, upon another cannot occur.

On the base of these considerations, the only possible collapse mode is the rotation of adjacent blocks about a common point, so that masonry behaves as an assemblage of rigid blocks held up by compressive contact forces. The collapse is characterized by the formation of hinges among the single parts.

Under the outlined hypotheses, collapse analysis of masonry structures basically consists in seeking a thrust line, which is actually the graphical representation of equilibrium conditions, passing through a number of hinges sufficient to transform the structure into a mechanism.

Therefore, the limit state analysis procedure is carried out by evaluating lower and upper thresholds in closed form for the seismic actions which can activate the local damage mechanisms under study, in relation to the meaningful geometrical and mechanical parameters. The collapse multiplier (λ) is computed by applying the Virtual Work Principle in terms of displacements according to the following equation:

$$\lambda \cdot \left[\sum_{i=1}^n P_i \cdot \delta_{ix} + \sum_{j=n+1}^{n+m} P_j \cdot \delta_{jx} \right] - \sum_{i=1}^n P_i \cdot \delta_{iy} - \sum_{h=1}^n P_i \cdot \delta_{iy} - \sum_{h=1}^o F_h \cdot \delta_h = L_{fi} \quad (3.26)$$

in which:

- n is the number of all the forces associated to the masses of the rigid blocks
- m is the number of the forces associated to the masses of the elements that generate horizontal actions under seismic loading condition
- o is the number of the external forces applied to the blocks
- P_i is the generic force associated to the mass of the block
- P_j is the generic force that, under seismic loading conditions, generates an horizontal actions on the blocks
- δ_{ix} is the virtual horizontal displacement of the application point of the force P_i
- δ_{jx} is the virtual horizontal displacement of the application point of the force P_j
- δ_{iy} is the virtual vertical displacement of the application point of the force P_i
- F_h is the absolute value of the generic external force applied to a block
- δ_h is the virtual displacement of the application point of the external force
- L_{fi} is the work of possible internal forces.

The displacements of the application point of the forces are calculated taking into account the structural geometry, by assigning a virtual rotation to the generic block. Therefore, the formulation (3.2) represents an equation of equilibrium between the stabilizing and the overturning moment.

The main collapse mechanisms are classified as follows (Beolchini et al., 2005):

- 1) *Overturning* (Fig. 3.17). The overturning mechanism represent one of the most diffused damage condition. This failure mode may be schematized as a rigid rotation around a horizontal cylindrical hinge on the base of the block. The movement is triggered off by out-of-plane actions when the connection with orthogonal walls or with floor structural system is poor.

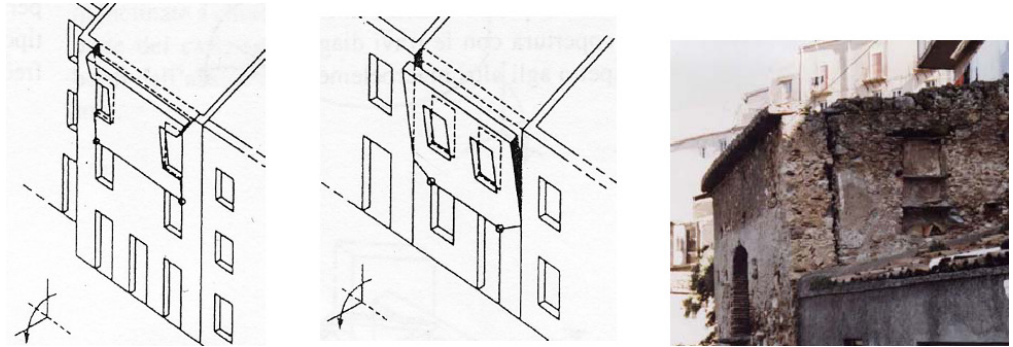


Figure 3.17 Overturning mechanism

- 2) *Vertical bending* (Fig. 3.18). This type of failure mode generally occurs when metal ties or other connecting devices at the top floor connect the façade to either the floor structural system or the lateral walls but there are no connecting system at intermediate floors (i.e. when a structural unit presents a roofing system with RC tie beams, but deformable intermediate floors). In this case, the overturning mode is not triggered, but the wall can be subjected to a failure mode due to vertical instability. This mechanism is dependent on the difference of macroelement geometry, on the openings distribution and on the pushing effect of other constructive elements. In particular, in case of sack masonry, the external curtain can reach the collapse due to vertical bending when only the internal curtain is connected with the horizontal structural system.



Figure 3.18 Vertical bending mechanism

- 3) *Horizontal bending* (Figs. 3.19 and 3.20). This collapse mode may occur when connection between façade and lateral walls is present over the entire building height. This is equivalent to a reduction of the free deflection horizontal width, which can be computed as a proportional increase in the restoring moment.

The structural response of the wall is characterized by the so-called horizontal arc effect inside the wall. In particular the floor horizontal pushing force is transmitted firstly to the façade wall and consequently to the orthogonal lateral walls. This action (R) is characterized by an horizontal component (I) orthogonal to the wall subjected to the seismic action and another one (H) parallel to the same wall. Thus, the mechanism heaviness depends on the capability of the lateral wall to support the horizontal arc thrusts.

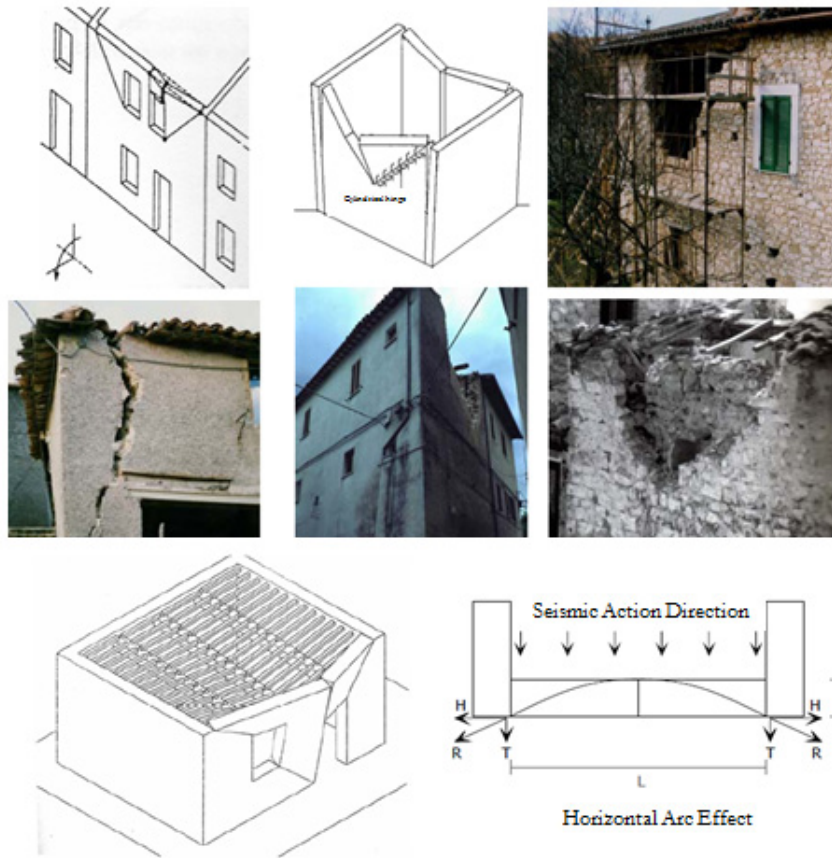


Figure 3.19 Horizontal bending mechanism

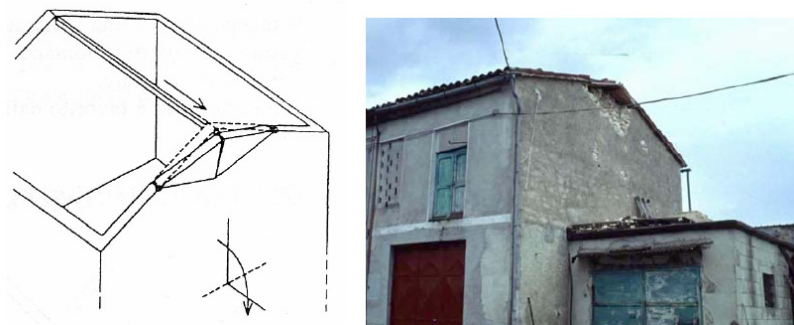


Figure 3.20 Sample of horizontal bending failure: gable collapse

- 4) *Composed overturning* (Figs. 3.21 and 3.22). This mechanism can be obtained as a combination of the two previous ones. It generally occurs when the walls are connected to the others by ties and quoins. This configuration represent the most frequent one.

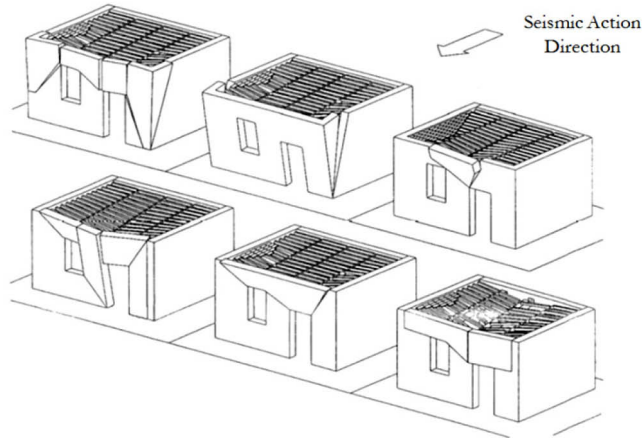


Figure 3.21 Possible composed overturning failure mode in case of good connections

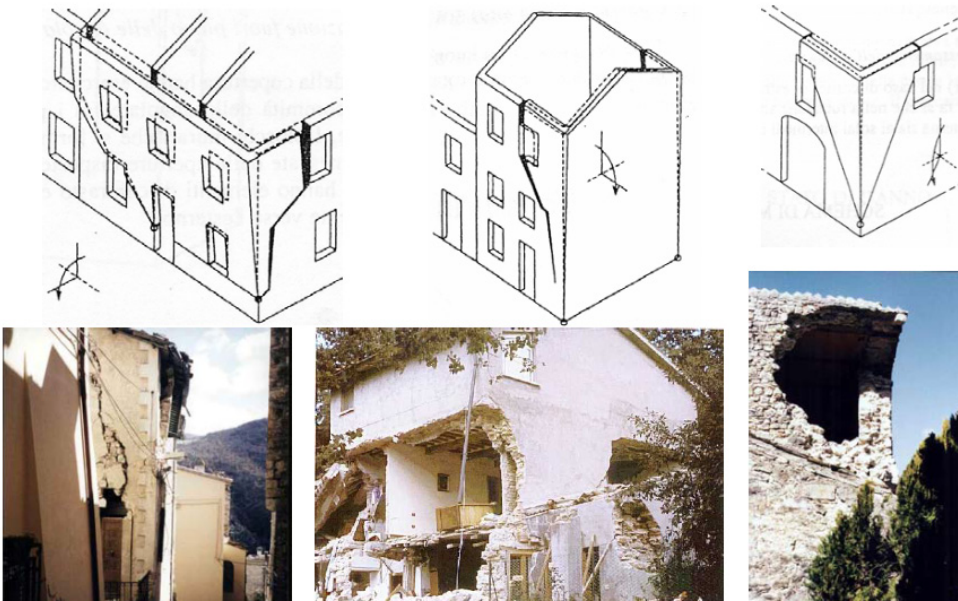


Figure 3.22 Composed overturning mechanism

Table 3.12 Resumptive draft of main failure out-of-plane modes

Overturing
One storey monolithic wall

Overturing moment:

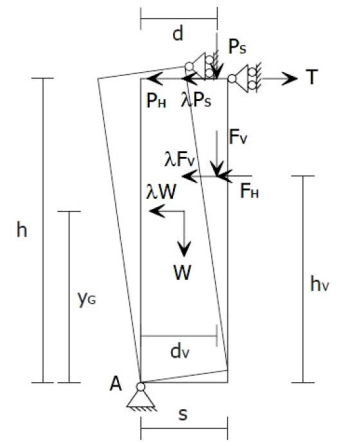
$$M_{S(A)} = W \cdot \frac{s}{2} + F_v \cdot d_v + P_s \cdot d + T \cdot h$$

Stabilizing moment:

$$M_{R(A)} = \lambda \cdot [W \cdot y_G + F_v \cdot h_v + P_s \cdot h] + F_H \cdot h_v + P_H \cdot h$$

Collapse load multiplier:

$$\lambda = \frac{W \cdot \frac{s}{2} + F_v \cdot d_v + P_s \cdot d + T \cdot h - F_H \cdot h_v - P_H \cdot h}{W \cdot y_G + F_v \cdot h_v + P_s \cdot h}$$



Calculation scheme

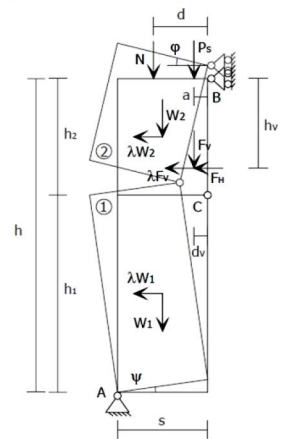
Vertical Bending
One storey monolithic wall

Collapse load multiplier:

$$\lambda = 2 \cdot \frac{(\mu - 1) \cdot (N \cdot d + P_s \cdot a + F_v \cdot d_v - F_H \cdot h_v) + s \cdot (W + N + P_s + F_v)}{(\mu - 1) \cdot \left(\frac{W \cdot h}{\mu} + 2 \cdot F_v \cdot h_v \right)}$$

in which μ is a coefficient >1 depending on λ value;
when the hinge height is equal to the vault skewback, the
formulation of collapse multiplier λ is:

$$\lambda = 2 \cdot \frac{(N \cdot d \cdot \frac{h_v}{h - h_v} + P_s \cdot a \cdot \frac{h_v}{h - h_v} + F_v \cdot d_v - F_H \cdot h_v + s \cdot (W + N + P_s))}{h_v \cdot (W + 2 \cdot F_v)}$$



Calculation scheme

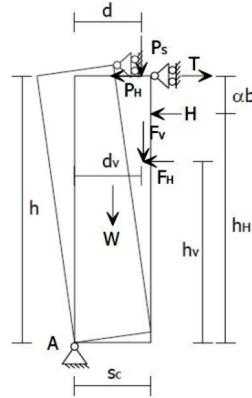
**Horizontal bending
Monolithic wall**

Collapse load multiplier:

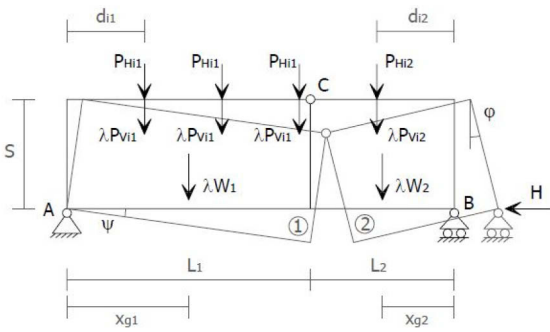
$$\lambda = \frac{H \cdot s \cdot \left(1 + \frac{L_1}{L_2}\right) - \sum_i P_{Hi1} \cdot d_{i1} - \sum_i P_{Hi2} \cdot \frac{L_1}{L_2} \cdot d_{i2}}{W_v \cdot x_{G1} + W \cdot \frac{L_1}{L_2} \cdot x_{G2} + \sum_i P_{Vi2} \cdot \frac{L_1}{L_2} \cdot d_{i2}}$$

H is the resistance of the lateral walls, equal to:

$$H = \frac{1}{h_H} \cdot \left(W \cdot \frac{s_C}{2} + F_v \cdot d_v + P_s \cdot d + T \cdot h - F_H \cdot h_v - P_H \cdot h\right)$$



Calculation scheme for H action



Calculation scheme

**Composed Overturning
Bending of diagonal quoins of monolithic wall**

Overturning moment:

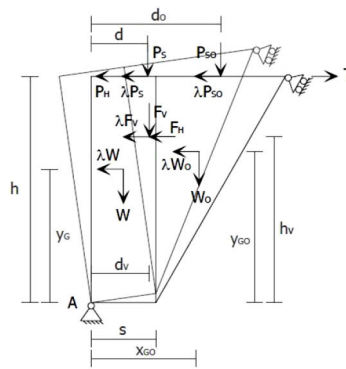
$$M_{S(A)} = W \cdot \frac{s}{2} + F_v \cdot d_v + W_o \cdot x_{Go} + P_s \cdot d + P_{so} \cdot d_o + T \cdot h$$

Stabilizing moment:

$$M_{R(A)} = \lambda \cdot [W \cdot y_G + W_o \cdot y_{Go} + F_v \cdot h_v + P_s \cdot h + P_{so} \cdot h] + F_H \cdot h_v + P_H \cdot h$$

Collapse load multiplier:

$$\lambda = \frac{W \cdot \frac{s}{2} + F_v \cdot d_v + W_o \cdot x_{Go} + P_s \cdot d + P_{so} \cdot d_o + T \cdot h - F_H \cdot h_v - P_H \cdot h}{W \cdot y_G + W_o \cdot y_{Go} + F_v \cdot h_v + P_s \cdot h + P_{so} \cdot h}$$



Calculation scheme

3.4.3. Proposal of a vulnerability assessment approach

3.4.3.1. Revision of the Benedetti and Petrini's form

The Benedetti e Petrini's procedure represents, as aforesaid, a milestone in the history of the quick vulnerability assessment methodologies of isolated masonry constructions. This limit make the technique inapplicable to the historical centre, generally constituted of aggregate of buildings. For this reason, the form herein proposed is aimed at extend the original one to masonry building blocks by taking into account the effects deriving from interaction among adjacent structures. To this purpose, the following five additional parameters have been introduced in the basic form:

1. Presence of adjacent buildings with different height;
2. Position of the building in the aggregate;
3. Number of staggered floors among aggregated buildings;
4. Effects of either structural or typological heterogeneity among adjacent structural units;
5. Percentage difference of opening areas among adjacent facades.

The synthetic vulnerability index is obtained in the same manner already described for the original form, that is the sum of class scores multiplied by the corresponding weights according to the equation (3.18). Therefore, the scores to be assigned to classes and weights of the new performance modifiers have been opportunely calibrated by means of the numerical model explained in the following section.

3.4.3.2. Numerical calibration of additional scores and weights

In order to calibrate scores and weights of the five additional parameters, some parametric analyses have been performed on the numerical model of a masonry structural unit typical of the urban tissue of the Campania region.

Such a calibration activity has been carried out by using the 3MURI non linear numerical software, distributed by S.T.A.DATA. (2010). This program is based on the Frame by Macro Element (FME) calculation approach and considers only two collapse mechanisms, namely the compression – bending failure and the shear one. In the first case, the effective redistribution of the compression due to the reduction of the section is considered when the maximum strength is reached. Therefore, the ultimate displacement depends on the maximum drift value expected for this mechanism (0.6%), as provided by the new technical Italian code (M. D., 2008). Instead, in case of shear mechanism, the phenomena is defined by the Mohr-Coulomb model on the basis of the Gambarotta - Lagomarsino joint (S.T.A.DATA, 2009). So, the assumed model allows to follow

the progressive decrease of the element strength and stiffness during the analysis, by modelling an hysteretic structural behaviour. The ultimate shear deformation is referred to the maximum drift value designated from the Italian code (0.4%). So, by using the calculation model of the 3MURI software, parametric analyses on a typical structural unit within a masonry building aggregate located in the municipality of Sessa Aurunca, a small town placed in the province of Caserta, have been implemented (Formisano et al., 2009a, Formisano et al., 2009b). The examined construction (Fig. 3.23) has a vertical structure made of 60 cm thick tuff squared stones with a reduction of 10 cm in thickness at each floor. Mixed RC - hollow tiles floors RC tie beams are used at each storey. In particular, the presence of these tie beams allows to assume that the walls were effectively connected to the floors and, therefore, only the in-plane seismic mechanisms have been investigated due to the high probability of occurrence. The values of the structure mechanical properties, that is compressive and shear stresses and the Young modulus, have been assigned as foreseen in the Italian Code (M. D., 2008).

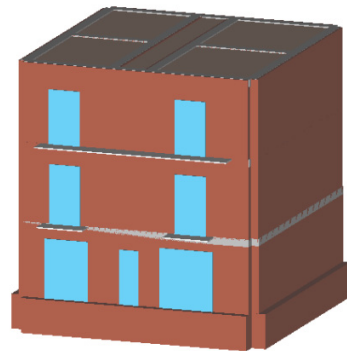


Figure 3.23 The 3MURI numerical model of a typical structural unit of Sessa Aurunca

Pushover analyses along the longitudinal (X) and transverse (Y) directions of the building have been performed by assigning horizontal forces proportional to its first vibration mode. For the spectrum definition the following parameters have been considered according to the aforesaid Code:

- subsoil type A; - topographic category T_i;
- ordinary building (class of use II) with nominal life of 50 years.

Thus, a mechanical vulnerability index I_M has been evaluated as the ratio between the maximum horizontal displacement of the building in the analysis direction under the assigned system of forces D_{max} and the ultimate one before collapse D_u , both of them provided in the pushover analysis, according to the simplified mechanical model described in section 3.3.1.4.

Several parametric analyses have been performed reproducing the boundary condition of each additional form parameter, in order to calculate a different index for each single case. In particular, the base structural unit has been modelled between two units having features so to reproduce from the numerical point of view the distinctive features of each class of each additional parameter introduced in the original survey form. The scores have been defined so that the difference among the indexes associated with different classes of each parameter is proportional to the difference among the corresponding mechanical vulnerability index values obtained in the analyses performed in the most severe direction (direction X).

Instead, the definition of weights has been performed for each parameter considering as a first step the absolute value differences of the vulnerability index among classes. Then, the weights have been assigned to each new parameter proportionally to this difference, representing the influence of each parameter on the building seismic behaviour. Finally, these weights have been homogenized with those of the original form.

The obtained results are the following:

- 1) *Presence of adjacent buildings with different height* (Fig. 3.24). This parameter generally positively influences the seismic behaviour of the structural unit. Considering the analyses, the classification has been resulted as follows:
 - Class A: score -20. The examined building is between two adjacent buildings having the same height.
 - Class B: score 0. The examined building is between two adjacent buildings higher than the examined one.
 - Class C: score 15. The examined building is between a building lower than the examined one and a building with the same height; the examined building is between a building lower than the examined one and a building higher.
 - Class D: score 45. Presence of adjacent buildings lower than the examined one.

The weight assigned to this parameter is equal to 1.

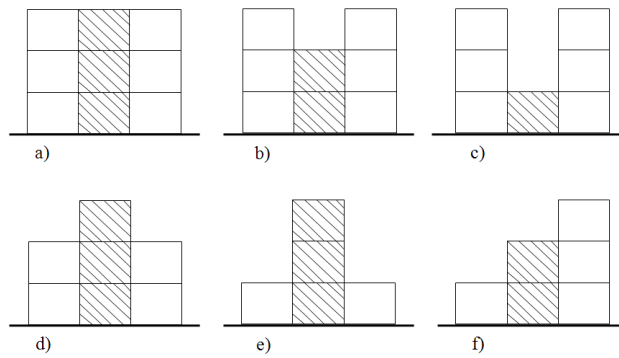


Figure 3.24 Presence of adjacent building with different height

- 2) *Position of the building in the aggregate* (Fig. 3.25). This parameter concerns the positions of the structural unit within the block and significantly influences the structural response. Generally, the positions are: internal or in the middle of the complex, corner or header. Thus, taking into consideration the analyses, the classification has been resulted as follows:
- Class A: score -45. The building has an internal position within the aggregate, it being bounded by three other units. The global vulnerability is decreased.
 - Class B: score -25. The building has an internal position within the aggregate, it being bounded by two other units. The global vulnerability is reduced.
 - Class C: score -15. The building has a corner position. The global vulnerability is reduced in this case too.
 - Class D: score 0. The building has a header position.
- The weight assigned to this parameter is equal to 1.5

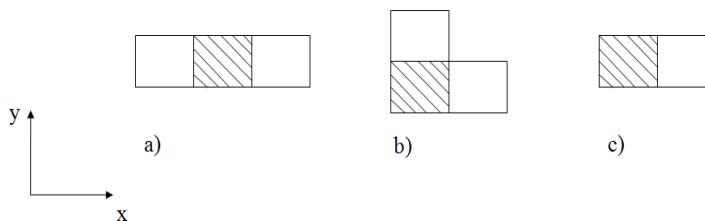


Figure 3.25 Possible positions of the building in the aggregate

- 3) *Number of staggered floors among aggregated buildings* (Fig. 3.26). This parameter concerns the possible presence of staggered floors among structural

units. This presence, indeed, can generate push and hammering effects between adjacent walls. The distance between the staggered floors have been established as equal to 0.5 m. So, taking into account the analyses, the classification has been resulted as follows:

- Class A: score 0. No staggered floors among adjacent units.
- Class B: score 15. Presence of a couple of staggered floors among adjacent units.
- Class C: score 25. Presence of two couples of staggered floors among adjacent units.
- Class D: score 45. Presence of more than two couples of staggered floors among adjacent units

The weight assigned to this parameter is equal to 0.5; the global vulnerability is increased in each case.

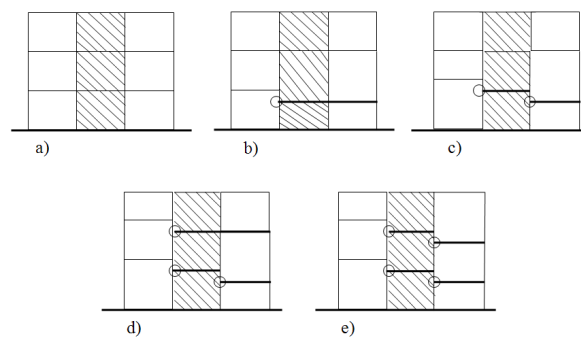


Figure 3.26 Number of staggered floors among aggregated buildings

4) *Effects of either structural or typological heterogeneity among adjacent structural units.*

Considering the analyses, the classification has been resulted as follows:

- Class A: score -15. The typological-structural continuity is assured.
- Class B: score -10. The structural continuity is assured, but not the typological one (for instance, it is the case of two masonry constructions made of two different types of natural stones).
- Class C: score 0. The structural continuity is assured, but not the typological one (for instance, it is the case of a natural stones masonry constructions and an artificial element masonry one).
- Class D: score 45. The typological-structural continuity is not assured (for instance, a masonry building adjacent to a RC structure).

The weight assigned to this parameter is equal to 1.2.

5) *Percentage difference of opening areas among adjacent facades.* The difference of percentage of opening areas may influence the distribution of the seismic forces. Therefore, the classification has been resulted as follows:

- Class A: score -20. Percentage difference < 5%.
- Class B: score 0. 5% < Percentage difference < 10%.
- Class C: score 25. 10% < Percentage difference < 20%.
- Class D: score 45. Percentage difference > 25%.

The weight assigned to this parameter is equal to 1.

The final version of the new form is depicted in Table 3.13, where the additional factors background is grey.

Table 3.13 Proposal of a survey data form for masonry block

Factors	Classes score (s)				Weight (w)
	A	B	C	D	
1. Organization of the vertical structures	0	5	20	45	1
2. Nature of the vertical structures	0	5	25	45	0.25
3. Location of the building and type of foundation	0	5	25	45	0.75
4. Planimetry	0	5	25	45	1.5
5. Planimetry: compactness	0	5	25	45	0.5
6. Regularity	0	5	25	45	variable
7. Type of slabs	0	5	15	45	variable
8. Roofing	0	15	25	45	0.75
9. Details	0	0	25	45	0.25
10. Physical conditions	0	5	25	45	1
11. Presence of adjacent buildings with different height	-20	0	15	45	1
12. Position of the building in the aggregate	-45	-25	-15	0	1.5
13. Number of staggered floors among aggregated building	0	15	25	45	0.5
14. Effects of either structural or typological heterogeneity among adjacent structural units	-15	-10	0	45	1.2
15. Percentage difference of opening areas among adjacent facades	-20	0	25	45	1

3.4.3.3. *Validation of the results: study cases in the historical centres of Sessa Aurunca (Ce)*

The effectiveness of the new proposed procedure has been proved by analysing a historical masonry aggregate located in Sessa Aurunca and shown in Figure 3.27.

The study case is a building block composed of five different structural units having a vertical structure made of squared tuff masonry stones.



Figure 3.27 The investigated aggregate: (a) plan view; (b) building n.1; (c) building n.2; (d) building n.3; (e) building n.4; (f) building n.5

The block develops along a curtain on the street and has an elongated shape. Its constitutive units have 2 or 3 stories and different types of floors, such as vaults with or without ties on the ground level and mixed steel-tile floors on other storeys, where in some cases also RC tie beams are allocated.

A numerical model of this building aggregate has been implemented by means of the 3MURI software (Fig. 3.28) in order to compare the achieved results with the ones deriving from the form application.

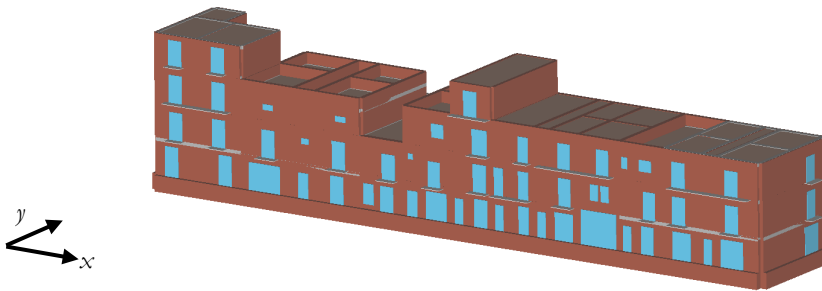


Figure 3.28 The implemented 3MURI model

The pushover analyses have been performed by modelling each of the single structural unit both as isolated and as part of the block. The seismic behaviour of buildings has been assessed along their longitudinal (X) and transverse (Y) direction and considering the force distribution proportional to their first vibration mode. Similarly to the case of the typical structural unit above described, the mechanical vulnerability index I_M has been obtained as the ratio between the maximum horizontal displacement of the building in the analysis direction under the assigned system of forces D_{max} and the ultimate one before collapse D_u . Finally, two different mechanical vulnerability indexes have been evaluated for each structure considered both as isolated (I_{M1}) and within the aggregate (I_{M2}). The results are shown in Table 3.14.

Table 3.14 Mechanical indexes obtained by means of the numerical model, considering the building both as isolated and as part of the aggregate

Building		Isolated			Within the aggregate		
		D_{max} (cm)	D_u (cm)	I_{M1}	D_{max} (cm)	D_u (cm)	I_{M2}
1	X	1.176	2.323	0.51	0.713	1.222	0.58
	Y	0.563	2.324	0.24	0.447	2.242	0.20
2	X	0.590	1.561	0.38	0.564	1.601	0.35
	Y	0.261	1.799	0.15	0.282	2.320	0.12
3	X	0.654	1.186	0.55	0.515	1.039	0.50
	Y	0.153	1.182	0.13	0.160	0.420	0.38
4	X	1.858	2.742	0.68	1.780	2.560	0.70
	Y	0.263	0.801	0.33	0.231	0.481	0.48
5	X	0.750	1.599	0.47	0.652	1.440	0.45
	Y	0.258	1.381	0.19	0.209	0.830	0.25

The global vulnerability indicator I_M has been computed as the ratio between I_{M2} and I_{M1} in the most vulnerable direction, that is the longitudinal one (X).

The following step has been the estimation of the vulnerability by applying both the original Benedetti and Petrini's procedure and the proposed one. Therefore, the quick vulnerability index I_V has been calculated as the ratio between the vulnerability index I_{V1} achieved by applying the Benedetti and Petrini's form and the index I_{V2} obtained by means of the compilation of the proposed form. Similarly to the application of the numerical model, the I_{V1} refers to the building considered as isolated, while the I_{V2} refers to the aggregate condition.

The comparison among results of the two different methodologies is shown in Table 3.15, while the values distribution is displayed in Figure 3.29. It is noticed that when the structural unit is within the block its seismic vulnerability is reduced if compared with the one of the same building considered as isolated. In addition, the classification of the building vulnerability is the same with the two applied methods. This proves the effectiveness of the proposed form.

Table 3.15 Comparison between the results of the two vulnerability assessment forms.

Unit	Numerical model			Vulnerability form		
	Isolated	Aggregate	I_{M1}/I_{M2}	Isolated	Aggregate	I_{V1}/I_{V2}
	I_{M1}	I_{M2}	I_M	I_{V1}	I_{V2}	I_V
1	0.51	0.58	1.15	25.00	29.75	1.19
2	0.38	0.35	0.93	12.15	12.15	1.00
3	0.55	0.50	0.90	34.38	24.88	0.72
4	0.68	0.70	1.03	51.74	48.89	0.94
5	0.47	0.45	0.97	20.49	20.96	1.02

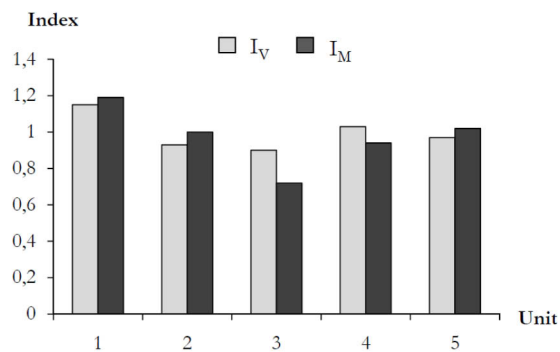


Figure 3.29 Distribution of the two calculated vulnerability indexes I_M and I_V

It is apparent that the simplified technique provides the same vulnerability classification as respect to the mechanical method applied in the longitudinal

direction. Therefore, the first application has shown a good result, although the methodology has been further validate.

3.3.4.1. *Further validation of the results: study cases in the historical centres of Torre del Greco (Na)*

Aiming at validating the proposed survey form, the analysis of a study case represented by an existing masonry building aggregate in the historical centre of Torre del Greco (Na), a town in the district of Naples, has been done. The study complex is within a pilot area, selected by the Working Group 4 (WG4) “Risk Assessment for Catastrophic Scenarios in Urban Areas” of the COST C26 Action “Urban Habitat Constructions under Catastrophic Events” (<http://www.civ.uth.gr/cost-c26/>) for evaluating the behaviour of both ordinary and public buildings under volcanic and seismic actions, the former related to a possible eruption activity of the Vesuvius (see paragraph 4.1).

The examined masonry block (Figure 3.30) consists of five structural units made of tuff stones having a regular layout but with different mechanical properties (Table 3.16). The horizontal structures consist of vaults without tie beams at the first level and mixed steel-hollow tiles floors at the other levels, while the roofing structures have a plain configuration.



Figure 3.30 Plan and bird-eye views of the study masonry aggregate in Torre del Greco

First of all, an in-situ inspection of this area has been made in order to assess all the main properties of the built-up. From this survey activity it is apparent that the typical ordinary houses of this part of the historical centre of Torre del Greco show a typological design completely fit with the features of the Vesuvius area. In particular, a large part of buildings are built before 1919, develops on 3 or 4

storeys and have the presence of sack tuff masonry as vertical structure typology. A large number of these constructions are attached each other, constituting historical blocks.

During the in-situ inspection, a survey of the above selected masonry block has been carried out, in order to evaluate the structural characteristics of its constituent units and, at the same time, to enable the collection of data necessary to apply the proposed vulnerability assessment procedure. This masonry aggregate is constituted by five units structurally dependent each other, having a total area equal to about 877 m².

The buildings, identified with numbers from 1 to 5 in Figure 3.31, present the following peculiarities:

- the building n.1 is placed at the internal corner of the block, so it shows two free sides only. The surface is about 97 m². It is composed of 4 storeys: the height of the ground level is 4 m, while the inter-storey height is 3.20 m;
- the building n.2 is placed at an internal position of the block, framed within three different buildings. The surface is about 137 m². It develops on 2 storeys having height of 4.00 m and 3.20 m at the ground level and the first level, respectively;
- the building n.3 is placed at the corner of the block, so it shows two free sides. The surface is about 194 m². It is developed on 3 storeys with a constant inter-storey height equal to 4.00 m;
- the building n.4 is adjacent to buildings 2, 3 and 5 and presents two free sides opposite each other. The surface is about 164 m². It develops on 3 storeys having the same inter-storey height of 4.90 m;
- the building n.5 occupies an external position within the block, so it is free on three sides. The surface is about 163 m². It is erected on 3 storeys: the height of the ground level is 5.40 m, while the inter-storey height is equal to 4.30 m.

Each building presents a tuff masonry structure with different quality; the mechanical parameters of each kind of masonry material are shown in Table 3.16.

Similarly to the aggregate in Sessa Aurunca, several static non linear analyses of the block has been carried out by means of both the proposed simplified methodology and the 3MURI numerical software (Formisano et al., 2010a, Formisano et al., 2010b).

Therefore, the first step has been the compilation of the form for each of the aggregate structural units. The results are depicted in Table 3.17, where both the absolute vulnerability indexes I_v and the relative ones $I_{v,rel}$, the latter normalized

into the range (0÷100), are reported.

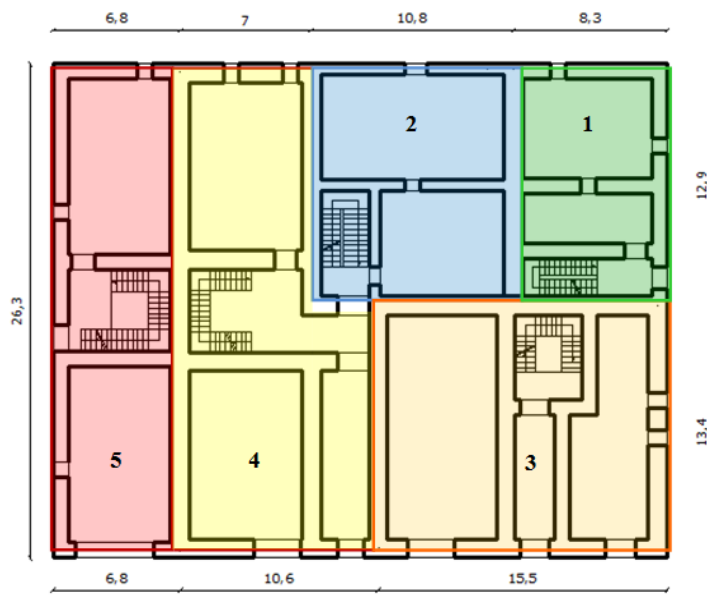


Figure 3.31 Plan view of the masonry block ground floor.

Table 3.16 Masonry mechanical properties of the aggregate structural units.

Unit	f_m [N/cm ²]	τ_0 [N/mm ²]	E [N/mm ²]	G [N/mm ²]	w [kN/m ³]
1	100	3,5	1080	180	16
2	80	2,8	900	150	16
3	110	3,5	1020	170	16
4	100	3,5	1080	180	16
5	120	4,2	1260	210	16

Table 3.17 Vulnerability index I_V according to the proposed procedure

Unit	I_V	$I_{V,rel}$
1	142.34	22.24
2	54.91	8.58
3	139.78	21.84
4	139.20	21.75
5	126.85	19.82

From the Table 3.17 it is evident that units having major height and placed at the aggregate corners are the most vulnerable ones.

Second, the pushover linear analyses have been performed on the FEM model of the aggregate (Figure 3.32) and, therefore, the relative pushover curves have been achieved by considering two different load conditions, namely a distribution of forces proportional to the masses and another one proportional to the masses by the corresponding first vibration mode displacements. Afterwards, these pushover curves have been compared with the demand spectrum at the Life Safety Limit State (LLS) provided by the Italian Code, according to the Capacity Spectrum Method, in order to obtain a vulnerability index, analogously to the analysis case of Sessa Aurunca. This spectrum is referred to an ordinary building with a service life of 50 years, located in Torre del Greco and based on a ground of type C of topographic category T_1 .

Each structural unit of the masonry aggregate has been modelled both as isolated and as part of the building complex. Two different pushover analyses have been carried out in the longitudinal direction (X) and along the transverse one (Y) of each building.

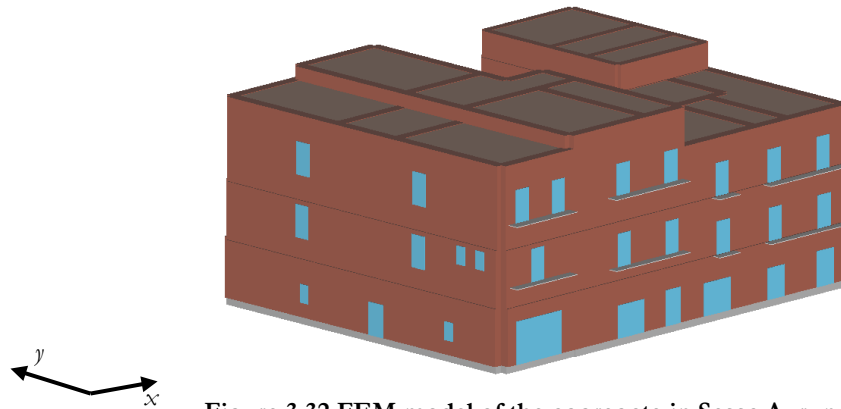


Figure 3.32 FEM model of the aggregate in Sessa Aurunca

The available ductility of structural units has been defined as the ratio between the ultimate displacement under the distribution of horizontal forces considered D_u and the maximum elastic displacement D_y . Then, the so-called mechanical seismic vulnerability index of the structure I_M , achieved under numerical way, has been calculated for each direction as the ratio between the maximum horizontal displacement required by earthquake D_{max} and the ultimate one before the collapse D_u , similarly to the case of Sessa Aurunca.

In Figure 3.33 the pushover curves of the whole aggregate in both plane directions are reported. Furthermore, in Table 3.18 the values of D_{max} and D_u , as

well as the vulnerability index I_M , are reported for each building numerically analysed both as single structure (I_{M1}) and as part of the aggregate (I_{M2}). From this table it can be noted that the aggregate condition of the structure reduced its seismic vulnerability if compared with the same building considered as isolated.

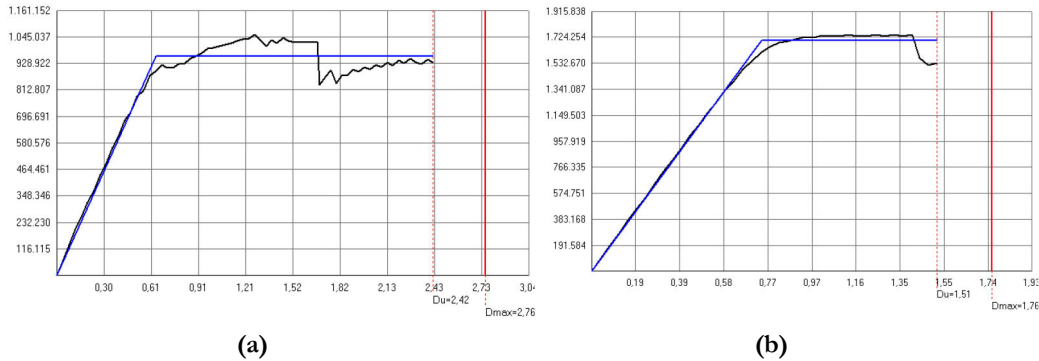


Figure 3.33 Pushover curves of the entire aggregate in the longitudinal (X) direction (a) and the transverse (Y) one (b)

Table 3.18 Mechanical vulnerability indexes obtained by means of the numerical analyses.

Unit	Dir.	Isolated			Aggregate condition		
		D_{max} (cm)	D_u (cm)	I_{M1}	D_{max} (cm)	D_u (cm)	I_{M2}
1	X	2.58	1.79	1.44	2.27	1.36	1.67
	Y	1.98	2.04	0.97	1.78	2.20	0.81
2	X	1.17	1.65	0.71	1.14	1.81	0.63
	Y	0.54	1.75	0.31	0.69	1.77	0.39
3	X	3.58	3.40	1.05	2.85	1.92	1.48
	Y	1.77	2.27	0.78	1.67	2.00	0.84
4	X	3.86	2.44	1.58	2.70	2.49	1.08
	Y	1.62	2.26	0.72	1.75	1.51	1.16
5	X	3.89	1.87	2.08	2.62	2.50	1.05
	Y	0.99	1.44	0.69	1.53	1.16	1.31

The comparison among the vulnerability index values related to the two examined methodologies with reference to the aggregate condition of buildings is also shown in Table 3.19, where it is perceptible that in the numerical analyses the most vulnerable direction is the longitudinal one (X).

According to the mechanical vulnerability classification in (X) direction, it is noticeable that the structural unit n. 1 is the most vulnerable. On the other hand, the building n. 2 is less vulnerable than others. In fact, such a structure is made of a good quality of tuff masonry and has a plan vertical regularity. Furthermore,

the building is protected by three higher buildings and it occupies an internal position in the aggregate. All these features reduce the seismic vulnerability, leading to the improvement of the building performance against earthquake.

In addition, if the results deriving from applying the two methods are compared, it is apparent that the simplified technique provides the same vulnerability classification as respect to the mechanical method applied in the longitudinal direction, as noted also for the aggregate in Sessa Aurunca.

Therefore, the comparison allows to validate the proposed quick evaluation methodology, so to consider the forms as a reliable indicator of the seismic vulnerability of masonry aggregates into historical centres. This methodology does not allow to evaluate the damage grade that the building into masonry aggregates should suffer under earthquakes, but permits to identify the most vulnerable units in order to program retrofitting interventions.

Table 3.19 Comparison between vulnerability indexes achieved by applying the two assessment methods

Unit	$I_{V,rel}$	I_{M2}	
		Longitudinal (X)	Transverse (Y)
1	22.24	1.67	0.81
2	8.58	0.63	0.39
3	21.84	1.48	0.84
4	21.75	1.08	1.16
5	19.82	1.05	1.31

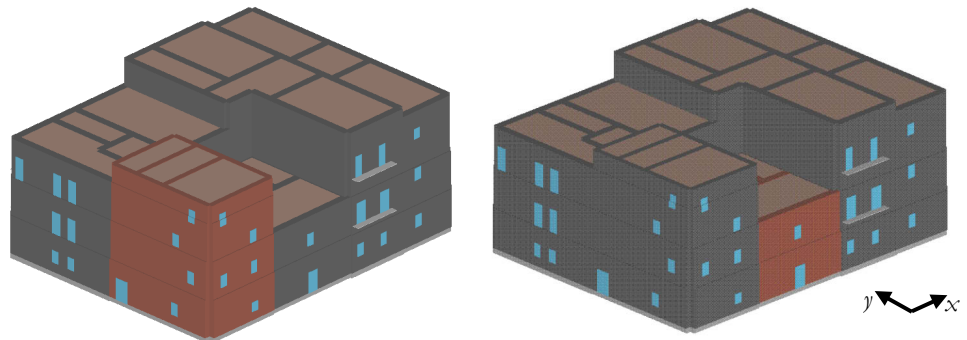


Figure 3.34 The building n. 1 and n. 2 within the masonry building block examined in Torre del Greco

3.3.4.2. Methodology application to the historical centre of Torre del Greco: seismic vulnerability and damage assessment by GIS

The proposed methodology has been used to assess the seismic vulnerability of the historic centre of Torre del Greco (Fig. 3.35). This city, about 20 km far from

Naples, is one of the municipalities most exposed to the Vesuvius risk, since it was destroyed in the eruption of 79 A. D. Furthermore, this town is interesting from the architectural and historical viewpoint, it presenting a large monumental heritage, such as Roman archaeological ruins, monasteries, churches, villas and museums. For this reason, the aforesaid WG4 of the COST C26 Action “Urban Habitat Constructions under Catastrophic Events” has selected the Vesuvius region and in particular the historic centre of Torre del Greco as investigation area, in order to evaluate the impact of the volcano on built up for both minimizing life loss and implementing protection measures for cultural heritage and ordinary buildings.



Figure 3.35 The pilot area selected within the historical centre of Torre del Greco.

The data used for the methodology application were collected during specific visual in-situ inspections of the aggregates of the investigated zone.

The activity of in situ collection data related to the pilot study area was achieved in January 2009 by the WG4 members, with the contribution of the PLINVS Centre (Hydrological, Volcanic and Seismic Engineering Centre, Director prof. Giulio Zuccaro). The data were collected by means a specific quick methodology, elaborated and commonly used by Civil Protection Department. The applied procedure is based on the identification of the construction typology and characteristics and on the compilation of a specific form. The element identification is performed through an external visual inspection and examination of the most influencing seismic and volcanic vulnerability factors.

This procedure is implemented in a synthetic form subdivided in the following eight different sections:

1. *Identification*, related to the geographical localization of the building given by Campania region;
2. *General information*, related to type (ordinary building, warehouse, electrical station, etc), use, destination and exposure of the structural unit;
3. *Condition*, related to the age, the state of conservation and the typology of the finishes;
4. *Descriptive Characteristics*, related to geometrical parameters, as the number of storeys above the ground, the number of residential apartments, the presence of occupied or not basement, the height of the first storey, minimum and maximum heights up to the roof, the presence of barriers with height bigger than 2 m, the orientation (angle between the longest or the main façade and the North) and the position of the structural unit in the aggregate;
5. *Structural Characteristics*, related to main typology (reinforced concrete, masonry, wood, steel and mixed), primary vertical structures (sack masonry with or without reinforcements, hewn stones masonry, masonry or tuff blocks, RC frames with weak or resistant cladding, etc.), primary horizontal structures (timber floor, floor with steel beams, concrete-tile structures, vaults, etc.), geometry of the roofing (plane, single pitched, multi pitched and vaults), thickness of the walls and the curtain walls and typology of the curtain walls (tuff blocks or squared stones, concrete blocks, etc);
6. *Openings*, referring to the dimensions and the percentage of openings in the façade, the number of small, typical and large windows, their material, protection and condition;
7. *Interventions*, about the type and the age;
8. *Regularity*, referring to the distribution of the curtain walls in plan and in elevation, the type of the structure (single or two-directional frames, single or two-directional walls and walls with frames), soft floor (pilotis on a part of the ground floor, totally open ground floor and intermediate soft storey) and possible presence of stocky beams or columns.

In the post-survey phase, all the collected data have been organized and put in a database, in order to have at disposal geometrical and structural characteristics of the built environment. In particular, a suitable elaboration of data acquired over the whole pilot area has been carried out in the GIS environment. By processing these data, homogeneous groups of buildings have been identified, their main features being displayed in several thematic maps created by means of the ArcGIS software (<http://www.esri.com/software/arcgis/index.html>).

These maps are related to the main structural typology (Fig. 3.36a), the class of age (Fig. 3.36b), the number of floors (Fig. 3.37a), the state of conservation (Fig.

3.37b) and the main vertical (Fig. 3.38) and horizontal (Fig. 3.39) structures of study constructions.

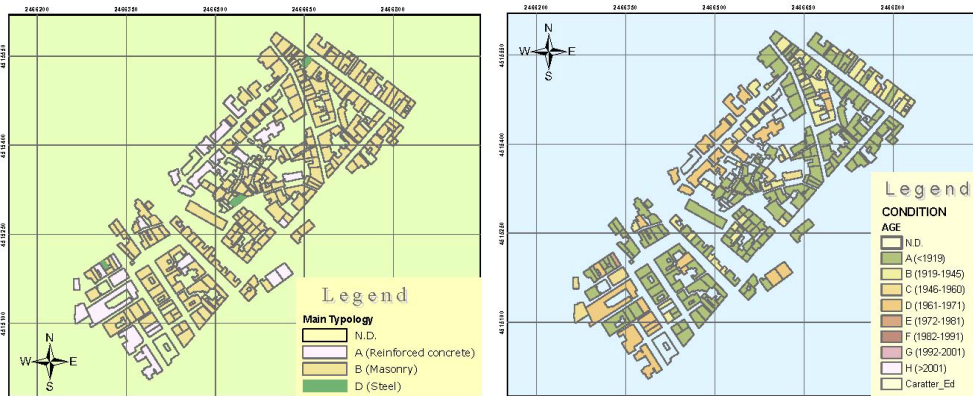


Figure 3.36 The investigated pilot area: a) main structural typologies; b) age classes

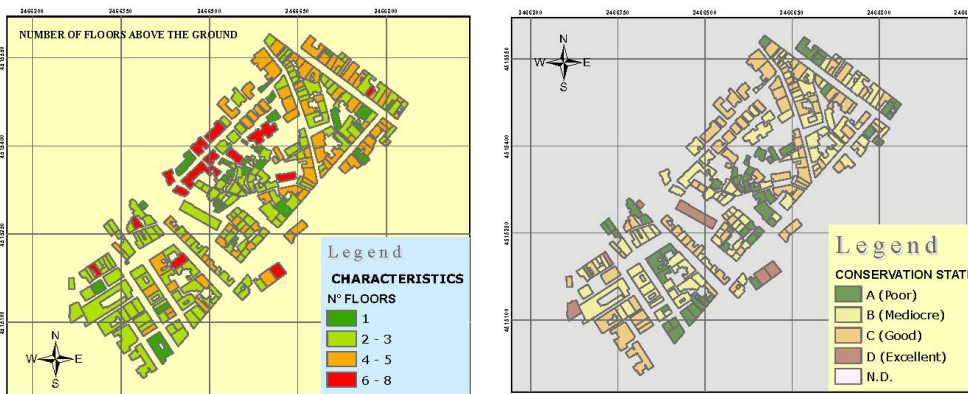


Figure 3.37 The investigated area: a) number of floors; b) conservation state

For each of the thematic groups, the percentage of buildings belonging to a specific subcategory is provided. In particular, for the main structural typology, it can be noted that the 80% of the buildings has a masonry structure, while the 9.5% is made of reinforced concrete. Other important information on the surveyed constructions are reported as follows:

- 1) 58% of buildings was built before 1919, while 18% of them was erected between 1919 and 1945;
- 2) the majority of buildings has 3 floors (38 %), whereas 25% of them has 4 floors and 17% of them has 2 floors;

- 3) 38% of the built up has a mediocre state of conservation, while 30% and 21% of buildings is in a good condition and in a poor state of maintenance, respectively;
- 4) 46% of buildings is made of tuff or squared masonry stones, 4% of them has a hewn stone masonry and 29% of them is composed of a sack masonry structure;
- 5) 51 % of buildings has floors consisting of steel beams and hollow flat tile, 16% of them is made of either mixed concrete-tile or RC floors and 16% and 5% of them has vaults without and with tie beams, respectively.

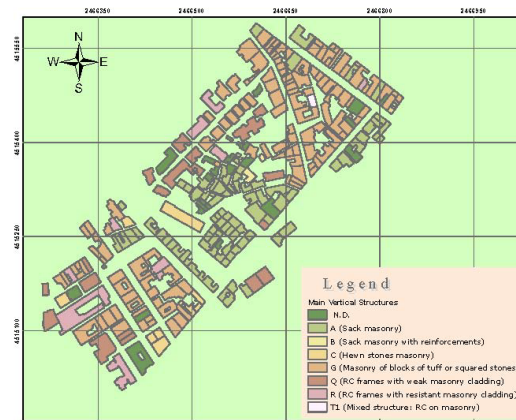


Figure 3.38 The investigated area: main vertical structures

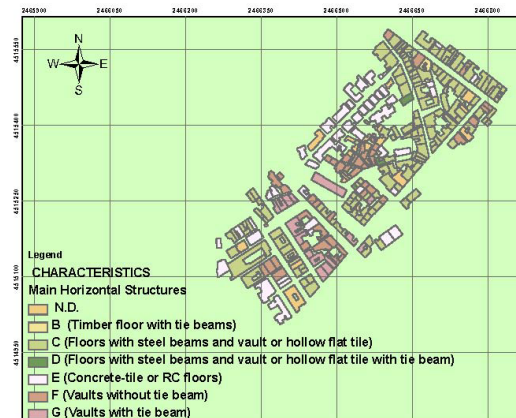


Figure 3.39 The investigated area: main horizontal structures

By observing the several thematic maps shown in the previous figures, the most relevant data and information necessary to the vulnerability management of the investigated area can be achieved.

Within the GIS tool, automatic procedures have been created and performed in order to process and share out the data collected from the identified building categories with the purpose to assess the seismic vulnerability of the historical aggregates within that area by using a rapid evaluation technique.

Therefore, the seismic vulnerability of the built up has been firstly estimated on the basis of the Benedetti and Petrini form and, later on, by means of the proposed one. The GIS application led to the vulnerability maps of Figure 3,40.

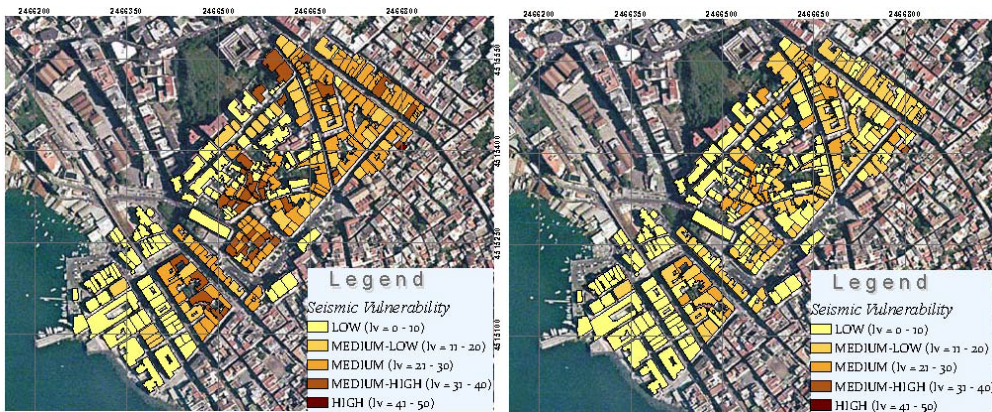


Figure 3.40 Seismic vulnerability maps developed by applying: (a) Benedetti and Petrini's procedure and (b) the proposed one

From figures, it is noted that the two applied methodologies keep the same vulnerability scale, although the original methodology overestimates the effective seismic vulnerability of the buildings in aggregate, since it does not take into account the significant parameters typical of the interaction among adjacent constructions. In fact, it is apparent that, in the case under question, the aggregate condition makes the structural units one level less vulnerable than the same units considered as isolated. So, the aggregate condition improves the seismic performance of the single buildings compared to the isolated ones. In addition, the analysis results show that the most vulnerable buildings were built before 1919, develop on 3-4 storeys and have a poor or mediocre conservation state. Moreover, their vertical structures, which sustain either mixed steel-hollow tile floors or vaults, are made of sack masonry. Instead, regarding the aggregate condition, it is apparent that the most vulnerable buildings are the ones

comprised between lower constructions and placed at either the corner or the end of the block.

Considering that the vulnerability index does not give information about the damage level caused by earthquakes, the mean damage grade μ_D have been evaluated on the base of the formulations (3.19) in order to estimate the seismic damage within the examined area

The earthquake scenario for different seismic intensities has been considered by changing the macro-seismic level (S), so to obtain different values of μ_D related to different values of the seismic acceleration (a_g) (Table 3.2). In particular, the mean damage grade has been calculated for 4 different seismic events, defined in the New Technical Italian Code and identified in Table 3.20 by both their return period (T_R) and the corresponding macro-seismic level.

Table 3.20 Earthquakes considered in the damage analysis.

T_R (years)	a_g (m/s ²)	MCS scale	Macro-seismic level S (MMI scale)
101	0,83	VII	8
475	1,61	VIII	10
975	2,06	IX	11
2475	2,72	X	12

The variation of the mean damage grade μ_D of each structure within the studied area for each of the seismic events listed in Table 3.20, is shown in the damage maps created by means of the GIS instrument (Figs 3.41 and 3.42), where the following damage levels can be identified (Grunthal, 1998):

- Light, for μ_D ranging from 0 to 1;
- Moderate, fo μ_D ranging from 1.1 to 2;
- Heavy, for μ_D ranging from 2.1 to 3;
- Very heavy, for μ_D ranging from 3.1 to 4;
- Destruction, for μ_D ranging from 4.1 to 5.

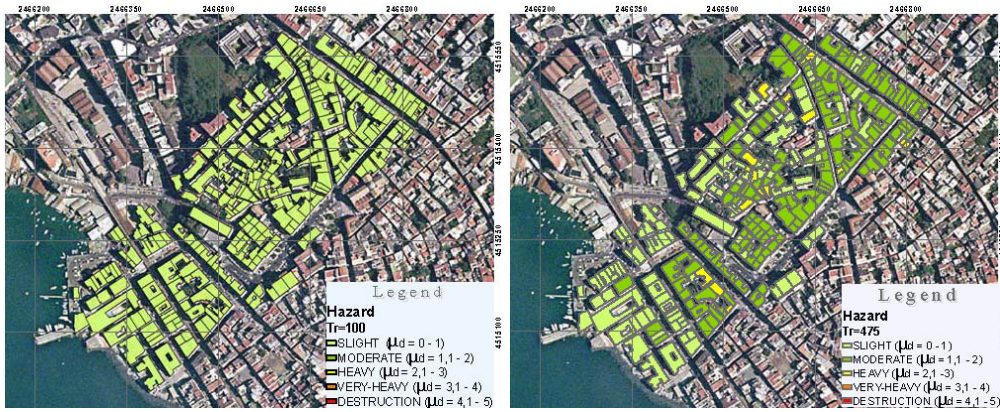


Figure 3.41 Damage map for an earthquake with: (a) $T_R = 101$ years; (b) $T_R = 475$ years

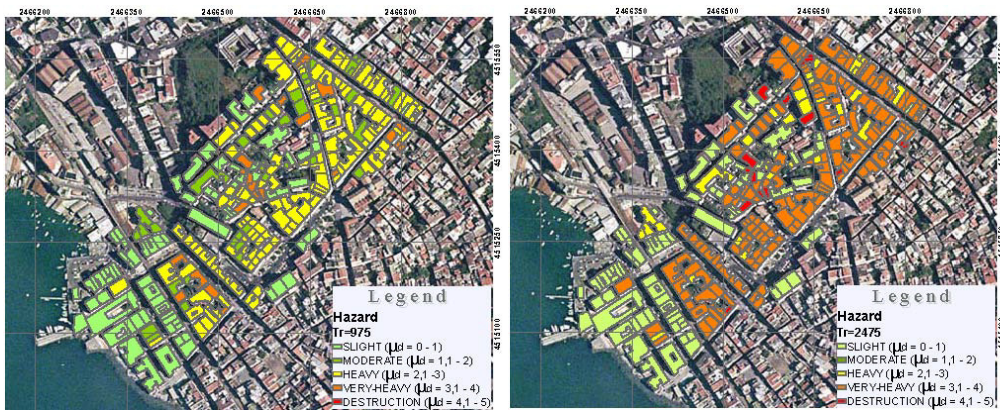


Figure 3.42 Damage map for an earthquake with: (a) $T_R = 975$ years; (b) $T_R = 2475$ years

The analysis results have shown that at Life Safety Limit State (LLS) the major part of buildings should suffer a heavy damage with large and extensive cracks in most walls and failure of roof tiles and chimneys. Instead, considering the possible earthquake occurring after the Vesuvius eruption, having a degree lower than tectonic quakes, it has been detected that the investigated masonry building aggregates should undergo a damage from light to moderate. In the first case, hair-line cracks in very few walls and fall of both small pieces of plaster and loose stones from upper part of buildings should occur. Instead, moderate damages should be represented by cracks into many walls, fall of large pieces of plaster and partial collapse of chimneys.

3.3.4.3. *Conclusions and further developments*

The described study shows that masonry exhibit a different behaviour as respect to isolated constructions, since adjacent buildings influence each other during earthquakes. So, in order to study their seismic behaviour, a simplified vulnerability assessment methodology has been proposed and validated on study cases in Sessa Aurunca and Torre del Greco, respectively. In particular, in the latter case, the validation has been done by comparing the achieved synthetic vulnerability indexes with the ones obtained under numerical way. The analysis results have shown that the proposed technique provides the same vulnerability classification defined in the numerical method. Also, the most vulnerable buildings are the ones having the major number of floors and located at the corner of the aggregate. Instead, the less vulnerable buildings occupy an internal position within the aggregate and are among taller buildings. Finally, the proposed form has been applied to a historical centre area of Torre del Greco, showing that, on average, the aggregate condition improves the seismic performance of the single buildings compared to the isolated ones.

Although the proposed procedure for masonry blocks have shown good results, this one should be confirm by means the application to other territorial zones having seismicity level different from Campania Region. In particular, the form is going to be applied to the whole historical centre of a town hit and damaged by the recent L'Aquila earthquake, as for instance Poggio Picenze (AQ), in order to show the procedure effectiveness by comparing the predicted damages with the real ones. The historical centre of Poggio Picenze, indeed, has been investigated by means of survey and experimental activities, thus it could be an interesting case study for the progress in this field.

Finally, another important aspect should be considered. The presented procedure does not examine the out-of-plane behaviour, that significantly influences the seismic structural response of a masonry aggregate. So, parametric analyses are going to perform in order to calibrate additional parameter for out-of-plane failure mechanisms.

Chapter 4

The Vesuvius study case: vulnerability evaluation of a monumental building

4.1. INTRODUCTION

The Research Project COST (European Cooperation in the field of Scientific and Technical Research) Action C26 “Urban Habitat Constructions under Catastrophic Events” has been an important three-year project (2007-2010) with the aim to develop research activities in the field of risk induced by exceptional actions. The main objective of the Action was to increase knowledge of the behaviour of constructions in the urban habitat when exposed to extreme events (e.g. earthquakes in non-seismic areas, fire, wind storms, impact, gas explosions, etc) in order to predict their response when both the applied loading and the inherent structural resistance are combined in such a way as to reduce the safety level below acceptable values, leading, in some cases, to a premature collapse.

This COST Action, therefore, was aimed at the protection of constructions in urban areas subjected to exceptional loading condition. In fact, buildings in the urban habitat are designed according to rules aimed at ensuring an adequate structural safety level under normal loading conditions. Nonetheless, all structures can be exposed to certain extreme conditions due to either natural or human-made hazards in their design lifetime. Thus, the main scope of this project was to establish an improved understanding of the response of constructions under extreme actions, in order to ensure a given adequate safety level.

In particular, the COST Action C26 was composed by the following four Working Groups:

- WG1: Fire Resistance
- WG2: Earthquake Resistance

- WG3: Impact and Explosions Resistance
- WG4: Risk Assessment for Catastrophic Scenarios in Urban Areas

In the framework of WG4, the Vesuvius region was identified as a multi-risk environment and, therefore, selected as a pilot study case.

Torre del Greco is one of the most exposed city to the Vesuvius risk, it being also very interesting from the cultural point of view, since a large historic built up heritage is present there. Therefore, in the historical centre of this town a sacrificial area has been selected (cfr. paragraph 3.4.3.4) in order to perform several studies for evaluating the behaviour of ordinary and strategic buildings subjected to both ordinary and extreme loads..

In particular, the object of this chapter is the investigation on the behaviour of a strategic monumental masonry building under volcanic actions. This palace, known as *Palazzo di Città* (City Palace), has been individuated as a pilot study case for the preservation of the cultural heritage (Fig. 4.1). Thus, quick, simplified and refined mechanical methodologies for seismic vulnerability assessment have been applied to the building under investigation in order to define its susceptibility at damage from earthquake. In addition, the comparison among the examined seismic vulnerability evaluation procedures has allowed to test the effectiveness of the employed procedures in order to outline a simplified approach for the vulnerability assessment of monuments.

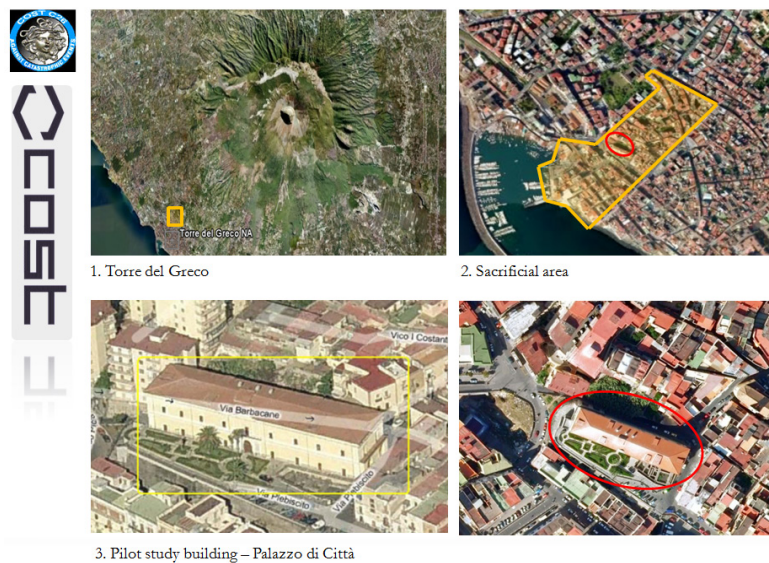


Figure 4.1 Pilot study building identification

In the final part of the study, a volcanic vulnerability analysis has been performed on the examined palace in order to estimate its structural response under exceptional loading conditions deriving from volcanic eruptions.

4.2. THE STUDY CASE: THE PALAZZO DI CITTÀ IN TORRE DEL GRECO (NA)

4.2.1 Historical and descriptive and information

Palazzo di Città was built as the ancient castle of the first urban nucleus of Torre del Greco, known as *Castrum Turris Octavae* (Castle of the Eighth Tower). During the Angevin Age, the eastern part of the castle was built, absorbing the first ancient norman- swabian tower.

In 1420 the castle became property of Alfonso D'Aragona, who decided to improve it with some special interventions, making it his occasionally residence until 1456, when the castle, in very bad conditions, was transferred to the Carafa family.

In 1698 the feud was annexed to the Regio Demanio and, after some issues of law, the castle became the common property of the University under the regency of the first democratic “dummy baron” Giovanni Langella (elected by people).

During the XVIII Century, the castle became a palace hosting a wide range of structures with different destination, such as public and private residencies, a public school, an archive, a prison and a chapel, which modified the old castle appearance.

In 1794, the castle was not destroyed by a disastrous volcanic eruption, thanks to its location far above the ground (28m on the sea level as it can be noted in Figure 4. b) and, therefore, it was equipped as “strategic” building to be used for the emergency management.

In the XIX century, the palace was refurbished and transformed in the building hosting the town Municipality. The historic façade was characterized by regular openings and was enhanced with several architectural ornaments. The entrance was constituted by an arch located in the central part of the façade.

Several oil paintings and period pictures depict the Palace appearance in the first half of the XX century (Figs. 4.2 and 4.3). In particular, the monumental character and the strategic position of the building is highlighted by these historical representations.

In 1927, the town Municipality decided to upgrade the building, by restructuring the masonry structures and by modernizing wiring and plumbing systems.

Some projects were rejected until 1980, when the final project of Eng. R. Sparacio and Arch. F. Parlato were approved, but the intervention was stopped by the Irpinia seismic event.

In 1989, the conservation state of the Palace was very poor, as depicted in Figure 4.4. Therefore, urgent structural intervention and retrofitting measures for the reuse of the entire built complex were necessary.



(a)



(b)

Figure 4.2 Oil paintings by: (a) N. De Corsi, “Le cento Fontane” (1939);
(b) L. Mazza, “Il Castello Baronale e Capri” (1928)



(a)



(b)

Figure 4.3 Historical photographs of the façades:
(a) from via Fontana (first half of XX cen.); (b) from Piazza Plebiscito (1980)



Figure 4.4 Views of the building before the refurbishment intervention started in 1989

The town Municipality commissioned the systems design and the structures one to prof. Eng. F. Reale and prof. Eng. F. M. Mazzolani, respectively. The restoration works were completed in 2003 (Figs. 4.5-4.7).



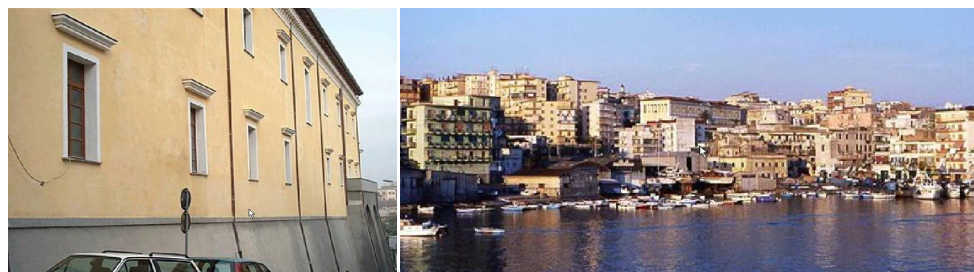
Figure 4.5 Views of the palace main façade after restoration works finished in 2003



(a)

(b)

Figure 4.6 Present-day pictures: (a) from via Fontana; (b) from via Barbacane



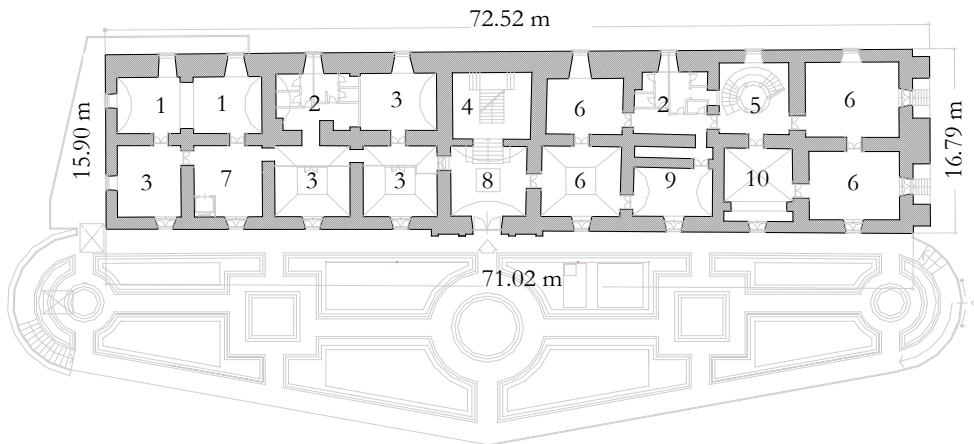
(a)

(b)

Figure 4.7 Present-day pictures: (a) from via Barbacane; (b) from the sea

Nowadays, *Palazzo di Città* has not only a historical and architectural importance, but also a strategic one, due to the fact that it hosts the public offices of the town

Municipality. In particular, the ground level is developed on a rectangular surface of about 1185 m² and hosts several public offices, as shown in Figure 4.8. In Figures 4.9-4.11 some geometrical views of the buildings are represented.



1. Contracts and competitive tenders office; 2. Sanitation; 3. Administration; 4. Grand staircase;
5. Backstairs; 6. Accounts department; 7. Room; 8. Entrance; 9. Steward's office; 10. Squad

Figure 4.8 Plan layout of the first floor of the building

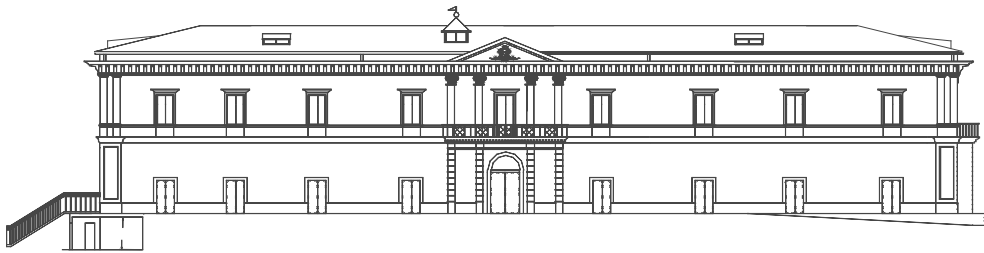


Figure 4.9 South geometrical view of the building (from Piazza Plebiscito)

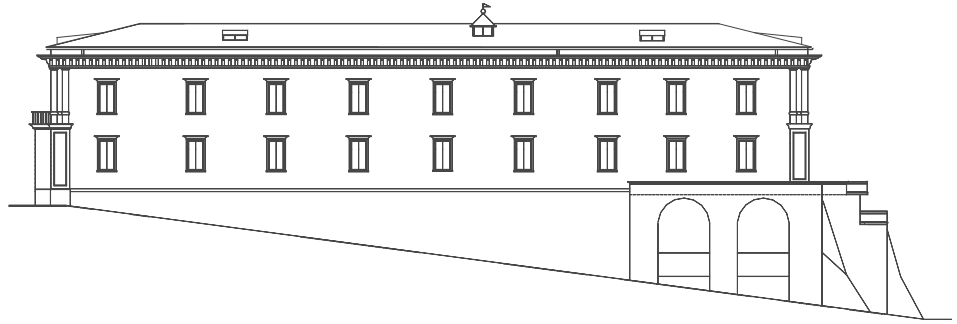


Figure 4.10 North geometrical view of the building (from via Barbacane)

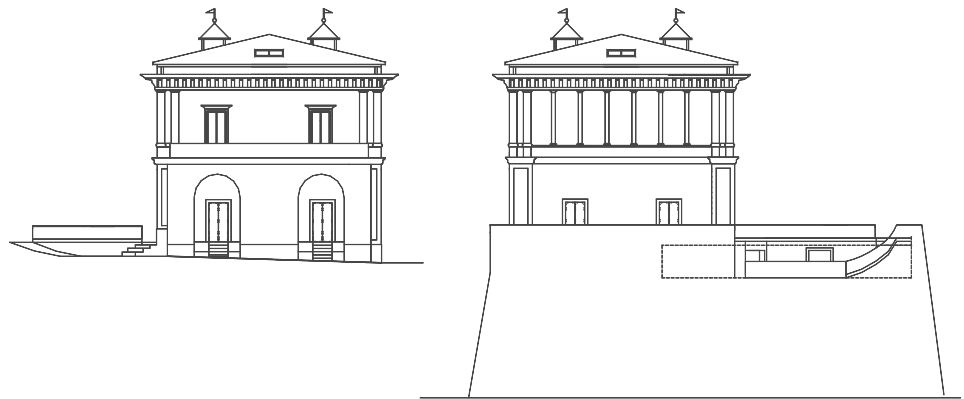


Figure 4.11 East and West geometrical views of the building

4.2.2 Structural features

Palazzo di Città has a tuff masonry structure and develops on two stories surmounted by a pitched roof. The original tuff walls have been consolidated by means of both concrete injection and spritz beton in the last restoration works.

The first floor is composed by original vaulted ceilings sustaining the more recent reinforced stiffening concrete slabs. The second horizontal structure level was completely restructured by substituting the old floor system with wooden and steel floors, as shown in Figure 4.12. The roof, which is supported on the left side of the building entrance by RC circular columns, has a wooden structure covered by clay tiles. A particularly significant intervention was the insertion of stringcourse in order to reduce the roof thrust.

The structural data related to the examined construction are shown in Table 4.1.

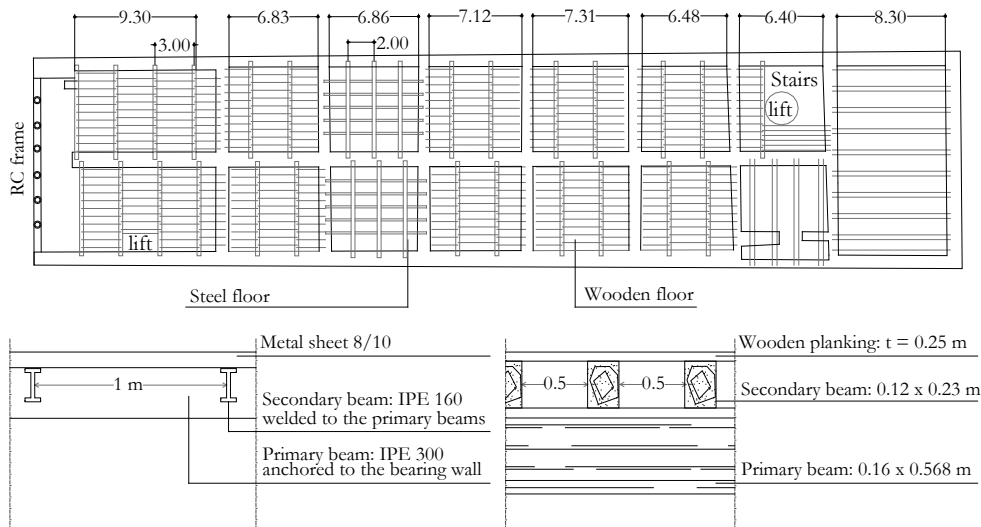


Figure 4.12 Structural plan view of the building and structural details

Table 4.1 Structural data of the examined construction

Floor typology	Weight P_s [kN·m ⁻²]	Mechanical properties of tuff masonry [M.D. 2008]	
Vault	15	Compressive strength σ_c [MPa]	1
Steel	5	Shear strength τ_0 [MPa]	3,5
Wooden	3.9	Elastic Modulus E [MPa]	1080
Roof	2.6	Shear Modulus G [MPa]	180
		Density w [kN·m ⁻³]	16

Since the structure is articulated into a rectangular shape with ratio between sides greater than four, it can be considered as irregular in plan. This condition is also confirmed from the fact that only some floors are infinitely rigid in their plane.

4.3. QUICK METHODOLOGY APPROACHES

4.3.1 The Benedetti and Petrini's form

The Benedetti and Petrini's quick methodology is used to assess the building seismic vulnerability through the assignment of a synthetic index I_v (cfr. section 3.2.3.3).

The procedure has been applied to the *Palazzo di Città* in order to quickly estimate the structural performance (Table 4.2) (Formisano et al., 2008; Florio et al. 2009).

Table 4.2 The Benedetti and Petrini's procedure applied to the Palazzo di Città

Factors	Classes score (s)				Weight (w)
	A	B	C	D	
1. Organization of the vertical structures	0	5	20	45	1
2. Nature of the vertical structures	0	5	25	45	0.25
3. Location of the building and type of foundation	0	5	25	45	0.75
4. Planimetry	0	5	25	45	1.5
5. Planimetry: compactness	0	5	25	45	0.5
6. Regularity	0	5	25	45	$0.5 < w < 1$
7. Type of slabs	0	5	15	45	$0.75 < w < 1$
8. Roofing	0	15	25	45	0.75
9. Details	0	0	25	45	0.25
10. Physical conditions	0	5	25	45	1

In the calculation of the vulnerability indicator, two different unsure parameters have been considered, namely the planimetry (n.4) and the regularity (n. 6). In particular, for the factor n.4, concerning the material mechanical properties of the masonry structure, three different medium shear resistances (τ_0) have been considered according to the Italian code (M. D., 2008):

- $\tau_{01} = 42 \text{ kN}\cdot\text{m}^{-2}$;
- $\tau_{02} = 28 \text{ kN}\cdot\text{m}^{-2}$
- $\tau_{03} = 35 \text{ kN}\cdot\text{m}^{-2}$

The parameter n.4, in fact, is based on the conventional and simplified computation of the ultimate strength of the masonry walls, according to the following formula:

$$C = \frac{a_0 \cdot \tau_0}{q \cdot N} \cdot \left[1 + \frac{q \cdot N}{1.5 \cdot a_0 \cdot \tau_0 \cdot (1 + \gamma)} \right]^{1/2} \quad (4.1)$$

in which:

- a_0 is the ratio between the minimum resistant area (A) in a given direction and the total resistant area (A_t);
- γ is the ratio between the maximum resistant area (B) in a given direction and the total resistant area (A_t);
- N is the number of stories;
- q is function of the masonry density (w) and of the weight for unit area (p_s) equal to:

$$q = \frac{(A + B) \cdot h}{A_t} \cdot w + p_s \quad (4.2)$$

The final score depends by the(α) value:

$$\alpha = \frac{C}{C^I_s} \quad (4.3)$$

where C is the ratio computed by means of the equation (4.1) and C^I represents the reference value of the shear strength assumed equal to 0.4.

All the parameters concerning the calculation of the factor n. 4 are listed in Table 4.3.

Table 4.3 Parameters related to the calculation of factor n.4

Parameter	Numeric value	Parameter	Numeric value
a_0 [A/A_t]	0.149668422	τ_{k1} [$\text{kN}\cdot\text{m}^{-2}$]	107.1
γ [B/A_t]	0.219217761	τ_{k2} [$\text{kN}\cdot\text{m}^{-2}$]	71.4
p_s [$\text{kN}\cdot\text{m}^{-2}$]	18.78743739	τ_{k3} [$\text{kN}\cdot\text{m}^{-2}$]	89.25
p_m [$\text{kN}\cdot\text{m}^{-3}$]	16	C_1	0.253030193
A [m]	177,355	C_2	0.201244927
B [m]	259.77	C_3	0.228010928
A_t [m]	1184.9861	C^I	0.4
h [m]	5.95	α^1	0.632575482
q [$\text{kN}\cdot\text{m}^{-2}$]	53.90540206	α_2	0.503112318
Number of storeis N	3	α_3	0.570027319

It is evident how the variability of this parameter depends on the uncertainties related to the mechanical properties of the material.

Instead, for the factor n.6, concerning the regularity of the mass distribution in elevation, since the real state of the building was not so clearly defined, both class A and class B have been considered one by one.

Therefore, the combination of the two variable parameters with others has led to the calculation of 16 different vulnerability indexes, whose absolute and relative values range from 63 to 98 and from 0.16 to 0.26, respectively. In particular, relative indexes have been calculated by the ratio between the absolute indexes and the upper one, which is obtained by assigning the maximum score to the ten analysis factors, it being equal to 382.02.

The elaboration of obtained indices has allowed to define two main final values, namely the relative mean value (I_{VM}), equal to 0.20, and the characteristic one (I_{VK}), equal to 0.21, the latter being considered as the effective vulnerability index of the study masonry structure as follows:

$$I_{VK} = I_{VM} \cdot (1 + k \cdot \delta) = 0.20 \cdot (1 + 0.05 \cdot 0.76) = 0.21 \quad (4.4)$$

in which δ represents the ratio between the I_{VM} value and the quadratic mean scatter (s) and k is a numerical coefficient provided by the code.

Since seismic vulnerability is the damage which a construction can undergo under earthquakes, it depends on both the earthquake grade and the construction parameters. For this reason, since I_{VK} does not give information about the damage level of the building, the mean damage grade (μ_D) of the building have been calculated on the basis of the aforementioned deterministic correlation between the seismic input and the expected damage expressed by equation (3.19). In particular, the index I_{VK} have been converted in the index V_I by means of the following equation directly derived from relationship (3.21):

$$V_I = \frac{76.25 + I_k}{156.25} = 1.01 \quad (4.5)$$

Thus, by changing the macro-seismic level S (Grunthal, 1998), according to the formulation (3.19), different values of μ_D have been obtained (Table 4.4).

Table 4.4 Mean damage grades related to macro-seismic levels of EMS 98

Macro-seismic level (S)	Mean damage grade (μ_D)
5	0.80
6	1.56
7	2.60
8	3.61
9	4.30
10	4.68
11	4.86
12	4.94

In particular, for an earthquake level S equal to 9, the factor μ_D , which represents the damage level caused by an earthquake corresponding to the Life Safety Limit State (LLS), is almost equal to the grade 4 of the EMS 98, while for an earthquake level S equal to 11, the factor μ_D , which represents the damage level caused by an earthquake corresponding to the Near Collapse Limit State (CLS), is almost equal to the grade 5 of the same scale (Fig. 4.13) (see par. 1.2).

The calculated damage grades can also be expressed in relative way by the ratio between this values and the maximum level of damage ($k_{\max}=5$), so leading to the following two indexes:

- $I_{SLS} = 0.860$
- $I_{CLS} = 0.972$

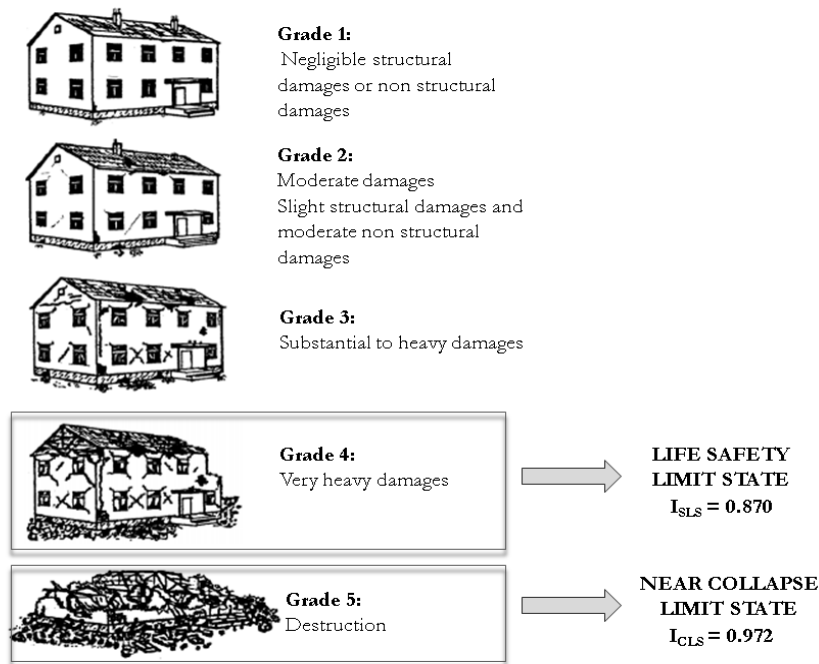


Figure 4.13 Relation between damage levels according to EMS 98 and vulnerability indexes

4.3.2 The Italian Guidelines

The Italian Guidelines for evaluation and reduction of the seismic risk of the cultural heritage according to the Italian Code (MiBAC, 2006), provide an approach to estimate the seismic vulnerability of a monumental building by

means of a simplified mechanical model. In fact, this method permits to calculate the collapse seismic acceleration of the structure, considering in-plane failure mechanisms also.

The ground failure acceleration is given by the following equation:

$$a_{CLS} = \frac{q \cdot V_{CLS}}{e^* \cdot M \cdot C(T)} \quad (4.67)$$

in which:

- V_{CLS} is the shear resistance of the examined structure;
- q is the structure factor, that is equal to 3 for the building regular in elevation and equal to 2,25 in the other cases;
- M is the total seismic mass of the system;
- e^* is the participant mass of the considered failure mode;
- $C(T)$ is the normalised spectrum, developed as the ratio between the elastic spectrum and the peak ground acceleration ($a_g \cdot S$).

The shear strength of the building is the minimum between the ones calculated considering two orthogonal direction (X and Y). According to this procedure, the structure collapses when the mean shear stress equals a fraction of the masonry shear strength.

In particular, the longitudinal shear strength (X direction) is evaluated as follows:

$$V_{CLS,X} = \frac{\mu_{xi} \cdot \xi_{xi} \cdot A_{xi} \tau_{di}}{\beta_{xi}} \quad (4.7)$$

in which:

- A_{xi} is the shear resistance area of the longitudinal walls of the generic i-level;
- β_{xi} is an irregularity plan factor of the generic i-level, dependent on the eccentricity e_{yi} (distance between stiffness centroid and mass centroid) and on the distance (d_{yi}) between the stiffness centroid and the more external wall in the considered direction; the parameter is calculated on the base of the following formula:

$$\beta_{xi} = 1 + 2 \cdot \frac{e_{yi}}{d_{yi}} \leq 1.25 \quad (4.8)$$

- μ_{xi} is a coefficient considering the stiffness and strength homogeneity of the masonry piers, it being equal to:

$$\mu_{xi} = 1 - 0.2 \cdot \sqrt{\frac{N_{mxi} \cdot \sum_j A_{x,ij}^2}{A_{x,i}^2}} - 1 \geq 0.8 \quad (4.9)$$

where N_{mxi} is the piers number in longitudinal direction at the generic i -level; $A_{x,ij}$ is the generic pier area in the x direction;

- ξ_{xi} is a coefficient dependent on the expected failure mode; it is equal to 1 in case of shear failure and to 0.8 in case of compressive-bending failure.
- τ_{di} is the calculus value of the masonry shear strength, given by:

$$\tau_{di} = \tau_{0d} \cdot \sqrt{1 + \frac{\sigma_{0i}}{1.5 \cdot \tau_{0d}}} \quad (4.10)$$

where τ_{0d} is the calculus value of the masonry shear strength computed by taking into account the confidential factor F_C (OPCM, 2003, cfr. paragraph 2.6.3) and σ_{0i} is the mean vertical given by the ratio between the mass of the generic i -level (M_i) and the shear resistance area ($A_{x,i}$).

The system mass (M) is associated to the vertical loads, as provided in the code (M.D., 2008); it is computed according to the following equation:

$$M = \frac{(G_k + \sum_i \psi_{2i} \cdot Q_{ki})}{g} \quad (4.11)$$

in which:

- G_k expresses the characteristic value of the permanent loads (e.g. self-weight of structures, fittings, ancillaries and fixed equipment);
- Q_{ki} expresses the characteristic value of the variable loads (e.g. live loads, wind loads or snow loads);
- g is the gravity acceleration;
- ψ_{2i} is the combination factor considering the probability of occurrence of the variable actions in case of earthquake.

In addition, in order to evaluate the participating mass of the e^* vibration mode, a collapse mode (Φ) must be a priori defined. Then, the participating mass according to the supposed failure mode is evaluated as follows:

$$e^* = \frac{(\sum_i m_i \cdot \varphi_i)^2}{M \sum_i m_i \cdot \varphi_i^2} \quad (4.12)$$

where: m_i is the generic i -level mass; φ_i is the horizontal displacement of the i^{th} level.

In general, when the failure mode Φ is not exactly defined, it is possible to make reference to the following common collapse mode for masonry structures:

- *soft k-level collapse mode*: it occurs when a floor system is definitely weaker than the other ones, so the dissipation and ductility capacity of the others structural levels is not exploited; in this case, the participating mass is calculated dealing with the following formula:

$$e^* = \frac{N+1-k}{N} \quad (4.13)$$

- *uniform failure collapse mode*: it occurs when lintels and masonry piers bases of the first-level collapse due to a compressive bending mechanism; in this case, the participating mass is expressed by:

$$e^* = 0.75 + 0.25 \cdot N^{-0.75} \quad (4.14)$$

The collapse acceleration assessment of the *Palazzo di Città* structure has been articulated in three steps:

1. Shear resistance (V_{CLS}) evaluation of the ground floor according to the longitudinal (X) and transverse (Y) directions and identification of the most vulnerable direction, that is the transverse one (Table 4.5);
2. Computation of the 1st level collapse acceleration by means of the (4.67), assuming an uniform failure mode;
3. Resistance evaluation according to the two orthogonal directions for the upper levels and identification of the most vulnerable direction (Y);
4. Computation of the collapse acceleration by means of relationship (4.67), assuming a soft-level failure mode;
5. Estimation of the global acceleration (a_{CLS}) as the minimum value among the previously calculated for each levels.

The final results are shown in Table 4.6.

In Figure 4.14 a graphic representation of the evaluated masonry shear strengths is depicted.

Table 4.5 Parameters for the evaluation of the masonry shear strengths at each levels

	V_{CLS} [kN]	μ	ξ	A [m ²]	β_{xi}	e_{yi}	d_{yi}
X	1 st lev	8994	0.92	1	177	1	0.013
	2 nd lev	5527	0.95	0.8	134	1	0.013
	3 rd lev	4047	1	0.8	144	1	0.013
	Total	19468			455		
Y	1 st lev	5437	0.82	1	150	1.16	1.63
	2 nd lev	2448	0.82	0.8	120	1.16	1.63
	Total	7886			270		

Table 4.6 Evaluation of the collapse acceleration

	a_{CLS}	a_{CLS}	Q	e^*	M_i [kN]	C(T)
X	1 st lev	0.076	0.075	2.25	1.33	55559
	2 nd lev	0.073	0.072	2.25	0.86	20040
	3 rd lev	0.065	0,064	2.25	0.86	6806
Y	1 st lev	0.046	0.045	2.25	1.33	55559
	2 nd lev	0.033	0.32	2.25	0.86	20040

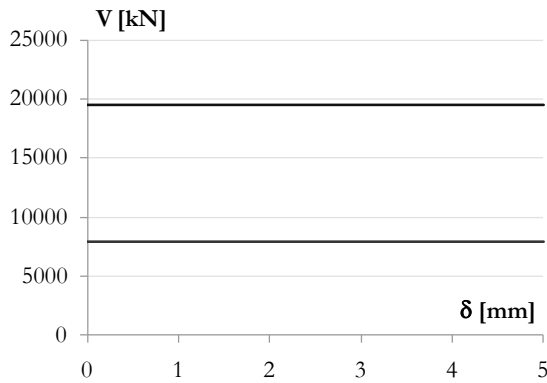


Figure 4.14 Graphic representation of the shear strength of the examined construction

Later on, considering the minimum value of the acceleration a_{CLS} among the calculated ones (Table 4.5, in bold), the vulnerability index has been calculated according to the following equation:

$$I_{SAVE,CLS} = 1 - \frac{a_{CLS}}{a_{PGA,CLS}} = 1 - \frac{0.032}{0.746} = 0.95 \quad (4.15)$$

The index so calculated shows the high vulnerability of the structure.

4.3.3 The SAVE Method

The application of the simplified SAVE (cfr. 3.3.1.1) methodology has permitted the evaluation of the building vulnerability in a more precise way as respect to the previous procedures.

The seismic accelerations corresponding to the Collapse Limit State (CLS) and the Operational Limit State (OLS) are shown in Tables 4.7 and 4.8. The minimum PGA value calculated represents the collapse acceleration of the structure.

The vulnerability index is calculated as the ratio between the collapse acceleration of the structure, represented by the minimum value provided by the program for the considered limit state, and the corresponding demand spectra peak accelerations given by the code for both CLS and LLS.

Table 4.7 Peak Ground Acceleration (Operational Limit State)

	PGA			PGA on rock		
	Ground Level	Level I	Level II	Ground Level	Level I	Level II
dir X	0.257	0.225	1.179	0.205	0.180	0.943
dir Y	0.167	0.117	0.164	0.134	0.093	0.131

Table 4.8 Peak Ground Acceleration (Near Collapse Limit State)

	PGA			PGA on rock		
	Ground Level	Level I	Level II	Ground Level	Level I	Level II
dir X	0.362	0.249	1.562	0,289	0,199	1,250
dir Y	0.242	0.132	0.214	0,194	0,106	0,171

The indexes have been, finally, calculated as follows:

$$I_{\text{SAVE,SLS}} = 1 - \frac{a_{\text{Collapse}}}{a_{\text{PGA,LLS}}} = 1 - \frac{0.132}{0.715} = 0.816 \quad (4.16)$$

$$I_{\text{SAVE,CLS}} = 1 - \frac{a_{\text{Collapse}}}{a_{\text{PGA,CLS}}} = 1 - \frac{0.132}{0.746} = 0.824 \quad (4.17)$$

The program also provides the masonry shear strength and the stiffness for each level (Tables 4.9 and 4.10).

Table 4.9 Shear resistance at each level

	Ground Level	Level I	Level II
V_{x,TOT} [kN]	40352	19062	25582
V_{y,TOT} [kN]	23018	8658	3126

Table 4.10 Structural stiffness at each level

	Ground Level	Level I	Level II
K_x [kN/m]	4431449	2269265	8693470
K_y [kN/m]	3321698	1310530	4154180

On the basis of the shear resistance and the stiffness, it is possible to represent only the elastic part of the shear-displacement [V-δ] curves for each storey of the structure, since the ultimate displacements are not known (Fig. 4.15).

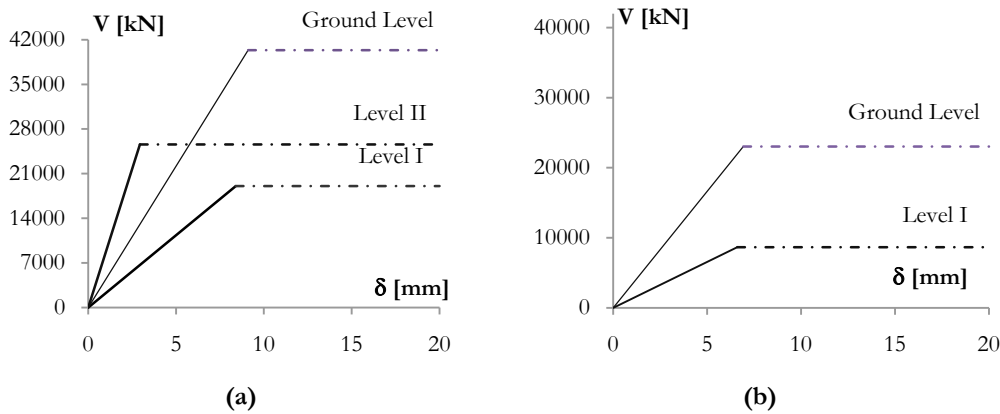


Figure 4.15 Shear-displacement relation according to (a) X direction and (b) Y direction

4.3.4 Mechanical model for masonry buildings

In this section, the seismic vulnerability has been assessed by means of a simplified mechanical model. This is based on the simplified definition of the bilinear capacity curve of the structure, dealing with a building stock characterised by a typological building homogeneity and by consolidated seismic design codes (Cattari et al., 2004, Giovinazzi, 2005).

In this way, the estimation of the parameters defining the capacity curve can be carried out referring to the values prescribed by national seismic design codes and to the construction material standards. On the other hand, for non designed structures, the bilinear capacity curve can be developed by taking into consideration the geometrical and the structural features characterising, on average, the typology (e.g. number of floors, code level, material strength, drift capacity, age, etc.) and hypothesising a certain failure mechanism.

Assuming a bilinear representation, the capacity spectrum is defined by only three parameters: the yielding (δ_y) and ultimate (δ_u) displacements and the shear resistance of the building. Thus, the curve is completely identified in terms of yield acceleration (a_y), true fundamental period of the structure (T) and structural ductility capacity (μ), depending on the constant part length of the graphic, since the hardening behaviour is totally neglected.

In fact, the yielding displacement and the ultimate may be respectively evaluated as follows:

$$\delta_y = \left(\frac{T}{2 \cdot \pi} \right)^2 \cdot a_y \quad (4.18)$$

$$\delta_u = \mu \cdot \delta_y \quad (4.19)$$

For the evaluation of the elastic period of the structure (T), it is possible to make reference to the simplified formula:

$$T = \theta \cdot H^{\frac{3}{4}} \quad (4.20)$$

where θ is a numeric coefficient depending on the typological class, defined on the basis of expert judgement, taking into account mechanical characteristics of the materials and the characteristic features of the building; H is the total height of the building.

Alternatively, it is possible to define the fundamental period by means of the relation for a SDOF (Single Degree Of Freedom) system:

$$T = 2 \cdot \pi \cdot \sqrt{\frac{m}{k}} \quad (4.21)$$

where m and k represent the mass and the stiffness of the system, respectively. The base shear capacity V (equation (4.22)) has been computed as function of the strength offered by the resistant area A_R in the considered direction:

$$V = 0.5 \cdot A_R \cdot \tau \quad (4.22)$$

In the formula (4.22), the 0.5 factor is introduced to take into account the hypothesis that, for a certain earthquake direction, only half of the walls are involved, whereas τ is the shear strength based on the characteristic shear strength τ_0 and on the compressive strength σ_0 values, calculated, similarly to τ_{di} (see eq. 4.10), by means of the following equation:

$$\tau = \tau_0 \cdot \sqrt{1 + \frac{\sigma_0}{\tau_0}} \quad (4.23)$$

In particular, when the resistant area is not known, it is possible to calculate the base shear strength by means of a simplified formulation:

$$V = 0.5 \cdot A \cdot \alpha \cdot \tau_k \cdot \beta_T \cdot \xi \quad (4.24)$$

in which:

- A is the floor area of the building;
- α is a numerical coefficient expressed as function of the building typology (Table 4.11);
- τ_k is the characteristic shear strength also provided in Table 4.11;
- β_T is a numerical coefficient expressed as function of the building floor numbers (N), taking into account geometrical rules belonging to the constructive traditions (Table 4.12), according to:

$$\beta_T = 1 + 0.2 \cdot (N - 1) \quad (4.25)$$

- ξ is a further coefficient introduced in order to consider the non uniform contribution of each masonry panel.

The yielding acceleration (A_y) is given by the following expression:

$$A_y = \frac{V}{m \cdot M} \quad (4.26)$$

where:

- m is the modal mass coefficient for the first natural mode, evaluated as follows:

$$m = \frac{\left(\sum m_i \cdot \varphi_i\right)^2}{\sum m_i \cdot \sum m_i \cdot \varphi_i^2} \quad (4.27)$$

The (4.27) may also be expressed as function of the number of the floors (N) of the building:

$$m = 0.75 + 0.25 \cdot \frac{1}{N^{0.75}} \quad (4.28)$$

- M is the total mass of the structure, expressed in terms of the geometrical and of the mechanical features as follows:

$$M = \sum_i^N A_i \cdot p_i + \sum_i^N \alpha \cdot A_i \cdot \gamma \cdot h \quad (4.29)$$

where:

- h is the inter-storey height;
- γ is the material density;
- A_i is the i -level floor area;
- p_i is the i -level overload.

Assuming the floor area and the overload constant for each i -level, the mass M may be simplified as follows:

$$M = A \cdot \left(N \cdot p + h \cdot \gamma \cdot \alpha \cdot \sum_i^N \beta_i \right) \quad (4.30)$$

in which the parameter β_i is defined for each i -level as the ratio between the resistant area at i -level and the resistant area computed at the upper level (4.28):

$$\beta_i = \frac{\alpha_i \cdot A_i}{\alpha_N \cdot A_N} \quad (4.31)$$

Therefore, the formula (4.26) provided for the evaluation of the acceleration A_y may be written as:

$$A_y = \frac{0.5 \cdot \alpha \cdot \tau_k \cdot \beta_T \cdot \xi}{m \cdot \left(N \cdot q + \gamma \cdot \alpha \cdot h \cdot \sum_i^N \beta_i \right)} \quad (4.32)$$

Finally, the ultimate displacement calculation depends on the hypothesised collapse mechanisms of the masonry panels. In particular, with respect to the

building total collapse mode, the following three limit situations, marked by a specific number, appear to be as significant:

- 0 : lintels failure collapse mode, with almost uniform deformations in masonry piers at the various storeys referred as uniform collapse mode;
- 1 : soft-storey collapse mode with prevailing rocking failures;
- 2 : soft-storey collapse mode with prevailing shear failures.

According to the present procedure, the collapse mode has been a priori established on the basis of the storey number (Table 4.11). Moreover, a specific value of the ultimate displacement D_u has been associated to each of possible collapse mechanisms.

With regard to the uniform collapse mode, the ultimate displacement capacity is given by the equation:

$$D_u = \delta_u \cdot \frac{N \cdot h}{\Gamma} \quad (4.33)$$

In case of soft-storey mechanism, both for rocking and shear failures, the expression becomes:

$$D_u = \delta_u \cdot h + D_y \cdot \left(1 - \frac{\Gamma}{N}\right) \quad (4.34)$$

where Γ is the modal participation factor for the first natural mode and δ_u is the ultimate drift ratio.

According to Table 4.10, the examined monumental building is classified in the M4 building typology: *Massive stones*, Constructions built with large and accurately squared stones are in general monumental buildings, castles, villas, palaces etc. As far as ordinary constructions are concerned, this type of masonry was used only in the Middle Ages when stones were worked with great accuracy. Therefore, these buildings generally are very resistant, have limited decay (due to the reduced use of mortar) and, consequently, good seismic behaviour.

The calculus values employed to estimate the aforesaid parameter are highlighted in Table 4.11. It is worth to precise that a linear interpolation has been adopted, since the investigated building develops on three storeys.

Table 4.10 Building typology classification

Unreinforced masonry typologies	
M1	Rubble stone
M2	Adobe (earth brick)
M3	Simple stone
M4	Massive stone
M5.w	Bricks with wooden floors
M5.v	Bricks with masonry vaults
M5.sm	Bricks with composite steel and masonry floors
M6	Unreinforced masonry with RC floors
M7	Reinforced confined masonry
M8	Retrofitted ancient buildings

Table 4.11 Values for the parameters involved in the capacity curves evaluation

	N	h [m]	θ	γ [kg·m ⁻³]	q [kg·m ⁻²]	τ_k [kg·m ⁻²]	Collapse mode	δ_u	α
M1	2	2.8	0.055	1900	200	3000	2	0.004	0.18
	4	2.8	0.055	1900	200	3000	2	0.004	0.18
M2	2	2.7	0.07	1500	350	2000	2	0.004	0.12
	2	3	0.05	2100	200	7000	2	0.004	0.16
M3	4	3	0.05	2100	250	7000	1	0.007	0.16
	6	3	0.05	2100	250	7000	1	0.007	0.16
M4	2	4	0.045	2200	350	12000	2	0.004	0.14
	4	4	0.045	2200	350	12000	1	0.007	0.14
	6	4	0.045	2200	350	12000	1	0.007	0.14
M5.w	2	3	0.045	1800	200	8000	2	0.004	0.1
	4	3	0.045	1800	200	8000	2	0.004	0.1
	6	3	0.045	1800	200	8000	2	0.004	0.1
M5.v	2	3.3	0.0525	1800	500	8000	1	0.007	0.12
	4	3.3	0.0525	1800	450	8000	1	0.007	0.12
	6	3.3	0.0525	1800	400	8000	1	0.007	0.12
M5.sm	2	3.3	0.05	1800	300	12000	2	0.004	0.1
	4	3.3	0.05	1800	300	12000	2	0.004	0.1
	6	3.3	0.05	1800	300	12000	2	0.004	0.1
M6	2	3.6	0.055	1600	400	15000	1	0.007	0.08
	4	3.6	0.055	1600	400	15000	1	0.007	0.08
	6	3.6	0.055	1600	400	15000	1	0.007	0.08
M7	2	3.6	0.04	1800	400	20000	2	0.01	0.08
	4	3.6	0.04	1800	400	20000	2	0.01	0.08
	6	3.6	0.04	1800	400	20000	2	0.01	0.08
M8	2	3	0.045	2000	400	9000	2	0.004	0.16
	4	3	0.045	2000	400	9000	2	0.004	0.16
	6	3	0.045	2000	400	9000	1	0.007	0.16

The parameters calculated by means of the linear interpolation are shown in Table 4.12, while the Table 4.13 depicts the results.

Table 4.12 Specific values of the parameter assumed for the investigated building

	N	h [m]	θ	γ [kg·m ⁻³]	q [kg·m ⁻²]	τ_k [kg·m ⁻²]	Collapse mode	δ_u	α
M4	3	5	0.045	2200	400	12000	2	0.004	0.14

Table 4.13 Simplified mechanical model results

	β_T	ξ	m	β_i	Γ	D_y [m]	T [s]	A_y	D_u [m]
M4	1.4	0.8	0.85	3.46	1.28	0.00233	0.233	0.17	0.021

The obtained capacity curve is shown in Figure 4.16, both in the acceleration-displacement domain and within the shear vs. displacement plane.

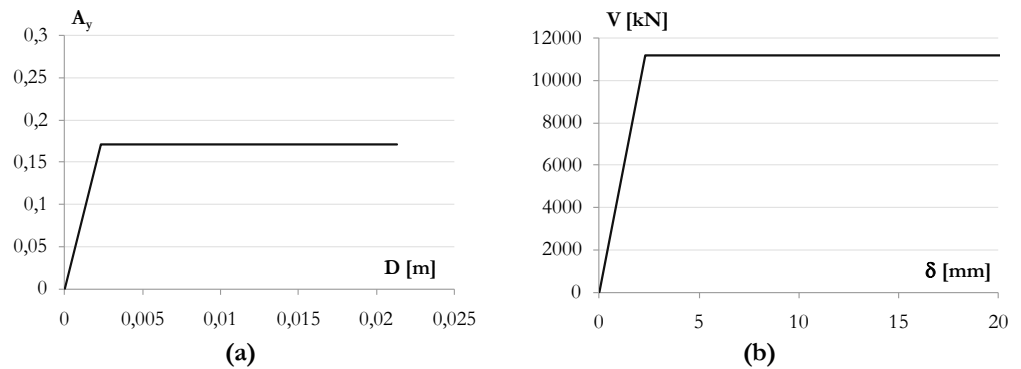


**Figure 4.16 Simplified capacity curve of the *Palazzo di Città*:
(a) acceleration-displacement domain; (b) shear-displacement plane**

According to the Performance Based Design methodology (PBD), four different damage limit states of the building S_{dk} ($k=1,2,3,4$) have been considered (see paragraph 3.3.1.4). These target displacements allow to individuate the damage level of the structure, they being computed as follows:

- $S_{d1} = 0.7 d_y = 1.6$ mm
- $S_{d2} = 1.5 d_y = 3.5$ mm
- $S_{d3} = 0.5 (d_y + d_u) = 11.8$ mm
- $S_{d4} = d_u = 21.3$ mm

Once the target displacement S_d , the displacement thresholds $S_{d,k}$ and the normalized standard deviation β_k have been evaluated according to the formula (3.14), the damage fragility curves have been drawn (Fig. 4.17).

These latter are expressed by means of the relationship (3.11), which is another time herein reported:

$$P[d_s/S_d] = \Phi \cdot \left[\frac{1}{\beta} \cdot \ln \left(\frac{S_d}{S_{d,ds}} \right) \right]$$

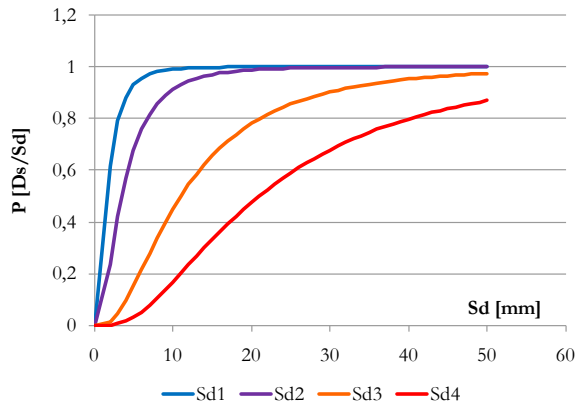


Figure 4.17 Fragility curves of the structure according to the simplified method

4.4. NUMERICAL ANALYSIS

4.4.1 Theoretical basis

4.4.2.1. The Capacity Spectrum Method

The Capacity Spectrum Method (CSM) was introduced in the 1970s as a rapid evaluation procedure in a pilot project for assessing seismic vulnerability of buildings at the Puget Sound Naval Shipyard (Freeman et al., 1975).

The CSM consists into the evaluation of the maximum displacement of the structure, it representing the intersection point, called performance point (PP), between the capacity curve with a response spectrum adequately reduced in order to take into account the inelastic behaviour of the structure. In other words, this procedure allows to estimate the expected seismic performance of a construction by comparing its seismic capacity (in spectral coordinates: S_d - S_d) with the seismic demand, described by the Acceleration-Displacement Response Spectra (ADRS). Capacity curves are developed by implementing static non-linear analyses and represent the building lateral load resistance V (static equivalent base shear) versus its characteristic lateral displacement δ_R (peak displacement of the building

roof). Thus, a capacity curve may be drawn from a pushover curve by means of the identification of two characteristic control points: the yield capacity V_y and the ultimate capacity V_u . The yield capacity represents the lateral load resistance strength of the building before structural system has developed non-linear response, while the ultimate capacity is the maximum strength of the building when the global structural system has reached a fully plastic state.

In order to apply the CSM, the construction is converted into an equivalent SDOF system. Therefore, the MDOF push-over curve characterising the building behaviour must be converted into the equivalent SDOF bilinear curve (OPCM, 2003) by means of appropriate formulations.

The CSM procedure synthetically consists in the following eight steps:

1. Development of the elastic spectrum as appropriate for the site;
2. Determination of the base shear-top displacement curve by a pushover analysis;
3. Conversion of the achieved force-deformation relationship of the MDOF into that of an equivalent SDOF system;
4. Idealization of the equivalent SDOF system curve into an elastic perfectly plastic form by means of the area equivalence criterion;
5. Conversion of the equivalent SDOF bilinear form into capacity spectrum (ADRS format);
6. Reduction of the 5% damped elastic spectrum;
7. Check of the performance at the expected maximum displacement, by identifying the performance point (PP)
8. Calculation of the vulnerability index.

4.4.2.2. *Horizontal elastic response spectra*

According to the European and Italian Code (CEN, 2005b, M.D., 2008), the seismic motion in a specific point of the Earth's crust may be represented by an elastic ground acceleration response spectrum. The canonical shape of the spectrum is the same for all the Limit States (LS) considered (Figure 4.18).

In particular, in the Italian Code, four different LS related to the seismic action are defined:

1. Operational Limit State (OLS);
2. Damage Limit State (DLS);
3. Life Safety Limit State (LLS);
4. Near Collapse Limit State (CLS).

The probability to be surpassed (P_{VR}) in the Reference Period for each defined LS is indicated in Table 4.13.

Table 4.14 Probability of each LS to be surpassed in the Reference Period

Limit State	P _{VR} : Probability to be surpassed in the Reference Period	
Exercise Limit States	OLS	81%
	DLS	63%
Ultimate Limit State	LLS	10%
	CLS	5%

Dealing with the New Technical Italian Code, the acceleration elastic response spectrum $S_e(T)$ for the horizontal components of the seismic action is expressed as function of the elastic vibration period (T) of a SDOF system, it being given by the following expressions:

$$0 \leq T \leq T_B \quad S_e(T) = a_g \cdot \eta \cdot F_0 \cdot S \cdot \left[\frac{T}{T_B} + \frac{1}{\eta \cdot F_0} \cdot \left(1 - \frac{T}{T_B} \right) \right] \quad (4.35)$$

$$T_B \leq T \leq T_C \quad S_e(T) = a_g \cdot \eta \cdot F_0 \cdot S$$

$$T_B \leq T \leq T_D \quad S_e(T) = a_g \cdot \eta \cdot F_0 \cdot \left(\frac{T_C}{T} \right)$$

$$T_D \leq T \quad S_e(T) = a_g \cdot \eta \cdot F_0 \cdot \left(\frac{T_C \cdot T_D}{T^2} \right)$$

where:

- a_g is the maximum horizontal ground acceleration, provided by the Code on the base of a given geographical zone;
- F_0 is the amplification factor, provided by the Code on the base of a given geographical zone;
- T_C is the upper limit of the period of the constant spectral acceleration branch, computed as follows:

$$T_C = C_C \cdot T_C^* \quad (4.36)$$

where T_C^* is the beginning of the constant velocity range of the spectrum, provided by the Code on the base of a given geographical zone; C_C is a numerical factor expressed as function of the subsoil category (Table 4.15);

- T_B is the lower limit of the period of the constant spectral acceleration branch, given by:

$$T_B = \frac{T_C}{3} \quad (4.37)$$

- T_D defines the beginning of the constant displacement response range of the spectrum, expressed by:

$$T_D = 4.0 \cdot \frac{a_g}{g} \cdot 1.6 \quad (4.38)$$

where g is the ground acceleration.

- S is the soil factor, evaluated as follows:

$$S = S_S \cdot S_T \quad (4.39)$$

where S_S is the coefficient of stratigraphical amplification (Table 4.15) and S_T is the coefficient of topographical amplification (Table 4.16);

- η is the the damping correction factor with a reference value equal to 1 for 5% viscous damping, given by:

$$\eta = \sqrt{\frac{10}{5 + \xi}} \geq 0.55 \quad (4.40)$$

where ξ is a factor depending on the constructive material, structural typology and soil foundation.

Table 4.15 Formulations for S_S and C_C

Subsoil Category	Stratigraphical factor S_S	C_C
A	1.00	1.00
B	$1.00 \leq 1.4 - 0.4 \cdot F_0 \cdot \frac{a_g}{g} \leq 1.20$	$1.10 \cdot (T_C^*)^{-0.20}$
C	$1.00 \leq 1.7 - 0.6 \cdot F_0 \cdot \frac{a_g}{g} \leq 1.50$	$1.05 \cdot (T_C^*)^{-0.33}$
D	$0.90 \leq 2.4 - 1.5 \cdot F_0 \cdot \frac{a_g}{g} \leq 1.80$	$1.25 \cdot (T_C^*)^{-0.50}$
E	$1.00 \leq 2.0 - 1.1 \cdot F_0 \cdot \frac{a_g}{g} \leq 1.60$	$1.15 \cdot (T_C^*)^{-0.40}$

Table 4.16 Maximum values of the coefficient of topographical amplification S_T

Topographical Category	Construction site position	S_T
T1	-	1.0
T2	On the top of a hill	1.2
T3	On the relief crest	1.2
T4	On the relief crest	1.4

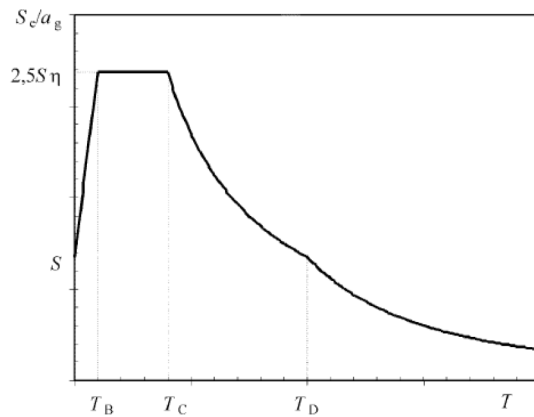


Figure 4.18 Canonical shape of the elastic response spectrum (EC8)

In order to apply the CSM, the elastic spectrum must be converted into Demand Spectrum, also called ADRS - Acceleration Displacement Response Spectrum, i.e. the representation of earthquake response spectra of acceleration and displacement into a unique diagram. Each point of the diagram, in spectral coordinates, corresponds to a different period of vibration (S_e - S_d format).

The ADRS is obtained by means of the following equation:

$$S_e(T) = S_d(T) \cdot \omega^2 = S_d(T) \cdot \left(\frac{2 \cdot \pi}{T} \right)^2 \quad (4.41)$$

On the basis of relationship (4.31), it is possible to develop the ADRS for an examined site. It is worth to notice that in the ADRS format inclined lines starting from the origin have constant period T , which can be computed for any point on the spectrum by using the following expression:

$$T = 2 \cdot \pi \cdot \frac{S_d}{S_a} \quad (4.42)$$

The traditional spectrum shape (Acceleration-Period) and the ADRS one are shown in Figure 4.19.

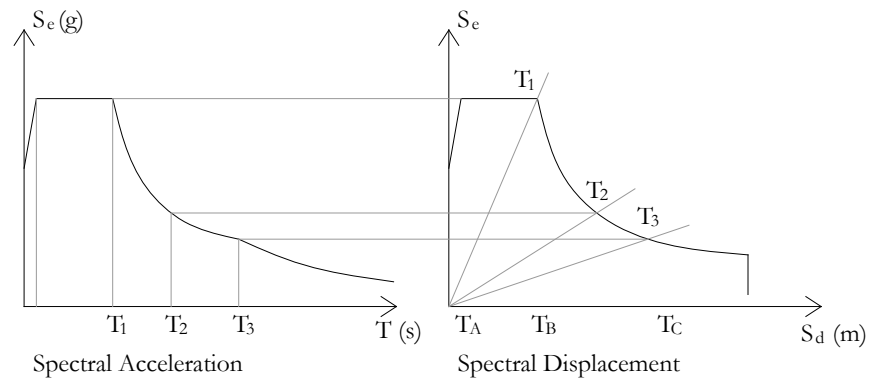


Figure 4.19 Traditional and ADRS formats for the response spectra representation

4.4.2.3. Conversion of the curve

The development of the capacity curve of a given structure represents a preliminary phase to employ the CSM approach.

In general, a capacity curve may be drawn by means of the implementation of a static non linear analysis. This push-over analysis allows to determine the MDOF capacity curve, that must be converted point by point into the equivalent SDOF curve and, subsequently, into the bilinear one by means of the area equivalence criterion (Figure 4.20).

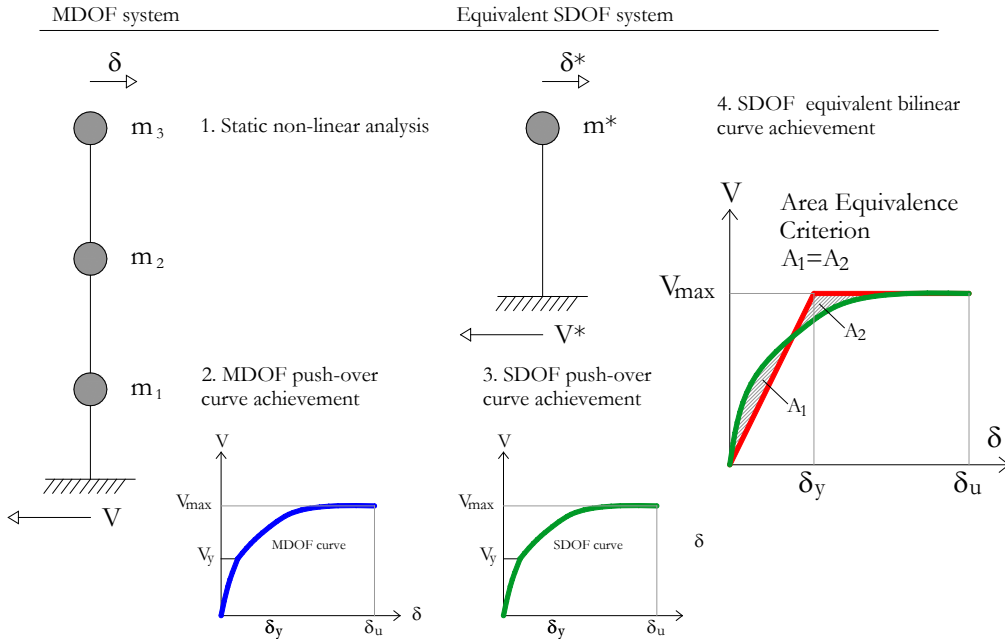


Figure 4.20 Phases of conversion of MDOF curve into SDOF equivalent bilinear one

The SDOF curve is obtained by dividing the MDOF coordinates for the modal participation factor (Γ), expressed by eq. (4.45), as follows:

$$V_{SDOF} = \frac{V_{MDOF}}{\Gamma} \tag{4.43}$$

$$\delta_{SDOF} = \frac{\delta_{MDOF}}{\Gamma} \tag{4.44}$$

$$\Gamma = \frac{\sum m_i \cdot \varphi_i}{\sum m_i \cdot \varphi_i^2} \tag{4.45}$$

where m_i is the story mass at i -level and φ_i is the amplitude of the first mode at i -level normalised to the roof displacement.

Finally, the SDOF equivalent bilinear form is derived from the SDOF curve by means of the area equivalence criterion.

Afterwards, the base shear forces vs. roof displacements diagram must be converted to the so-called capacity spectrum (ADRS plane), in order to achieve the PP. Therefore, any point on the push-over curve having V_i and δ_i roof as coordinates is converted into the corresponding point (S_{ei} , S_{di}) on the capacity spectrum using the following relationships:

$$S_{ci} = \frac{V_i}{m \cdot M} \quad (4.46)$$

$$S_{di} = \frac{\delta_i}{\Gamma \cdot \varphi_R} \quad (4.47)$$

in which:

- V_i is the base shear;
- δ_i is the point displacement;
- m is the story mass at i -level;
- M is the building dead weight plus likely live loads;
- φ_R is the roof level amplitude of the first vibration mode;
- Γ is the modal participation factor as expressed in (4.45);
- m is the modal mass coefficient for the first natural mode of the structure, defined according to the equation (4.27).

The capacity spectrum so defined may be finally compared with the elastic spectrum in order to obtain the PP.

4.4.2.4. *The index calculation: N2 and ATC 40 Methods*

The performance point PP is, as described above, the intersection between the capacity spectrum and the demand one. However, in order to consider the structural inelastic behaviour, the elastic spectrum, representing the seismic demand, must be reduced.

In fact, the building capacity and the seismic demand are mutually interconnected, depending on both the system stiffness and the system damping change during the earthquake. When a structure surmounts its yield point, indeed, its effective damping and period increase, due to the energy lost because of the hysteretic damping. So, when the structure has a more heavily damped, it responds to the quake motion with a longer period and therefore the 5% damped elastic spectrum has to be reduced towards a lower spectrum in order to be consistent with the structure response.

Several procedures exist for the reduction operation, such as the N2 method (Fajfar, 1999, Fajfar, 2000) and the Overdamped Spectrum one (Freeman, 1998; ATC-40, 1996).

The N2 method consists in developing an inelastic spectrum obtained by applying a strength reduction factor (R_μ) due to the ductility. Therefore, the elastic 5% damped response spectrum may be converted point by point into a constant-ductility inelastic response spectrum, by means of the following relationships:

$$S_a = \frac{S_e}{R_\mu} \quad (4.48)$$

$$S_d = \frac{\mu}{R_\mu} \cdot S_{de} = \frac{\mu}{R_\mu} \cdot \frac{T^2}{4 \cdot \pi^2} \cdot S_e = \mu \cdot \frac{T}{4 \cdot \pi^2} \cdot S_a \quad (4.49)$$

in which:

- S_a and S_d are acceleration and displacement of the inelastic spectrum, respectively;
- S_e and S_{de} are acceleration and displacement of the elastic spectrum, respectively;
- μ is the ductility factor, defined as the ratio between the ultimate displacement and the yielding one of the structure;
- R_μ is the reduction factor due to the hysteretic energy dissipation of ductile structures, expressed as a function of the elastic period and given by the following equations (Vidic et al., 1994):

$$\text{if } T \leq T_0 : \quad R_\mu = (\mu - 1) \cdot \frac{T}{T_0} + 1 \quad (4.50)$$

$$\text{if } T \geq T_0 : \quad R_\mu = \mu \quad (4.51)$$

$$T_0 = 0.65 \cdot \mu^{0.3} \cdot T_C \leq T_C \quad (4.52)$$

Observing eqs. (4.45) and (4.46), it can be noted that the reduction factor R_μ depends on the structural stiffness. In fact, if the structure is characterized by a fundamental period T higher than T_C , it may be classified as flexible structure and the R_μ value is equal to the ductility μ ; on the other hand, if the structure presents a fundamental period T lower than T_C , it may be classified as rigid and the R_μ parameter is lower than μ .

The Figure 4.21 shows an example of performance point identification by means of this reduction technique.

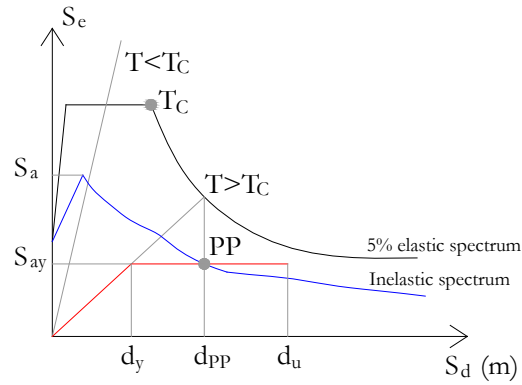


Figure 4.21 Performance point identification by means of the N2 method

The vulnerability index is finally evaluated as the ratio between the performance point PP and the ultimate displacement of the structure.

The Overdamped Spectrum Reduction Method was proposed by ATC 40. This consist in the estimation of the equivalent damping as a function of the displacement and the evaluation of the performance point by means of an interactive procedure.

Therefore, after the aforementioned preliminary steps, the procedure consist in:

- 2 calculation of the spectral reduction factors and development of the inelastic demand spectrum, choosing a trial point (a_{pi}, d_{pi}) ;
- 3 check if the demand spectrum intersects the capacity one at the point (a_{pi}, d_{pi}) or if the displacement (d_i) at which the demand spectrum intersects the capacity one is within the acceptable tolerance established for d_{pi} ;
- 4 selection of a new (a_{pi}, d_{pi}) point, if the demand spectrum does not intersect the capacity one within acceptable tolerance and return to the step 1;
- 5 calculation of the PP if the demand spectrum intersects the capacity one within acceptable tolerance, so the trial performance point (a_{pi}, d_{pi}) is the effective performance point (a_p, d_p) and d_p represents the maximum displacement expected for the demand earthquake.

In particular, the equivalent viscous damping, β_{eq} , associated with a maximum displacement of d_{pi} , can be estimated by the following expression:

$$\beta_{equ} = \beta_0 + 0.05 \quad (4.53)$$

where β_0 is the hysteretic damping represented as equivalent viscous damping, given by:

$$\beta_0 = \frac{1}{4 \cdot \pi} \cdot \frac{E_D}{E_{so}} \quad (4.54)$$

in which:

- E_D is the energy dissipated by damping, calculated as follows:

$$E_D = 4 \cdot (a_{pi} \cdot d_{pi} - 2 \cdot A_1 - 2 \cdot A_2 - 2 \cdot A_3) = 4 \cdot (a_y \cdot d_{pi} - d_y \cdot a_{pi}) \quad (4.55)$$

- E_{so} is the maximum strain energy, determined by:

$$E_{so} = \frac{a_{pi} \cdot d_{pi}}{2} \quad (4.56)$$

The reference system is shown in Figures 4.22 and 4.23.

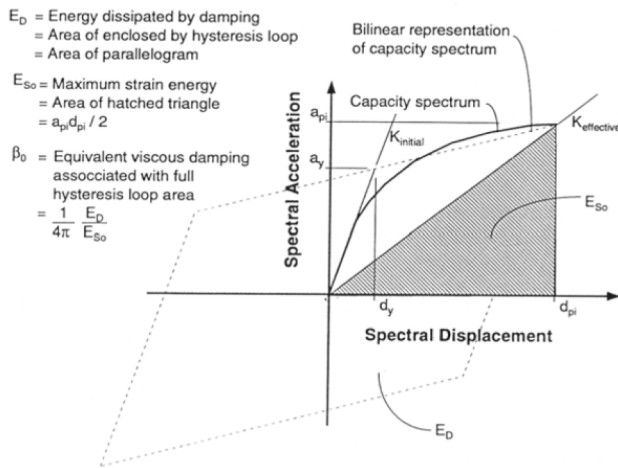


Figure 4.22 Derivation of damping for spectral reduction

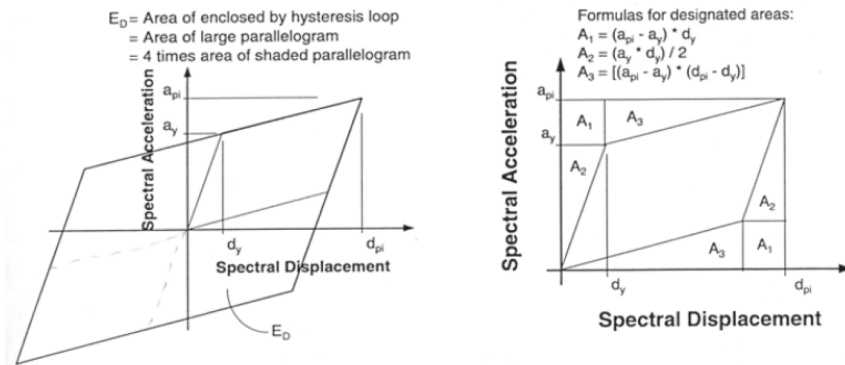


Figure 4.23 Derivation of energy dissipated by damping E_D

Considering the (4.55) and the (4.56), the (4.54) becomes:

$$\beta_0 = \frac{63.7 \cdot (a_y \cdot d_{pi} - d_y \cdot a_{pi})}{a_{pi} \cdot d_{pi}} \quad (4.57)$$

and the (4.48) assumes the following formulation:

$$\beta_{equ} = \beta_0 + 5 = \frac{63.7 \cdot (a_y \cdot d_{pi} - d_y \cdot a_{pi})}{a_{pi} \cdot d_{pi}} + 5 \quad (4.58)$$

However, the effective viscous damping (β_{eff}) is estimated according to the following eq. (4.59) in order to take into account the presence of imperfect hysteretic loops:

$$\beta_{eff} = \kappa \cdot \beta_0 + 5 = \frac{\kappa \cdot 63.7 \cdot (a_y \cdot d_{pi} - d_y \cdot a_{pi})}{a_{pi} \cdot d_{pi}} + 5 \quad (4.59)$$

where the κ -factor represents a damping modification factor, it depending on the structural behaviour of the building, which is influenced by both the quality of the seismic resisting system and the duration of the ground shaking.

Similarly to the N2 procedure, the vulnerability index is assessed as the ratio between the performance point PP and the ultimate displacement of the structure.

4.4.2 The AeDES software

4.4.2.1 The FEM Model

The first preliminary phase for the application of the Capacity Spectrum Method is the implementation of a push-over analysis. To this scope, a FEM model by means of the AeDes non linear numerical code, specific for masonry buildings modelling, has been set up. The program is constituted by two different analysis components (Aedes, 2009):

- PC.M (*Progettazione di Costruzioni in Muratura* – Design of Masonry Structure), used for the model implementation. In this module, a macroelement model is created by defining geometrical and structural features, material properties, loading conditions. In particular, the program is able to directly define the material physical properties on the basis of a database referring to the regulation in force.
- PC.E (Programma per il Calcolo agli Elementi finiti – Finite Element Calculation Code). This section is specific for structural analyses.

Therefore, the numerical model of *Palazzo di Città* has been implemented in PC.M environment (Figs. 4.24 and 4.25) and then imported in PC.E (Fig. 4.26), where a frame equivalent model is automatically created in order to perform the

static push-over analysis (Formisano et al., 2008; Florio et al. 2009). The equivalent frame model allows to represent solid walls and lintels as columns and beams elements. Therefore, the structural model consists of an assemblage of a finite number of vertical and horizontal frames linked by means of a rigid offset.

In particular, in the equivalent frame model based on finite element method, nonlinear flexural springs are inserted into the model at the ends of the piers and spandrels, in terms of moment–rotation laws. Translational shear springs, instead, are added at each pier and spandrel at mid-points, expressed in terms of shear force–displacement laws. Both the New Technical Italian Code (M.D.,2008) and the EC8 allows this modelling method.

The Aedes modelling technique is able to automatically take into consideration the possible mechanical non-linearity by means of the automatic definition of plastic hinges at the end of the frame elements.

Therefore, this software represents a suitable instrument to quickly implement a numerical model of a masonry construction and to easily manage all the inserted data related to the model.

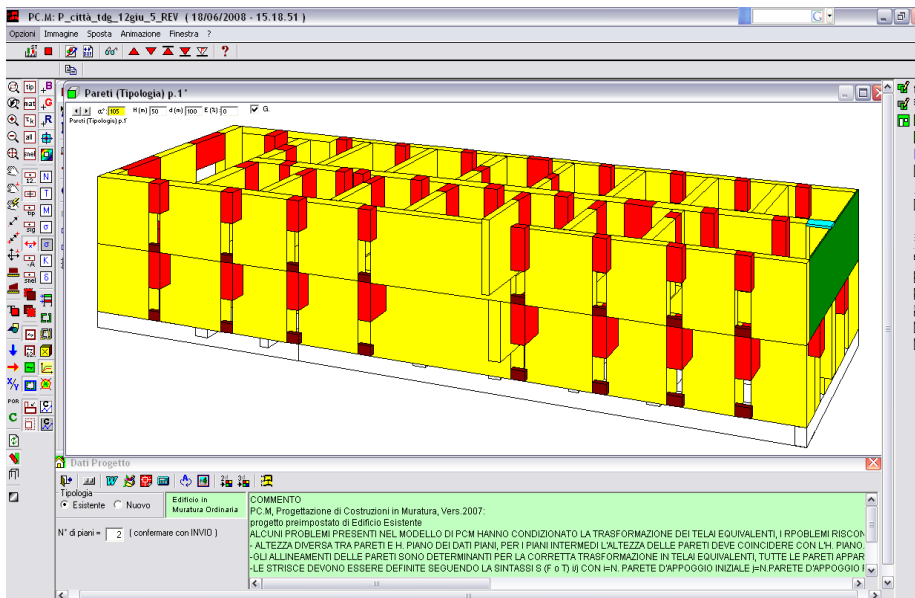


Figure 4.24 PC.M model 3D view

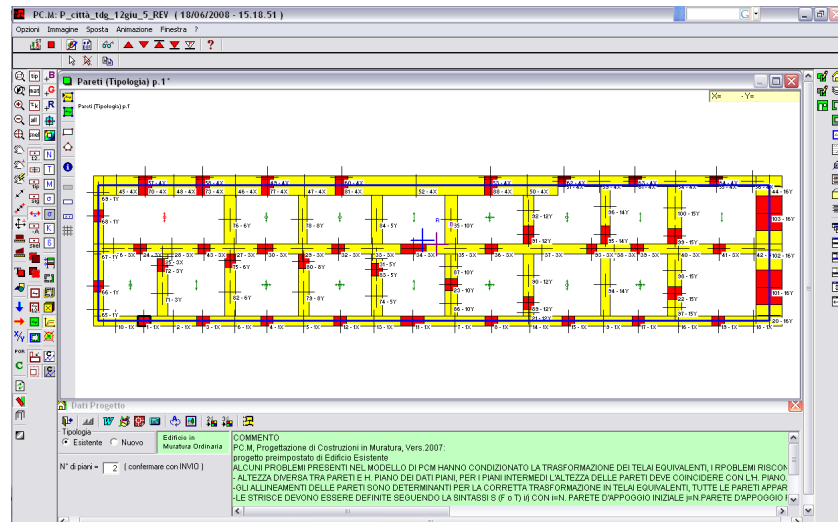


Figure 4.25 FEM model plan within the PC.M software

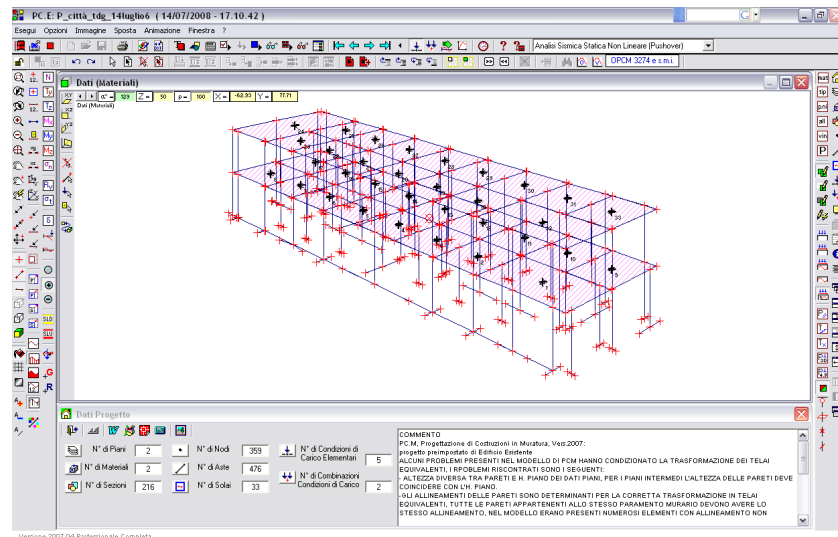


Figure 4.26 3D View of the equivalent frame model in PC.E environment

The first fundamental elastic period of the structure has been detected by means of a preliminary modal dynamic analysis, it being equal to 0.223 s. Furthermore, the first mode is in transverse direction, the second one is a rotational mode and the third one is characterised by longitudinal movements.

4.4.2.2. *The static non linear analysis*

In the successive phase, seismic pushover analyses have been performed both in longitudinal (X) and in transverse (Y) direction in order to obtain the capacity curves of the investigated structure. According to the M.D. 2008, the combination (2.24) of the loading conditions has been considered (cfr. section 2.5.3.3).

In each pushover analysis, two different load distributions have been considered according to the New Technical Italian code M.D., 2008):

- the first one proportional to masses (A);
- the second one proportional to masses multiplied by the displacements corresponding to the first vibration mode (B).

Therefore, for each plane direction and for each force distribution, the shear-displacement curve has been achieved along longitudinal (Fig. 4.27) and transverse directions (Fig. 4.28). It is worth to note that the PC:E software automatically converts the MDOF curve (green curve in the diagrams) into the SDOF system curve by dividing each coordinates for the participation factor and then in the SDOF equivalent bilinear form (red line in the diagrams) by means of the equivalence area criterion (cfr. section 4.4.1.4). The parameter identifying the bilinear curve are depicted in Table 4.17, while the bilinear representation is shown in Figure 4.29.

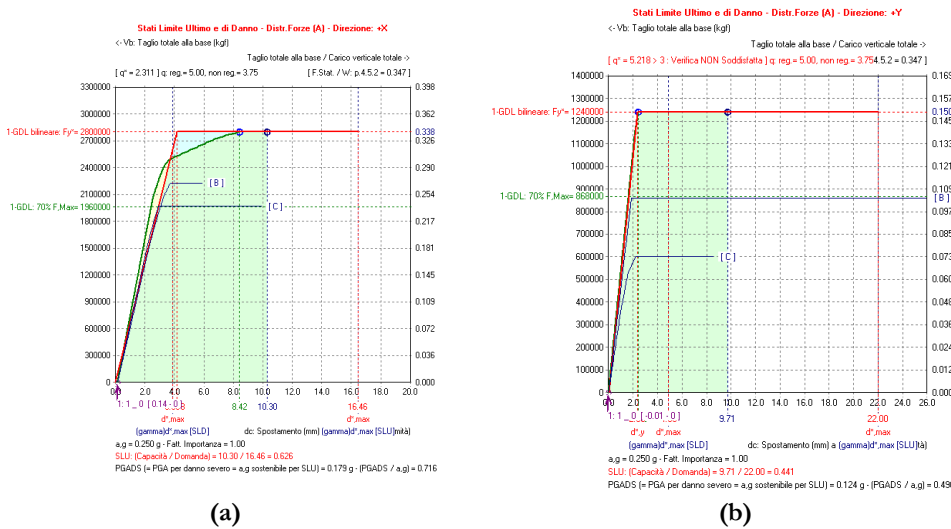


Figure 4.27 Push-over curves in (a) longitudinal and (b) in transverse direction according to the load distribution (A)

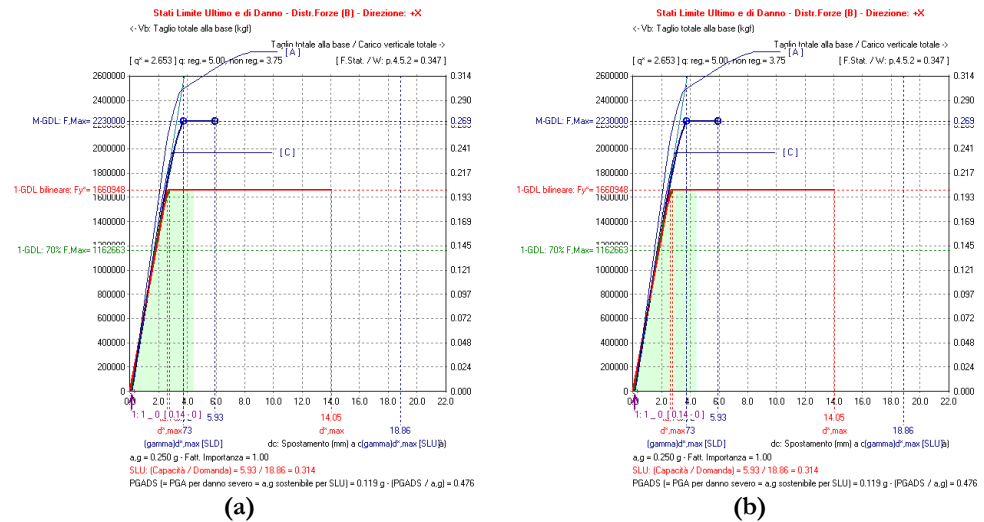


Figure 4.28 Push-over curves in (a) longitudinal and (b) in transverse direction according to the load distribution (B)

Table 4.17 Aedes results: SDOF bilinear curves parameters

Direction	Load distribution	δ_u [mm]	δ_y [mm]	F_y [kgf]	F_y [kN]
X	A	16.46	4	2800000	28000
	B	14.5	2.5	1660948	16609,48
Y	A	22	2	1240000	12400
	B	22.56	2	431900	4319,45

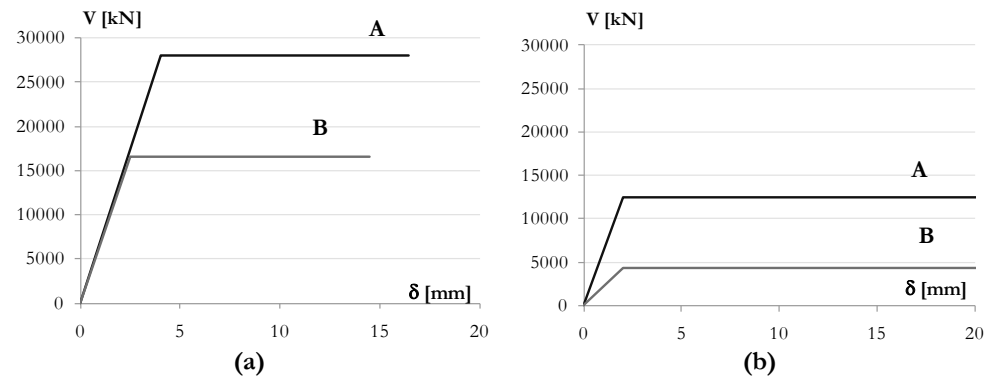


Figure 4.29 Aedes results: SDOF curves for (a) longitudinal (X) and (b) transverse (Y) directions according to the force distributions considered (A and B)

Afterwards, the mean curves between distributions A and B have been developed according the two examined directions. These latter have been considered as the

push over curves representative of the effective structural behaviour of the investigated construction (Fig. 4.30).

The parameter identifying the mean curves are summarized in Table 4.18.

Table 4.18 Aedes results: SDOF mean curves between A and B load distribution

Direction	δ_u [mm]	δ_y [mm]	F_y [kgf]	F_y [kN]
X	15.48	3.25	2230474	22304.74
Y	22.28	2	835972.5	8359.725

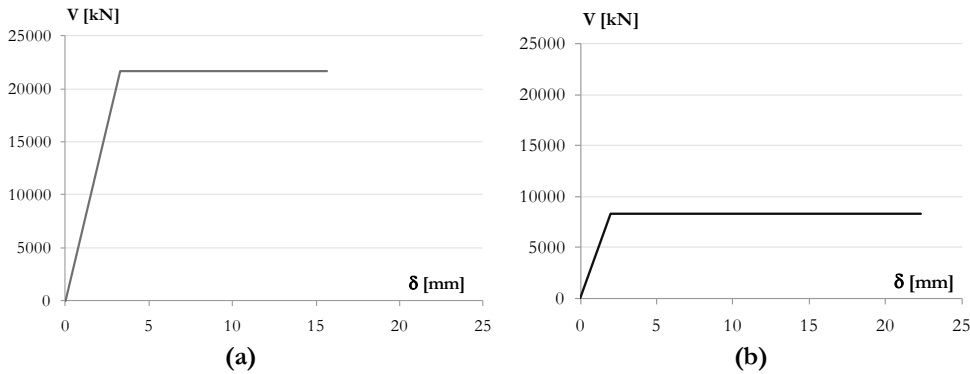


Figure 4.30 Aedes results: SDOF mean curves between distribution A and B for longitudinal (X) and transverse (Y) directions

The results of the static non linear analysis have shown that in terms of resistance, the structure behaves in a best way in the longitudinal direction in terms of ductility, it exhibiting a better response in the transverse direction.

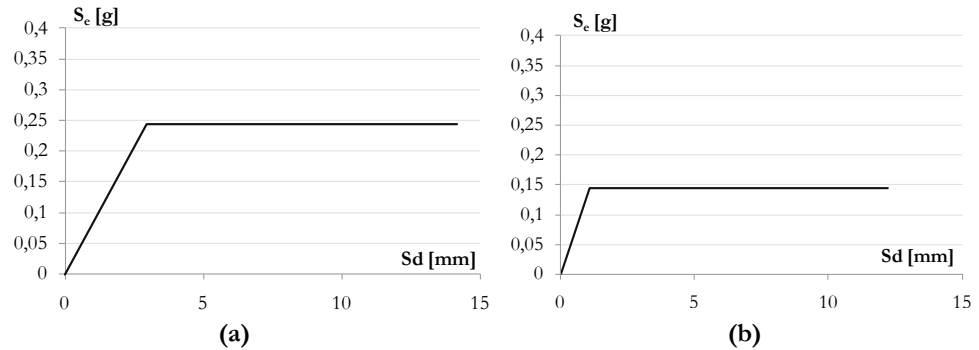
4.4.2.3. Vulnerability indexes assessment

In order to apply the CSM procedure and to assess the vulnerability index, it is necessary, as explained in section 4.4.1.1, to transform the capacity curve into the capacity spectrum.

Therefore, the curves displayed in Figure 4.28 have been appropriately converted in terms of spectral acceleration S_e and spectral displacement S_d by means of the formulation (4.46) and (4.47). The capacity spectra and its characterising parameters are shown in Figure 4.31 and in Table 4.19, respectively.

Table 4.19 Capacity spectrum parameter according to X and Y directions

Direction	δ_u [mm]	δ_y [mm]	a_y [g]	a_u [g]
X	14.14	2.94	0.244	0.244
Y	12.24	1.10	0.144	0.144

**Figure 4.31 Capacity spectrum for (a) longitudinal (X) and (b) transverse (Y) directions**

According to M. D. 2008, two different earthquake design spectra, namely the life safety limit state (LLS) and the collapse limit one (CLS), characterised by the probability to be exceeded during the structure life equal to 10% and 5%, respectively (cfr. 4.4.1.3), have been used. Consequently, these two spectra have been converted in the ADRS domain with the purpose to identify the performance points. Later on, these elastic response spectra have been adequately reduced according to the N2 Method and the ATC 40 one (section 4.4.1.4).

Dealing with the N2 procedure, four different performance points, two for each limit states considered, have been obtained from intersecting the capacity curve of the structure with the developed demand spectra (Figs. 4.32-4.33).

Later on, the vulnerability indexes have been calculated as the ratio between the displacement corresponding to performance point (PP) and the ultimate one (δ_u), according to the following formula:

$$I_{M_{aedes}} = \frac{PP}{\delta_u} \quad (4.60)$$

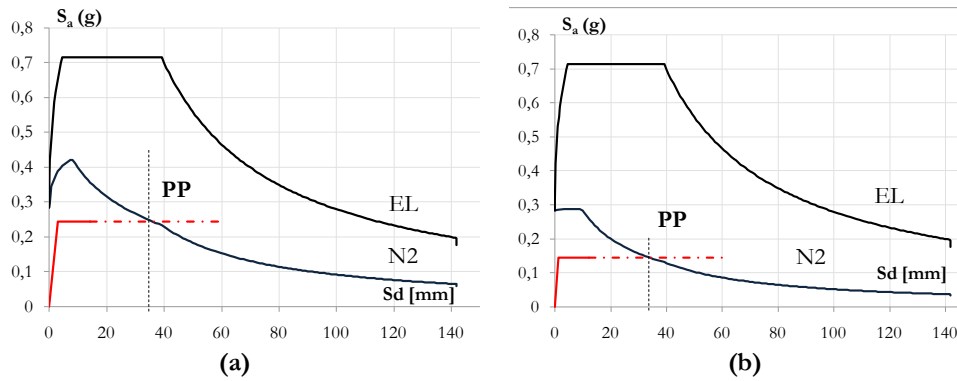


Figure 4.32 Performance Point detection at LLS according to the N2 method:
(a) longitudinal (X) and (b) transverse (Y) directions

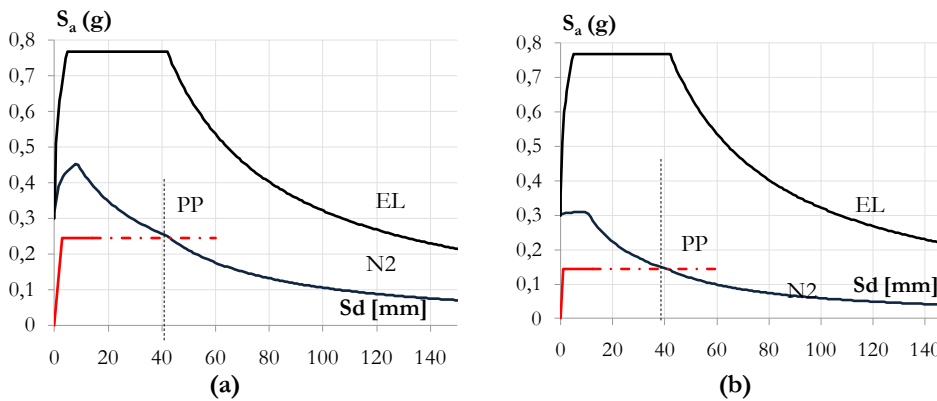


Figure 4.33 Performance Point detection at CLS according to the N2 method:
(a) longitudinal (X) and (b) transverse (Y) directions

According to the Performance Based Design methodology (PSB), four different damage limit states of the building S_{dk} ($k = 1, 2, 3, 4$) have been considered as a function of both the yielding (δ_y) and the ultimate (δ_u) displacements (Cattari et al., 2004):

- $S_{d1} = 0.7 d_y =$ no damage;
- $S_{d2} = 1.5 d_y =$ light damages;
- $S_{d3} = 0.5 (d_y + d_u) =$ significant damages;
- $S_{d4} = d_u =$ near collapse.

These target displacements, which have been determined for the capacity curves in directions X and Y (Table 4.20), allow to individuate the damage level of the structure versus lateral loads. Also, the results of the performed analyses in terms of vulnerability indexes are summarized in Table 4.20.

Table 4.20 Target displacement of the structure capacity curve

Direction	Damage state S_d [mm]	
X	S_{d1} – No Damage	2.06
	S_{d2} – Light Damage	4.41
	S_{d3} – Significant Damage	8.54
	S_{d4} – Near Collapse	14.14
Y	S_{d1} – No Damage	0.77
	S_{d2} – Light Damage	1.65
	S_{d3} – Significant Damage	6.67
	S_{d4} – Near Collapse	12.24

According to the Overdamped Spectrum Method, four different performance points have been similarly calculated (Figure 4.32 and Figure 4.33).

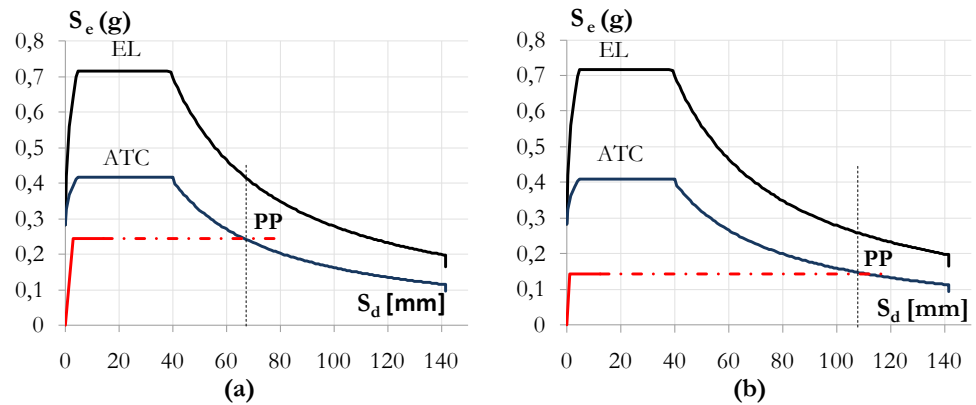


Figure 4.34 Performance Point detection at LLS according to the ATC method: (a) longitudinal (X) and (b) transverse (Y) directions

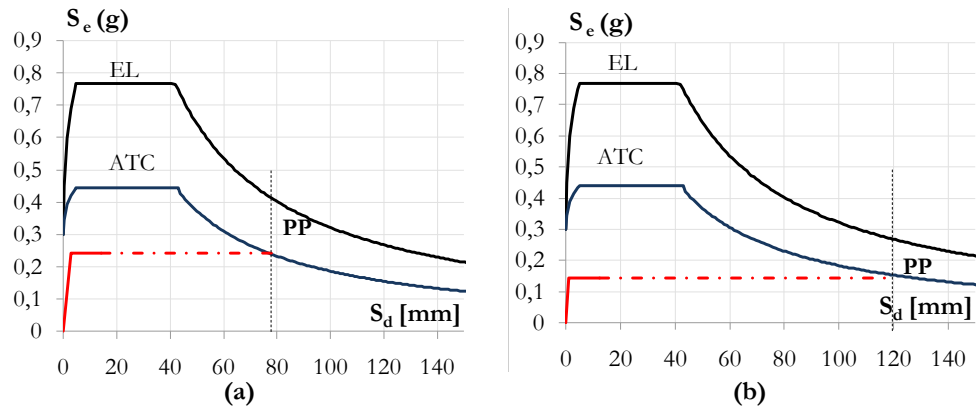


Figure 4.35 Performance Point detection at LLS according to the ATC method: (a) longitudinal (X) and (b) transverse (Y) directions

Later on, the vulnerability indexes have been assessed, as shown in Table 4.21.

Table 4.21 Seismic vulnerability indexes according to the numerical model

Limit State	Vulnerability Indexes			
	N2		ATC 40	
	X	Y	X	Y
LLS	2.68	3.10	1.66	1.88
CLS	2.97	3.26	1.70	1.96

The evaluated indexes show that the most vulnerable direction is the transverse one. It may be noted that the index is larger than 1; this means that the performance point, corresponding to expected damage level for the considered seismic event, is greater than the ultimate structural displacement. Therefore, the seismic vulnerability is very high.

4.4.3 The SAP 2000 program

4.4.3.1. Theoretical basis

In order to model masonry structure by means of the SAP 2000 non linear numerical software (CSI, 2000), it is necessary to develop an equivalent frame model, which allows to carry out a global analysis on the construction. So, several possible collapse mechanisms occurring inside each macroelement may be considered by modelling spandrels and piers as elastic frame fully rigid linked.

The SAP 2000 non linear code represents a generic structural calculation program. For this reason, the non linear mechanical behaviour of masonry may be modelled by defining plastic hinges for each element of the equivalent frame model. In fact, the plastic hinges allow to accurately investigate the non linear structural response of the building at each step of the incremental analysis.

In Pasticier et al. (2007), according to modern seismic codes, a technique to define the plastic hinges is provided. The Figure 4.35 shows the elasto-plastic behaviour with brittle fracture assumed for the entire pier and the rigid-perfectly plastic behaviour assumed, instead, for the pier plastic hinge. In particular, two rocking hinges are defined at the end of the deformable part of the vertical frame, while a shear hinge is defined at the mid-height of the same element.

The ultimate moment M_u is calculated according to eq. (2.25), assuming that the ultimate rotation (φ_u) corresponding to an ultimate lateral deflection δ_u^l is equal to the 0.8% of the deformable height of the pier minus the elastic lateral deflection.

The shear strength is, instead, evaluated as the minimum value between the shear strengths calculated according to two different criteria, both recommended in the OPCM 3274 (2003). The first one, recommended for existing constructions, is based on the original Turnšek and Čavic criterion (1971) and is referred to shear failure with diagonal cracking (cfr. section 2.5.3.4). This criterion is expressed by the formula (2.26). The second criterion, recommended for new constructions, refers to shear failure with sliding and is defined by the Mohr-Coulomb criterion according to the formulation (2.27).

In particular, the ultimate shear displacement δ_u is assumed to be equal to 0.4% of the deformable height of the pier minus the elastic lateral deflection.

As far as the modelling of the spandrel beams is concerned, assuming the presence of a lintel properly restrained at both supports, only one shear hinge is introduced at mid-span with the shear strength V_u given by the equation (2.29).

A brittle-elastic behaviour with residual strength after cracking equal to a quarter of the maximum strength is assumed for the entire element, with no limit in deflection.

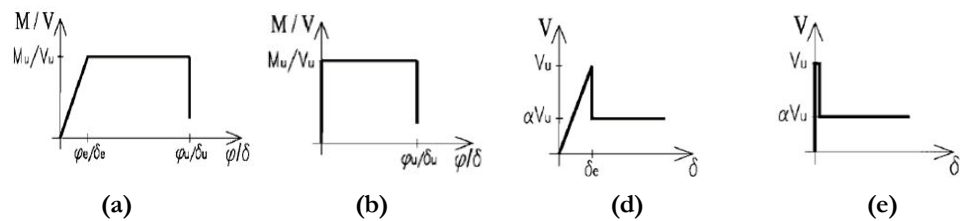


Figure 4.36 Relationships assumed in SAP 2000 v.10 (Pasticier et al., 2007):
(a) behaviour assumed for the entire pier; (b) pier plastic hinge;
(c) behaviour assumed for the entire spandrel; (d) spandrel plastic hinge

4.4.3.2. The FEM model

The *Palazzo di Città* model was implemented in SAP environment in accordance with the above described modelling method proposed in Pasticier et al. (2007), in which the non linear mechanical behaviour of masonry is modelled by introducing plastic hinges.

The implemented FEM model is shown in Figures 4.37 and 4.38.

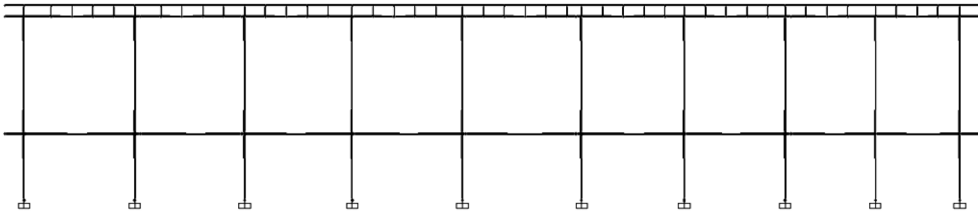


Figure 4.37 Plane Equivalent Frame Model of the examined building

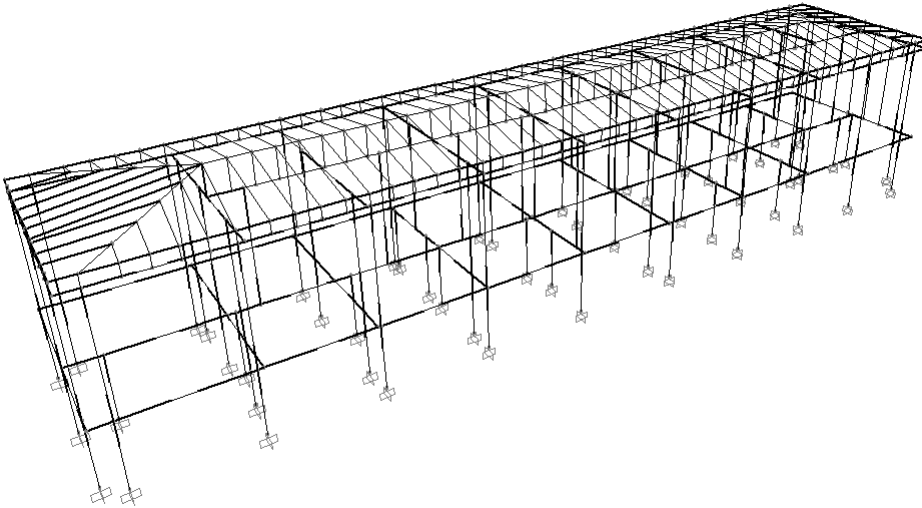


Figure 4.38 3D Equivalent Frame Model of the *Palazzo di Città*

Preliminary modal dynamic analysis has provided the shape of the vibration modes and the corresponding elastic periods of the structure. In particular, the first vibration mode is of transversal type ($T_1=0.228s$), the second mode is rotational ($T_2=0.251s$) and the third one is longitudinal ($T_3=0.185s$).

4.4.3.3. *The static non linear analysis*

Static non linear analysis have been carried out both in longitudinal and transverse direction in order to obtain the static push-over curve of the structure. Similarly to the analyse performed with Aedes , the combination of the actions given by expression (2.24) has been considered. Analogously, the analysis have been performed referring to the same load distributions: the first one

proportional to masses (A) and the second one proportional to masses multiplied by the displacements corresponding to the first vibration mode (B).

The deformed shapes related to the examined directions are represented in Figures 4.39 and 4.40; in both cases plastic hinges appear.

Therefore, for each plane direction and for each force distribution, the shear-displacement curve has been achieved along longitudinal (Fig. 4.41) and transverse (Fig. 4.42) directions.

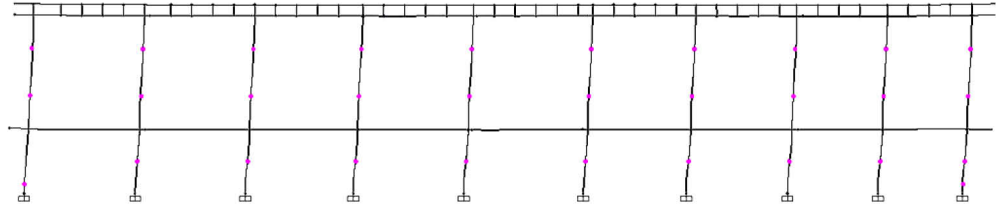


Figure 4.39 Deformed shape of the structure in the longitudinal direction

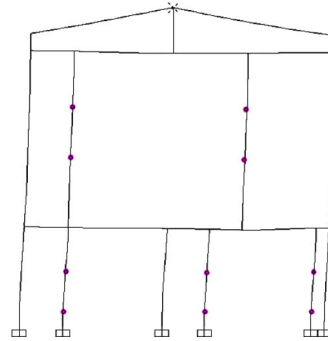


Figure 4.40 Deformed shape of the structure in the transverse direction

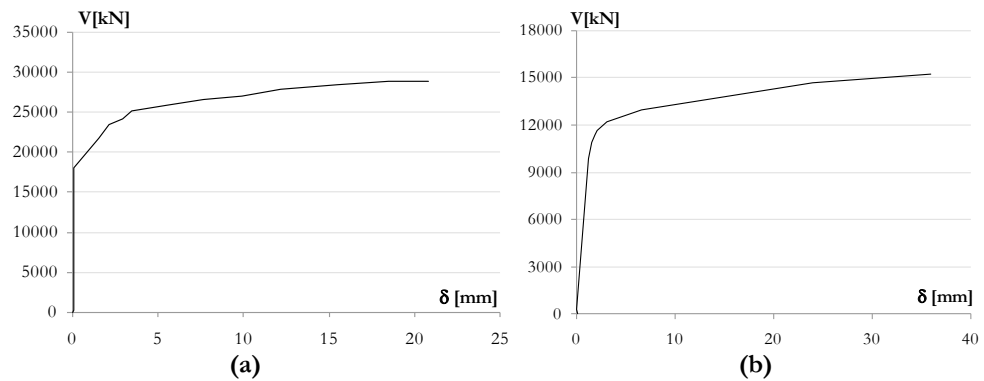


Figure 4.41 MDOF static push over curves for load distribution proportional to masses: (a) longitudinal and (b) transverse direction

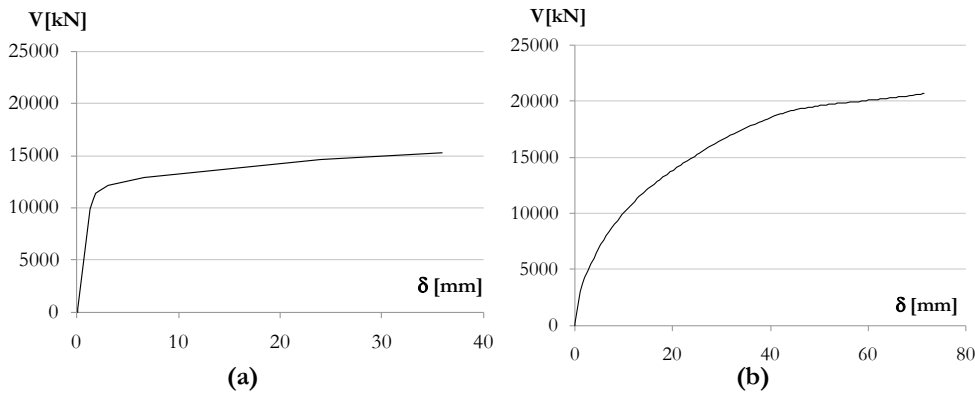


Figure 4.42 MDOF static push over curves for load distribution proportional to vibration mode displacements: (a) longitudinal and (b) transverse direction

The MDOF static push over curves have been subsequently transformed in the correspondent SDOF curves and, then, in the SDOF bilinear form according to the equations (4.43) and (4.44). Referring to the push-over curves in transverse direction, it is worth to precise that the maximum shear strength does not coincide with the effective structural strength. In fact, the shear strength value corresponding to the occurrence of collapse mechanisms in each elements is about 8000 kN for the distribution (A) and 5000 for the distribution (B). On the basis of these considerations, the bilinear curves have been drawn as shown in Table 4.22 and in Figure 4.43.

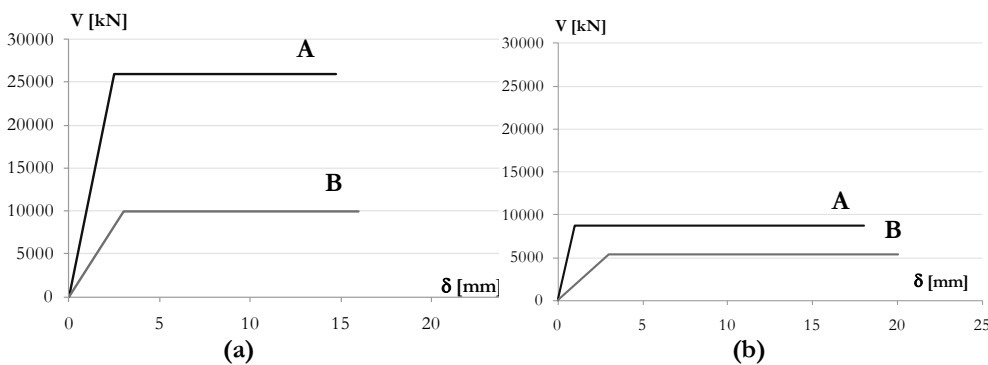


Figure 4.43 SAP results: SDOF curves for (a) longitudinal (X) and (b) transverse (Y) directions according to the force distributions considered (A and B)

Table 4.22 SAP results: SDOF bilinear parameters

Direction	Load distribution	δ_u [mm]	δ_y [mm]	F_y [kgf]	F_y [kN]
X	A	14.71	2.5	2600000	26000
	B	16	3	1000000	10000
Y	A	18	1	869200	8692
	B	20	3	540700	5407

Afterwards, the mean curves between distributions A and B have been developed according the two examined directions. These latter have been considered as the push over curves representative of the effective structural behaviour of the investigated construction (Fig. 4.44).

The parameter identifying the mean curves are summarized in Table 4.24.

Table 4.23 SAP results: SDOF bilinear parameters of the mean curve

Direction	δ_u [mm]	δ_y [mm]	F_y [kgf]	F_y [kN]
X	15.35	2.75	1800000	18000
Y	19	2	704900	7049

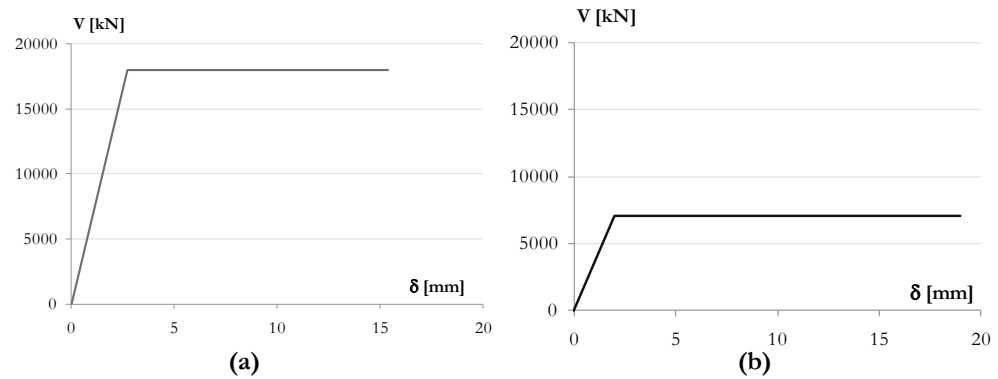


Figure 4.44 SAP results: SDOF mean curves between distribution A and B for longitudinal (X) and transverse (Y) directions

The results of the static non linear analysis are coherent with the ones provided by Aedes analysis. In fact, also according to the SAP analysis, the structure better behaves in longitudinal direction in terms of resistance, but it exhibits a more ductile response in the transverse direction than the longitudinal one.

4.4.3.4. Vulnerability indexes assessment

The achieved capacity curves have been subsequently converted into capacity spectra. So, the curves displayed in Figure 4.42 have been appropriately converted into the ADRS format by means of the (4.46) and (4.47) relationships. The capacity spectra and their constitutive parameters are shown in Figure 4.45 and in Table 4.24, respectively.

Table 4.24 Capacity spectrum parameter according to X and Y directions

Direction	δ_u [mm]	δ_y [mm]	a_y [g]	a_u [g]
X	12.23	2.17	0.290	0.244
Y	10.35	0.98	0.134	0.144

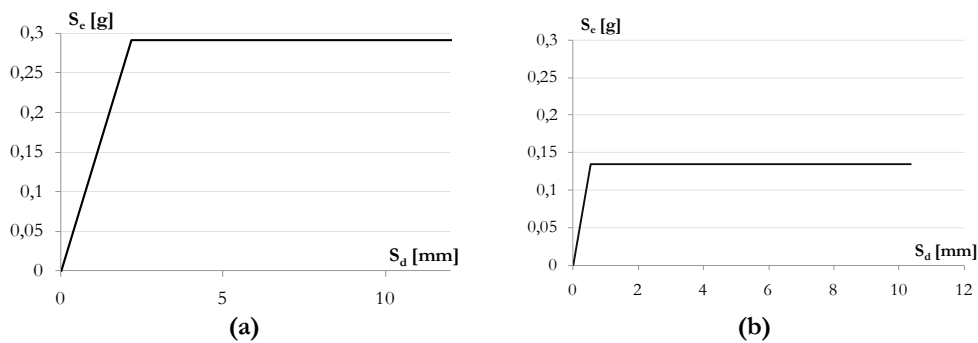


Figure 4.45 Capacity spectrum for (a) longitudinal (X) and (b) transverse (Y) directions

Therefore, according to CSM, the performance point has been detected by intersecting the reduced inelastic spectrum representing the seismic demand with the capacity spectrum. Similarly to the procedure described in section 4.4.1.4, four different performance points have been obtained according to the N2 method (Figs. 4.46-4.47).

Later on, the vulnerability index have been calculated as the ratio between the displacement corresponding to performance point (PP) and the ultimate one (δ_u).

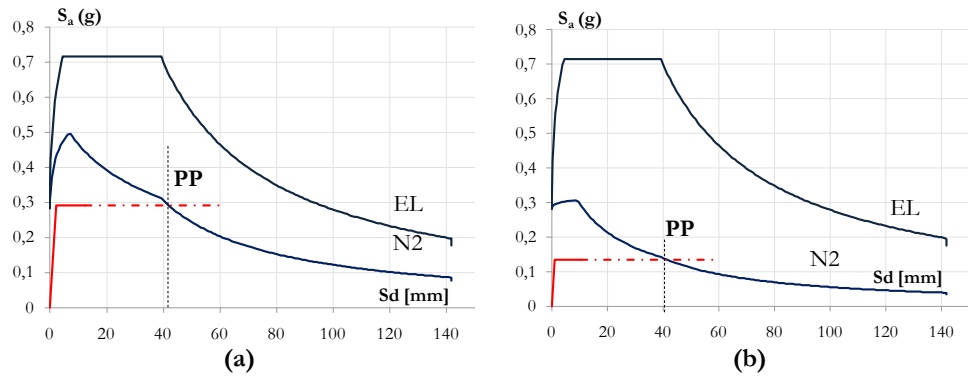


Figure 4.46 Performance Point detection at LLS according to the N2 method: (a) longitudinal (X) and (b) transverse (Y) directions

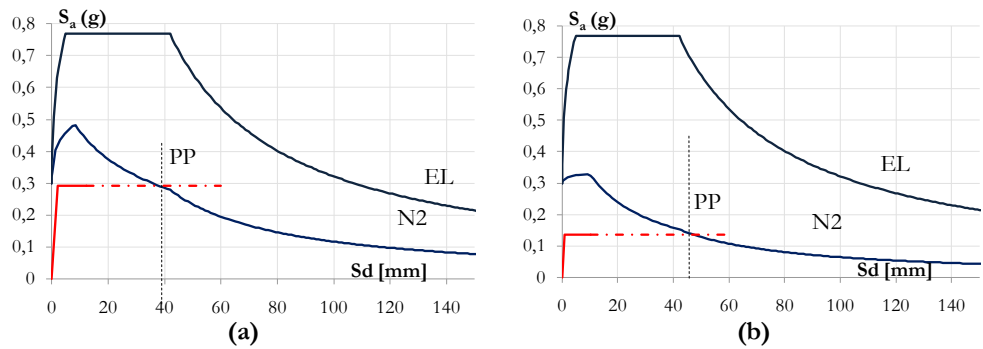


Figure 4.47 Performance Point detection at CLS according to the N2 method: (a) longitudinal (X) and (b) transverse (Y) directions

According to the PSB, four different damage limit states of the building S_{dk} have been considered as a function of both the yielding (δ_y) and the ultimate (δ_u) displacements. These target displacements are indicated in Table 4.25.

Table 4.25 Target displacement of the structure capacity curve

Direction	Damage state S_d [mm]	
X	S_{d1} – No Damage	1.52
	S_{d2} – Light Damage	3.26
	S_{d3} – Significant Damage	7.20
	S_{d4} – Near Collapse	12.23
Y	S_{d1} – No Damage	0.68
	S_{d2} – Light Damage	1.47
	S_{d3} – Significant Damage	5.66
	S_{d4} – Near Collapse	10.35

Afterwards, in accordance to the Overdamped Spectrum Method, four different performance points have been similarly calculated (Figs. 4.48-4.49).

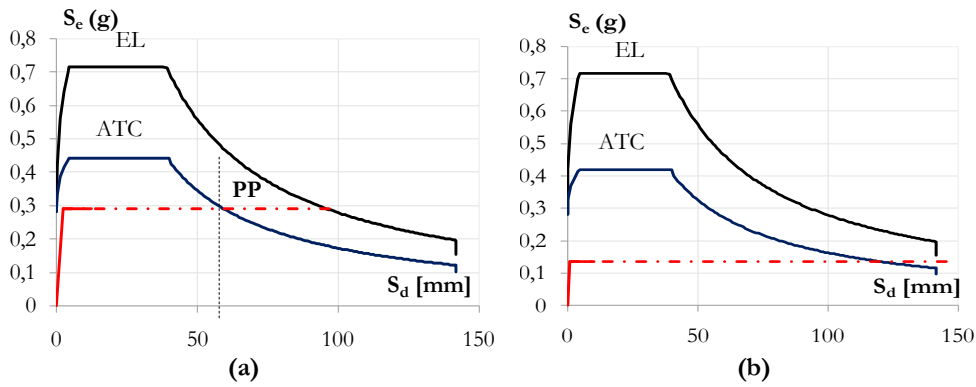


Figure 4.48 Performance Point detection at LLS according to the ATC method: (a) longitudinal (X) and (b) transverse (Y) directions

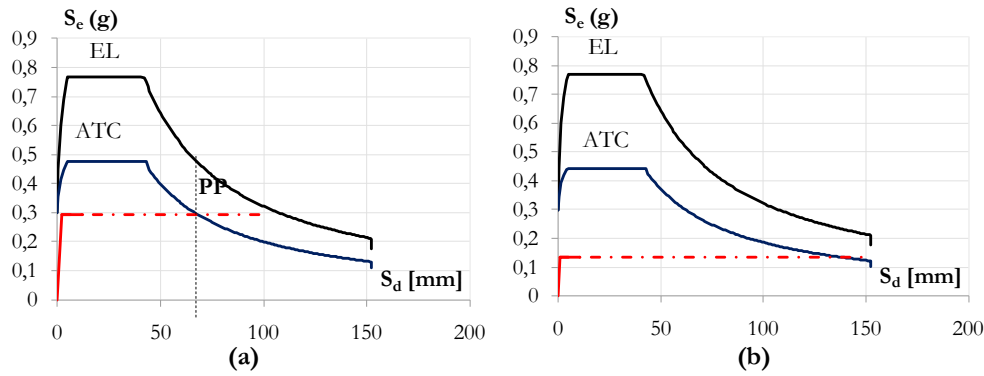


Figure 4.47 Performance Point detection at LLS according to the ATC method: (a) longitudinal (X) and (b) transverse (Y) directions

The estimated vulnerability indexes have been listed in Table 4.26.

Table 4.26 Seismic vulnerability indexes according to the numerical analysis performed

Limit State	Vulnerability Indexes			
	N2		ATC 40	
	X	Y	X	Y
LLS	3.43	3.96	1.57	1.70
CLS	3.92	4.34	1.68	1.75

4.4.4 Comparison among results

The CSM have been applied to the *Palazzo di Città* in order to assess its response under earthquake. To this purpose, mechanical models have been implemented by using two different computer calculation codes, namely Aedes and SAP 2000. A comparison between the two models in terms of capacity curve is depicted in Figures 4.49.

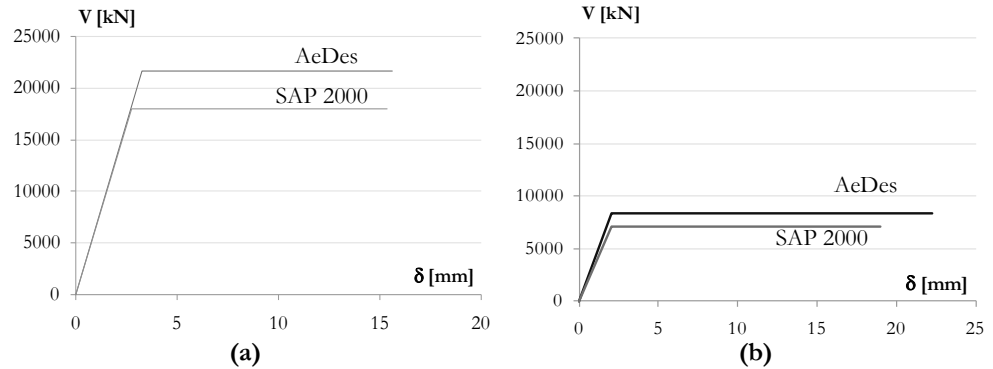


Figure 4.49 Comparison between SDOF curves both for (a) longitudinal (X) and (b) transverse (Y) directions developed by means of the AeDes and SAP 2000 programs

It may be noted that the results between the two programs are coherent, both in terms of stiffness and in terms of ductility. In terms of resistance, although the percentage gap in the two directions is similar (about 25%), the SAP 2000 code underestimates the shear strength, since it cannot be representative of the real behaviour of the structure. In fact, AeDes has been created with the specific purpose of numerical analysis of masonry structures, while SAP 2000 is a program used for modelling each type of structural typology, especially steel or concrete framed structures. Therefore, Aedes provides results more accurate than SAP 2000, since the former better estimates the real behaviour of masonry buildings.

With regard to the results provided by the CSM, it is possible to notice that the application of the two reduction approaches has led to the same vulnerability estimation. In fact, both according to the N2 method and the Overdamped Spectrum, the most vulnerability direction is the transverse one (Y) for the two considered limit states (LLS and CLS). In particular, the N2 method gives results on the safe side as respect to ATC ones; for this reason, it is the one recommended by the seismic Italian regulations.

The summary draft showing all the evaluated vulnerability indexes according to the N2 method and the ATC40 one is shown in Table 4.27.

Table 4.27 Summary draft of the vulnerability indexes assessed by means of the two applied methodologies

Program	Dir.	Method	LSV	CLS
			Index	Index
Aedes	X	N2	2.68	2.97
		ATC 40	1.66	1.70
	Y	N2	3.10	3.26
		ATC 40	1.88	1.96
SAP	X	N2	3.43	3.67
		ATC 40	1.57	1.68
	Y	N2	3.96	4.34
		ATC 40	1.68	1.75

Finally, the mean values between all indexes calculated along X and Y directions have been calculated. The value achieved in the direction Y has been considered as the effective vulnerability index of the structure (Table 4.28).

Table 4.28 Summary draft of the vulnerability indexes assessed by means of the two applied methodologies

Direction	LSV	CLS
	Index	Index
X	2.35	2.50
Y	2.65	2.82

4.5. COMPARISON AMONG VULNERABILITY ASSESSMENT PROCEDURES

In the final part of the study, all the analysis results have been critically analysed and compared each other.

The vulnerability index from simplified procedure has evidenced that the structure is not able to sustain the collapse limit state considered in the Italian code. In particular, the Benedetti and Petrini's methodology is not able to represent the real structure seismic vulnerability, because it gives a relative indication of the vulnerability of the structure. However, when the method is used with the damage analysis, it estimates well the seismic damage that the structure should undergo under earthquakes with different return periods.

The Italian guidelines (ITA G) provides a quick approach for the seismic vulnerability estimation, based on the calculation of the seismic collapse acceleration. According to this technique, the investigated structure should suffer heavy damages under a seismic actions corresponding to both LLS and CLS spectra.

Similarly, the failure acceleration of the structure has been estimated by means of the SAVE procedure and, then, the vulnerability indexes have been calculated. Also this method have evidenced the high vulnerability of the structure.

As last quick methodology, the simplified mechanical model (SM) has been applied. The method has permitted to draw a simplified capacity curve of the structure, referring to some mechanical parameters. In this case the vulnerability index has been calculated by using the CSM, adopting the N2 method to reduce the response spectrum.

Ultimately, the quick methodologies are able to foresee the damage state of the structure under high grade earthquakes. Although these approaches should be improved in order to correctly evaluate the real structural behaviour, they give a well estimation of the building vulnerability. Furthermore, the simplified procedures provides one vulnerability index, without considering different seismic directions.

The CSM procedure, which is based on refined FEM analyses performed along two plane directions, provides vulnerability values greater than 1 (collapse) and can be considered as the most reliable seismic vulnerability appraisal method, (Fig. 4.50). The summary draft is shown in Table 4.29.

Table 4.29 Summary draft of all the vulnerability indexes assessed

Methodology	Type	Dir	SLS	CLS
Benedetti and Petrini (B&P)	Quick	-	0.860	0.972
Italian Guidelines (ITA G)	Simplified	-	0.950	0.980
SAVE	Simplified	-	0.816	0.824
Simplified model (SM)	Simplified	-	1.64	1.96
CSM	Analytic	X	2.35	2.50
		Y	2.79	2.98

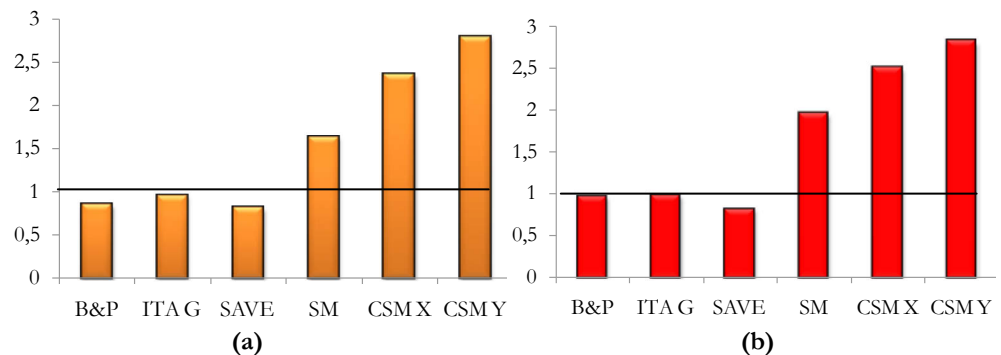


Figure 4.50 Vulnerability index distribution : (a) SLS; (b) CLS

A further comparison has been achieved among the structure capacity curves achieved along both the plane directions examined (Figs. 4.51 and 4.52).

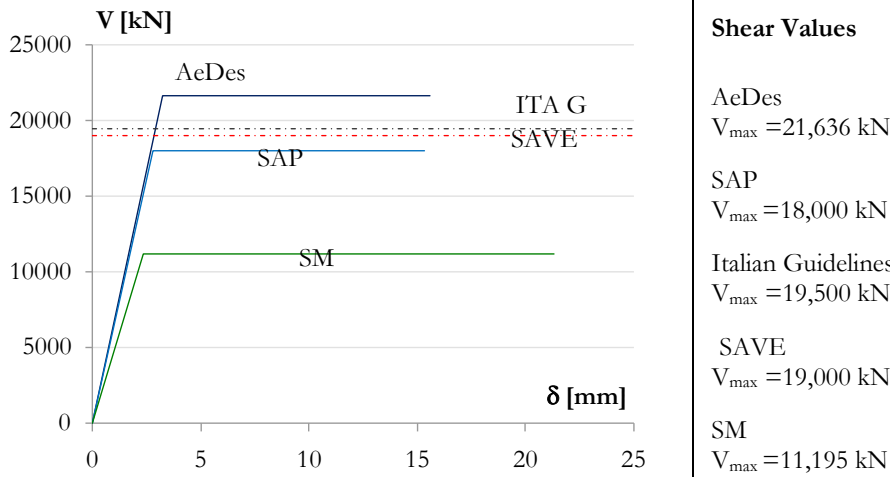


Figure 4.51 Capacity curves of the examined structure for longitudinal direction (X) according to different analysis methodologies

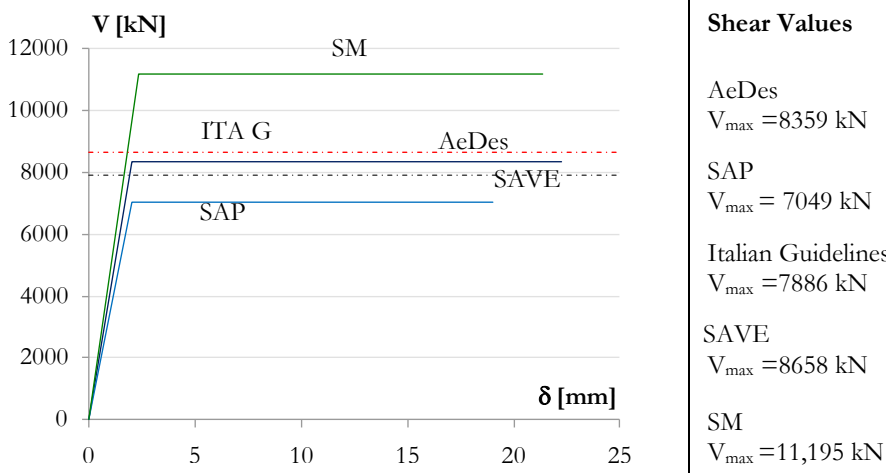


Figure 4.49 Capacity curves of the examined structure for transverse direction (Y) according to different analysis methodologies

The main observations on the performed comparison are:

1. The Italian guidelines approach predicts well the shear resistance only;

2. The SAVE procedure provides both the shear strength and the structural stiffness, but it does not give information about the ultimate displacement of the structure;
3. The SM provides one capacity curve only, without distinguishing X direction from Y one. Also, this curve is between the ones developed by means of the mechanical models.

4.6. VOLCANIC VULNERABILITY ASSESSMENT

4.6.1 Introductory observations

The analysed monumental building is within an area characterized by the potential existence of different kinds of risks. One of this directly derives from the high probability of occurrence of a large or medium Vesuvius eruption in the next decades, that should provoke many fatalities and economic losses. In fact, in the course of its history, Vesuvius has always represented a serious danger for the population living within its surroundings.

The main aspects determining the Vesuvius high risk are the elevated exposed values, due to the urban population density and to the built up heritage, and the vulnerability of the urban settlements to eruptive events, which make very difficult the risk management (Mazzolani et. al, 2009a, 2009b). A possible vesuvian eruption, indeed, should provoke the evacuation of about 600.000 people from an area of about 200 km² around it (Nunziata et al., 2000). This area is nowadays subjected to environmental crisis, represented by anthropic pressures, expansions towards agricultural areas, processes of degradation, abandonment and congestion, could be seriously compromised from a possible eruption, also deriving from the sea.

On the basis of these considerations, the final part of this study has concerned the volcanic vulnerability assessment of *Palazzo di Città* by means of the investigation of its behaviour under loads caused by volcanic effects, in order to emphasize its safety level against the volcanic actions.

4.6.2 Volcanic eruption effects

4.6.2.1. General remarks

Volcanic eruptions represents exceptional actions. In the course of history, these phenomena have always constituted a risk for the populations who live in the

proximity of the volcanic vents. Generally, the severity and dangerousness of the eruptive scenarios depends on the volcanic typology.

In particular, effusive and explosive eruptions may be distinguished (Fig. 4.52) (Mazzolani et al., 2009a). An effusive volcano emits the magma in the form of a lava flow, while an explosive volcano emits the magma violently through the so-called eruptive column, formed by gas-solid dispersal. The effusive eruptions are the least hazardous, because they can be in a state of continuous activity or erupt with annual frequency, while the explosive ones present long rest periods and explode unexpectedly.

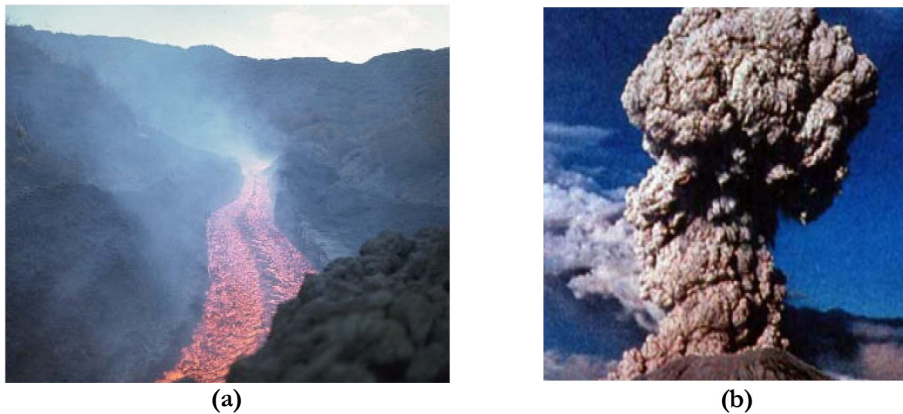


Figure 4.52 Eruption typologies: (a) effusive; (b) explosive

The most dangerous volcanoes are explosive ones, they characterizing by an eruptive column, which vertically rises from the eruptive centre and then it laterally moves for the action of the wind, according to its direction. Therefore, part of clasts get into gas-solid dispersals called pyroclastic flows and surges, respectively with high or low concentration of particles, and the rest of the clasts falls by gravity (air fall deposits) or is exploded directly in air from the crater (flying fragments).

Vesuvius is an explosive volcanic complex, located about 10km away from Naples. The volcano has summit elevation of 1281 m and is located at latitude 40.821°N and longitude 14.426°E.

While the typical products of effusive eruption are the lavas, those ones of explosive eruptions are the pyroclastics, originated by the magma fragmentation and classified, according to their size, in bombs and blocks (>64 mm), lapillus (2÷64 mm) and ashes (<2 mm). The deposits of pyroclasts are generically called tephra and divided in three basic types: air fall, pyroclastic flows and surges.

The typical eruption is also accompanied by the seismic movements, produced by cracking of rocks for the rise of the magma, and the lahars, constituted by flows of pyroclastic material and water, set in motion by the rains that often engendered by the explosive volcanic events, for the change of atmospheric state in the proximity of the volcano.

Definitely a construction invested by an eruption can be subjected to different actions: accelerations due to volcanic earthquake; horizontal dynamic pressures; static vertical pressures produced by pyroclastic deposits, together with elevated temperatures causing fires and possible explosions. Henceforth, each of these phenomena will be examined and expressed in terms of actions on constructions.

4.6.2.2. *Tephra deposits*

Tephra deposits are formed by the accretion of clasts which fall down by gravity from the eruptive column, at a distance which depends on the speed and the initial ejection angle. The largest pyroclasts fall in the environs of the emission point, the most fragmented ones at greater distance and the smallest ones can be transported long distance far from the vent by stratospheric winds.

Generally, air fall deposits cover the topography with uniform thickness, but, because of their poor consistency, they are removed from the most steep slopes (less than 20°-30°) and accumulated in the valleys.

During violent explosive eruptions, i.e. Plinian and sub-Plinian, large deposits of pumice cover an area of elliptical shape around the crater, which is elongated in the direction of winds. Contrary, a moderately explosive eruption produces deposit of clasts, whose distribution is symmetrical around the crater, because the launches are not sufficiently high to be influenced by the wind. In general, the thickness of tephra deposits decreases with the distance from the eruptive centre. The static load from air fall deposits may be considered a gravitational distributed load and it may be calculated according to the following relationship:

$$q_s = h \cdot g \cdot \rho \quad (4.61)$$

in which:

- g is the gravity acceleration
- h is the deposit thickness
- ρ is the deposit density

In particular, the density is dependent on the composition of pyroclasts, their compactness, the deposit moisture and the subsequent rains.

With reference to Vesuvius, the deposit density ranges from 400 to 1600 kg·m⁻³ in dry conditions and from 800 to 2000 kg·m⁻³ in damp conditions (Spence et al., 2005).

The weight of air fall certainly increases vertical load, producing the collapse of roofs, columns and walls, or of the entire structure. Moreover, another important feature concerns the further damaging effect due to elevated temperatures, which cause a substantial degradation of the mechanical properties of the construction materials.

4.6.2.3. *Pyroclastic flows*

Pyroclastic flows consist of a mixture of gases with dispersed solid particles of various sizes, which slides off the volcano slope with a speed up to $100 \text{ km}\cdot\text{h}^{-1}$, like a snow avalanche. They represent the most violent action that may occur during an explosive eruption.

The pyroclastic flow effect on the hit constructions is a dynamic pressure on the building lateral surface exposed to the volcano, accompanied by temperature ranges between 200 and 400°C .

The pyroclastic flows effect is very complex to model, since it depends on several variable factors difficult to catch, among them the pyroclastics erupted per unity of time (mass eruption rate), the volcano topographic profile and the magma properties, such as the water content and the temperature at the crater exit.

Aiming at examining the evolution of a pyroclastic flow, several models have been adopted. For instance, specific model that allows to determine the dynamic pressure produced by a flow may be find in Todesco et. al (2002), Esposti Ongaro et al. (2002) and Dobran (2007).

4.6.2.4. *Flying fragments and ballistic missiles*

Flying fragments are pyroclasts of different dimensions: the largest clasts are exploded directly from the crater according to pure ballistic trajectories, while the smaller clasts can be sustained by convection in the eruptive column, thrown in the atmosphere from the main flow to fall or be transported along the mountainside in gravitational currents.

The ejection distance of a volcanic fragment (R) with ballistic trajectory is expressed by the following law:

$$R = \frac{(u_0^2 \cdot \sin 2\theta)}{g} \quad (4.62)$$

where:

- u_0 is the ejection velocity,
- θ is the initial ejection angle of the fragment as respect to the horizontal plane

- g is the acceleration of the free fall.

The distance R depends on the wind velocity, on the air density, the cross-sectional area, the mass of the ballistic block and the drag coefficient (Dobran, 2006).

Ballistic missiles are flying objects generated by pyroclastic flows, as for instance particulates, debris, stones, loose flower pots and dustbins. They are incorporated into the main current and add to the destructive impact.

In Spence et al. (2007) a study on the probability of failure of the window produced by missiles may be found.

4.6.2.5. Lahars

The term lahars has an Indonesian origin and indicates any type of muddy flow containing volcanic material. Lahars and mudslides are produced by the combination the rain with the pyroclasts of poor coherence.

Lahars and mudslide are extremely dangerous because of their high kinetic energy, they being generally characterized by high speed. Furthermore, lahars are influenced by the same mechanisms of transportation and sedimentation of the non volcanic material landslides. Indeed, the lahars movements under gravity depends on the shear stress, the concentration of the flow and the slope gradient. Generally, the lahars deposits have very heterogeneous granulometry and extremely variable thickness, from few meters to few tens meters, with thickening in the anterior part of the flow. The density and the transportation energy of the mudslides can be so elevated to drag rocks of considerable dimension for many kilometres.

The lahars motion is regulated by the following equation:

$$\sigma = \sigma_0 + \mu \cdot \left(\frac{dv}{dy} \right) \cdot n \quad (4.63)$$

where:

- σ is the total shear stress
- σ_0 is the threshold of yielding,
- μ is the viscosity
- dv/dy is the velocity gradient
- n is a coefficient depending on the fluid model.

The effects of lahars on the constructions are comparable to those ones produced by the debris flows. According to a specific study related to the damages in the buildings impacted by the debris flows during the hydrogeological disaster of may 1998 in Campania (Faella and Nigro, 2002), the damage extent is dependent on the position of the construction, the impact direction, the level of

kinetic energy of the flow and the structural typology. The results of the analysis have permitted to identify the main collapse mechanism of RC and masonry structures. Moreover, a range value of the lahar hydrodynamic pressure to assume in volcanic analysis has been established. However, in a volcanic analysis, the additional variable of the temperature may be considered.

4.6.2.6. Earthquakes

Volcanic eruptions are always accompanied by local seismic activity, because the going up of the magma across the Earth's crust produces cracking of rocks. However, volcanic earthquakes are different from tectonic ones, they affecting narrow areas due to the superficial hypocenters.

The intensity of a volcanic earthquake is a function of the entity of the eruptive event. With particular reference to the Vesuvius case, the seismic crisis preceding the 1631 Sub-Plinian Vesuvius eruption was characterized by an earthquake intensity equal to 4.0 degree of the Richter scale, temporally limited to some hours before the eruption (Cubellis e Marturano, 2006) while after the last Vesuvian eruption (1944) the volcanic seismic activity has been characterized by an earthquake of low intensity.

A remarkable comparison between the volcanic and tectonic earthquakes is shown in Figure 4.53. The response spectrum of the Vesuvian earthquake of 9th October 1999 is compared with the one of the Irpinia seismic event of 1980, with reference to the registered seismograms of the Torre del Greco accelerometric station (Mazzolani et. al, 2009b).

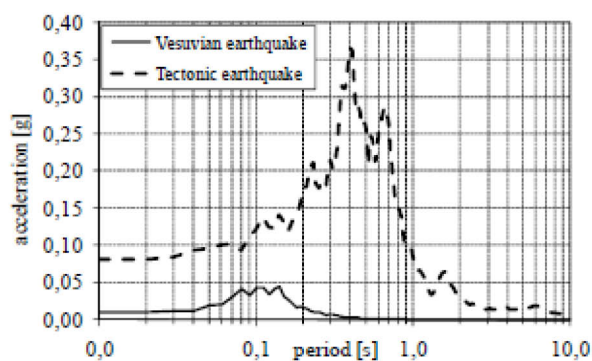


Figure 4.53 Comparison between the response spectra of the tectonic (1980) and the volcanic (1999) earthquakes in the Vesuvius area

The spectra give a significant comparison between the volcanic and tectonic earthquakes. The substantial difference between the two seism types is related to

the peak maximum acceleration periods T , which are equal to 0.40s and 0.14s, respectively. This means that, for constructions with ordinary height, the masonry structures suffered much more the volcanic earthquake, since its frequency is close to that of the building, while RC buildings are more sensible to tectonic earthquakes

4.6.3 Volcanic analysis

4.6.3.1 Tephra

In order to assess the volcanic vulnerability of the *Palazzo di Città*, firstly the effect due to tephra loads has been estimated.

The evaluation of tephra loads has been done according to the same relationship provided by the New Technical Italian Code (M.D., 2008) for snow loads.

Therefore, such a load has been computed by means of the following formula:

$$q_{sk} = \mu_i \cdot q_s \cdot C_E \quad (4.64)$$

where:

- μ_i is the shape coefficient depending on the roof slope (α); this value is equal to 0.8 for the investigated building (Table 4.30);
- C_E is the exposure coefficient, depending on the geographic position of the construction; for the examined zone C_E is equal to 0.9;
- q_s is the characteristic load of tephra on the ground level referring to past eruptions, expressed by the formulation (4.61).

Table 4.30 Values of the shape coefficient μ_i

Shape Coefficient	$0 \leq \alpha \leq 30^\circ$	$30^\circ \leq \alpha \leq 60^\circ$	$\alpha \geq 60^\circ$
μ_i	0.8	$0.8 \cdot \frac{60 - \alpha}{30}$	0

In particular, the tephra thickness has been estimated with reference to the map of the Vesuvius region where the extent of the area affected by tephra fall is shown. Within this map the isopachs of the ash deposits during the eruption occurred in 1631 are plotted (Fig. 4.54). Since the investigated area is about 7 km from the crater in South-West direction, the deposit thickness, which is related to the isopach highlighted in red on the map, is equal to 0.1 m.

Later on, the tephra load has been estimated considering different density, providing different values of the characteristic distributed load (q_s) according to the formulation (4.61) and q_{sk} according to the formula (4.64) (Table 4.31).

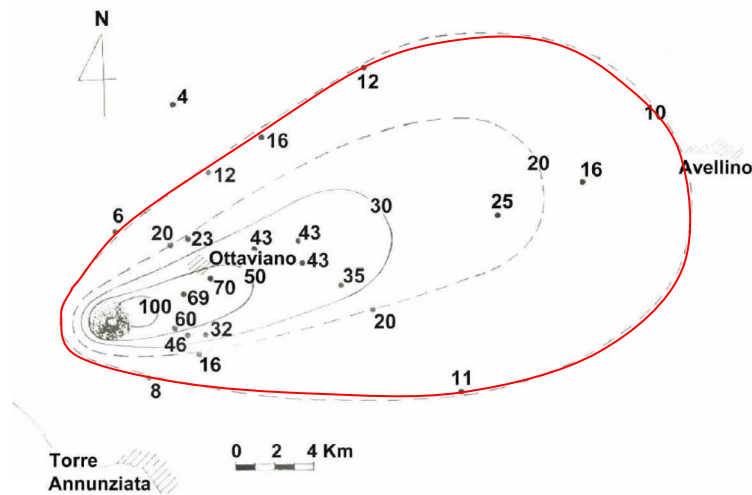


Figure 4.54 Map of the isopachs of the ash deposits during the eruption occurred in 1631

Table 4.31 Tephra load evaluation

ρ [$\text{kg}\cdot\text{m}^{-3}$]	q_s [$\text{kN}\cdot\text{m}^{-2}$]	q_{sk} [$\text{kN}\cdot\text{m}^{-2}$]
400	0.392	0.28
800	0.784	0.56
1400	1.3	0.98
1600	1.6	1.13
2000	1.9	1.41

Subsequently, the effect of the high temperature of the load has been considered by reducing the mechanical properties of the roofing timber structure, according to Eurocode 5 (UNI EN 1995 – 1 -2, 2005). In fact, this regulation provides specific formulas to decrease the wood strength under fire condition.

Thus, the local values of wood strength parallel to grain have been appropriately modified by multiplying the original value for the temperature dependent reduction factor (k_0). This factor has been detected in accordance to the diagram displayed in Figure 4.55. The modulus of elasticity, instead, has been directly reduced by means of the diagram of Figure 4.56.

Three different temperatures, namely 20°C, 100°C, and 200°C, have been considered in the analysis.

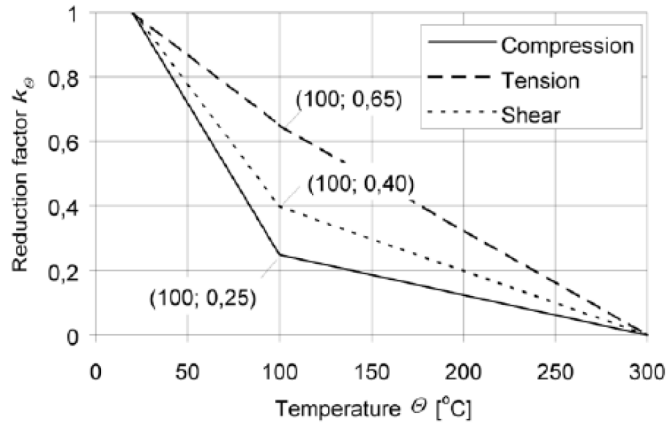


Figure 4.55 Reduction factor detection for strength parallel to grain softwood

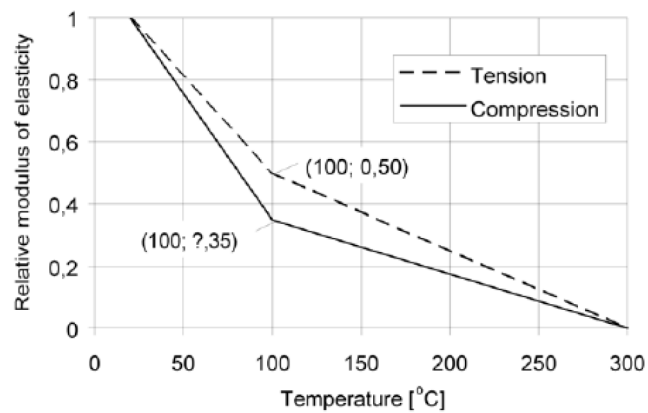


Figure 4.56 Effect of temperature on modulus of elasticity parallel to grain of softwood

Afterwards, a static linear analysis have been performed by means of the SAP 2000 numerical code, considering the application of tephra loads indicated in Table 4.32 for the three aforesaid temperature values.

In particular, the following exceptional combination of the actions have been considered, according to the M.D. 2008:

$$F_D = G_{k1} + G_{k2} + P + A_d + \sum_i \psi_{2i} \cdot Q_{ki} \tag{4.65}$$

in which:

- G_{k1} and G_{k2} express the characteristic value of the permanent loads;
- Q_{ki} expresses the characteristic value of the variable loads;

- A_d is the exceptional action;
- ψ_{2i} is the combination factor considering the probability of occurrence of the variable actions when the extreme event occurs.

Thus, the building assessment towards tephra has been done by checking the stress level in the roof timber beams, made of a chestnut wood characterized by a flexural strength of 30 MPa, according to the following formula:

$$s = \frac{M_{SD}}{M_{RD}} \quad (4.66)$$

The evaluated s ratios are shown in Table 4.32.

Table 4.32 Performance ratios for different value of the tephra density

ρ [$\text{kg}\cdot\text{m}^{-3}$]	T =20 °C	T =100°C	T =200°C
400	$s = 0.14$	$s = 0.25$	$s = 0.57$
800	$s = 0.28$	$s = 0.51$	$s = 1.4$
1400	$s = 0.50$	$s = 0.90$	$s = 2.00$
1600	$s = 0.57$	$s = 1.00$	$s = 2.28$
2000	$s = 0.71$	$s = 1.28$	$s = 2.85$

It is evident that the collapse due to tephra loads occurs when the s ratio is greater than 1, that is in the following cases (in bold in Table 4.33):

- for a T = 100°C when $\rho > 1600 \text{ kg}\cdot\text{m}^{-3}$;
- for T= 200°C when $\rho > 800 \text{ kg}\cdot\text{m}^{-3}$.

4.6.3.2. Ground motion

The CSM procedure applied in order to estimate the seismic vulnerability of *Palazzo di Città*, has been herein also used to assess its vulnerability towards volcanic earthquakes. The reference seismic event is the one occurred in 1631, characterized by an earthquake intensity equal to the 4th degree of the Richter scale and by a Peak Ground Acceleration of 0.07g. Therefore, the corresponding elastic response spectrum can be approximately referred to a seismic event with a return period T_R equal to 72 years.

Similarly to the seismic analysis already carried out, firstly the building response has been estimated by means of AeDes and SAP 2000 programmes. Later on, the achieved response spectra have been adequately reduced by using both the N2 and the ATC 40 methodologies and, finally, the performance points have been determined, they providing the vulnerability indexes summarised in Table 4.33.

Table 4.33 Vulnerability indexes of the building towards a volcanic earthquake

DIR		AeDes	Sap 2000
X		0.17	0.16
Y	N2	0.81	0.91
	ATC 40	0.75	0.90

From the above table, where it is apparent that in the longitudinal direction (X) the two methods provide the same result, it has been detected that the examined structure should suffer heavy damages under a volcanic earthquake in transverse direction.

4.7. CONCLUSIVE REMARKS

The vulnerability analysis of an isolated monumental building in Torre del Greco, characterised by strategic and historic importance, has been performed with reference to two different phases, represented by seismic and volcanic analyses.

In the first step, quick, simplified and refined vulnerability assessment methods have been applied. In particular, in order to use the CSM, a numerical model has been implemented by means of two computer codes. Thus the vulnerability indicators have been estimated for each of the employed methods and then compared each other.

The analysis results deriving from both techniques have shown the high vulnerability of the structure, so that this building cannot be considered as strategic, since its failure should occur under the collapse limit state demand spectrum considered in the new technical Italian code.

Afterwards, the vulnerability due to the Vesuvius risk has been assessed, considering exceptional loadings related to the effect of this phenomenon. Volcanic actions, in fact, represents exceptional loads, producing extreme conditions for ancient constructions, often designed to resist ordinary vertical loads only and in compliance with the technical rules of their time of constructions.

Therefore, the effect of tephra load on the structure has been investigated by performing a linear static analysis considering the deposit material at both different temperature levels and load densities. The results have provided the conditions of major vulnerability for the examined building.

Finally, the vulnerability due to a volcanic quake have been estimated. Such an analysis has demonstrated that the building should suffer heavy damages under this volcanic ground motion in transverse direction.

In conclusions, the study has been useful to assess the high vulnerability of the study building under exceptional actions. Because of its architectural and historical values, as well as its strategic role in the municipality, seismic retrofitting interventions should be therefore made in a next analysis phase.

Chapter 5

Seismic behaviour of a monumental palace under exceptional actions: the L'Aquila earthquake study case

5.1. L'AQUILA EARTHQUAKE

5.1.1. Characteristics of the seism

On April 6th, 2009 at 3:32 a.m. (1.32 UTC) (Fig. 5.1a) an earthquake stroke the Abruzzo region, a 5000 km² area located within the Central Apennines of Italy. In particular, the capital of the region, namely L'Aquila, a city of about 73.000 people, and several villages of the middle Aterno valley were mostly hit by the seism.

The mainshock was rated 5.8 on the Richter Scale (M_I) and 6.3 on the Moment Magnitude Scale (M_W).

This earthquake was generated by a normal fault, located in a valley contained between two parallel mountain located along the direction North - South (Figs. 5.1b and 5.1c) (Fanale et al., 2009), with a maximum vertical dislocation of 25 cm and hypocentre depth of about 8.8 Km.

The main event was recorded by 56 digital strong motion stations which are part of the Italian Strong Motion Network (in Italian *Rete Accelerometrica Nazionale*, RAN), owned and maintained by the Department of Civil Protection (DPC).

The distribution of damage within the affected area was non-uniform and asymmetric, as may be pointed out from the map of the observed MCS intensity (Fig. 5.3a). Observing this map, it may be noted that the mainshock caused heavy damages in the centre of L'Aquila, where intensity value was reported varying between VIII and IX. Damages were even more significant in some villages

located in the middle Aterno valley, where intensities as high as IX-X were experienced in Castelnuovo, Onna and Paganica. In total, 14 municipalities experienced a MCS intensity between VIII and IX, whereas those characterized by MCS intensity I larger than VII were altogether 45 (Galli and Camassi, 2009).

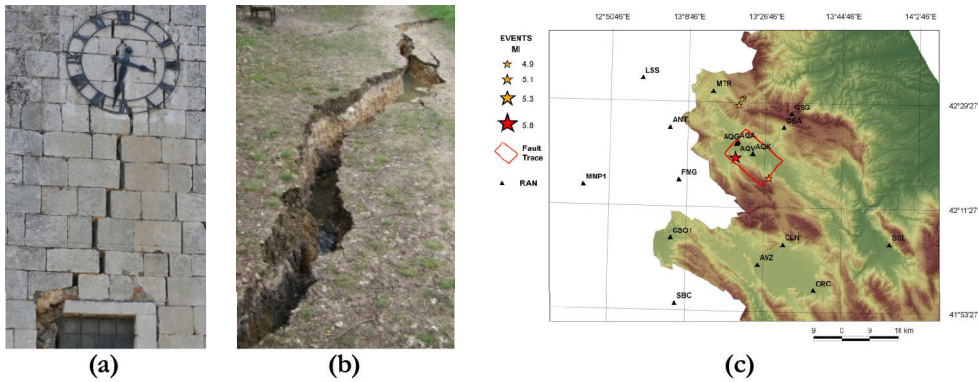


Figure 5.1 Traces of L'Aquila earthquake: (a) the hour of the event; (b) the surface fracture; (b) the fault geometry

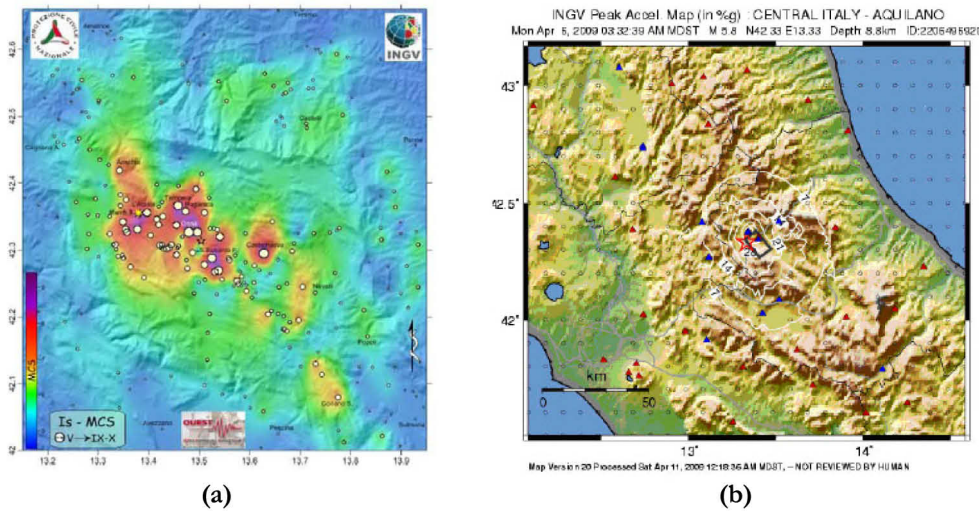


Figure 5.2 Mainshock maps (Italian National Institute of Geophysics and Vulcanology - INGV): (a) MCS map; (b) (PGA) map

Although the epicentre depth was not so deep, the seismic waves associated with shallow quakes produced very strong shaking and many damages; therefore, the main shock was followed by many aftershocks.

5.1.2. Why an exceptional action

L'Aquila earthquake is regarded an exceptional seismic action.

The main reasons are closely correlated to the following aspects:

1. the maximum recorded horizontal and vertical acceleration components within the epicentral area were larger than PGAs of the elastic spectra given by the Italian Code (M. D., 2008) (see Table 5.1);
2. it was a near-field quake, representing the first well-documented strong-motion earthquake instrumentally recorded in Italy in a near-fault area (Monaco et al., 2010).

Referring to the first point, this event was the third main ground motion recorded in Italy since 1972, after the Friuli event (1976; $M_w=6.4$) and the Irpinia one (1980; $M_w=6.9$). Furthermore, it was the strongest among a sequence of 23 earthquakes having M_w greater than 4 and occurred between 2009 March, 30th and 2009 April, 23rd (Fig. 5.3a), it providing strong motion recordings from accelerometer stations placed very close to the epicentre, that is 4-5 Km (Fig. 5.3b).

Table 5. 1 Earthquake effects at different epicentre distances

Record identifier	Dir. x	Dir. y	Dir. z	Epicentre distance [Km]
	PGA (g)			
GX066	0.626	0.597	0.420	4.8
FA030	0.416	0.434	0.215	4.3
CU104	0.394	0.451	0.380	5.8
AM043	0.342	0.340	0.350	5.6
EF021	0.153	0.149	0.112	18.0
TK003	0.081	0.089	0.045	31.6

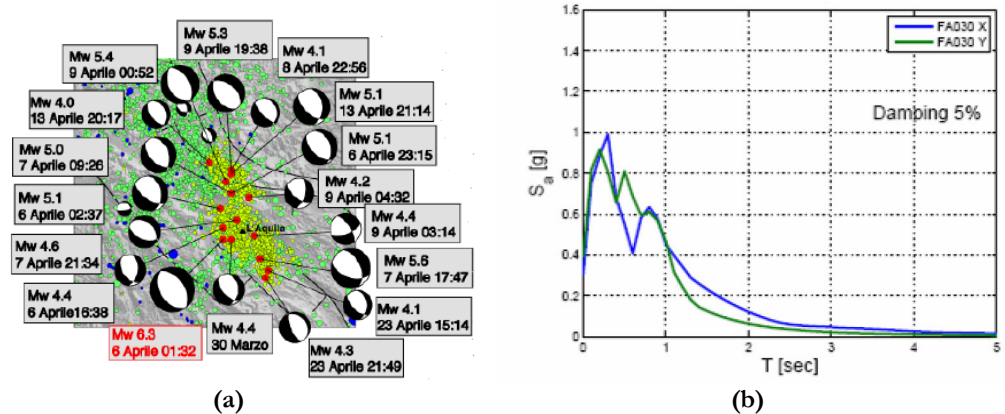


Figure 5.3 (a) Sequence of seismic events occurred in the L'Aquila district (INGV); (b) elastic acceleration spectrum 4.3 Km far from the epicentre

The second aspect is related to near field effects. A near- field earthquake (Fig. 5.4) is an impulse motion and not a cyclic one, generally characterized by the following aspects (Ohmaci and Jalali, 1999): large pulses occur at the beginning of the S waves motion with rather short duration; the pulse of the motion is polarized in the direction normal to the fault strike; the pulse shows large amplitude in both horizontal and vertical directions. Thus the quake vertical component cannot be disregarded, since it has a high value as respect to the horizontal one. As a consequence, the dynamic motions are dominated by a large long period pulse of motion.

The near-fault earthquake directly affects the seismic response of structures, especially in the nonlinear range. Therefore, the most important effects on construction as respect a far-field earthquake are:

- the superior modes are dominant as respect the fundamental ones;
- the vertical component causes second order effects, i.e. local or soft-floor mechanisms;
- the structural ductility depends on the global stiffness rather than the soil condition.

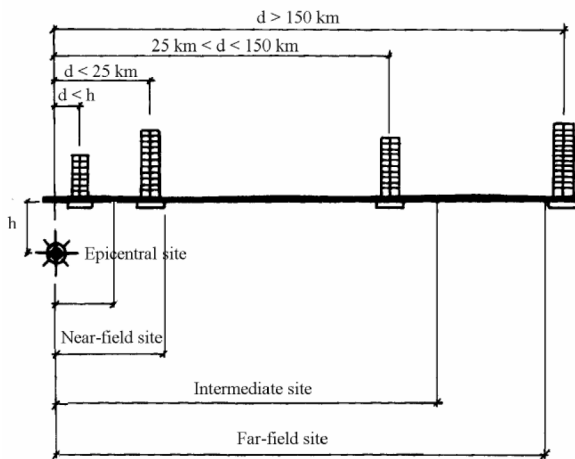


Figure 5.4 Near-field and far-field site distances

Another important aspect of L'Aquila earthquake, is related to seismic local amplification effects. In fact, L'Aquila was built on the bed of an ancient lake, characterized by a soil structure that amplifies seismic waves. In particular, the historic centre of L'Aquila is located on a fluvial terrace on the left bank of the Aterno River (Monaco et al., 2009).

Therefore, the current geological setting of the L'Aquila basin results from a complex sequence of depositional events, due to erosion and tectonics (Fig. 5.5).

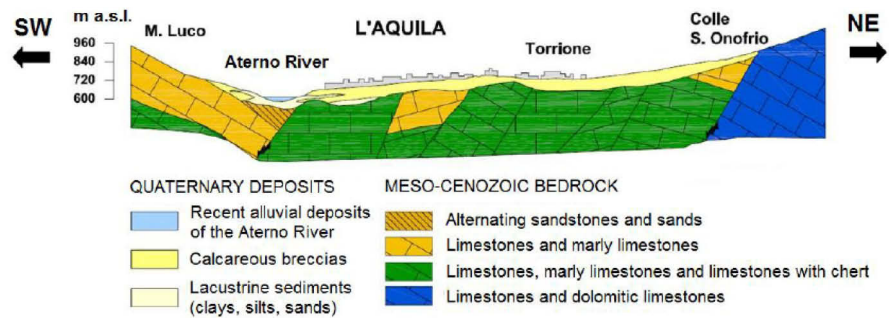


Figure 5.5 Geologic section corresponding to the centre of L'Aquila (Bertini et al. 1992)

Coupling near-fault conditions with site effects induced by the complex geological structures further contributes to the complexity of the earthquake ground motion.

5.1.3. Post-event consequences

The earthquake occurred when most people were sleeping. So, a large number of people were killed (305) or injured (1.500). The fatalities were concentrated in two age groups, namely 20-29 years and over-70 years, but this does not reflect the demographic age of L'Aquila province. In fact, the peak in the 20-29 years group was due to the collapse of a student hall in the downtown of L'Aquila. Moreover, the earthquake produced the temporary evacuation of 70,000-80,000 residents and 24,000 of them remained without home (AA.VV., 2009).

The whole population of the towns listed in the official earthquake damage declaration was 60,352. Generally, towns were composed of people in the range [1.000 ÷ 3.000], with only two larger municipalities having 5.000 and 8.500 inhabitants.

After the earthquake about 10,000 - 15,000 buildings were destroyed or damaged. Above all, many of the region cultural sites, including Romanesque churches, palaces and other monuments dating from the Middle Ages and Renaissance, were harmed in a severe way or demolished. The total damage was estimated larger than 25 billion €.

L'Aquila and the surrounding districts suffered significant damages to historic buildings. In particular, the historic centre of L'Aquila, which in English means "*The Eagle*", was partially destroyed. The built up heritage of this city is represented by churches and monuments, which includes the Fountain of the Ninety-Nine Spouts, the 16th century Spanish Castle, the Basilica of St.

Bernardino (Fig. 5.7a), the Church of St. Massimo (Fig. 5.6), the Church of St. Mary in Collemaggio and the Government Palace (Fig. 5.7b).

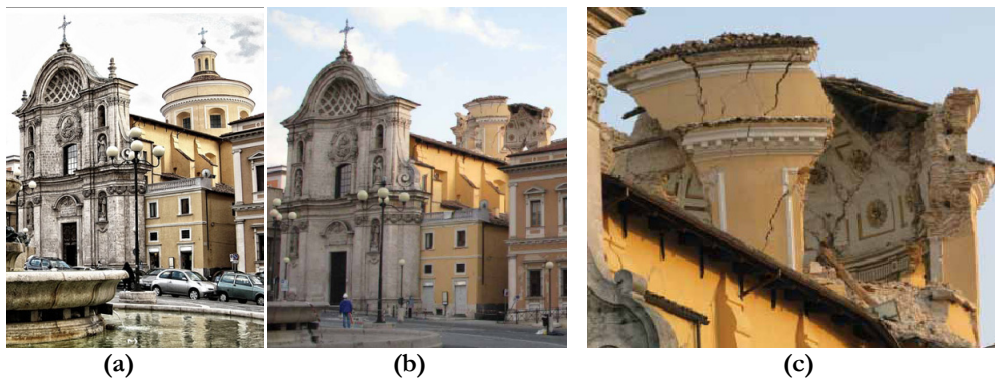


Figure 5.6 The Church of St. Massimo: (a) before and (b) after the earthquake; (c) detail of the damaged dome



Figure 5.7 Monumental buildings of L'Aquila after the earthquake:
(a) The Basilica of St. Bernardino; (b) the Government Palace

Also the so called "minor" architecture, consisting of the surroundings small historic centres, was grievously damaged, e.g. Fossa, Onna, Paganica, Castelnuovo and Poggio Picenze, these latter being study cases of this PhD thesis.

Starting from the days immediately after the seismic event, the Civil Defense Department members, in cooperation with a large number of Italian University Institutions researchers, visited those places in order to evaluate the usability of the whole built-up of L'Aquila and its districts.

In the following months, the emergency have been handled by the Civil Protection Department, as concerns the housing managements.

In particular, two types of dwelling have been provided for the homeless people:

1. apartments of the CASE Project (*Anti-Seismic, Sustainable and Environment-Friendly buildings*), called by the inhabitants of L'Aquila and surroundings the *New Town* (Fig. 5.8a);
2. wooden cabins of the MAP Plan (*Temporary Accommodation in Modular Housing Unit*) (Fig. 5.8b).



Figure 5.8 (a) Building of the New Town; (b) wooden cabin in Onna

5.2. MEASUREMENTS IN ABRUZZO

5.2.1 Introduction

In order to evaluate the seismic behaviour and response of historical buildings, several important aspects should be considered. One important aspect is the estimation of earthquake ground motions based on amplitudes as well as on the frequency content of both local and distant seismic sources considering the modification by local soil conditions. Other important factors that influence the determination of seismic response are the strength and deformability characteristics of the materials, as well as the interaction between the local soil and the structure. Further, the dynamic properties of the structure - the natural (resonant) frequencies, mode shapes, and damping capacity should be considered also as one of the main aspects. Therefore, the definition of the actual state of a monument in respect to its dynamic characteristics should be performed by experimental in-situ testing, applying ambient or forced vibration testing method. For this reasons, in May 2010, an experimental activity has been performed in the frames of the COST Action C26 (cfr. paragraph 4.1), as cooperation between the Institute of Earthquake Engineering and Engineering Seismology (IZIIS) of the

“Ss. Cyril and Methodius” University (Skopje, Republic of Macedonia) and the University of Naples “Federico II”. This testing campaign has been developed by the working team depicted in Figure 5.9 in order to investigate the actual state of four selected monumental constructions in the historical centres of Poggio Picenze and Castelnuovo of San Pio.



Figure 5.9 The work team

Besides the description of the tested buildings and the main collapse mechanisms provoked by the earthquake, the applied testing procedure and the main obtained experimental results are presented and discussed.

Furthermore, the numerical analysis of one of the measured building has been carried out by means of the ABAQUS numerical code, in order to assess the building behaviour and design adequate restructuring measures (see paragraph 5.3).

5.2.2 Poggio Picenze and Castelnuovo historical centres

The measurements in Abruzzo have been performed in the historical centres of Poggio Picenze and Castelnuovo of San Pio, both of them in the South - East territory of L'Aquila (Fig. 5.10).

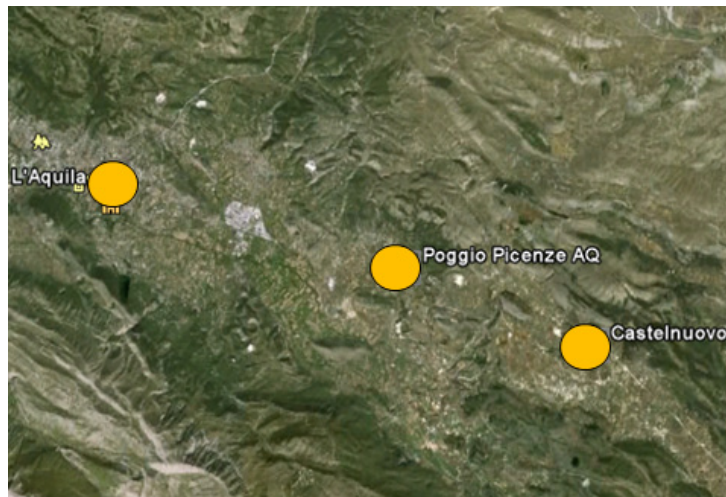


Figure 5.10 Location of Poggio Picenze and Castelnuovo as respect L'Aquila

Poggio Picenze is a small town situated on the top of a hill, 760 meters above sea level, and it is located about 10 km to the South-East of L'Aquila; it lies along a slope located at the left (north) side of the river Aterno valley. The municipality has a population of about 1000 inhabitants. It is one of the most damaged towns under the Abruzzo mainshock with a grade of 5.8 and 6.3 on the Richter scale and the moment magnitude one, respectively. Also, several thousands of aftershocks occurred, more than thirty of which had a Richter magnitude greater than 3.5.

Most of the centre of Poggio Picenze was partially destroyed by the earthquake, which produced both significant damages to buildings of the historical centre and death of 5 people. The historical centre is the result of the process of continuous urban growth from the ancient times up to the present days. In particular, the farming town can be divided into two different urban areas (Fig. 5.11a). The oldest nucleus was founded by Piceni around the 3rd century B.C. on the slope of Mount Picenze. The subsequent urban configuration developed around the medieval castle built approximately in the 1st century A.C. Originally, the ancient castle had fortified walls and six towers, including a high one in the middle. Therefore, in the oldest part, the urban planning is typical of a medieval town with buildings arranged in almost concentric arrays which follow the contours. On the contrary, the other area, which is the new one, has an irregular urban plan with some important palaces, like the mercantile Medieval House, built in the 13th century (Fig. 5.11b). The entire town suffered heavy damages during the 1762 October 6th earthquake, which required substantial reconstruction works. In fact, the castle of Poggio Picenze became unsafe and it

was demolished. Ruins of this structure are still visible in the oldest part of the town.

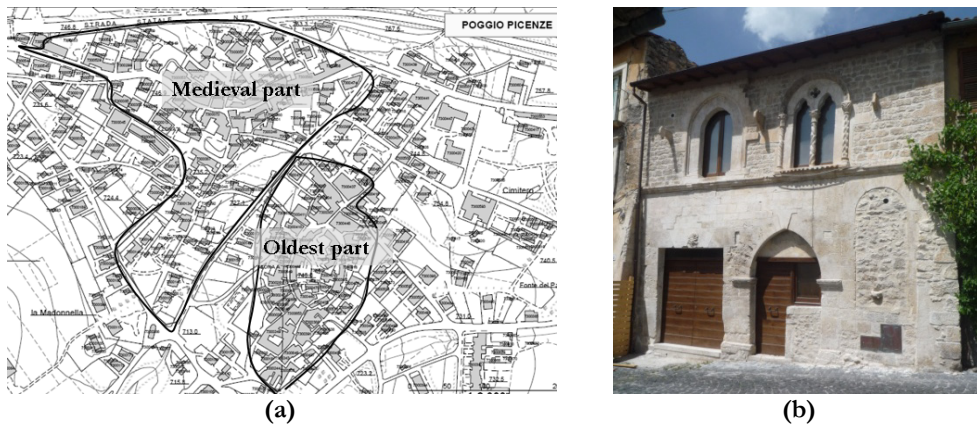


Figure 5.11 Poggio Pienze: (a) plan view; (b) the Medieval House

Nowadays, the historical centre consists of masonry complex, generally ranging from 2 to 3 stories. Sack masonry with chaotic texture inside and bad quality mortar is the typical structure for load-bearing walls, which are, in some cases, connected to each other by metal ties. In general, the first level horizontal structure represents vaulted floors, while the other levels are constituted by either wooden or steel floors. The most common roof typology is the pitched one. Moreover, from the architectural viewpoint, finishing, doorways, balconies, patios and porches are usually embellished with local limestone, the so-called white stone of Poggio Pienze, which has a gentle appearance and is easy to work.

The most important monumental buildings of the town are the three churches, namely San Felice Martire, Visitazione and St. Giuliano. and two palaces, namely Galeota and Ferrari. More information on the history and the most important buildings of Poggio Pienze are reported in (Galeota, 2006).

The historical centre of Poggio Pienze has suffered heavy damages during the earthquake of 2009 (Fig. 5.12).



Figure 5.12 Part of the destroyed centre of Poggio Picenze

Castelnuovo of San Pio is a hamlet of the municipality of San Pio delle Camere. The ancient walled nucleus is situated on the top of a hill, while an irregular urban area following the contours develops on the mountainside. The urban scheme of the town high part is regular and develops according to the so-called *chessboard* or *hippodamian* plan, in which all the streets are orthogonal to each other. The whole rectangular area identified by these streets has dimensions of 70 m x 56 m and is divided into four blocks. Formerly, the entrance of the ancient village was a round arch and, probably, the walled zone was surrounded by a moat (<http://www.castelnuovoonline.com/castelnuovo>).

The most important monuments in Castelnuovo are the St. Giovanni Battista Church built in 1703 on the ruins of another church previously destroyed by the earthquake, and the Sidoni Palace, that represents the study case of this thesis (cfr. section 5.3). The historical centre consisted of 2-3 stories masonry buildings of poor quality.

Also Castelnuovo of San Pio was seriously damaged by the Abruzzo earthquake, which produced several collapses in the historical centre.

It is worth to be noted that a lower damage level has been observed on the buildings at the toe of the hill (Figure 5.13a) as respect to the constructions located on the hilltop (Fig. 5.13b), where is Sidoni Palace. This is due to some factors related to topographic amplification which may have contributed to the strong shaking at the highest elevations of the village (Monaco et al., 2009).



Figure 5.13 The historical centre of Castelnuovo: (a) collapse of old masonry building on the hilltop; (b) limited damage to masonry building at the toe of the hill

5.2.3 The investigated buildings in Poggio Picenze

During the experimental campaign based on environmental vibration measurements in Poggio Picenze, three monumental constructions were investigated: two churches and one palace (Fig. 5.14).

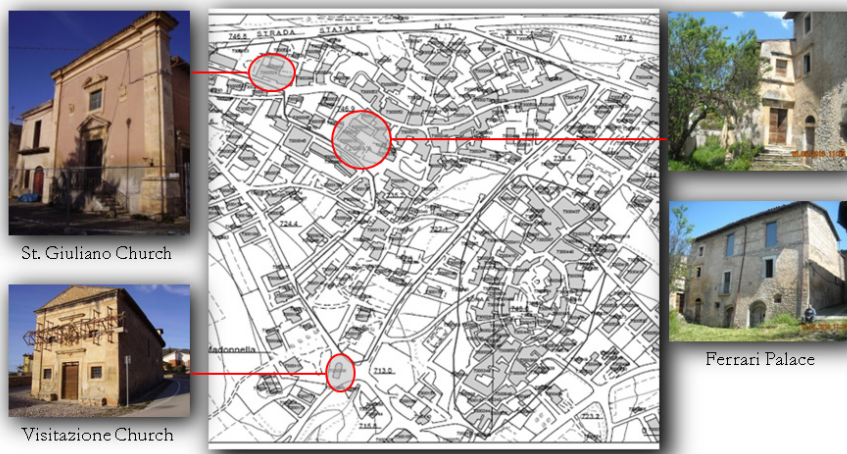


Figure 5.14 Detection of the monumental building investigated in Poggio Picenze

The first structure tested was the Visitazione church (Fig. 5.15a), an isolated building located in the lowest part of the centre of Poggio Picenze. This small parish church was built probably between the 14th and 15th century and it was

enlarged in 1832, as declared also on an internal epigraph. The church has a long central rectangular shape with a 18 m long unique nave. The building is constructed as a local stone masonry structure surmounted by a wooden pitched roof, probably rebuilt after the collapse of the original one. The main façade contains elegant architectural decorations typical of the Romanesque - Aquilano style. Due to the earthquake, the main façade of the church suffered an out of plane overturning mechanism, which is now stopped by an appropriate retaining system.

The second investigated structure was the St. Giuliano church, which was built in the 14th century (Fig 5.15b). This building was originally constructed within a small hospital, whereas presently, time it is within a masonry building complex. The remaining part of the original hospital consists of two rooms: one at the ground floor with vaulted ceilings and the other at the mezzanine floor. The church has a central layout with a unique nave. The main vertical structure is constructed of sack local stone masonry walls surmounted by a wooden pitched roof. This structure is more damaged than the Visitazione church, since its façade suffered a more pronounced out-of-plane collapse mechanism.



(a)



(b)

Figure 5.15 Churches in Poggio Picenze: (a); Visitazione (b) St. Giuliano

The Ferrari palace is a monumental building placed in the post-medieval part of Poggio Picenze. It was originally a small independent district, characterized by the presence of farms built over the years around the central nucleus. In the subsequent years, the original owners sold part of the building complex. Nowadays the palace has an irregular plan shape, due to the several interventions performed over the years. Indeed, the original sack masonry structure was reinforced with stone buttresses, stretches of listed masonry and concrete lintels. In addition, the horizontal structures were reinforced with metal ties at various

levels. These structures suffered some serious damages to masonry walls and vaults due to the earthquake.

The results of the ambient vibration test are presented in the following sections.

5.2.4 Environmental dynamic tests

5.2.4.1. Theoretical basis

The ambient vibration test is a non-destructive test, thus it is a very important test, especially for building having an historical and artistic importance.

The following equipment is used to perform the testing: three seismometers Ranger type (Fig. 5.16) and a Kinematics product (Fig. 5.17a) for the ambient vibration measurements; a Four Channel Signal Conditioner (Fig. 5.17b) for filtering and amplifying the measured signals.

The seismometers measure the vibration signals recorded in different point of the structure. Since the input – output correlation is not a priori noted, a steady point must be fixed as a Reference Point (RP), in order to normalise each measured point as respect the RP amplification and identify the global dynamic response. Afterwards, the amplified and filtered signals from the seismometers is collected by a high-speed data acquisition system (Fig. 5.17c) which transforms the analogue signals into digital. PC and special software for online data processing were used to plot the time histories of the recorded velocities together with the Fourier Amplitude Spectra (FAS) of the response at each measured point.

More precisely, the Fast Fourier Transform (FFT), obtained for each measured point (P) is simultaneously compared with the RP recorded response. This latter is constantly monitored during the vibration test in order to determine a transform function ((H(ω)) which constitutes an intrinsic function of the structure. Thus the following ratio is used to define the transform function:

$$H(\omega) = \frac{FFT_{P_{ij}}(\omega)}{FFT_{RP_j}(\omega)} \quad (5.1)$$

where:

- i is the spatial position of the i -seismometer
- j is the testing direction (X or Y)

Finally, for post-processing and analysis of the recorded vibrations at all the measuring points, ARTeMIS software is used. In this software the natural frequencies and the mode shapes of vibrations can be determined using the Peak Picking technique and the Frequency Domain Decomposition (FDD) technique.

This program has possibilities for very good graphical presentation of the obtained data (Krstevska et al., 2008).



Figure 5.16 (a) Seismometer Ranger type; (b) adjustment of the seismometer

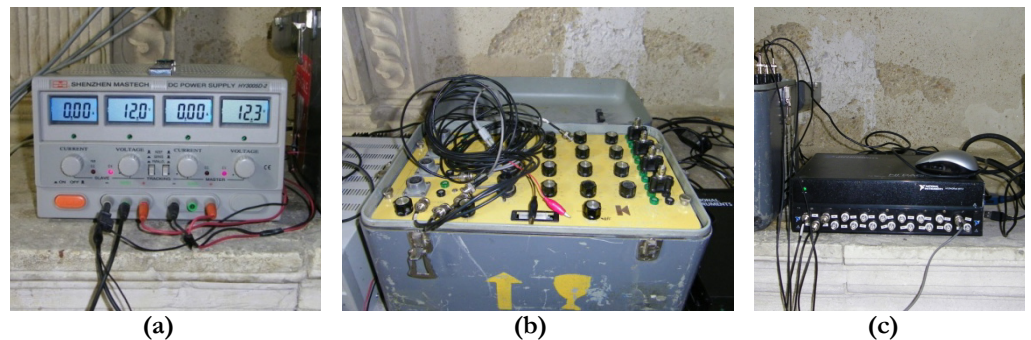


Figure 5.17 Applied equipment for ambient vibration measurements: (a) Kinemetrics product; (b) Four Channel Signal Conditioner; (c) high-speed data acquisition system

5.2.4.2. *Experimental results*

The buildings in Poggio Picenze have been tested by ambient vibration method, measuring the vibrations in selected internal and external (along the façades) points of the structure and then processing the recorded signals to obtain the dynamic characteristics.

All the measurements were performed in transversal and longitudinal direction of the monuments, enabling the obtaining of the frequencies and mode shapes in both orthogonal directions and torsion (Krstevska et al., 2010).

The results of the dynamic identification test are described in the following.

1. *Visitazione Church*. The measured points are presented on the generated geometry of the monument by ARTeMIS testor (Fig. 5.18a). Several frequencies are dominating on the obtained spectrum, as shown in Figure 18b and specified in Table 5.2.

The mode shapes of vibration are presented for the frequency of transversal vibrations, $f=3.51\text{Hz}$, for the frequency in torsion $f=5.08\text{Hz}$ as well as for the frequency of longitudinal vibration $f=7.32\text{Hz}$ (Fig. 5.19).

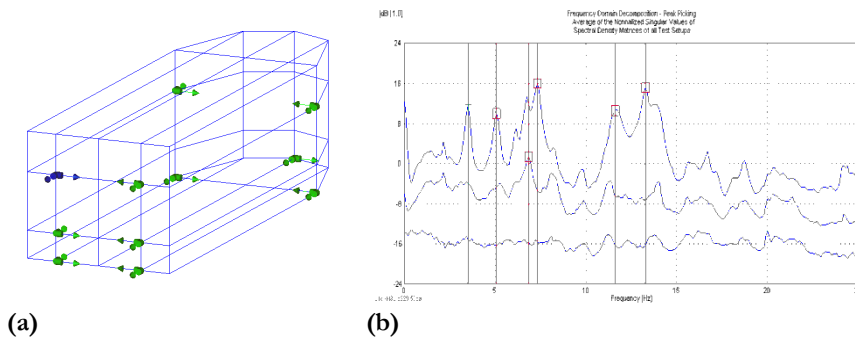


Figure 5.18 *Visitazione Church*: (a) Test set-up (the RP is highlighted in blue); (b) Peak-picking of the dominant frequencies

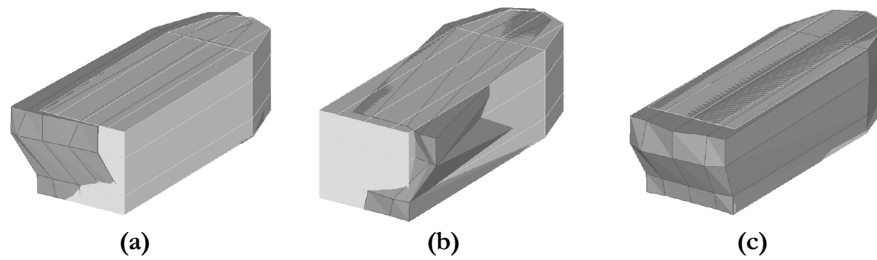


Figure 5.19 Mode shapes of vibration: (a) transverse, $f = 3.51\text{ Hz}$; (b) rotational, $f = 5.08$; (c) longitudinal, $f=7.32\text{Hz}$

Table 5.2 Dominant frequencies and damping coefficients

Dominant frequency (Hz)	Damping coeff. (%)
3.52	3.3
5.08	2.6
6.84	2.4
7.32	1.5
11.62	-
13.28	-

2. *St Giuliano Church*. The points of measurement on this monument are presented on the generated geometry (Fig. 5.20a). The dominating frequencies in the obtained spectrum are presented in Fig. 5.20b and Table 5.3, along with the corresponding damping coefficients.

The mode shapes of vibration are presented in Figures 5.21a and 5.21b for frequencies of 5.37Hz and 6.64Hz under which the structure is vibrating in longitudinal direction, with dominant separation of the façade wall, and frequency of 7.03Hz in which the torsional effect is noticeable as a result of the influence of the neighbouring connected structures (Fig. 5.21c), which prevent free transversal vibration of the monument.

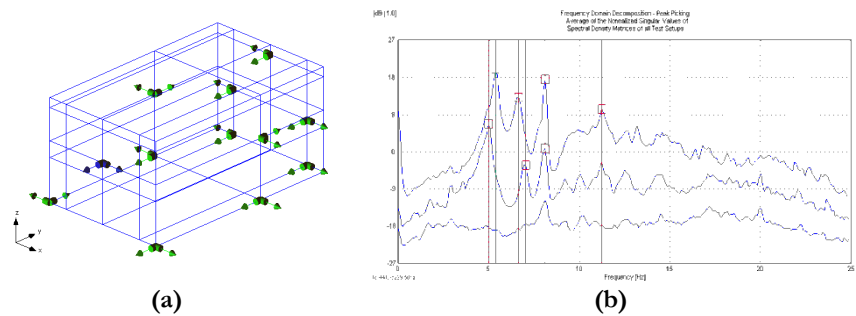


Figure 5.20 St. Giuliano Church: (a) Test set-up (the RP is highlighted in blue); (b) Peak-picking of the dominant frequencies

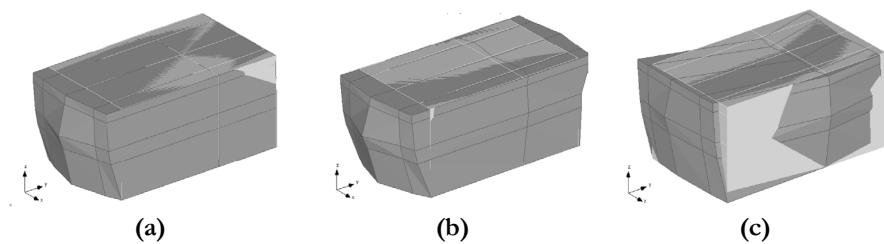


Figure 5.21 Mode shapes of vibration: (a) longitudinal $f=5.37$ Hz; (b) longitudinal $f=6.64$ Hz; (c) rotational, $f=7.03$ Hz

Table 5.3 Dominant frequencies and damping coefficients

Dominant frequency (Hz)	Damping coeff. (%)
4.98	1.4
5.37	2.2
6.64	2.2
7.03	1.9

1. *Ferrari Palace*. The generated geometry of the measured part of this palace and the test set-up are presented in Figure 5.22a. The dominating frequencies are presented in Figure 5.22b and in Table 5.4, together with the corresponding damping coefficients.

The first two mode shapes of vibration are presented in Figure 5.23. They are indicating non-uniform and complex vibration, which is the result of the heavy damage state and the extreme irregularity of the building.

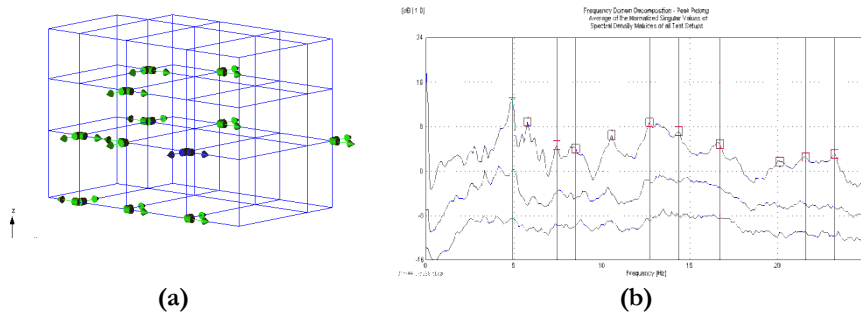


Figure 5.22 Ferrari Palace: (a) Test set-up (the RP is highlighted in blue); (b) Peak-picking of the dominant frequencies

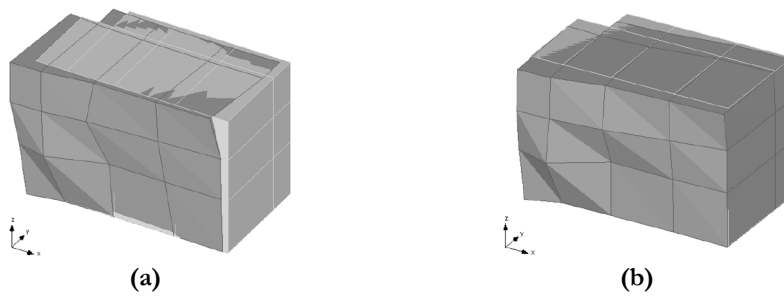


Figure 5.23 Mode shapes of vibration: (a) longitudinal; (b) transverse; (c) rotational

Table 5.4 Dominant frequencies and damping coefficients

Dominant frequency (Hz)	Damping coeff. (%)
4.88	2.8
5.76	2.5
7.42	1.6
8.50	1.4
10.55	1.8

5.3. THE STUDY CASE: PALAZZO SIDONI IN CASTELNUOVO

5.3.1 Historical news and structural features

The Sidoni palace (Fig. 5.24b) is a monumental building in the old medieval nucleus of Castelnuovo. It is an isolated building, having a regular and symmetric plan shape (Fig. 5.25). The façade is also symmetric, and is characterized by regular openings and several architectural ornaments (Fig. 5.26). The entrance is constituted by an arch located in the central part of the façade. The building represents a sack stone masonry two storey structure surmounted by a wooden pitched roof covered by clay tiles, that was rebuilt after the demolition of the original vaulted one. The first floor is developed on a rectangular surface of about 366 m². The first level floors are composed of tunnel vaults, while the second level horizontal structure is realised with steel floors.

The building also presents a basement, as it may be noted from the section in Figure 5.27. Furthermore, the first floor level is partially a basement floor.

No damage was recorded in the building facade as shown in Figure 5.24b, whereas significant damages and collapse of the masonry vault, took place inside (Fig. 5.29). Furthermore, part of the steel floors was destroyed by the quake, as shows the view in Figure 5.29.



Figure 5.24 Palazzo Sidoni: (a) before earthquake (b) after earthquake

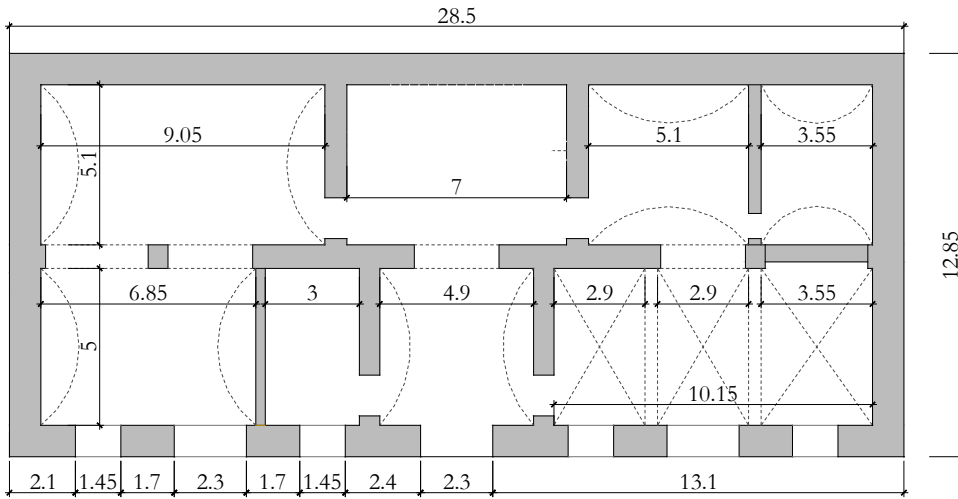


Figure 5.25 Palazzo Sidoni: plan view

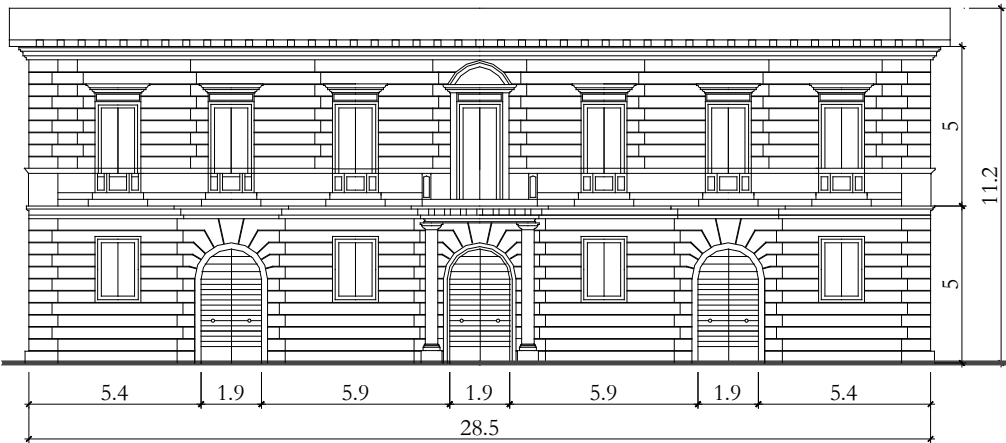


Figure 5.26 Palazzo Sidoni: front view

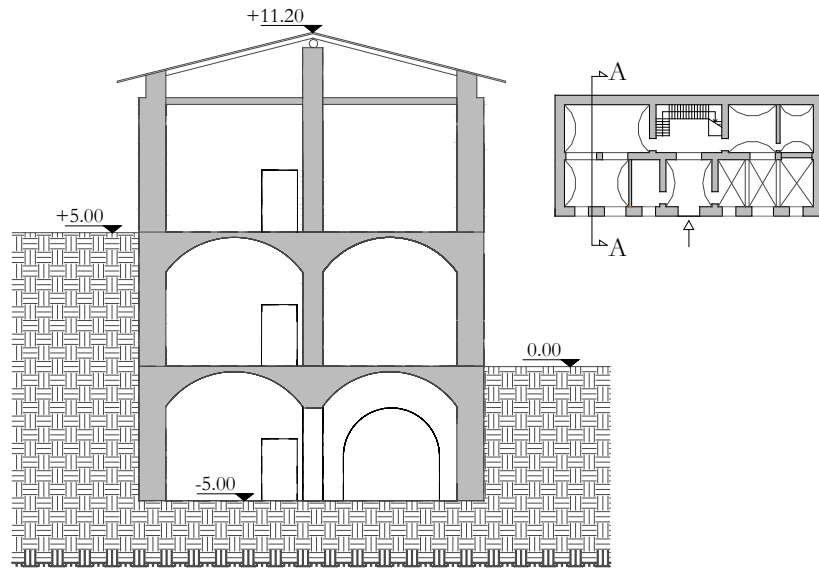


Figure 5.27 Section AA



(a)



(b)



(c)



(d)

Figure 5.28 Main damages: (a) and (b) vaults; (c) debris and (d) remaining part of the collapsed vault over the stairs

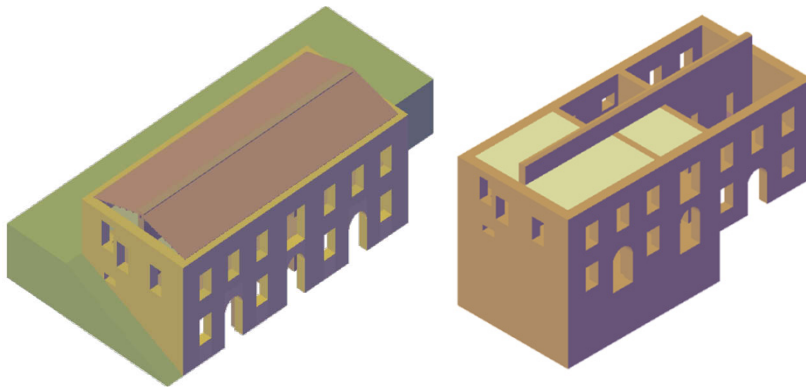


Figure 5.29 3D views of Palazzo Sidoni

5.3.2 Experimental tests on masonry

The study building has been subjected to double flat jack test (Fig. 5.30) after the earthquake in order to determine the mechanical properties of masonry.

In general, this type of test is used to measure the state of stress of masonry, to estimate the local value of the compression and also to determine the deformability characteristics. Even if this test was firstly set up for brick-masonries, it has now been developed also for stone-masonries made with irregular stones, like the investigated material.

A flat jack test is articulated in the following steps:

1. Two reference points are marked on the wall and their initial distance is measured;
2. A cut perpendicular to the wall surface is made in order to produce a stress relaxation; in particular, the stress release is caused by a partial closing of the cutting. Thus the distance between the reference points is measured again, it resulting lower than the initial one.
3. A thin flat-jack is placed inside the achieved slot.
4. The initial distance between the reference points is restored by gradually increasing the pressure of the flat jack.

During the test, the following equilibrium equation must be satisfied:

$$\sigma_f = K_j \cdot K_a \cdot P_f \quad (5.2)$$

in which:

- σ_f is the calculated stress value;
- K_j is the jack constant calibrated in laboratory;

- K_a expresses the ratio between the jack surface (A_j) and the cutting surface (A_c);
- P_f is the flat jack pressure.

Subsequently, in order to determine the deformability characteristics of masonry, a second cut parallel to the previous one is made and a second jack is inserted in the new slot. Generally, the second jack is made at a distance of about 40 to 50cm from the other one, so that a masonry sample of appreciable size is considered. Later on, an uniaxial compression stress is applied to the sample of masonry. In each phase of the test, the vertical and lateral displacements are measured by a removable strain gauge.

Numerous loading cycles are carried out, they characterizing by a gradual increment of the stress level in order to establish the deformability parameters of masonry in loading and unloading condition.



(a)



(b)

Figure 5.30 (a) Flat jack test; (b) present state

The experimental in-situ test performed on the study case masonry has provided the stress-strain laws shown in Figure 5.31. The parameters characterizing the test are listed in Table 5.5.

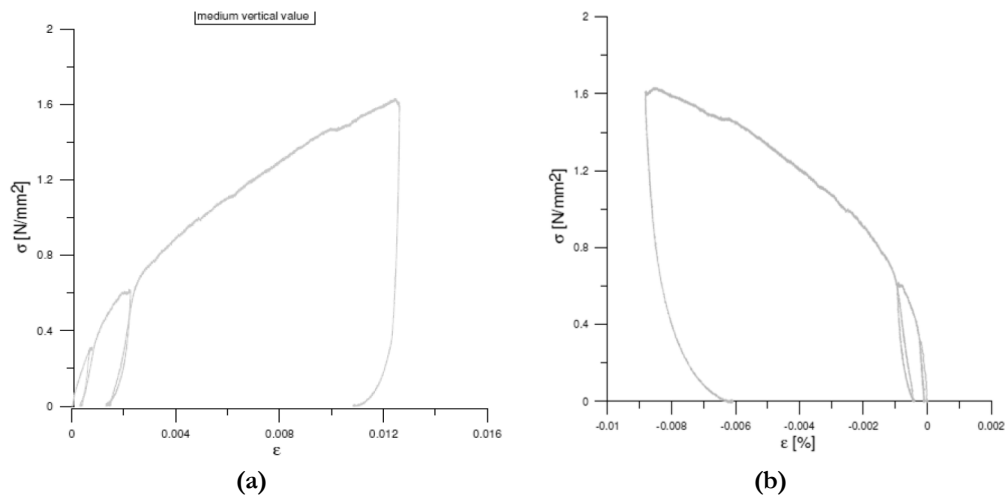


Figure 5.31 Stress-strain law: (a) mean vertical deformations; (b) horizontal deformations

Table 5.5 Double flat jack test: parameters

Parameter	Value
A_C , Cutting area [cm ²]	882
A_J , Flat jack area [cm ²]	778
Jacks distance [cm]	30
K_m	0.78
K_a [A_J/A_C]	0.88

The test shows the very low compressive strength of masonry ($f_k=1.6$ MPa), that may be identified as a type 1 masonry according to the OPCM 3431 (2005).

5.3.3 Dynamic identification tests

In the section, the results of the ambient vibration test on Sidoni Palace are reported, similarly to the monuments in Poggio Pienze (cfr. section 5.2.4.2).

The measured points on the Sidoni palace are presented in the geometry of the monument generated by the ARTeMIS testor (Fig. 5.33a) (Krstevska et al., 2010). The RP was placed at a height of 10m in the left part of the palace, as depicted in Figure 5.32.

Several frequencies dominate on the obtained spectrum, as given in Fig. 5.33b and specified in Table 5.6.

The frequency in transversal direction is 5.08Hz, while longitudinal vibration is expressed at frequency of 5.27Hz, as presented on the mode shapes in Fig. 5.34.



Figure 5.32 Sidoni Palace: (a) seismometer; (b) detection of the RP;

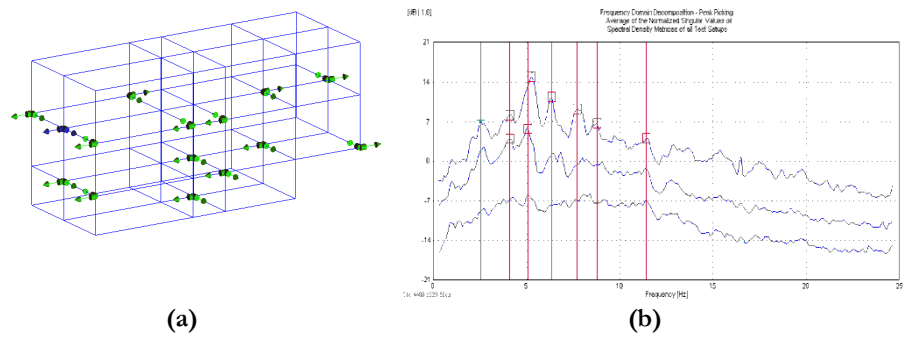


Figure 5.33 Sidoni Palace: (a) test set-up (the RP is highlighted in blue);
(b) peak-picking of the dominant frequencies

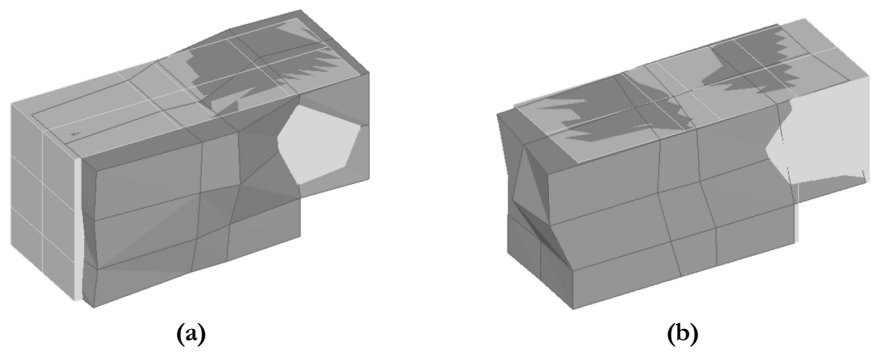


Figure 5.34 Mode shapes of vibration: (a) transverse, $f = 5.08\text{Hz}$;
(b) longitudinal, $f=5.27\text{Hz}$

Table 5.6 Dominant frequencies and damping coefficients

Dominant frequency (Hz)	Damping coeff. (%)
2.54	5.8
4.10	3.3
5.08	4.8
5.27	4.8
6.35	3.8
7.7	2.3
8.8	1.4

5.3.4 Numerical activity

5.3.4.1. Calibration of the experimental results

The dynamic response of Sidoni Palace has been subsequently investigated by means of numerical frequency analysis. The FE (Finite Element, cfr. chapter 2) model has been implemented in the computer code ABAQUS.

In particular, this model has been generated by importing in the FE program a three-dimensional solid model of the structure created in a computer aided design system (AutoCad 2010).

In order to properly assess the structural interaction among the different constituent parts, the geometrical model accurately reproduces all the main components of the building, including the openings, the vaults and the horizontal floors.

It is worth to precise that the collapsed floors have not been included in the model, in order to take into account the present damage state of the building.

Therefore, the whole masonry structure has been discretized by means of tetrahedral 3D solid elements, namely C3D4 (4-node linear tetrahedron) elements (HKS, 2004).

As far as the material modelling is concerned, a continuum homogeneous material has assumed since the analysis is aimed at the structural global response identification.

Since frequency analysis is purely a linear perturbation type, it required only linear elastic properties of the elements.

The density has been established by referring to the OPCM 3431 (2005) classification, while the elastic modulus (E) have been opportunely calibrated on the basis of the ambient vibration tests. In fact, even if the Young modulus (E) may be defined by means of the Hook's relationship applicable to the stress-strain law provided by the flat jack test (cfr. section 5.3.2), the elastic phase may not clearly recognised in the diagram. Therefore, dealing with the indications

provided in literature, a Young modulus ranging between $500 \cdot f_k$ and $1000 \cdot f_k$, where f_k is the compressive strength of masonry, has been considered for the calibration of the model, as follows:

$$800 \leq E \leq 1600 \quad (5.3)$$

So, several analyses have been achieved in order to find the frequencies and the mode shapes that better approximated the experimental ones.

Thus the most significant results are shown in Table 5.7, in which it is noted that the best results is achieved for E equal to 1200 MPa; such value is not between the range provided by the OPCM ($600 \leq E \leq 1050$) for the considered type of masonry.

Table 5.7 Dominant frequencies corresponding to different value of E

	Transverse f [Hz]	Longitudinal f [Hz]
E = 800 MPa	4.33	5.10
E = 1000 MPa	4.80	5.07
E = 1200MPa	5.26	5.30
E = 1300MPa	5.47	5.52
E = 1600MPa	6.07	6.12

The elastic mechanical properties adopted in the material modelling are reported in Table 5.8.

Table 5.8 Parameter used in the adopted numerical model

Properties	Masonry
Density [kg]	1900
Yung Modulus (E) [MPa]	1200
Poisson Coefficient	0.25

Later on a mesh sensitivity analysis has been carried out in order to refine the obtained results.

In macro model approaches, the mesh is usually generated in such a way that each element contains at least a portion of horizontal as well as vertical mortar joint surrounding the masonry unit. However, in the examined case it is not possible to distinctly identify the mortar joints, since it is a chaotic masonry.

Thus, in the calibration of the elastic modulus a trial mesh size 0.4m has been used, adopting the criterion that each element contains at least two stones or little more than two stones along the length.

Three mesh type has been analysed:

- Coarse Mesh: 0.50 m
- Medium Mesh: 0.40m

- Fine Mesh: 0.30m

Therefore, a frequency analysis has been performed for all the three defined meshes individually and natural frequencies have been found for the first 10 modes of vibration.

Conclusively, the mesh refined type has shown the results that better approximate the experimental ones (Table 5.9).

Table 5.9 Dominant frequencies corresponding to different value of t

	Transverse f [Hz]	Longitudinal f [Hz]
0.30m	5.06	5.17
0.40m	5.26	5.30
0.50m	5.36	5.42

Finally as far as the boundary condition are concerned, full restraints were assumed at the base of the structure in the performed analysis.

The fundamental modal shapes are depicted in the Figures 5.35, 5.36 and 5.37.

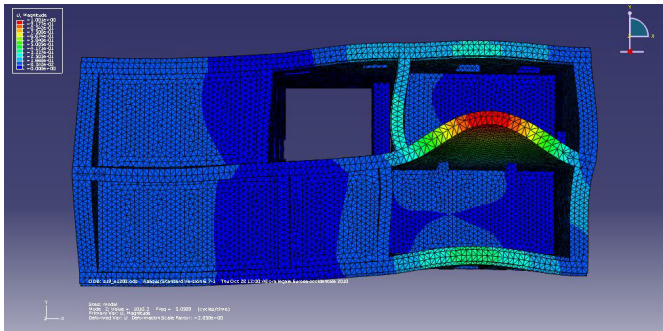


Figure 5.35 Transversal vibration mode of the damaged model: $f = 5.06$ Hz;

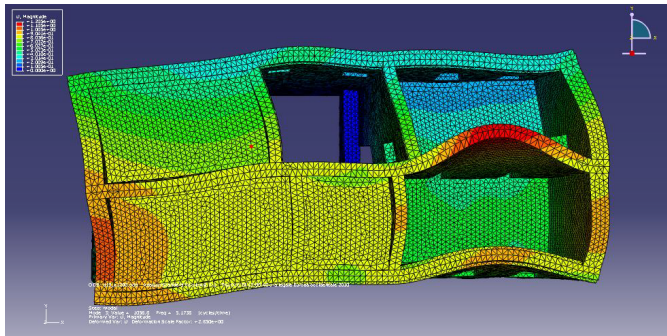


Figure 5.36 Longitudinal vibration mode of the damaged model: $f = 5.17$ Hz;

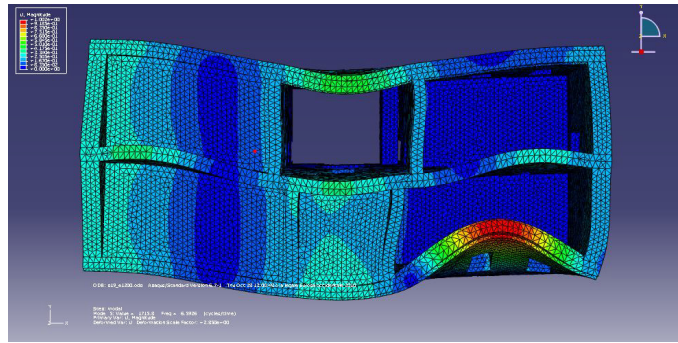


Figure 5.37 Torsional vibration mode of the damaged model corresponding to $f = 6.59$ Hz

From the previous figures, it may be pointed out that the most deformable part is that one in which the floors are collapsed, also according to the experimental results.

5.3.4.2. *Modal behaviour of the undamaged building*

The frequency analysis has been also performed on the model representative of the structural configuration of Sidoni Palace before the seismic event of the 6th April.

The essential difference between the damaged and the undamaged numerical model is the presence of the floors collapsed for the effect of the seismic action. The global modal shapes of vibration in Figure 5.38. In particular, it may be noticed that the global mode shapes are clearly defined in each directions in the undamaged configuration. Furthermore, in this case the third vibration mode is the rotational one, while the transverse mode (cfr. Fig. 5.35) due to the lack of the floors is missed.

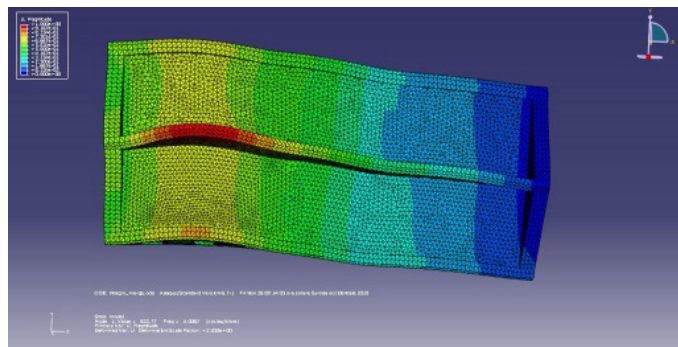


Figure 5.38 Transversal vibration mode of the undamaged model: $f = 4.00$ Hz;

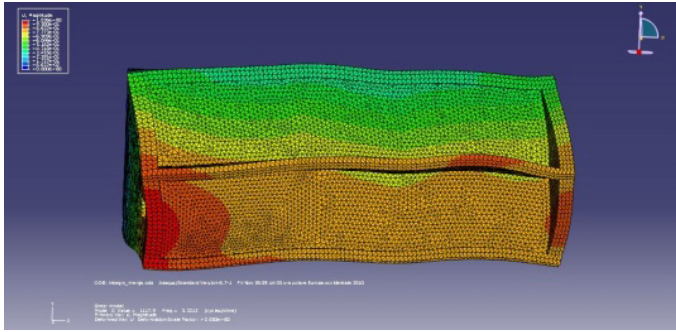


Figure 5.39 Longitudinal vibration mode of the undamaged model: $f = 5.32$ Hz;

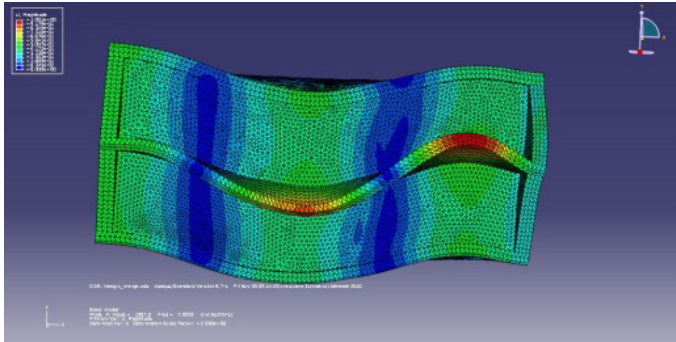


Figure 5.40 Torsional vibration mode of the undamaged model: $f = 7.09$ Hz;

A difference of stiffness may be estimated between the two examined configuration (Table 5.10). In particular, the stiffness of the damaged model averagely decreases of the 4% as respect the configuration before earthquake.

Table 5.10 Comparison among frequencies

Damaged model f [Hz]	Undamaged model f [Hz]	Stiffness decrease [%]
3.92	4.00	2
5.17	5.32	3
6.59	7.09	7

5.3.5 Interpretation and comparison of results

Presented in Table 5.11 are the values of the natural frequencies obtained numerically comparatively to the experimental ones. It can be seen that there is a satisfactory agreement between the vibration modes as well as the respective

values of the natural frequencies obtained for the Sidoni Palace by different ways: experimentally and numerically.

Table 5.11 Comparison among experimental and numerical frequencies

Experimental frequency [Hz]	Numerical frequency [Hz]
4.10	3.92
5.08	5.06
5.27	5.17
6.35	6.59
7.70	7.21

Finally, after the identification of the dynamic properties of the structures measured by means of the experimental in-situ testing and successively confirmed by the numerical analysis, the damage evolution curve of Sidoni Palace has been developed. As the numerical model have shown, the reduction of the natural frequencies is related to the stiffness variation and, consequently, to the evolution of the damage. Therefore, a simplified damage indicator ($d_{k,i}$) based on the variation of the natural frequencies due to the damage level may be obtained as follows (Mendes et al., 2010):

$$d_{ki} = 1 - \left(\frac{f_{k,i}}{f_{k,0}} \right)^2 \quad (5.4)$$

where:

- $f_{k,i}$ is the natural frequency of the mode shape k after the earthquake
- $f_{k,0}$ is the natural frequency of the mode shape k before the earthquake

The damage evolution curve has been drawn by means of the graphic relationship between the number of modes ($f_{k,i}$, abscissa) and the simplified damage indicator ($d_{k,i}$, ordinate) according to the value in Table 5.12; the final curve is shown in Figure 5.40.

Table 5.12 Dominant frequencies

	f_{k0} [Hz]	f_{ki} [Hz]	d_{ki}
Longitudinal (X)	5.17	5.32	0.055596
	6.59	9.08	0.528853
	8.26	9.2	0.722761
	8.79	9.66	0.894774
Transverse (X)	3.92	4	0
	5.06	5.54	0.0396
	5.85	7.09	0.205378
	7.21	7.76	0.524579
	8.07	8.64	0,661308

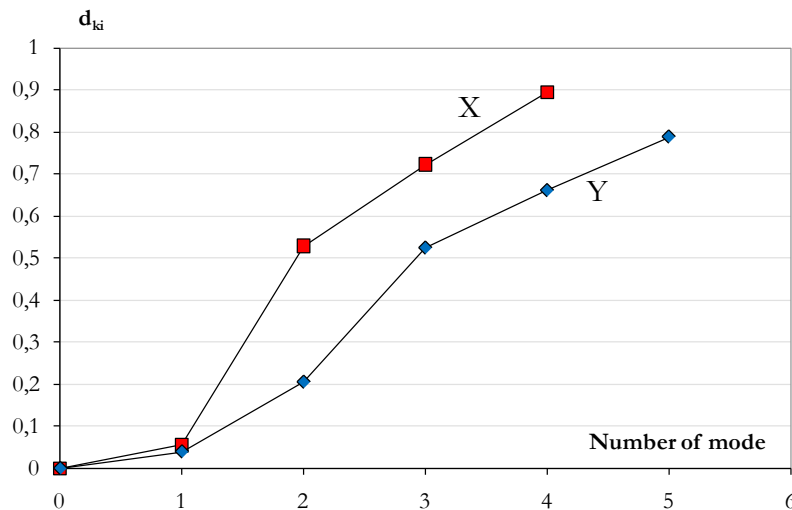


Figure 5.41 Damage evolution curve of Sidoni Palace

From the curves illustrated in Figure 5.41, it is apparent that:

- the damage is greater in longitudinal direction (X);
- the major damage occurs between 1st and 2nd vibration modes in direction (X) and between 2nd and 3rd ones in direction (Y);
- after these damages, the increase of the damage indicator (d_{ki}) is almost constant in both directions.

5.3.6 Retrofitting interventions

The recent seismic event has evidenced the high structural vulnerability of Sidoni Palace, mostly due to low effectiveness of both walls and floor-to-wall connections. Thus on the basis of the achieved study, retrofitting measures is herein proposed for the restoration of the examined monumental Palace.

At first, the rebuilding of the collapsed floors and the replacement of the existing ones with RC floors. In fact, RC floors behave as rigid diaphragms, assuring an adequate distribution of the seismic forces to all the bearing walls. These floors have to be well connected to the walls by means of the arrangement of stringcourses.

Second, the repair of the damaged vaults and the placements of metal ties. The use of metal ties, indeed, represents an ancient and widespread intervention technique used to eliminate the horizontal thrust of arches, vaults and roofs. This system is an effective and reliable technique to obtain a better connection between structural elements at the floor level, ensuring a box-type behaviour of

the entire structure. Moreover, this technique allows to avoid all the out-of-plane overturning mechanisms of masonry walls.

The tie-bars intervention technique herein proposed consists of the insertion of metal profiles in the wall along the vault length in both the two orthogonal directions.

Furthermore, other possible interventions may be: the replacement of fractured brackets; relocation of the fallen stones and joints filling; the consolidation of the wooden roof by means the arrangements of perimetrical stringcourses.

Taking into account all the aforesaid intervention, a retrofitted model has been implemented in ABAQUS. In particular, the constraints condition among the new RC floors and the walls have been improved in order to consider the presence of the stringcourses. Moreover, beam elements have been inserted in the wall in order to model the metal ties.

Afterwards, a frequency analysis has been achieved on this retrofitted model, providing the results shown in Figure 5.41 and in Table 5.13.

The results have shown an increase of stiffness of 6%, especially in the first floor. The modal shape are clearly defined and the local modes coincide with the superior ones.

Definitively, the behaviour of the structure is totally improved.

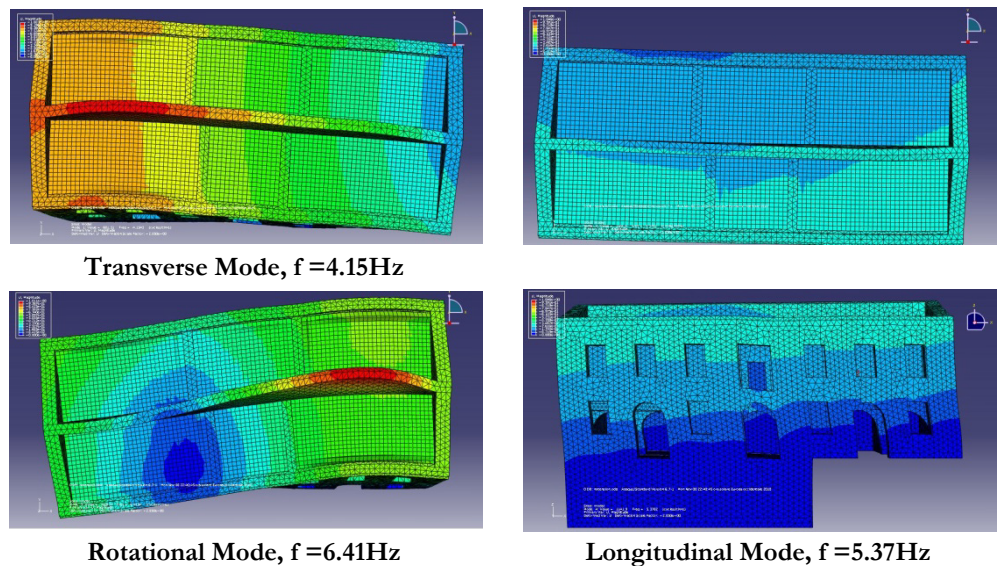


Figure 5.42 Modes shape of vibrations of the retrofitted building

Table 5.13 Dominant frequencies and damping coefficients

Damaged f [Hz]	Retrofitted f [Hz]	Stiffness decrease [%]
3.92	4.15	6
5.06	-	-
5.17	5.37	6
-	6.41	-
6.59	9.21	-

5.3.1 Vulnerability curves

The achieved analyses enable to plot the vulnerability curves of Sidoni Palace for each of the three structural configuration examined (undamaged, damaged and retrofitted), by means of the following relationship:

$$d^*_{ki} = \frac{1}{\left(\frac{f_{k0}}{f_1}\right)^2 - 1} + d^*_{ki-1} \quad (5.5)$$

where:

- f_k is the natural frequency of the k-mode;
- f_1 is the natural frequency of the first mode;
- d^*_{ki} is the damage indicator of the (k-1) mode.

In the Figures 5.43 and 5.44 the damage index of the building into the considered conditions has been plotted as a function of the mode number according to both the longitudinal (X) and transverse (Y) directions.

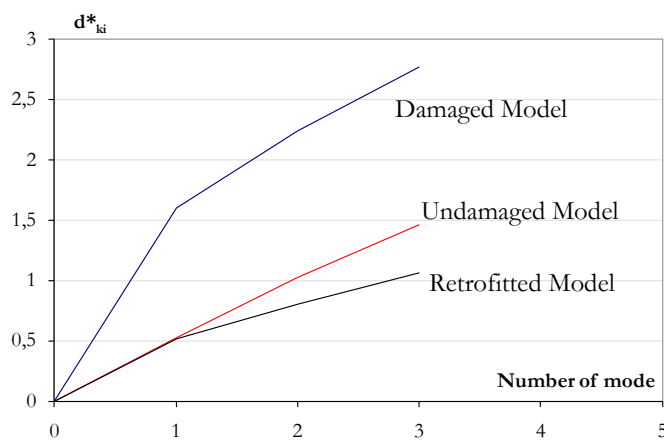


Figure 5.43 Vulnerability curve of Sidoni Palace according to (X) direction

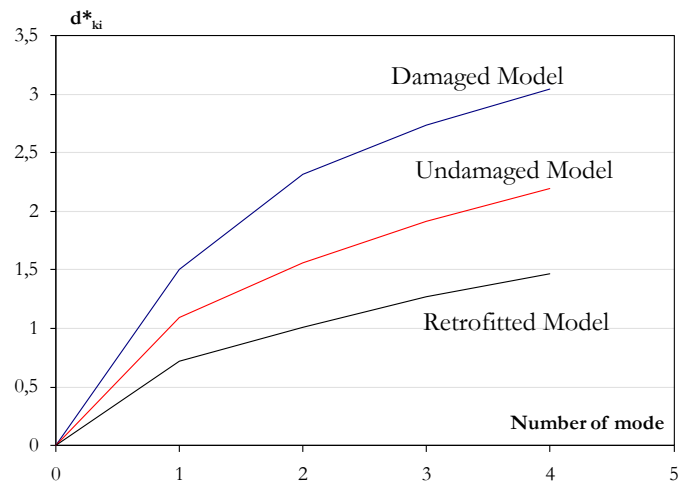


Figure 5.44 Vulnerability curve of Sidoni Palace according to (Y) direction

In transverse direction, the achieved curves have shown that:

- the damaged building and the retrofitted one suffers major and minor damages, respectively;
- the undamaged building shows damages of intermediate level as respect to the others;
- in all cases, the major damage occurs in the first mode;
- in all cases, damage is reduced as number of mode increases;
- the reduction of the d^* factor with mode number is less evident as the structural behaviour improve.

Also in direction X the d^*_{ki} factor is more large for the building damaged from the quake. Moreover, the damage suffered by undamaged and retrofitted buildings is similar in the first mode. It is noteworthy that the efficiency of retrofitting interventions is detected starting from the 2nd vibration mode.

Finally, as in direction Y, in all cases, damage is reduced as number of mode increases.

5.4. CONCLUSIVE REMARKS

L'Aquila earthquake has represented a significant catastrophic event which has profoundly affected Italy. It has been an exceptional action and, for this reason, it has been elected as a pilot study case in the framework of this thesis.

Therefore, the presented study was aimed at the investigation of the seismic behaviour of a damaged monumental building in Castelnuovo, namely Sidoni Palace, gravely hit by the quake.

The dynamic characteristics of the study building have been obtained by ambient vibration testing method in frequency range up to 30 Hz in two directions: transversal and longitudinal ones. So, the natural frequencies of the structure as well as the shapes of vibration have been clearly expressed by the tests.

Afterwards, a numerical model in ABAQUS environment has been implemented. To this purpose, the elastic parameters of masonry material have been adequately calibrated on the basis of the experimental frequencies. The comparison between the natural frequency values and the mode shapes of vibration to the ones obtained by numerical analysis has shown good agreement. Thus, in this phase the experimental tests have been fundamental for the study of the damaged model.

Frequency analysis has also carried out considering an undamaged model, characterized by the original structural configuration. This investigation has permitted to evaluate the difference of the structural performance between the two models. Furthermore, the frequencies related to damage model have allowed to calculate the vulnerability curve of the structure.

Finally, frequency analysis has been also performed on a proposed retrofitted model. The output of the analysis represents a further demonstration on the effectiveness of metal ties strengthening system.

Conclusive remarks

The current Ph.D. thesis presents the study of the behaviour of ancient masonry building subjected to exceptional loading conditions, which has been performed by means of both numerical analyses and experimental in-situ tests.

The vulnerability of masonry blocks and isolated monumental buildings have been examined with the main objective of analysing their vulnerability under extreme events.

In case of building aggregates, a simple and reliable vulnerability assessment form, based on refined numerical analysis, has been calibrated and validated relatively to two towns (Sessa Aurunca and Torre del Greco) of the Campania Region. The application of the validated quick procedure has shown the high damage level which should be experienced by historical centre aggregates under the earthquakes foreseen by the new Italian code. However, even if the quick vulnerability assessment form for masonry blocks has provided important results, the implemented analysis procedure must be also applied to other territorial zones having a seismicity level different from that of the Campania Region in order to further certify its efficiency. To this purpose, the form is going to be applied to some historical centres of the Abruzzo region damaged by the L'Aquila earthquake in order to compare the predicted damages with the real ones.

On the other hand, in case of monumental buildings, the structural performance of two palaces has been investigated.

In the first case, the vulnerability of a historical palace in the Vesuvius area has been assessed. This study consists of two types of analysis, namely seismic and volcanic. So, in the first phase, the seismic vulnerability has been estimated by means of the application of both refined methodological approaches and

simplified ones, in order to both evaluate the building vulnerability and test the effective reliability of the latter procedures.

First of all, the building vulnerability has been estimated with reference to a refined method based on a mechanical approach. To this purpose, the implementation of a numerical model of the palace by using two distinct computer codes, that is AeDes, specific for masonry structures, and SAP 2000, both based on the equivalent frame modelling approach, has been done. Later on, pushover analyses in longitudinal and transverse directions have been achieved by considering the two force distributions given by the Italian code.

A comparison among the capacity curves developed by the two programs has shown the coherence of the structural response both in terms of stiffness and ductility. Instead, in terms of resistance, the SAP 2000 code underestimates the building strength, it providing therefore results on the safe side with respect to the Aedes ones, whose use should be more advisable for masonry structures.

Then, the Capacity Spectrum Method has been applied in order to detect the performance points and, consequently, the vulnerability indexes of the palace. The application of this mechanical procedure, which represents the most reliable approach to study the global behaviour of masonry buildings, has revealed the high vulnerability of the examined construction. Subsequently, several simple vulnerability assessment methodologies, namely the Benedetti and Petrini's form (1987), the SAVE procedure (Dolce and Moroni, 2005), the Italian Guidelines approach (2005) and the Simplified Mechanical Model for building typologies (Cattari et al., 2004), have been applied to the study case. All these procedures have provided both the vulnerability indicator, expressed by an index, and the shear strength of the structure. As in the previous case, the results achieved through the application of the aforesaid simplified techniques, has confirmed the high vulnerability of the building. In addition, among the used simplified assessment procedures, all of them providing a rather good forecast of the structural response, the indications of the Italian Guidelines approach and the SAVE in terms of strength and of the Simplified mechanical Model in terms of stiffness seem to be the most reliable.

Afterwards, the building vulnerability due to the Vesuvius risk has been evaluated. In particular, two loading conditions have been considered as representative of the volcanic effects: tephra and ground motion. The analyses under tephra loads have shown that the collapse occurs for a temperature of 100°C, when the material density is larger than 1600 kg·m⁻³, and for a temperature of 200°C, when the material density is larger than 800 °C. Instead, the seismic analysis has shown that the building should suffer heavy damages in the weakest direction (Y), which coincides with the transverse one, under a

volcanic ground motion, but no damages should occur in the longitudinal one. All the achieved results have proved the inefficiency of the building to withstand seismic and volcanic actions, so to program future retrofitting interventions in a next study activity.

In the second case, the vulnerability of a monumental building under L'Aquila exceptional earthquake has been examined under experimental and numerical way. Environment vibration tests have provided the fundamental vibration modes of the building, which have been numerically calibrated by means of the ABAQUS non linear numerical code.

Frequency analysis has been carried out also considering an undamaged model of the palace, which represented its structural configuration before the earthquake.

This investigation has allowed to quantify the decrease of the structural performance of the building after the seismic event. In other words, it has been possible to estimate the reduction in stiffness of the palace after the seismic event by comparing, for each vibration mode, the corresponding frequency in the two examined models. Such a comparison has allowed to calculate the structural damage indicator and, therefore, to plot the vulnerability curve of the building. Finally, some retrofitting interventions have been set up, their effectiveness to improve the building seismic behaviour being proved by numerical analyses. The output of this analysis phase represents a clear demonstration of the usefulness of metal ties as simple and very reliable retrofitting system of existing masonry buildings.

In conclusion, all the above results allow to recognize the extreme vulnerability of monumental masonry buildings under exceptional actions. Nevertheless, different analysis methods can be usefully applied for estimating their vulnerability before catastrophic events. Firstly, the available simplified assessment procedures are a good tools both to individuate the cases most at risk within a group of buildings and to estimate in a rather good way the global structural response. At last, refined numerical analysis methods are efficient instruments to evaluate exactly the building performance and to implement correctly seismic retrofitting measures under both ordinary and extreme events.

References

- AA. VV. (2009). Learning from Earthquakes - The M_w 6.3 Abruzzo, Italy, Earthquake of April 6, 2009. *EERI Special Earthquake Report*, June.
- AeDes Software (2009), PCM – PCE User Manual. San Miniato (PI)
- Anderson D., Brzev D. (2009). Seismic Design Guide for Masonry Buildings. Canadian Concrete Masonry Producers Association, Toronto.
- Applied Technology Council (ATC) - 40, (1996). Seismic evaluation and retrofit of concrete buildings. Vol.1, Report No. SSC 96-01.
- Augenti N., (2004). Il calcolo sismico degli edifici in muratura, UTET, Torino.
- Benedetti D., Petrini V. (1984). On the seismic vulnerability of masonry buildings: an evaluation method (in Italian), *L'Industria delle Costruzioni*, 149: 66-74.
- Beolchini G. C., Milano L., Antonacci E. (cured by) (2005). Repertorio dei meccanismi di danno, delle tecniche di intervento e dei relativi costi negli edifici in muratura - Definizione di Modelli per l'analisi Strutturale degli Edifici in Muratura (in Italian). Vol. II – Part I. Research Convention with Marche Region; National Research Council – Institute for Constructions Technology, DISAT, University of L'Aquila, L'Aquila.

- Bernardini A. (a cura di) (2000). *La Vulnerabilità Degli Edifici: Valutazione a Scala Nazionale Della Vulnerabilità Sismica Degli Edifici Ordinari*. Research Report, CNR-GNDT, Rome, Italy (in Italian).
- Bernardini A., Gori R., Moden C. (1990). *Application of Coupled Analytical Models and Experimental Knowledge to Seismic Vulnerability Analyses of Masonry Buildings*. Engineering Damage Evaluation and Vulnerability Analysis of Building Structures (edited by A. Koridze), Omega Scientific, Oxon, U.K.
- Bertini T, Farroni A, Totani G (1992). *Idrogeologia della conca aquilana*. University of L'Aquila, Dipartimento Ingegneria Strutture Acque e Terreno, Publ. DISAT 92/6 (in Italian).
- Binda L., Saisi A. (2005). Research on historic structures in seismic areas in Italy. *Prog. Struct. Engng Mater.*, 7: 71-85.
- Braga F., Dolce M., Liberatore D. (1982). A statistical study on damaged buildings and an ensuing review of the M.S.K76 scale. *Proc. of the 7th European Conference on Earthquake Engineering*, Athens.
- Braga F., Dolce M. (1982). Un metodo per l'analisi di edifici multipiano in muratura antisismica. *Proc. of the 6th I.B.M.A.C - International Brick Masonry Conference*, Rome.
- Brencich A., Gambarotta L., Lagomarsino S. (1998). A macroelement approach to the three-dimensional seismic analysis of masonry buildings. *Proc. of 11th European Conference on Earthquake Engineering*, Rotterdam.
- Calderini C., Cattari S., Lagomarsino S. (2009). In plane seismic response of unreinforced masonry walls: comparison between detailed and equivalent frame models. *Proc. of COMPDYN 2009 ECCOMAS Thematic Conference on Computational Methods in Structural Dynamics and Earthquake Engineering*, Rhodes, Greece, June, 22–24.
- Calvi G.M. (1999). A displacement-based approach for vulnerability evaluation of classes of buildings, *Journal of Earthquake Engineering*, 3, 3, pp. 411-438.

- Calvi G.M., Magenes G. (1994). Experimental Results of Unreinforced Masonry Shear Walls Damaged and Reipared. *Proceedings of the 10th I.B.M.A.C - International Brick Masonry Conference*, Calgary.
- Cattari S., Curti E., Giovinazzi S., Lagomarsino S., Parodi S., Penna A. (2004). A mechanical model for the vulnerability analysis of the masonry built-up at urban scale (in Italian), *Proc. of the 11th Italian Congress "L'Ingegneria Sismica in Italia"*, Genova, January, 25-29.
- CEN (European Committee for Standardization) – UNI EN 1052-1 (2001a). Method of test for masonry – Compressive strenght determination.
- CEN (European Committee for Standardization) – UNI EN 1052-3 (2001b). Method of test for masonry – Initial shear strenght determination.
- CEN (European Committee for Standardization) – UNI EN 998-2 (2003). Specification for mortar for masonry - Part 2: Masonry mortar.
- CEN (European Committee for Standardization) – UNI EN 771-1 (2004a). Specifications for masonry units.
- CEN (European Committee for Standardization) – UNI EN 772-1 (2004b). Methods of test for masonry units.
- CEN (European Committee for Standardization) EN 1996-1-1 (2005a). Eurocode 6. Design of masonry structures. Brussels, Belgium.
- CEN (European Committee for Standardization) – EN 1998-3 (2005b). Eurocode 8. Design of structures for earthquake resistance, Part 3: Assessment and retrofitting of buildings, Brussels, Belgium.
- CEN (European Committee for Standardization) EN 1995-2 (2005c). Eurocode 5. Design of timber structures. Brussels, Belgium.
- Coburn A.W., Spence R.J.S., Pomonis A. (1994). Vulnerability and Risk Assessment. Disaster Management Training Programme. Cambridge Architectural Research Limited, The Oast House, Malting Lane, Cambridge, United Kingdom.

- Cornell C. A. (1968). Engineering Seismic Risk Analysis. Bulletin of Seismological Society of America, Vol.58, No5, pp.1583-1606.
- Corsanego A., Petrini V. (1994). Evaluation criteria of seismic vulnerability of the existing building patrimony on the national territory. Seismic Engineering, Patron ed., Vol. 1.
- CSI (2006) SAP 2000: Users Manual, Version 11. Berkley, California, USA.
- Cubellis E., Marturano A. (2006). Analysis of historical and present earthquakes at Vesuvius for seismic hazard evaluation. Volcanic Hazard and Risk, Vienna, Austria, July 2.
- D'Ayala D., Speranza E. (2002) An integrated procedure for the assessment of seismic vulnerability of historic buildings. *Proc. of 12th European Conference on Earthquake Engineering, London*, Paper n. 561.
- D'Ayala D., Speranza E. (2003). Definition of Collapse Mechanisms and Seismic Vulnerability of Masonry Structures. *Earthquake Spectra* 19 (3), 479-509.
- De Rossi M.S. (1883), Programma dell'osservatorio ed archivio centrale geodinamico presso il R. Comitato Geologico d'Italia (in Italian). Italian Volcanism Bulletin - 10, 3-128.
- Dobran F. (2007). Urban Habitat Constructions Around Vesuvius, Environmental Risk and Engineering Challenges. GVES, Naples, Italy, Hofstra University, New York, U.S.A.
- Dong W., Shah H., Wong F. (1988). Expert System in Construction and Structural Engineering. New York: Chapman and Hall, London.
- Drysdale R.G., Hamid A.A., Baker, L.R. (1999). Masonry structures. Behaviour and design. The Masonry Society, Boulder, Colorado, USA.
- Esposti Ongaro T., Neri A., Menconi G., De Michieli Vitturi M., Marianelli P., Cavazzoni C., Erbacci G., Baxter P.J. (2008). Transient 3D numerical simulations of column collapse and pyroclastic density current scenarios at Vesuvius, *Journal of Volcanology and Geothermal Research*. 178: 378-396.

- Faella C., Nigro E. (2002). Debris flow effects on constructions. Damage analysis , collapse mechanisms , impact velocities, code provisions. Internal Report COST-C12/WG2, Volos, Greece, 14–15 June.
- Fajfar P. (2000). A non linear analysis method for performance-based seismic design, *Earthquake Spectra*, 16, 3, pp. 573-591.
- Fajfar P., (1999). Capacity spectrum method based on inelastic demand spectra, *Earthquake Engineering and Structural Dynamics*, 28.
- Fanale L., Lepidi M., Gattulli V., Potenza F. (2009). Analysis of buildings damaged from the 2009 April seismic event in the town of L'Aquila and in some neighbouring minor centres (in Italian). DISAT publication n. 03.
- Federal Emergency Management Agency (FEMA) – 154 (1988). Rapid visual screening of buildings for potential seismic hazards: a handbook. Washington (DC).
- Federal Emergency Management Agency (FEMA). 1999. Hazus 1999. Earthquake loss estimation methodology. Technical Manual. FEMA, Washington D.C.
- Florio G., Landolfo R., Formisano A., Mazzolani F.M. (2009). Vulnerability of a historical masonry building in the Vesuvius area. *Proc. of PROHITECH 2009 International Conference*, Rome, June, 21-24.
- Fields N., Spedaliere D., Sulemsohn S. (2004). Troy c. 1700-1250 BC. Osprey Publishing Ltd, UK.
- Formisano A., Florio G., Landolfo R., Mazzolani F. M. (2008). The Vesuvius risk scenario, the seismic vulnerability of the “Palazzo di Città” in Torre del Greco (NA). *Proc. of COST Action C26 Symposium*, Malta, October, 23-25.
- Formisano A., Florio G., Landolfo R., Mazzolani F.M. (2009a). Seismic vulnerability of a masonry block in Sessa Aurunca (CE) (in Italian). *Proc. of the 13th Italian Congress “L’Ingegneria Sismica in Italia”*, Bologna, June, 28 - July, 2.
- Formisano A., Florio G., Landolfo R., Mazzolani F.M., (2010b). A method for seismic vulnerability assessment of historical aggregates (in Italian). *Proc of the*

- Workshop Wondermasonry "Design for Rehabilitation of Masonry Structures"*, Ischia, October, 8-10.
- Formisano A., Florio G., Mazzolani F.M., Landolfo R., Terracciano G. (2010a). The behaviour of masonry building aggregates under earthquake: a study case. *Proc. of the 14th European Conference on Earthquake Engineering*, Ohrid, Republic of Macedonia, August.
- Formisano A., Florio G., Mazzolani F.M., Landolfo R. (2010b). A quick methodology for seismic vulnerability assessment of historical masonry aggregates. *Proc. of COST C26 Final International Conference*, Napoli, September, 16-18.
- Frassine L., Giovinazzi S. (2004). Comparison of databases for the seismic vulnerability analysis of residential buildings: an application for the city of Catania (in Italian), *Proc. of the 11th Italian Congress "L'Ingegneria Sismica in Italia"*, Genova, January, 25-29.
- Freeman S.A., (1998). The Capacity Spectrum Method. *Proc. of 11th European Conference on Earthquake Engineering*, Paris.
- Freeman S.A., Nicoletti J.P., Tyrell J.V. (1975). Evaluations of Existing Buildings for Seismic Risk - A Case Study of Puget Sound Naval Shipyard, Bremerton, Washington. *Proc. of U.S. National Conference on Earthquake Engineering, Berkeley*, U.S.A., pp. 113-122.
- Fusier F., Vignoli A. (1993). Proposal of a calculation method for masonry buildings subjected to horizontal actions. *Ingegneria Sismica*, n.1.
- Galeota, A. (2006). *Dizionario Poggiano*. Associazione culturale il castello, Poggio Pienze.
- Galli P., Camassi R. (2009). Report on L'Aquila earthquake of 6th April 2009 effects (in Italian). Joint Report DPC-INGV.
- Giovinazzi S. (2005). The Vulnerability Assessment and the Damage Scenario in Seismic Risk Analysis, PhD Thesis, Technical University Carolo-Wilhelmina at Braunschweig, Braunschweig, Germany and University of Florence, Florence, Italy.

- Giovinazzi S., Lagomarsino S. (2001). A methodology for the seismic vulnerability analysis of the built up. *Proc. of the X Congresso Nazionale on L'Ingegneria Sismica in Italia*, Potenza-Matera, Italy, Paper No. 121 (on CD).
- Giovinazzi S., Lagomarsino S. (2004) A Macro seismic Method for the Vulnerability Assessment of Buildings, *Proc. of the 13th World Conference on Earthquake Engineering*, Vancouver, Canada, Paper No. 896 (on CD).
- GNDT, 1994. 1st and 2nd level vulnerability and damages detection forms (masonry and RC structures) (in Italian).
- Grunthal G. (1998). European Macro seismic Scale 1998. *Chaiers du Centre Européen de Géodynamique et de Séismologie*, Vol. 15, Luxembourg.
- Guagenti E., Petrini V. (1989). Il caso delle vecchie costruzioni: verso una nuova legge danni-intensità. *Proc. of 4th Italian Conference on Earthquake Engineering*, Milano, Vol. I, pp. 145-153.
- HKS, 2004.ABAQUS Theory Manual. USA
- Kircher C. A., Nassar A.A., Kuster O., Holmes W.T. (1997). Development of building damage functions for earthquake loss estimation. *Earthquake Spectra*, 13(4), pp. 663-682.
- Krstevska L., Kustura M., Tashkov L. (2008). Experimental in-situ testing of reconstructed old bridge in mostar. *Proc. of the 14th World Conference on Earthquake Engineering*, Beijing, China, October 12-17.
- Krstevska L., Tashkov L., Naumovski N., Florio G., Formisano A., Fornaro A., Landolfo R. (2010). In-situ experimental testing of four historical buildings damaged during the 2009 L'Aquila earthquake. *Proc. of COST C26 Final International Conference*, Naples, September 16-18.
- Lourenço P.B. (1998). Experimental and numerical issues in the modelling of the mechanical behaviour of masonry. *Structural Analysis of Historical Constructions II*. CIMNE. Barcelona. pp 57-91.

- Macchi G., Magenes G. (2002). Le strutture in muratura. In Giangreco E. (cured by) “Ingegneria delle strutture”, Vol. 3, UTET, Torino.
- Magenes G., Calvi G.M. (1997). In-plane seismic response of brick masonry walls. *Earthquake Engineering and Structural Dynamics*, Vol. 26, 1091-1112.
- Magenes. G. (2006). Masonry building design in seismic areas: recent experiences and prospects from a European standpoint. *Proceedings of 1st European Conference on Earthquake Engineering and Seismology*, Geneva, Switzerland, 3-8 September.
- Mazzolani F.M, Indirli M., Zuccaro G, Faggiato B., Formisano A., De Gregorio D. (2009a). Catastrophic Effects of a Vesuvian Eruption on the Built Environment, *Proc. of Protect* .
- Mazzolani F.M., Faggiato B., De Gregorio D. (2009b). The catastrophic Scenario in explosive volcanic eruptions in urban area. *Proc. of PROHITECH 2009 International Conference*, Rome, June, 21-24.
- McKenzie W.M.C. (2001). Design of structural masonry. Great Britain.
- McGuire R. K. (2007). Probabilistic seismic hazard analysis: Early history, in Wiley InterScience, <http://www.interscience.wiley.com>, DOI: 10.1002/eqe.765.
- Mendes N., Lourenço P B., Campos-Costa A. (2010). Seismic Vulnerability Assessment of Ancient Masonry Building: and Experimental Method. *Advanced Materials Research Vols. 133-134*, pp 635-640, Trans Tech Publication, Switzerland.
- Ministerial Decree of the Ministry of Public Works (M.D. 24/01/1986) Technical regulations for seismic constructions.
- Ministerial Decree of the Ministry of Public Works (M.D. 20/11/1987) Technical regulations for design, execution and testing on masonry structures and for their strengthening.
- Ministerial Decree (M. D. 16/01/1996). Technical regulation for constructions in seismic areas.

- Ministerial Decree (M. D. 14/09/2005) (2005). *Technical codes for constructions*. Official Gazette of the Italian Republic.
- Ministerial Decree (M. D., 14/11/2008) (2008). *Technical codes for constructions*. Official Gazette of the Italian Republic published on January 14th.
- MiBAC (Ministry of Cultural Heritage and Activities) (2006). Guidelines for the seismic risk evaluation and reduction of the cultural heritage with reference to the technical regulations of constructions (in Italian).
- Modena C., Valluzzi M. R., Da Porto F., Casarin F., Garbin E., Munari M., Mazzon N., Panizza M., Dalla Benetta M. (2009). Recent advances in the structural analysis and intervention criteria for historic stone masonry constructions subjected to seismic actions. *Proc. of ISCARSAH Symposium on Assessment and strengthening of historical stone masonry constructions subjected to seismic actions*, Mostar 12th July 2009.
- Monaco P., Totani G., Barla G., Cavallaro A., Costanzo A., D'Onofrio A., Evangelista L., Foti S., Grasso S., Lanzo G., Madià C., Maraschini M., Marchetti S., Maugeri M., Pagliaroli A., Pallara O., Penna A., Saccenti A., Santucci de Magistris F., Scasserra G., Silvestri F., Simonelli A. L., Simoni G., Tommasi P., Vannucchi G., Verrucci L.. (2009). Geotechnical aspects of the L'Aquila earthquake. *Proc. of Earthquake Geotechnical Engineering Satellite Conference XVIIth International Conference on Soil Mechanics & Geotechnical Engineering*, Alexandria, Egypt.
- Nocilla N., Viviano D., Aversa S. (1999). Applicazione della fotogrammetria al rilievo strutturale di costoni Rocciosi, *Proc. XX Italian Geotechnical Conference*: 231-238. Parma: Patron Editore.
- Nunziata C., Luongo G., Panza G.F. (2000). Mitigation of seismic hazard in Naples and the protection of cultural heritage. *Proc. of the EuroConference on Global Change and Catastrophe Risk Management: Earthquake Risks in Europe*, Laxenburg.
- Ohmachi T., Jalali A. (1999). Fundamental study on near-field effects on earthquake response of arch dams. *Earthquake Engineering and Engineering Seismology*, Vol. 1, n. 1, pp. 1-11, September.

- Omori, F. (1900). Intensity scale. Earthquake Investigation Committee publication in foreign languages, 4, 137-141.
- OPCM (Decree of the cabinet president) n. 3274 (2003). First elements in the matter of general criteria for seismic classification of the national territory and of technical codes for structures in seismic zones (in italian). Official Gazette of the Italian Republic
- OPCM (Decree of the cabinet president) 3431, (2005). Further changes and upgrade to the OPCM 3274/2003; Official Gazette of the Italian Republic.
- Page A.W., Samarasinghe W., Hendry A.W. (1980). The failure of masonry shear walls. *Int. J. Masonry Constr.*, 1(2), pp. 52-57.
- Page, A.W. (1981). The biaxial compressive strength of brick masonry”, *Proc. Instn. Civ. Engrs.*, Part 2, 71, 893-906.
- Pasticier. L, Amadio C., Fragiacommo. M. (2007). Non-linear seismic analysis and vulnerability evaluation of a masonry building by means of the SAP2000 V.10 code. *Earthquake Engng Struct. Dyn.* 2008; 37:467–485.
- Picarelli L, Urciuoli G. (1993). Effetti dell’erosione in argilliti di alta plasticità. *Rivista Italiana di Geotecnica*, XXVIII (No.1): 29-47.
- R. L. (Region Law) Friuli Venezia Giulia n.30, 20th July 1977.
- Restrepo Vélez L. F. (2005). A Simplified Mechanics-Based Procedure for the Seismic Risk Assessment of Unreinforced Masonry Building. Ph.D Thesis, European School for Advanced Studies in Reduction of Seismic Risk (ROSE School), I.U.S.S, Pavia, Italy.
- Ruscetti M., Carniel R., Cecotti C. (1997). Seismic Vulnerability assessment of masonry buildings in a region of moderate seismicity. *Geophysics Annals*, Vol. XL, N.5, pp. 1405-1413.
- Romano A. (2005). Modelling, Analysis and Testing of Masonry Structures. Phd Thesis, Naples.
- S.T.A. DATA (2009). 3Muri User Manual, Release 4.0.0, Torino.

- Sandi H. (1986). Report of the Working Group: Vulnerability and risk analysis for individual structures and systems, of the European Association of Earthquake Engineering, Proceedings of the 8th European Conference on Earthquake Engineering, Lisbon.
- Spence R., Kelman I., Baxter P.J., Zuccaro G., Petrazzuoli S. (2005). Residential building and occupant vulnerability to tephra fall. *Natural Hazard and Earth System Sciences*, 5, 477–494.
- Stucchi M., Calvi G. M., Meletti C. (2007). Project S1 - Continuation of assistance to DPC for improving and using the seismic hazard map compiled according to the Prime Minister “Ordinanza” 3274/2003 and planning future initiatives. Scientific Reports of the Research Units, <http://esse1.mi.ingv.it>, Milano-Pisa.
- Suckale J., Grunthal G., Regnier M., Bosse C. (2005). Probabilistic Seismic Hazard Assessment for Vanuatu, Scientific Technical Report STR 05/16.
- Todesco M., Neri A., Esposti Ongaro T., Papale P., Macedonio G., Santacroce R., Longo A. (2002). Pyroclastic flow hazard assessment at Vesuvius (Italy) by using numerical modelling. I. Large-scale dynamics, *Bull. Volcanol.* 64:155–177. DOI 10.1007/s00445-001- 0189-7.
- Tomazevic M. (1999). Earthquake resistant design of masonry buildings, Innovation in structures and constructions. Vol. I, 5-12, A.S. Elnashai & P.J. Dowling, Singapore.
- Turnšek V., Cačovic F. (1971). Some experimental results on the strength of brick masonry walls. *Proc. of the 6th I.B.M.A.C - International Brick Masonry Conference*, Stoke-on- Trent, pp. 149-156
- Turnšek V., Cačovic F. (1970). Some Experimental Results on the Strength of Brick Masonry Walls, *Proc. of the 2nd International Brick Masonry Conference*, Stock on Trent.
- U.N.D.R.O. (1979). Natural Disasters and Vulnerability Analysis. Report of Expert Group Meeting. Geneva: Office of the United Nations Disaster Relief Coordinator.

- Valensise G., Amato A., Montone P., Pantosti D. (2003). Earthquakes in Italy: past, present and future. Episodes, Vol. 26, n.3. Istituto Nazionale di Geofisica e Vulcanologia (INGV), Rome, Italy.
- Vidic T., Fajfar P., Fischinger M. (1994). Consistent inelastic design spectra: strength and displacement, Earthquake Engineering and Structural Dynamics 23, pp. 507-521.
- Zuccaro G., Papa F., (2001). Multimedial MEDEA CD-ROM – Tutorial manual on damage and usability of ordinary masonry buildings (in Italian). CAR Progetti srl, October.
- Zuccaro G., Papa. F. (2002) Multimedial handbook for seismic damage evaluation and post event macroseismic assessment. 50th Anniversary of the European Seismological Commission (ESC): XXVIII General Assembly. Genova.
- Zucchini A., Lourenço P.B. (2006). Mechanics of masonry in compression: Results from a homogenisation approach. Computers and structures.